

**Republic of Iraq**  
**Ministry of Higher Education and**  
**Scientific research**  
**Baghdad University**  
**Collage of Education for Pure**  
**Science (Ibn Al-Haitham)**  
**Department of Chemistry**



# **Synthesis , characterization and biological activity evaluation of some metal ions with selective drug**

**A Thesis**

**Submitted to the Council of the College of Education for Pure Sciences\**

**(Ibn-AL-Haitham),**

**University of Baghdad in partial fulfilment**

**of the requirements for the Degree of MSc in Chemistry**

**By**

**Saja Ahmed Abdulla**

**B.Sc. in Chemistry (2016) Baghdad University**

**Supervised by**

**Prof.Dr. Taghreed Hashim Al-Noor**

**2019 A.D.**

**1441 A.H.**

بِسْمِ اللَّهِ الرَّحْمَنِ الرَّحِيمِ

بَلْ هُوَ آيَاتٌ بَيِّنَاتٌ

فِي صُدُورِ الَّذِينَ أُوتُوا الْعِلْمَ

وَمَا يَجْعَدُ بآيَاتِنَا إِلَّا الظَّالِمُونَ

صَدَقَ اللَّهُ الْعَلِيِّ الْعَظِيمِ

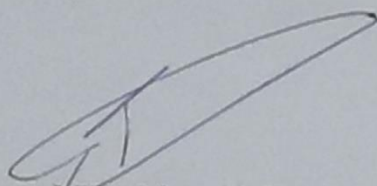
سورة العنكبوت - الآية ٤٩

## Declaration of the Supervisor

I hereby declare that this thesis has been performed under my supervision in chemistry department, College of Education for pure science Ibn Al-Haitham of Baghdad University in partial fulfillment of the requirements for the degree of master of science in chemistry.

Supervisor

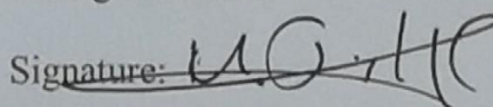
Signature:



**Prof. Dr. Tghreed Hashim Al-Noor**  
Department of Chemistry  
College of education  
For pure science Ibn Al-Haitham  
University of Baghdad

Date: 20/11 / 2019

In view of the available recommendation .I forward thesis for debate by the examining committee

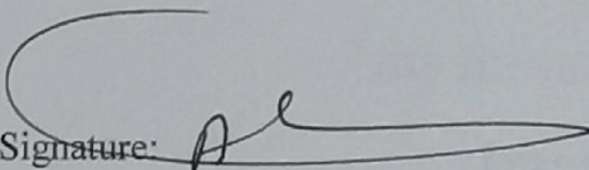
Signature: 

**Prof. Dr. Mohamad Jaber Al-Jeboori**  
Head of Chemistry Department  
College of Education  
For pure Science Ibn Al-Haitham  
University of Baghdad

Date: 20/11 / 2019

## Certification

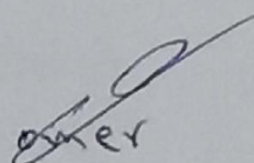
We, the examining committee, after reading this thesis " **Synthesis , characterization and biological activity evaluation of some metal ions with selective drug** " and examining the student, " **Saja Ahmed Abdulla** " in its contents, found that it is qualified for the degree of Master of Science in Chemistry with grade of (**Excellent**) on ( 12 / 11 / 2019 ).

Signature: 

Name : Prof. Dr. Ahmed Thabit Numan

Date: 19 / 11 / 2019

(Chairman)

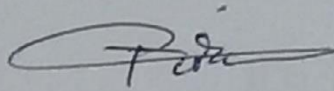
Signature: 

Name: Prof. Dr. Omar H. Al-Obaidi

Date: 17 / 11 / 2019

(Member)

Signature:

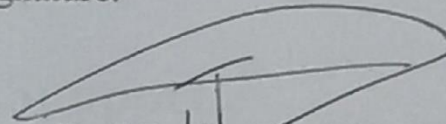


Name: Asst. Prof. Dr. Tariq H. Almgheer

Date: 18 / 11 / 2019

(Member)

Signature:

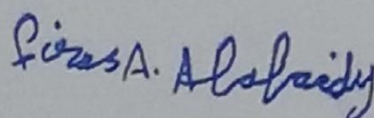


Name: Prof. Dr. Taghreed Hashim

Date: 20 / 11 / 2019

Member (Supervisor)

Address: Behalf / The Dean of College of Education for pure Science  
(Ibn-Al-Haitham) University of Baghdad

Signature 

Assit. Prof. Dr. Firas Abdulhameed Abdullatif

Date: 24 / 11 / 2019

# **Dedication**

This thesis is dedicated to

**Imam Mehdi**

and to

**My Family**

For their

**Endless love, Support**

And

**Encouragement.**

## Acknowledgements

Every Challenging Work Need self-efforts as well as guidance of elderly especially those who were very close to my heart.

- I would like to thank my dear supervisor who was supported me in everything **Prof. Dr. Taghreed Hashim Al-Noor**. Thanks be to Allah and then to her for what I finally achieved.

\_ To who missed from my eyes and did not lose sight of my heart “ my dear father “

\_ My humble effort. I thanks to my sweet and lovely “ My Mather and sisters “

\_ I am very grateful to my partner and my fatigue and companion laughed and tear “ my husband Gabriel “ and all thanks for his family

\_ To my little heart walking on the ground “ my son Ahmed “

\_ Whose affection , love , encouragement and prays of day and night make me able to get such success, I personally thankful to my friends especially Hamsa , Maryam , rand , Bayader , Yosra ,Asmaa , Alaa , Ammar , Naail

**Saja**

## Summary

The work in this thesis is described as follows:

### A: Mixed-Ligand metal complexes

A A: Sulphamethoxazole (**SMZ**) (antibiotics) are used as primary ligands and/or L-Proline(**L-ProH**), and L-Valine (**L-ValH**) as secondary ligands with M(II) and M' (III) complexes (as listed in the Table below.

Type Mixed ligand complexes	Primary ligand	Secondary Ligand amino acid	Compositions
Style 1 L-ProH -M - SMZ 2.1.1 1.1.1	Sulfamethoxazole (SMZ)	L-Proline ( L-ProH)	[ ( L-Pro) <sub>2</sub> M (SMZ)] M= Mn(II), Fe (II),Ni(II), Cu(II),Cd(II), Hg(II) and Sn(II)
	Sulfamethoxazole (SMZ)	L-Proline ( L-ProH)	[L-Pro) <sub>2</sub> M' (SMZ)]Cl M' = Al(III) ,Cr(III) and Fe(III)
	Sulfamethoxazole (SMZ)	L-Proline ( L-ProH)	[ Sn(SMZ)( L-Pro)]Cl
Style 2 L-Val- M - SMZ 2.1.1	Sulfamethoxazole (SMZ)	L-Valine ( L-ValH)	[ ( L-Val) <sub>2</sub> M (SMZ)]Cl M= Mn (II), Fe (II), Co(II),Ni(II), Cu(II), ,Cd(II), Hg(II) and Sn(II)
	Sulfamethoxazole (SMZ)	L-Valine ( L-ValH)	[ ( L-Val ) <sub>2</sub> M' (SMZ) ]Cl M' = Fe(III) ,Cr(III) and Al(III)

## B : Mono Ligand Complexes

Sulphamethoxazole (*antibiotics*) , L-Proline and L-Valine

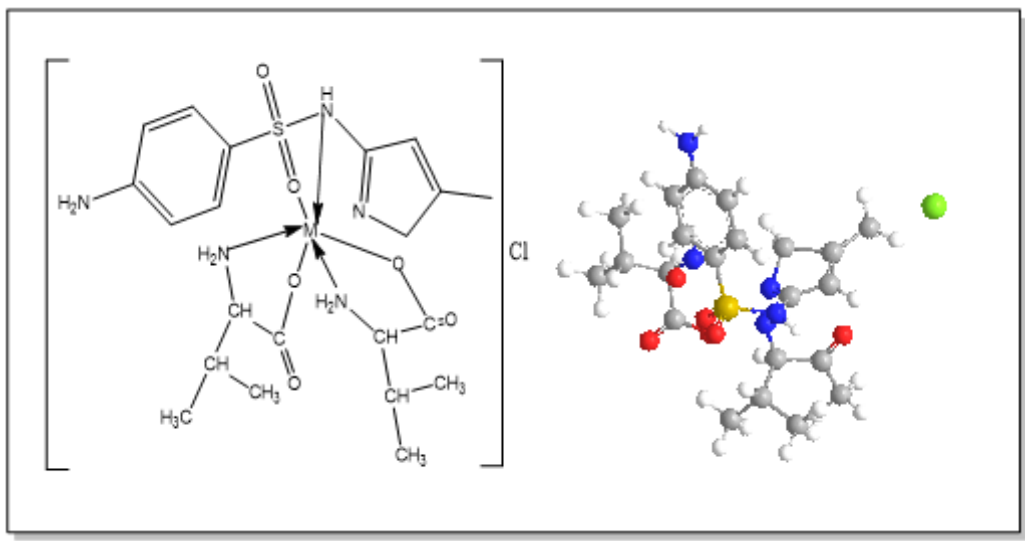
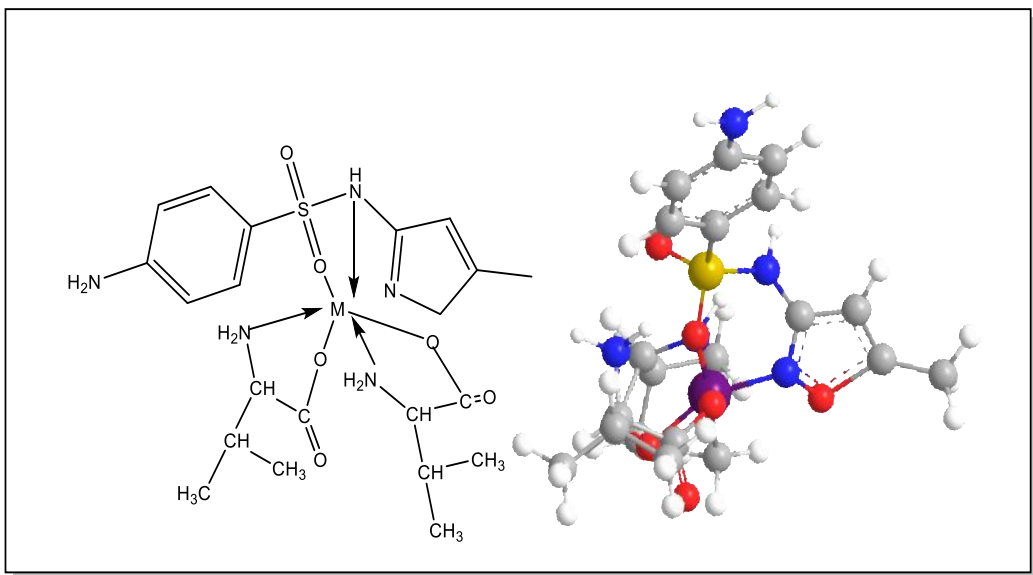
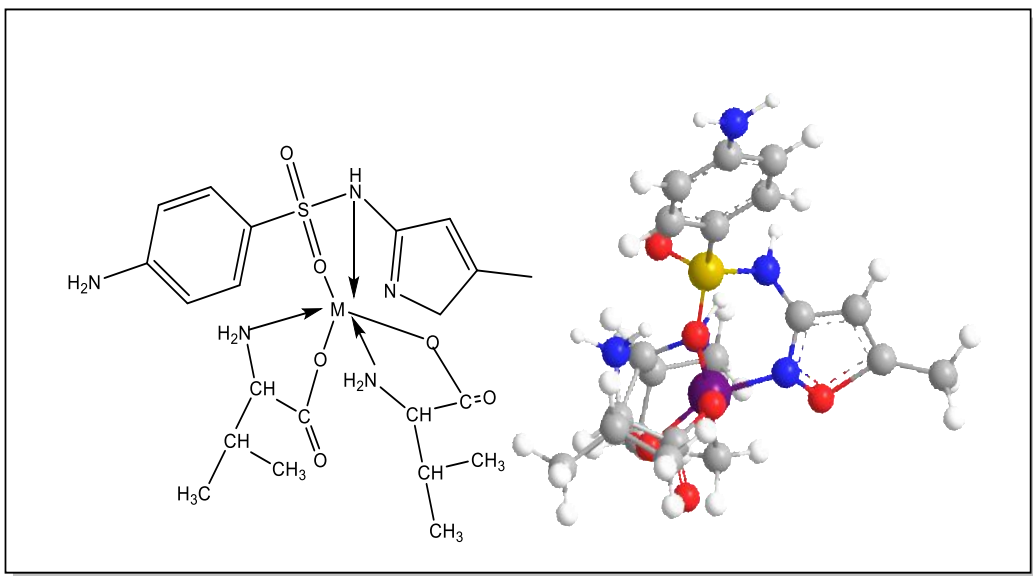
Were used as mono ligand complexes (as listed in the Table

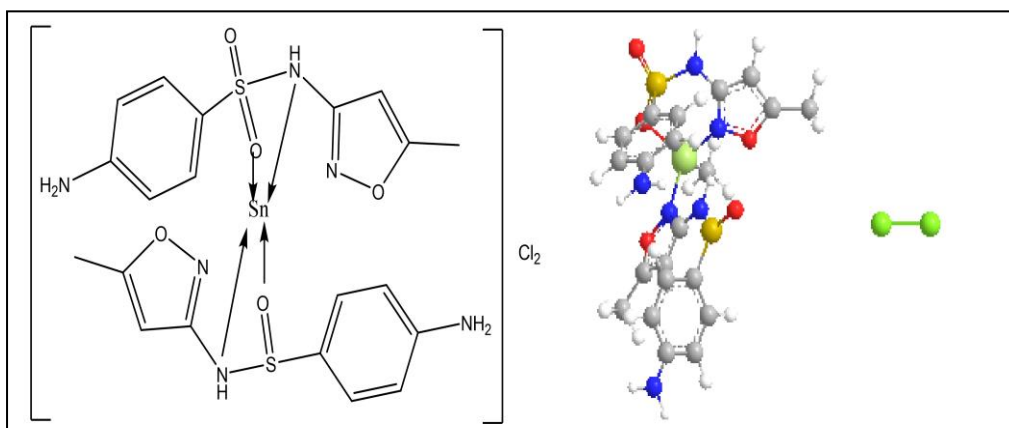
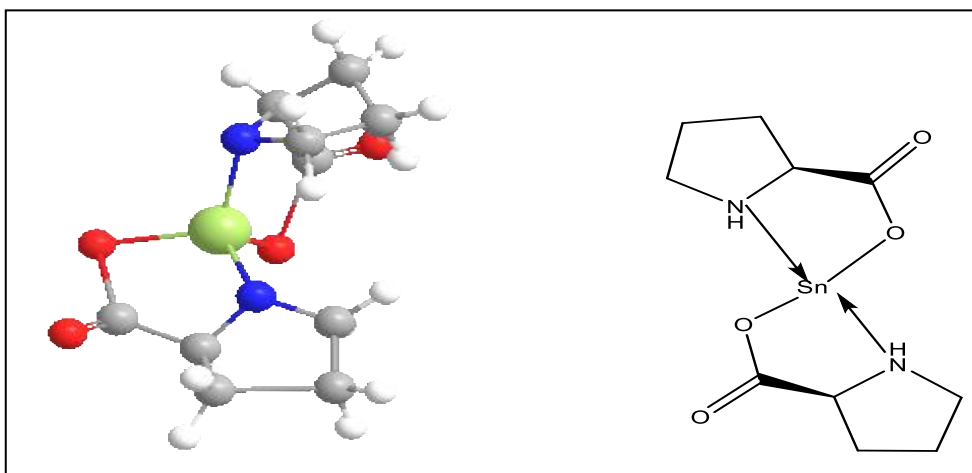
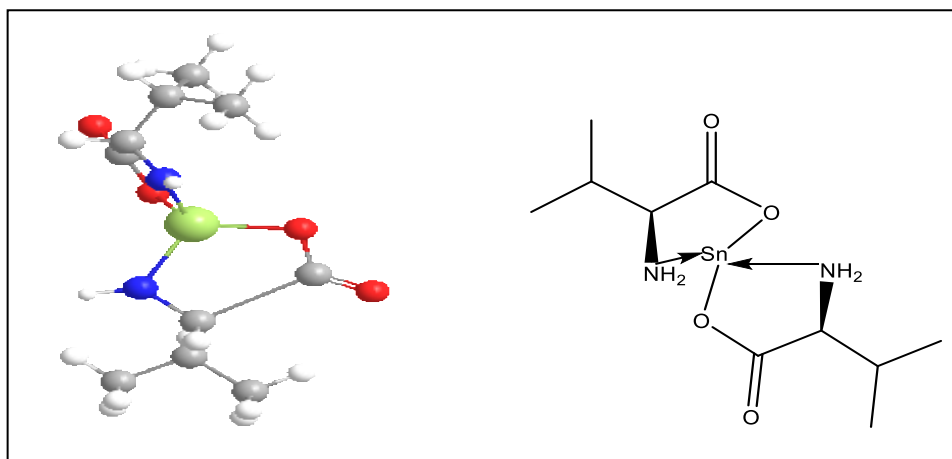
below:

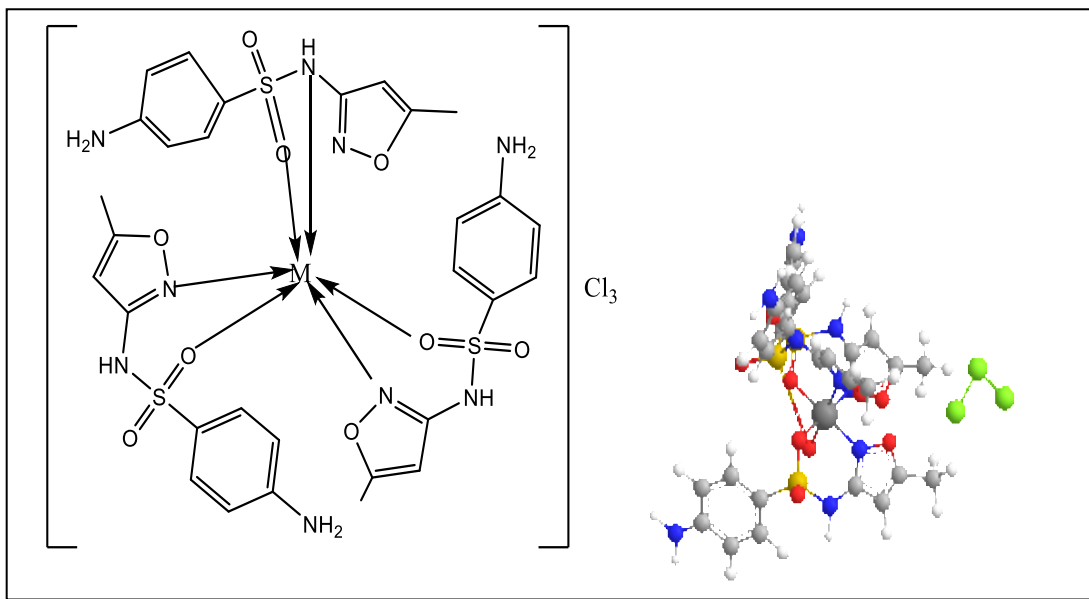
Type	ligands	Compositions
Style 1	Sulfamethoxazole (SMZ)	$[\text{Sn}(\text{SMZ})_2]\text{Cl}_2$
Style 2	amino acid L-Proline ( L-ProH)	$[\text{Sn}(\text{L-Pro})_2]$
Style 3	amino acid L-Valine ( L-ValH)	$[\text{Sn}(\text{L-Val})_2]$
Style 4	Sulfamethoxazole (SMZ)	$[\text{M}'(\text{SMZ})_3]\text{Cl}_3$ M'=Fe(III),Cr(III)and Al(III)

Products were found to be solid complexes, which were characterized through the following techniques: Molar conductance, Melting point measurements and spectroscopic methods i.e., [FT-IR, UV-Vis and AA]. According to the results obtained from the different techniques, the following structures are suggested.









The biological activity of the synthesized compound as well as their free ligands was studied by the zone of inhibition (ZI) .

<b>Subject</b>		<b>Page No.</b>
<b>Chapter one : Introduction</b>		
1	General Introduction	1
1.1	Antibiotics Drugs and elemental medicine	1
1.2	Sulfamethoxazole and its complexes	5
1.3	Amino acids	14
1.3.1	Structure, classification and biochemical role.	14
1.3.2	Basicity of Nitrogen L- $\alpha$ -amino-acid	18
1.4	L- Valine complexes	23
1.5	L- Proline complexe	30
1.6	Aim of The present Work	37
<b>Chapter Two : Experimental</b>		
2	The Experimental	38
2.1	Chemicals	38
2.2	Instruments and apparatus	38
2.2.1	The Melting point measurements	38
2.2.2	Electrical conductivity measurements	39
2.2.3	Metal determination	39
2.2.4	Chloride contents	39
2.2.5	Electronic (U.V-Vis) spectra	39
2.2.6	Magnetic susceptibility	39
2.2.7	Elemental micro analysis	40
2.2.8	The infrared spectra	40
2.3	Procedures For (Biological ) Evaluation	40
2.4	General Preparation of Mixed- ligand Metal Complexes with some metal ions	42
2.4.1	preparation of potassium L-prolinate	42
2.4.2	preparation of [M(SMZ)(L-Pro) <sub>2</sub> ] and [M'(SMZ)(L-Pro) <sub>2</sub> ] Cl complexes.	42
2.4.3	Preparation of potassium L-Valinate	44
2.4.4	Preparation of [M(SMZ)(L-Val) <sub>2</sub> ] and [M'(SMZ)(L-Val) <sub>2</sub> ] Cl complexes	45
2.4.5	Preparation of [ Sn(SMZ)( L-Pro)]Cl	45
2.5	Preparation of mono - ligand Metal Complexes	46
2.5.1	Preparation of [Sn(L-Pro) <sub>2</sub> ]	46
2.5.2	Preparation of [Sn(L-Val) <sub>2</sub> ]	47
2.5.3	Preparation of [Sn(SMZ) <sub>2</sub> ]Cl <sub>2</sub>	48

<b>Chapter Three : Results &amp; Discussion</b>		
3.1.	General Methodology:	51
3.2.	(U.V-Vis) Spectra of the Ligands:	52
3.2.1	(U.V-Vis) Spectrum of the (SMZ)	52
3.2.2	(U.V-Vis) Spectrum of the (proH)	53
3.2.3	(U.V-Vis) Spectrum of the (L-ValH)	54
3.3	FT-IR Spectra of the Ligands	54
3.3.1	FT-IR Spectrum of (SMZ)	54
3.3.2	FT-IR Spectrum of L- proline	57
3.3.3	FT-IR Spectrum of L- Valine	58
3.4	Physico-Chemical Characterization of Mixed – ligand (L-prolin -Metal - SMZ) Complexes	60
3.4.1	FT-IR spectra of [SMZ -M-L-ProH] and [SMZ - M'-L-ProH] complexes	64
3.4.2	Ultraviolet–visible UV/Vis spectra , magnetic properties of compounds	74
3.4.3	Ultraviolet / Visible [UV/Vis] spectra of [SMZ - M-L-ProH] and [SMZ - M'-L-ProH] complexes	79
3.4.3.1	UV/Vis spectrum of [Mn(SMZ)(Pro) <sub>2</sub> ]	79
3.4.3.2	UV/Vis Spectrum of [Fe(SMZ)(L-Pro) <sub>2</sub> ]	81
3.4.3.3	UV/Vis Spectrum of [Ni (SMZ)(L-Pro) <sub>2</sub> ]	82
3.4.3.4	UV/Vis Spectrum of [Cu(SMZ)(L-Pro) <sub>2</sub> ]	82
3.4.3.5	UV/Vis Spectrum of [Cd(SMZ)(L-Pro) <sub>2</sub> ]	84
3.4.3.6	UV/Vis Spectrum of [Hg(SMZ)(L-Pro) <sub>2</sub> ]	84
3.4.3.7	UV/Vis Spectrum of [Al (SMZ)(L-pro) <sub>2</sub> ]Cl	85
3.4.3.8	UV/Vis Spectrum of [Cr (SMZ)(L-pro) <sub>2</sub> ]Cl	86
3.4.3.9	UV/Vis Spectrum of [Fe (SMZ)(L-pro) <sub>2</sub> ]Cl	86
3.4.3.10	UV/Vis Spectrum of [Sn(SMZ)(L-Pro) <sub>2</sub> ]	87
3.4.3.11	UV/Vis Spectrum of [Sn(SMZ)(L-Pro)] Cl	88
3.4.4	The Proposed Molecular Structure for [L- pro H-Metal - (SMZ) ] Complexes M-(II) , M'-(III)	88
3.5	Physico-Chemical Characterization of Mixed – ligand (L-Valine -Metal-SMZ) Complexes.	90
3.5.1	FT-IR spectra of [SMZ -M-L-ValH] and [SMZ - M'-L-ValH] complexes	96
3.5.2	Ultraviolet / Visible [UV/Vis]	102
3.5.2.1	UV/Vis Spectrum of [Mn(SMZ)(L- Val) <sub>2</sub> ]	103
3.5.2.2	UV/Vis Spectrum of [Co (SMZ)(L- Val) <sub>2</sub> ]	105
3.5.2.3	UV/Vis Spectrum of [Ni (SMZ)(L- Val) <sub>2</sub> ]	107

3.5.2.4	UV/Vis Spectrum of [Cu (SMZ)(L- Val) <sub>2</sub> ]	108
3.5.2.5	UV/Vis Spectrum of [Cd (SMZ)(L- Val) <sub>2</sub> ]	109
3.5.2.6	UV/Vis Spectrum of [Hg(SMZ)( L- Val) <sub>2</sub> ]	110
3.5.2.7	UV/Vis Spectrum of [Sn(SMZ)(L- Val) <sub>2</sub> ]	111
3.5.2.8	UV/Vis Spectrum of [Al(SMZ)(L- Val) <sub>2</sub> ]Cl	112
3.5.2.9	UV/Vis Spectrum of [Cr (SMZ)( L-Val) <sub>2</sub> ]Cl	113
3.5.2.10	UV/Vis Spectrum of [Fe (SMZ)( L-Val) <sub>2</sub> ]Cl	114
3.5.3	The Proposed Molecular Structure for [L-Valin - Metal - (SMZ) ] Complexes	115
3.6	Synthesis and Characterization of Mono Ligand Complexes	117
3.6.1	Sn (II) Complexes	117
3.6.1.1	. Synthesis and Characterization of [Sn(L-pro) <sub>2</sub> ] , [Sn(L-Val) <sub>2</sub> ] and [Sn(SMZ) <sub>2</sub> ]Cl <sub>2</sub> Complexes	117
3.6.1.2	FT-IR spectra of [Sn(L-Val) <sub>2</sub> ] and [Sn(L-pro) <sub>2</sub> ] complexes	119
3.6.1.3	UV/Vis Spectrum of [Sn(L-Val) <sub>2</sub> ] and [Sn(L-pro) <sub>2</sub> ] complexes	122
3.6.1.4	The proposed molecular structure [Sn(L-Val) <sub>2</sub> ] and [Sn(L-pro) <sub>2</sub> ] complexes	123
3.6.1.5	Synthesis and Characterization of [Sn(SMZ) <sub>2</sub> ]Cl <sub>2</sub>	125
3.6.2	Synthesis and Characterization of [M' (SMZ) <sub>3</sub> ]Cl <sub>3</sub> Complexes	131
3.6.2.1	Ftr FT-IR spectra of [Al(SMZ) <sub>3</sub> ]Cl <sub>3</sub> , [Cr(SMZ) <sub>3</sub> ]Cl <sub>3</sub> , and [Fe (SMZ) <sub>3</sub> ]Cl <sub>3</sub> , complexes	132
3.6.2.2 .1	UV/Vis Spectrum of [Al(SMZ) <sub>3</sub> ]Cl <sub>3</sub>	136
3.6.2.2 .2	UV/Vis Spectrum of [Cr(SMZ) <sub>3</sub> ]Cl <sub>3</sub>	136
3.6.2.2. 3	UV/Vis Spectrum of [Fe(SMZ) <sub>3</sub> ]Cl <sub>3</sub>	137
3.7	The proposed molecular structure for M' (III)-SMZ) complexes	138
<b>Chapter Four: Biological activity</b>		
4	Biological activity	139
4.1	Introduction	139
4.2	Material & equipment's	141
4.3	Principle of antimicrobial susceptibility test	141
4.4	Types of Pathogenic Bacteria and fungus in this Study	142
4.5	Results and Discussion	143

## List of Tables

<b>Tables</b>		<b>Page No.</b>
<b>Chapter one</b>		
1-1	Some medical uses of complexes	3
1-2	structural of Amino acids	16
1-3	common amino acid abbreviations	17
1-4	Classification of Amino Acids According to Biological value	18
1-5	UPAC names and some physical properties of L- Proline and L- Valine	23
<b>Chapter Two</b>		
2-1	Chemicals used in this work and their Suppliers	38
2-2	Weights metals Chloride	43
2-3	Data for (CVM)of Determining Stoichiometry of Complex	50
<b>Chapter Three</b>		
3-1	Compositions of synthesised Mixed- Ligand Metals Complexesc	51
3-2	Compositions of synthesised Mono ligand Metals Complexes	52
3-3	Electronic data of starting materials and synthesized ligands	52
3-4	FT-R spectral data ( $\nu'$ ) $\text{cm}^{-1}$ for the SMZ	56
3-5	FT-IR Spectrum of L- proline	57
3-6	Infrared Spectrum Data (wave number $\hat{\nu}$ ) $\text{cm}^{-1}$ for the L- Valine	59
3-7	The Physical Properties & Atomic Absorption Results of the [SMZ -M-L-ProH] and [SMZ - M'-L-ProH] Complexes.	61
3-8	Microanalysis results	62
3-9	Solubility of all complexes in different solvents	63

3-10	Molar Conductivity ( $\Omega^{-1}\text{cm}^2\text{mol}^{-1}$ ) in water and some organic solvents	64
3-11	Infrared spectral data(wave number $\nu$ ) $\text{cm}^{-1}$ for [SMZ – M -L-ProH] complexes	66
3-12	Infrared spectral data(wave number $\nu$ ) $\text{cm}^{-1}$ for [SMZ – M -L-ProH] complexes	68
3-13	Racah's (B')values for some Ions( $\text{Cm}^{-1}$ )	77
3-14	Visible and U.V. region	78
3-15	Electronic Spectral Data of the [SMZ -M-L-ProH] complexes	78
3-16	Electronic Spectral Data of the [SMZ - M'-L-ProH] Complexes	79
3-17	The Physical Properties & Atomic Absorption Results of the [SMZ -M-L-ValH] and [SMZ - M'-L-ValH] Complexes	92
3-18	The solubility of complexes	92
3-19	Infrared spectral data(wave number $\nu$ ) $\text{cm}^{-1}$ for [SMZ – M -L-ValH] complexes	94
3-20	Infrared spectral data(wave number $\nu$ ) $\text{cm}^{-1}$ for [SMZ – M -L-ValH] complexes	95
3-21	Electronic Spectral Data of the Mixed- Ligand (L-Valin - Metal(II) -(SMZ) Complexes	102
3-22	Electronic Spectral Data of the Mixed- Ligand (L-Valin - Metal(III) -(SMZ) Complexes	103
3-23	Electronic Spectral Data of the [Mn(SMZ)( L-Val) <sub>2</sub> ]	104
3-24	The Physical Properties & Atomic Absorption Results of the Tin (II) Complexes	118
3-25	Microanalysis and analytical data for [Sn(SMZ) <sub>2</sub> ]Cl <sub>2</sub>	118
3-26	Solubility of [Sn (II)] complexes in different solvents	118
3-27	Infrared spectral data( $\nu$ ) $\text{cm}^{-1}$ for Tin -amino acids complexes	121
3-28	Electronic Spectral Data of the [Sn (L-Val) <sub>2</sub> ] and [Sn (L-Pro) <sub>2</sub> ]	122
3-29	FT-R spectral data ( $\nu$ ) $\text{cm}^{-1}$ for the SMZ	126
3-30	Data for (CVM)of Determining Stoichiometry of Complex	129
3-31	Results of continues variation method	130
3-32	The Physical Properties & Atomic Absorption Results of the [ [SMZ - M'-] Complexes	132
3-33	Solubility of [SMZ - M'-] Complexes in different solvents	132
3-34	Infrared spectral data (wave number $\nu$ ) $\text{cm}^{-1}$ for [SMZ –M']	133



3-35	Electronic Spectral Data of $[Al(SMZ)_3]Cl_3$ . $[Cr(SMZ)_3]Cl_3$ and $[Fe(SMZ)_3]Cl_3$ Complexes	135
<b>Chapter Four</b>		
4-1	Observation and Report of Diameter of the (IZ) around the Hole (mm) by scale	141
4-2	Types of bacteria , fungus and their report	142
4-3	The (IZ mm) data of ligands	144
4-4	The (IZ mm) data of $[M(SMZ)(L-Pro)_2]$ and $[M'(SMZ)(L-Pro)_2]$	144
4-5	The (IZ mm) data of $[M(SMZ)(L-Val)_2]$ and $[M'(SMZ)(L-Val)_2]$	145
4-6	The (IZ mm) data of $M'$ (III)and Sn(II) mono ligand complexes	145

### List of Figures

Figures		Page No.
<b>Chapter One</b>		
<b>1-1</b>	The major key areas of medical inorganic chemistry	1
<b>1-2</b>	The major key areas of metal complexes , on corrosion inhibition biological , and optical properties.	2
<b>1-3</b>	Sulfamethoxazole structure	6
<b>1-4</b>	$[Ca(SMZ)(Cl)_2].8H_2O$ , $[Zn(SMZ)(Cl)_2].2H_2O$ and $[Au(SMZ)(Cl)_2].Cl$ complexes .	7
<b>1-5</b>	Lanthanide (III)– (SMZ) complexes	9
<b>1-6</b>	Structure of (SMZ-SDZ)	9
<b>1-7</b>	Structure of $[(SMZ-SDZ)-VO]$	10
<b>1-8</b>	Structure of $[(SMZ-SDZ)-M]$ $M(II) = Cu, Ni$	10
<b>1-9</b>	Structure of $[(SMZ-SDZ)-M]$ $M = Hg(II)$	10
<b>1-10</b>	$[Ag(I) - (SFM) - (SFT)]$	11
<b>1-11</b>	(SMZ) - metal ion complexes	12
<b>1-12</b>	(SMZ) - (2-hydroxypropyl) beta-cyclodextrin	12
<b>1-13</b>	Sulfabenzamide –M complexes	14
<b>1-14</b>	The basic structure of an amino acid	15
<b>1-15</b>	Structure of the Schiff base and Mn(III) -Schiff base	19
<b>1-16</b>	Structure of Amino Acid-Schiff bases	20
<b>1-17</b>	General structure of (5-FU) - amino acids	21

<b>1-18</b>	Multiple functions of proline in plants	22
<b>1-19</b>	structure 3D-geometrical $[M(\text{Val})_2(\text{SacH})_2]$	25
<b>1-20</b>	<i>Metal binding with L-valine</i>	26
<b>1-21</b>	Four Molecular structures of Cu(II) complexes	27
<b>1-22</b>	A chiral Schiff base Zn(II)	27
<b>1-23</b>	mixed ligand complex of $[\text{Cu}(\text{L-Val})(\text{pzta})(\text{H}_2\text{O})]\text{ClO}_4$ and $[\text{Cu}(\text{L-Thr})(\text{pzta})(\text{H}_2\text{O})]\text{ClO}_4$	28
<b>1-24</b>	Structures of $[\text{Ce}(\text{1N2N})_2(\text{AA}) \cdot 2\text{H}_2\text{O}]$ (AA) = (a) (L-Val), (b) (Ser), (c) (Iso)	29
<b>1-25</b>	Structures of Cu (II) complex 1 and 2	29
<b>1-26</b>	Structure of Copper (II) - methyleneda(4-hydroxy-L-proline)	30
<b>1-27</b>	Structure of [(L-proline)-Pt(II)]	30
<b>1-28</b>	Structure of Complexes 1 and 2 and the heterocyclic bases	31
<b>1-29</b>	(a) $[\text{RuCl}_3(\text{L-Pro-H})(\text{NO})]$ – (b) $[\text{RuCl}_3(\text{D-Pro-H})(\text{NO})]$	33
<b>1-30</b>	Fe(IV)–oxo complex bearing an L-proline-derived aminopyridine	34
<b>1-31</b>	Molecular structure of studied inhibitors	34
<b>1-32</b>	Quantum chemical results of Proline in the absence and presence of NaBenz calculated by the ORCA programme: (A) optimized molecular structure, (B) HOMO; (C) LUMO (D) Mulliken charges (E) MEP.	35
<b>1-33</b>	di-/tri-organotin(IV) derivatives of mandelic acid - ,L-proline and mixed ligand complexes of 1,10 phenanthroline	36
<b>Chapter Two</b>		
<b>2-1</b>	Antibiotic sensitivity testing	41
<b>Chapter Three</b>		
<b>3-1</b>	U.V-Vis- Spectrum of the SMZ	35
<b>3-2</b>	U.V-Vis- Spectrum of the L-proH	35
<b>3-3</b>	U.V-Vis- Spectrum of the L-ValH	45
<b>3-4</b>	FT-IR spectrum of SMZ	55
<b>3-5</b>	FT- IR spectrum of L- Proline	85
<b>3-6</b>	FT-IR spectrum of L-Valine	59
<b>3-7</b>	FT-IR Spectrum of $[\text{Mn}(\text{SMZ})(\text{L-Pro})_2]$	69
<b>3-8</b>	FT-IR Spectrum of $[\text{Fe}(\text{SMZ})(\text{L-Pro})_2]$	69
<b>3-9</b>	FT-IR Spectrum of $[\text{Ni}(\text{SMZ})(\text{L-Pro})_2]$	70

<b>3-10</b>	FT-IR Spectrum of [Cu(SMZ)( L-Pro) <sub>2</sub> ]	70
<b>3-11</b>	FT-IR Spectrum of [Cd(SMZ)( L-Pro) <sub>2</sub> ]	17
<b>3-12</b>	FT-IR Spectrum of [Hg(SMZ)( L-Pro) <sub>2</sub> ]	17
<b>3-13</b>	FT-IR Spectrum of [Al (SMZ)(L-pro) <sub>2</sub> ]Cl	27
<b>3-14</b>	FT-IR Spectrum of [Cr (SMZ)(L-pro) <sub>2</sub> ]Cl	27
<b>3-15</b>	FT-IR Spectrum of [Fe (SMZ)(L-pro) <sub>2</sub> ]Cl	37
<b>3-16</b>	FT-IR Spectrum of [Sn(SMZ)( L-Pro) <sub>2</sub> ]	37
<b>3-17</b>	FT-IR Spectrum of [Sn(SMZ)( L-Pro)]Cl	47
<b>3-18</b>	Laport Selection rule	57
<b>3-19</b>	The Orgel- diagrams	57
<b>3-20</b>	Types Of Charge transfer (CT) transition	67
<b>3-21</b>	Involve Electron from Ligand based orbital	67
<b>3-22</b>	Tanabe-Sugano diagram for d5 system for Mn(II)	80
<b>3-23</b>	Electronic Spectrum of [Mn(SMZ)( L-Pro) <sub>2</sub> ]	18
<b>3-24</b>	UV/Vis Spectrum of [Fe(SMZ)( L-Pro) <sub>2</sub> ]	18
<b>3-25</b>	Electronic Spectrum of [Ni(SMZ)( L-Pro) <sub>2</sub> ]	28
<b>3-26</b>	overlapping of bands which occurs in the case of Cu(II)	38
<b>3-27</b>	UV/Vis Spectrum of [Cu(SMZ)( L-Pro) <sub>2</sub> ]	38
<b>3-28</b>	UV/Vis Spectrum of [Cd(SMZ)( L-Pro) <sub>2</sub> ]	48
<b>3-29</b>	UV/Vis Spectrum of [Hg(SMZ)( L-Pro) <sub>2</sub> ]	58
<b>3-30</b>	UV/Vis Spectrum of [Al (SMZ)(L-pro) <sub>2</sub> ]Cl	58
<b>3-31</b>	UV/Vis Spectrum of [Cr (SMZ)(L-pro) <sub>2</sub> ]Cl	68
<b>3-32</b>	UV/Vis Spectrum of [Fe (SMZ)(L-pro) <sub>2</sub> ]Cl	78
<b>3-33</b>	UV/Vis Spectrum of [Sn (SMZ)(L-pro) <sub>2</sub> ]	78
<b>3-34</b>	UV/Vis Spectrum of [Sn(SMZ)( L-Pro)] Cl	88
<b>3-35</b>	3D Molecular Modeling Proposed [M(SMZ)(L-pro) <sub>2</sub> ]	89
<b>3-36</b>	3D Molecular Modeling Proposed [M'(SMZ)(L-pro) <sub>2</sub> ]	89
<b>3-37</b>	3D Molecular Modeling Proposed [Sn(SMZ)(L-pro)]Cl	90
<b>3-38</b>	FT-IR Spectrum of [Mn(SMZ) (L-Val) <sub>2</sub> ]	79
<b>3-39</b>	FT-IR Spectrum of [Co(SMZ) (L-Val) <sub>2</sub> ]	79
<b>3-40</b>	FT-IR Spectrum of [Ni(SMZ) (L-Val) <sub>2</sub> ]	89
<b>3-41</b>	FT-IR Spectrum of [Cu(SMZ) (L-Val) <sub>2</sub> ]	89
<b>3-42</b>	FT-IR Spectrum of [Cd(SMZ) (L-Val) <sub>2</sub> ]	99
<b>3-43</b>	FT-IR Spectrum of [Hg(SMZ) (L-Val) <sub>2</sub> ]	99
<b>3-44</b>	FT-IR Spectrum of [Al (SMZ) (L-Val) <sub>2</sub> ]Cl	100
<b>3-45</b>	FT-IR Spectrum of [Cr (SMZ) (L-Val) <sub>2</sub> ]Cl	100
<b>3-46</b>	FT-IR Spectrum of [Fe (SMZ) (L-Val) <sub>2</sub> ]Cl	101
<b>3-47</b>	FT-IR Spectrum of [Sn(SMZ) (L-Val) <sub>2</sub> ]	101
<b>3-48</b>	UV/Vis Spectrum of [Mn(SMZ)(L- Val) <sub>2</sub> ]	410
<b>3-49</b>	Electronic transition for d7 system for Co(II)	510
<b>3-50</b>	Electronic Spectrum of [Co(SMZ)( L-Val) <sub>2</sub> ]	610
<b>3-51</b>	Tanabe-Sugano diagram for d7 system	610

<b>3-52</b>	Electronic Spectrum of [Ni (SMZ)( L-Val) <sub>2</sub> ]	810
<b>3-53</b>	Tanabe-Sugano diagram for d <sup>7</sup> system	810
<b>3-54</b>	Electronic Spectrum of [Cu (SMZ)( L-Val) <sub>2</sub> ]	910
<b>3-55</b>	Electronic Spectrum of [Cd (SMZ)( L-Val) <sub>2</sub> ]	110
<b>3-56</b>	Electronic Spectrum of [Hg (SMZ)( L-Val) <sub>2</sub> ]	111
<b>3-57</b>	Electronic Spectrum of [Sn (SMZ)( L-Val) <sub>2</sub> ]	112
<b>3-58</b>	Electronic Spectrum of [Al(SMZ)( L-Val) <sub>2</sub> ]Cl	113
<b>3-59</b>	Electronic Spectrum of [Cr(SMZ)( L-Val) <sub>2</sub> ]Cl	114
<b>3-60</b>	Electronic Spectrum of [Fe (SMZ)( L-Val) <sub>2</sub> ]Cl	115
<b>3-61</b>	3D Molecular Modeling Proposed Complexes [M(SMZ)(L-Val) <sub>2</sub> ]. [Sn(II),Mn(II), Co(II), Ni(II), Cu(II), Zn(II), Cd(II) and Hg(II)]	116
<b>3-62</b>	3D Molecular Modeling Proposed [M' (SMZ)(L-Val) <sub>2</sub> ] Cl [Al(III), Cr (III), and Fe(III)]	116
<b>3-63</b>	FT-IR Spectrum of [Sn(L-Val) <sub>2</sub> ]	120
<b>3-64</b>	FT-IR Spectrum of [Sn(L-pro) <sub>2</sub> ]	120
<b>3-65</b>	Electronic Spectrum of [Sn (L-Val) <sub>2</sub> ]	122
<b>3-66</b>	Electronic Spectrum of [Sn ( L-Pro) <sub>2</sub> ]	123
<b>3-67</b>	The geometry structure , 3D of [Sn(L-Val) <sub>2</sub> ] (3S,8S)-3,8-diisopropyl-1,6-dioxa-4,9-diaza-5-stannaspiro[4.4]nonane-2,7-dione	124
<b>3-68</b>	The geometry structure , 3D of [Sn(L-Pro) <sub>2</sub> ] (3aS,3a'S)-octahydro-3H,3'H-1,1'-spirobi[pyrrolo[1,2-c][1,3,2]oxazastannole]-3,3'-dione	124
<b>3-69</b>	FT-IR Spectrum of [Sn(SMZ) <sub>2</sub> ]Cl <sub>2</sub>	127
<b>3-70</b>	UV -Vis spectrum of the [Sn(SMZ) <sub>2</sub> ]Cl <sub>2</sub>	128
<b>3-71</b>	Mole ratio (M:2L) by continues variation method	129
<b>3-72</b>	Probable 3-D structure of the [Sn(SMZ) <sub>2</sub> ]Cl <sub>2</sub>	131
<b>3-73</b>	FT-IR Spectrum of [Al(SMZ) <sub>3</sub> ]Cl <sub>3</sub>	134
<b>3-74</b>	FT-IR Spectrum of [Cr (SMZ) <sub>3</sub> ]Cl <sub>3</sub>	134
<b>3-75</b>	FT-IR Spectrum of Fe (SMZ) <sub>3</sub> ]Cl <sub>3</sub>	135
<b>3-76</b>	Electronic Spectrum of [Al(SMZ) <sub>3</sub> ]Cl <sub>3</sub>	136
<b>3-77</b>	Electronic Spectrum of [Cr (SMZ) <sub>3</sub> ]Cl <sub>3</sub>	137
<b>3-78</b>	Electronic Spectrum of [Fe (SMZ) <sub>3</sub> ]Cl <sub>3</sub>	137
<b>3-79</b>	3D Molecular Modeling Proposed [M' (SMX) <sub>3</sub> ]Cl <sub>3</sub> [M' Al(III), Cr(III), and Fe(III)]	138
<b>Chapter Four</b>		
<b>4-1</b>	The mechanisms of action of antimicrobial drugs	81
<b>4-2</b>	applications of antimicrobial drugs	81
<b>4-3</b>	Aerobic And anaerobes organisms	82

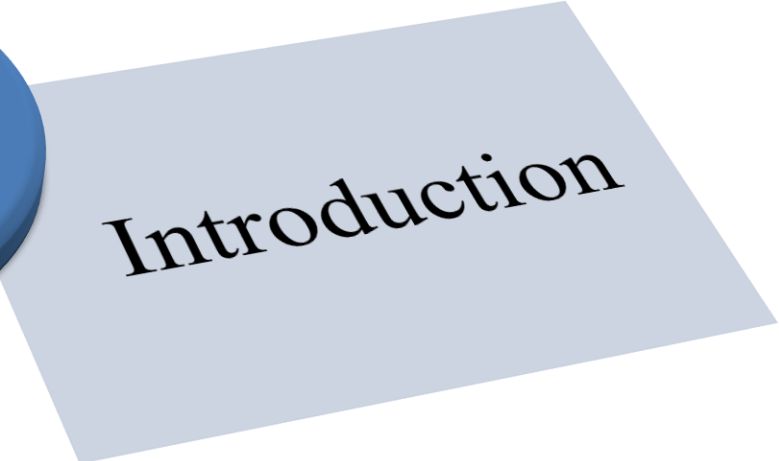
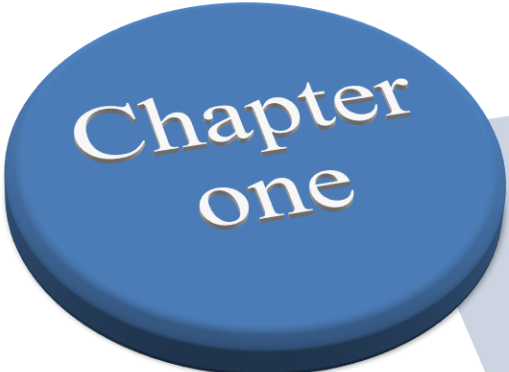
<b>4-4</b>	(a) <i>S. aureus</i> cells and (b) skin infection by <i>S. aureus</i>	82
<b>4-5</b>	<i>Candida albicans</i>	83
<b>4-6</b>	Photograph of Antimicrobial Activity of complexes	84

## List of Schemes

<b>Schemes</b>		<b>Page No.</b>
<b>Chapter One</b>		
1-1	Synthesis 1-4. metal of azo-dye- sulfonamide complexes; n= number of crystalline H <sub>2</sub> O.	13
1-2	synthesis of nickel (II) and copper (II) complexes of L-valine from benzyl	24
<b>Chapter Two</b>		
1-2	synthesis of nickel (II) and copper (II) complexes of L-valine from benzyl	24
2-1	preparation of potassium L-prolinate	42
2-2	preparation of [M(SMZ)(L-Pro) <sub>2</sub> ] and [M'(SMZ)(L-pro) <sub>2</sub> ] Cl	44
2-3	Preparation of Potassium L- Valinate	44
2-4	Preparation of [M(SMZ)(L-Val) <sub>2</sub> ] and [M'(SMZ)(L-Val) <sub>2</sub> ] Cl	45
2-5	Preparation of [ Sn(SMZ)( L-Pro)]Cl	46
2-6	Preparation of [Sn(L-Pro) <sub>2</sub> ]	47
2-7	Preparation of [Sn(L-Val) <sub>2</sub> ]	48
2-8	Preparation of [Sn(SMZ) <sub>2</sub> ]Cl <sub>2</sub>	49
<b>Chapter Three</b>		
3-1	Zwitter ion of L-proline	57
3-2	Zwitter ion of L-Valine	59

## List of Abbreviations

Symbol	Full name
M.p	Melting point
DMF	N,N-Dimethyl Formamide
CT	change transfer
FTIR	Fourier Transform Infra Red
$^1\text{H}$ NMR	Proton Nuclear Magnetic Resonance
No.	Number
$T_m$	Melting temperature
M.Wt	Molecular weight
I Z	Inhibition Zone
A.A	Atomic Absorption
SMZ	Sulfamethoxazole
L-ValH	Ligand Valine
L-ProH	Ligand Proline
DMSO	Dimethylsulfoxide
TGA	Thermal gravimetric analysis
CVM	Continuous variations method
INCT	Intra ligand change transfer



## Introduction and Literatures Review

### 1. General Introduction

The field of bioinorganic chemistry, explores the roles that metals play in biology. A large number of compounds are important and using various bioanalytical and spectroscopic techniques. They synthesize metal enzymes, catalysts and materials structures chemistry, and study their mechanism of action. <sup>[1]</sup>

#### 1.1. Antibiotics Drugs and elemental medicine:

Elemental medicine " Medical inorganic - chemistry " is an important major key area of chemistry for many researches <sup>[1-5]</sup> who are interested in coordination field between metal ions and antibiotics. Many diseases which are currently intractable

Figures (1-1) and (1-2) <sup>[5]</sup>

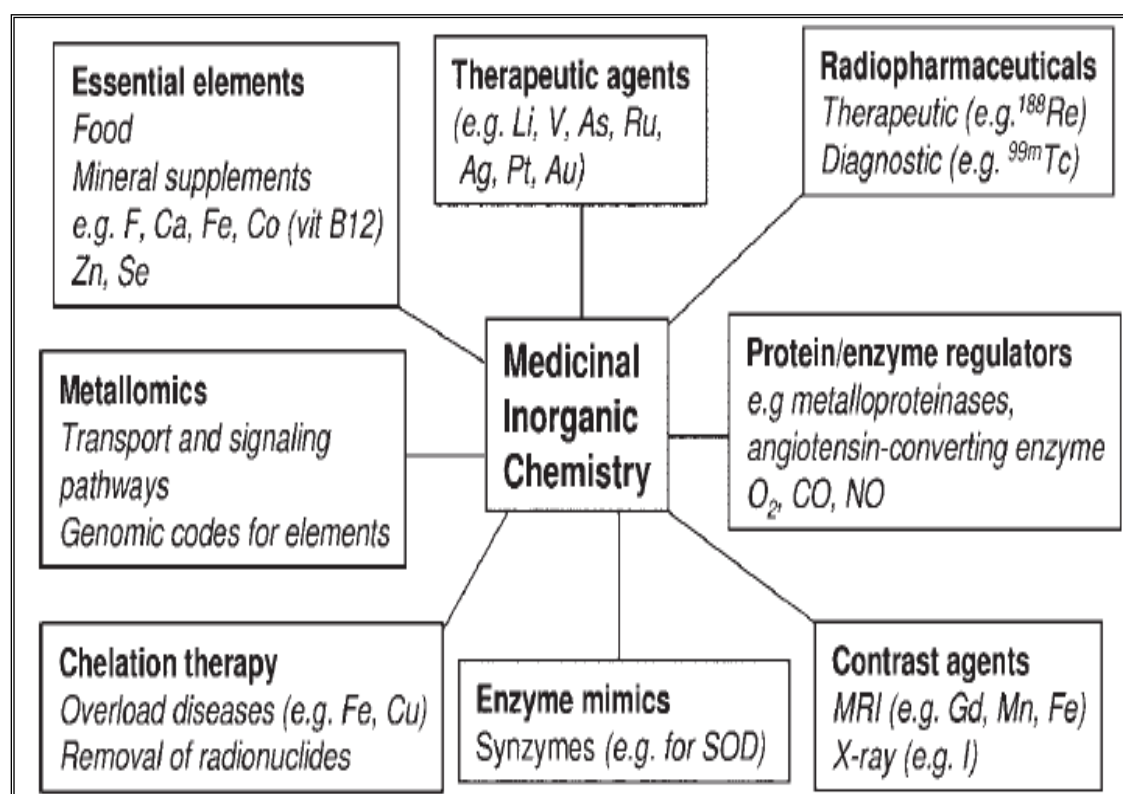


Figure (1-1): The major key areas of medical inorganic chemistry. <sup>[1]</sup>



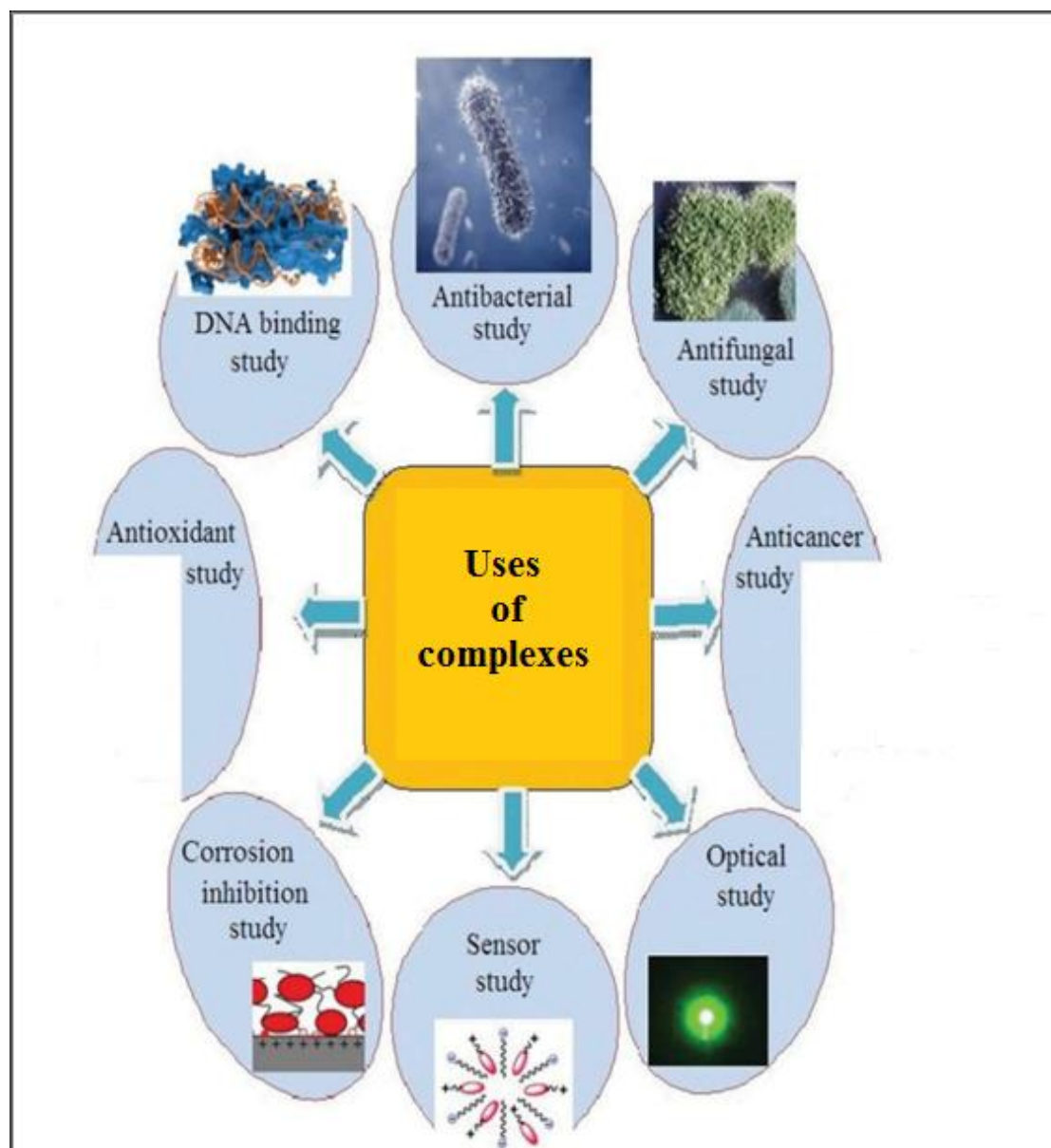
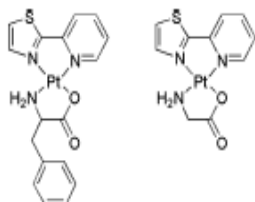
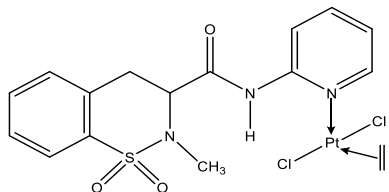
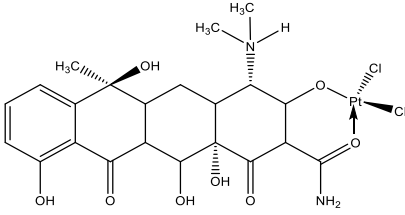
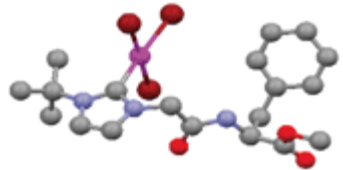
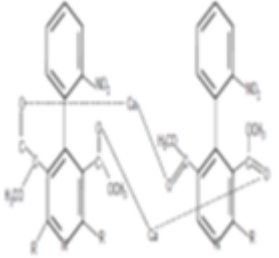


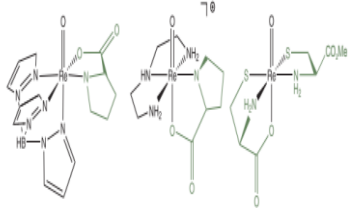
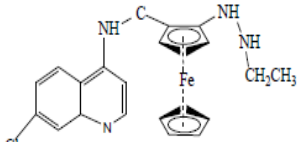
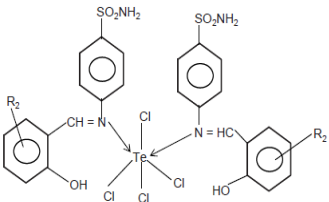
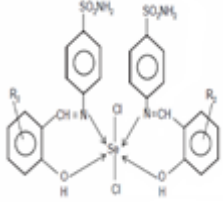
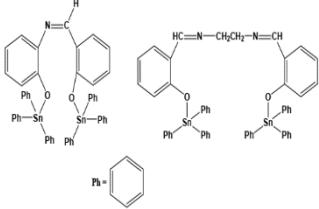
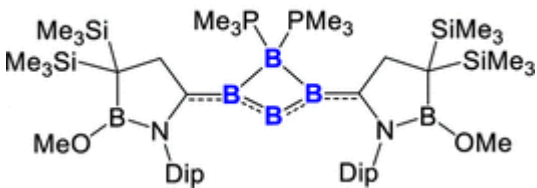
Figure (1-2): The major key areas of metal complexes , on corrosion inhibition biological and optical properties.

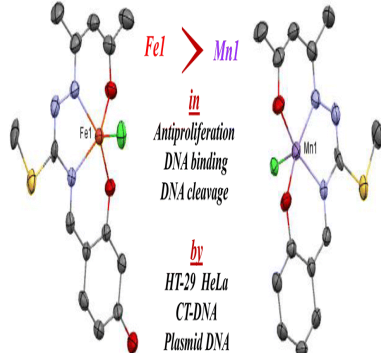
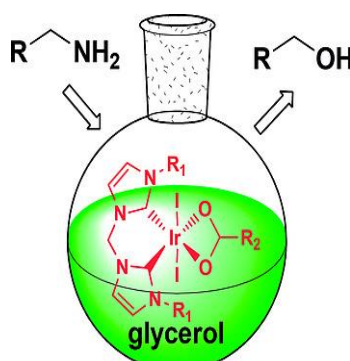
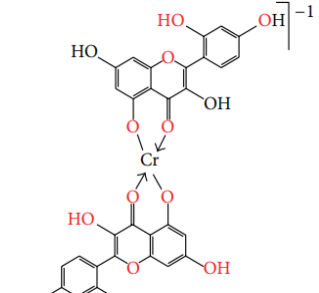
The term "antibiotic" originally referred to natural compounds produced by a fungus or other microorganisms that kill disease causing by bacteria. Introducing metal ions into a biological system may be carried out for diagnostic purposes or therapeutic [2-3]. Increasing knowledge of metal biochemistry will provide the design of new drugs both inorganic and organic in many other areas too. [4-6].

Many organic drugs require interaction with metals as complexes for activity, as shown in Table (1-1).

Table (1-1): Some medical uses of complexes

Element	Compounds	Uses	references
Pt <sup>II</sup>	 <p>Pt<sup>II</sup>-amino acid complexes</p>	high binding affinities toward human serum albumin in buffer solutions.	[7]
Pt <sup>II</sup>	 <p>Platinum (II)-Piroxicam</p>	Anti-inflammatory agents	[8]
Pt <sup>II</sup>	 <p>tetracycline Pt(II) complex</p>	Antibacterial agents	[9]
Au (I) and Au (III)	 <p>NHC gold amino acid</p>	anti-cancer drug	[10]
Ca <sup>II</sup>		Anti-Hypertensive Drug	[11]

Re (V)	 <p>[ReO(tpb)(L-pro)]</p>	Pharmacology	[12]
Fe II	 <p>ferroquine</p>	Malaria Parasite.	[13]
Te (IV)	 <p>Tellurium (IV) sulphonamide Schiff base complex</p>	Antibiotics	[14]
Se (IV)	 <p>Selenium (IV) Sulphonamide Schiff base complex</p>	antibiotics	[14]
Sn (IV)	 <p>Sn(IV) Schiff bases</p>	fungicidal activity	[15]
Tetraatomic Boron(0)		Crystalline Research	[16]

Fe (III) and Mn (III)	 <p>iron(III)– and manganese(III)– thiosemicarbazone</p>	<p>vitro anti-proliferative activity on human cancer cells, DNA binding and cleavage studies</p>	[17]
Ir (III)	 <p>glycerol</p>	<p>Ir(bis-NHC)-Catalyzed Direct Conversion of Amines to Alcohols</p>	[18]
Cr (III)	 <p>Cr(III)-Morin Complex</p>	<p>Antioxidant</p>	[19]

## 1.2. Sulfamethoxazole and its complexes

Sulfamethoxazole, Sulfa-drug (abbreviated SMZ or SMX) molecular formula:  $C_{10}H_{11}N_3O_3S$  is a sulfonamide bacteriostatic antibiotic. Figure (1-3) <sup>[20]</sup> trade names ; ( Bactrim, Septrin , or Septra ). Systematic (IUPAC) name:4-aminoN(5methylisoxazol3yl) benzene sulfonamide combination with trimethoprim (TMA) in a 5:1 ratio in co-trimoxazole, trade names such as Bactrim, Septrin or Septra. Other names include sulfadimerazine , sulfadimezine and sulphadimethyl-pyrimidine. is an off-

white and crystalline powder. Sulfamethoxazole Figure (1-3) is commonly used to treat urinary tract infections and it affects primarily patients with HIV choice for *Pneumocystis pneumonia*.<sup>[21]</sup> Larson et al (2005). were reported Sulfamethoxazole is in the class of Sulfonamides, with para amino benzoic acid which are used as antibacterial agent interfere in the biosynthesis of tetrahydrofolic acid,<sup>[22]</sup>. In literature survey, many authors have reported the antimicrobial activity of Sulfamethoxazole and their metal complexes Bellú et al (2005)<sup>[23]</sup>. Ma et al (2007); and Monti et al (2010)<sup>[24]</sup>.

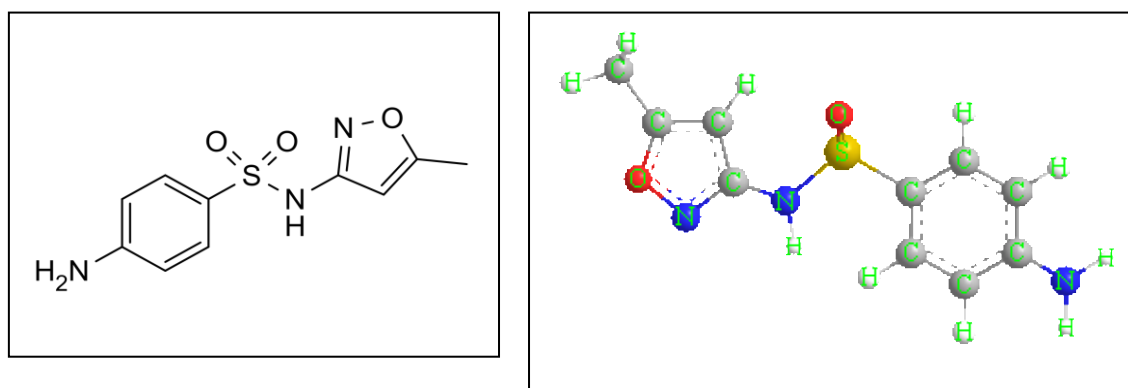


Figure (1-3): Sulfamethoxazole structure

The metal sulfamethoxazole complexes have a great pharmacological and physiological rather than their free drugs itself<sup>[25-26]</sup>. Complexes of Co (II) and Cd (II) - sulfamethoxazole (SMZ) have been prepared for the first time and their Infra-red spectra were investigated. The SMZ wave numbers observed in the Infra-red of the metal complexes were compared with those of free SMZ indicated the vibrations due to the sulfonamide and amino groups are shifted with respect to the free molecule in line with their coordination to the metal. In the Cd (II) complex, the active binding sites of (SMZ) are the sulfonamide nitrogen (N) and sulfonic oxygen(O); in cobalt compound, the metal atom coordinates through the sulfonamide and amino nitrogen<sup>[27]</sup>. The coordination site of (SMZ) chelating via

M(II) = Cu (II), Ni (II), Mn (II), Zn (II), Ln(III)) = Y(III) , La(III), Nd(III) , and Gd(III) metal ions have been investigated by Yasmin et al (2017), [28] and formulated for all these complexes as:  $[M (SMZ)_2Cl_2].2H_2O$  and  $[Ln (SMZ)_2Cl_3].3H_2O$

Fatima and AL-khodir (2015) [29] have been reported synthesis, anticancer evaluation and spectroscopic studies Ca(II), Zn(II) and Au(III) sulfamethoxazole complexes are formulated as shown  $[Ca(SMZ)(Cl)_2].8H_2O$  ,  $[Zn(SMZ)(Cl)_2].2H_2O$  and  $[Au(SMZ)(Cl)_2]Cl$  .The (SMZ)-complexes were discussed with the conductance and spectroscopic study. indicated the vibrations due to the sulfonamido (–NH and SO<sub>2</sub>) and isoxazole (C=N) groups are shifted with respect to the free molecule compared with their coordination to the metal.

Ca (II) and Zn(II) complexes , the coordination site of (SMZ) are the sulfonyl oxygen and SO<sub>2</sub> -NH sulfonamide- N, but in  $[Au(SMZ)(Cl)_2]Cl$  complex, the Au(III) coordinates through the sulfonyl - O and isoxazole – N ,as shown in Figure (1-4).

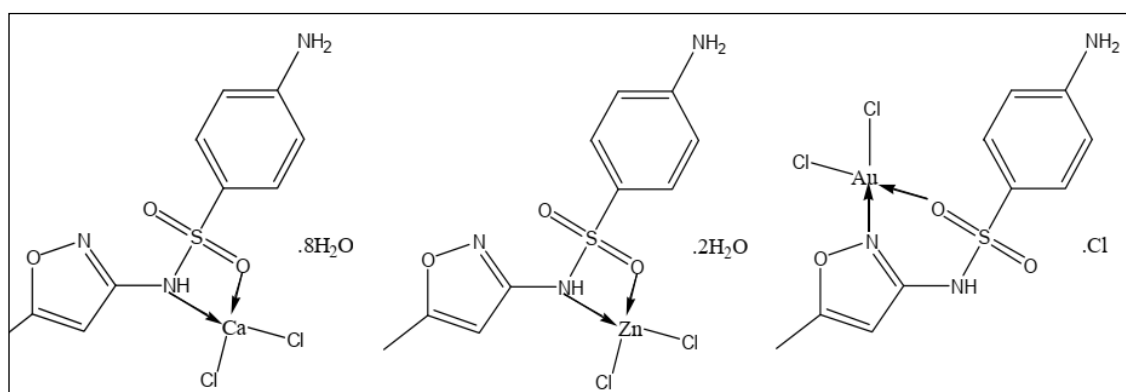


Figure (1-4):  $[Ca(SMZ)(Cl)_2].8H_2O$ ,  $[Zn(SMZ)(Cl)_2].2H_2O$  and  $[Au(SMZ)(Cl)_2]Cl$  complexes .

Mixed [Sulfamethoxazole – Cloxacillin ] complexes were synthesized by Bamigboye et al., (2012).<sup>[30]</sup> The complexes were characterized using solubility, Thin layer - chromatography, M.p, Conductivity measurement, and FT-IR spectroscopy. Both Sulfamethoxazole (SMZ) and Cloxacillin (Clox) acts as bidentate ligands. Evaluation of biological activities of the complexes against the tested;(*Escherichia coli*, *Pseudomonas aureginosa* and *klebsiella pneumonia*), revealed that the complexes were found to be more active against the organisms than SMZ and Clox ligands. Karthikeyan *et al.*, (2006) <sup>[31]</sup> reported the synthesis and evaluation of non -electrolytic lanthanide(III) complexes ,  $[M(SMZ)_2Cl_3].2H_2O$ , Figure (1-5) where M is Ln(III) = [ La, pr, Nd, Sm, Gd, Y and Dy ] containing (SMZ) ligand. Figure (1-6) The structures and site bonding of the ligand are studied by C.H.N , magnetic susceptibility, FT-IR,<sup>1</sup>HNMR, X-ray and UV, VIS spectra studies of the complexes . The stereochemistry around the Ln(III) is (a mono capped trigonal prism ) in which 4 of the coordination sites are occupied by two each from two chelating ligands, sulfonyl oxygen (O) and nitrogen (N) of the amide group and the remaining three positions are occupied by 3 (Cl atoms). The ligand and the complexes were tested in vitro to evaluate their activity against the *Escherichia coli*. and *Staphylococcus aureus*.

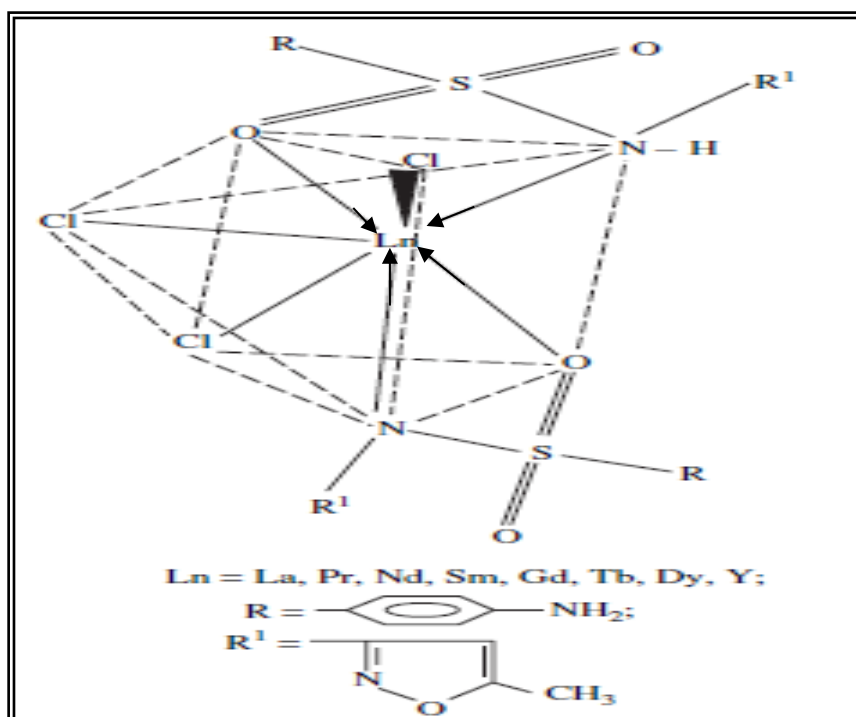


Figure (1-5): Lanthanide (III)– (SMZ) complexes

Sulfamethoxazole (SMZ) and sulfadiazine (SDZ) have exhibited activity against *Mycobacterium tuberculosis* <sup>[32]</sup> and atypical mycobacteria (NTM) as nontuberculous <sup>[33]</sup>

Shrikant et al 2013 -2014 <sup>[34-35]</sup> have reported synthesis complexes of Schiff bases of [sulfamethoxazole – salicylaldehyde] (SMZ– SDZ) Figure (1-6) and VO(II) , Ni(II) Cu(II), Hg(II) complexes, Figure (1-7) To (1-9).

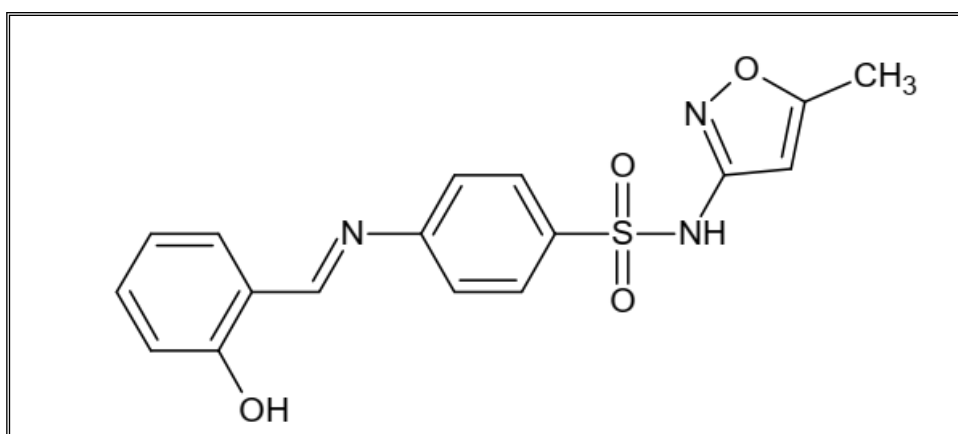


Figure (1-6) : Structure of (SMZ-SDZ)



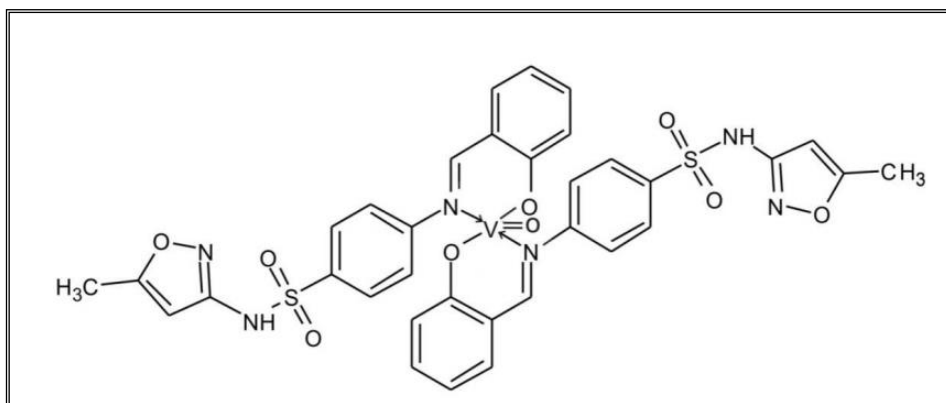


Figure (1-7) : Structure of [ (SMZ-SDZ)-VO ]

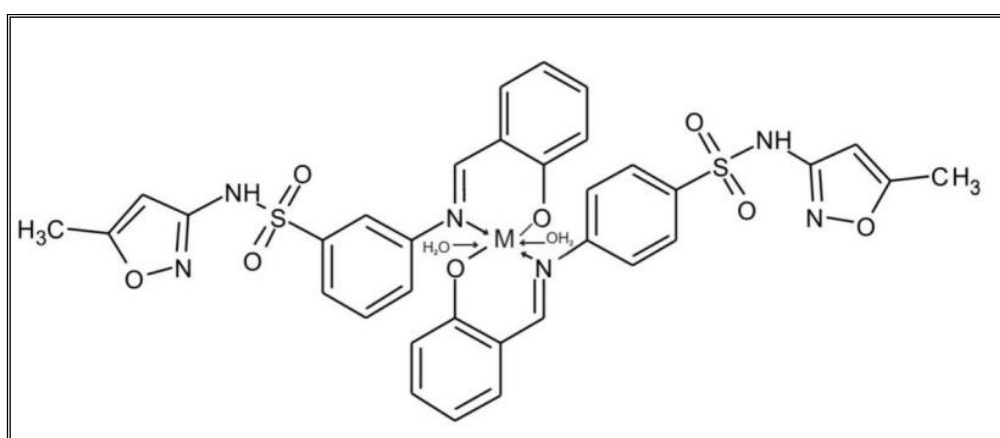


Figure (1-8) : Structure of [ (SMZ-SDZ)-M ] M(II) = Cu, Ni

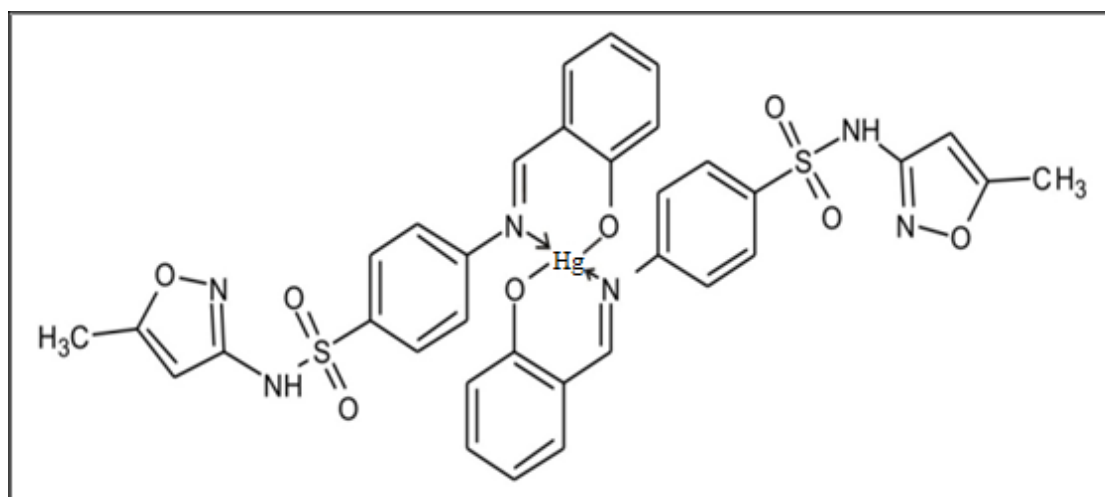


Figure (1-9) : Structure of [ (SMZ-SDZ)-Hg ]

Julia et al (2015) <sup>[36]</sup> have been reported synthesis Ag (I) - Sulfonamides (SFM ) sulfathiazole (SFT) complexes : C.H.N indicate a 1:1 ligand / metal composition for  $[AgC_9H_8N_3O_2S_2, Ag-SFT]$  and  $[AgC_{10}H_{10}N_3O_3S, Ag-SFM]$  complexes . <sup>1</sup>H,NMR and FT-IR evidence the coordination of (SFM ) and (SFT) to Ag (I) through the N atom of the sulfonamide group, Figure (1-10) and also indicate the participation of the 5-membered N-heterocyclic ring in the coordination.

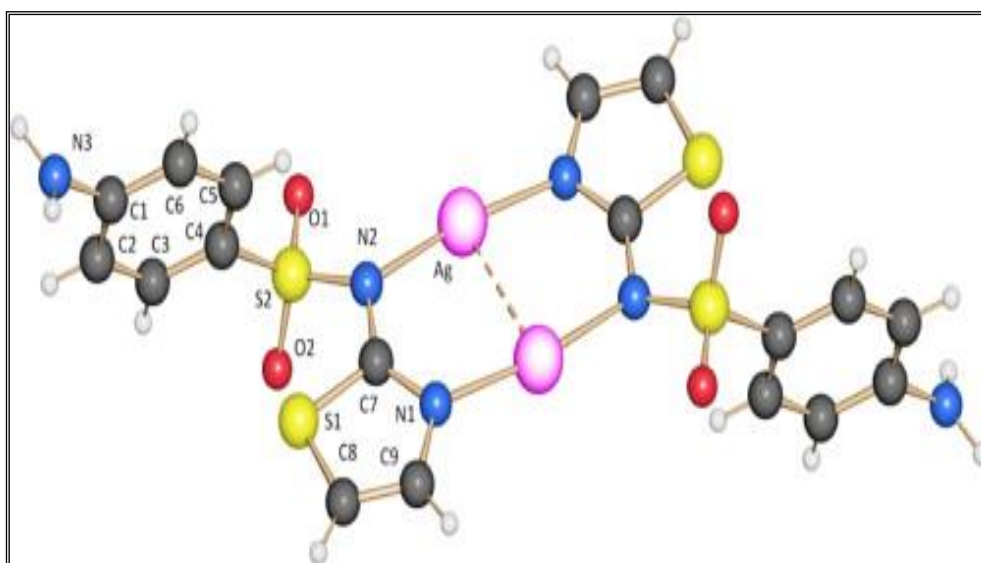


Figure (1-10) : [ Ag (I) - (SFM ) -(SFT) ]

Naggar et al ( 2016) have been reported synthesis complexes of binary and ternary complexes of (SMZ) and glycine (Gly) with metal ions; Fe(III), Al(III), La (III), pb (II), Co(II), Sr(II), Cr(III), Th(IV), Sn(II) and Zr (IV). The stoichiometry's of all complexes were determined conductometrically and indicated that the formation of 1: 3 ,1: 2 and/or 1: 1, (M:L) (metal M: ligand) complexes . Also, the species distribution diagrams of (SMZ) and its metal ion complexes Figure (1-11) were reported. <sup>[37]</sup>

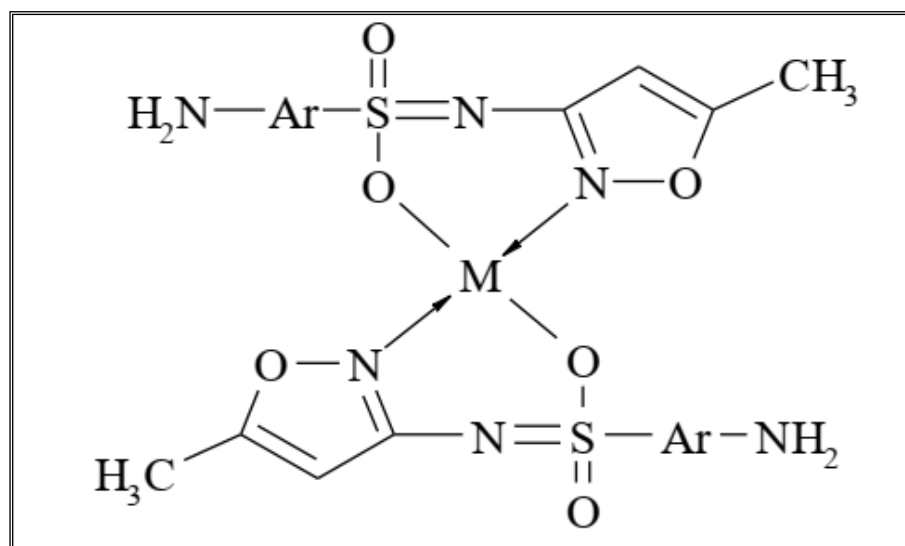


Figure (1-11) : (SMZ) - metal ion complexes .

Varghese, et al 2018 <sup>[38]</sup> have reported synthesis complexes of (SMZ) with (2-hydroxypropyl) beta-cyclodextrin, Figure (1-12) and beta-cyclodextrin in solid state and characterized by X-ray diffraction, (Raman and FT-IR ) techniques. The association constants ( $K_a$ ) and stoichiometry's of all complexes have been determined by the fluorescence data .The results showed that complexes of (SMZ) with both beta-cyclodextrin are stabilized in aqueous media by strong hydrogen bonding interactions.

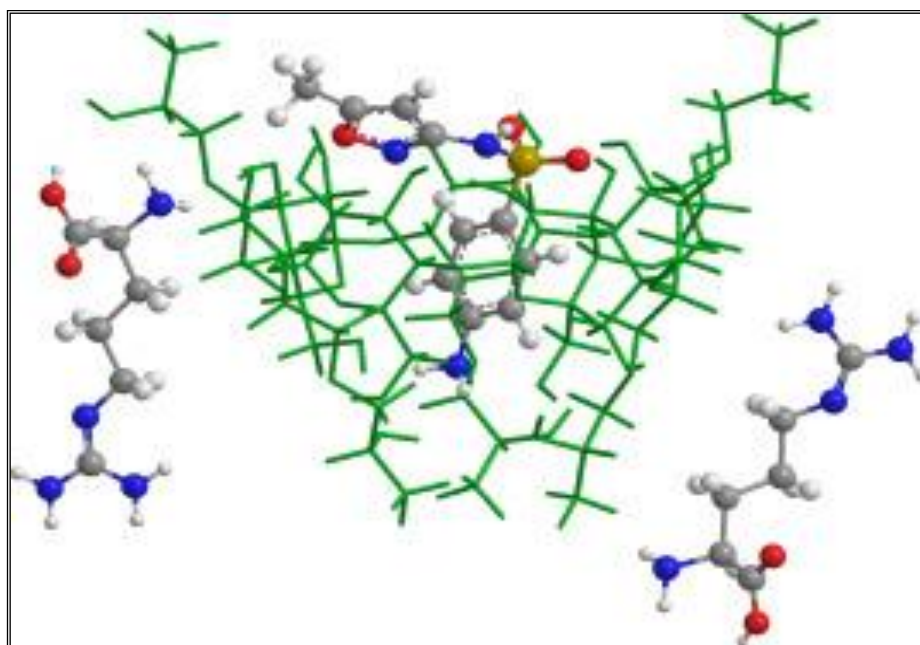
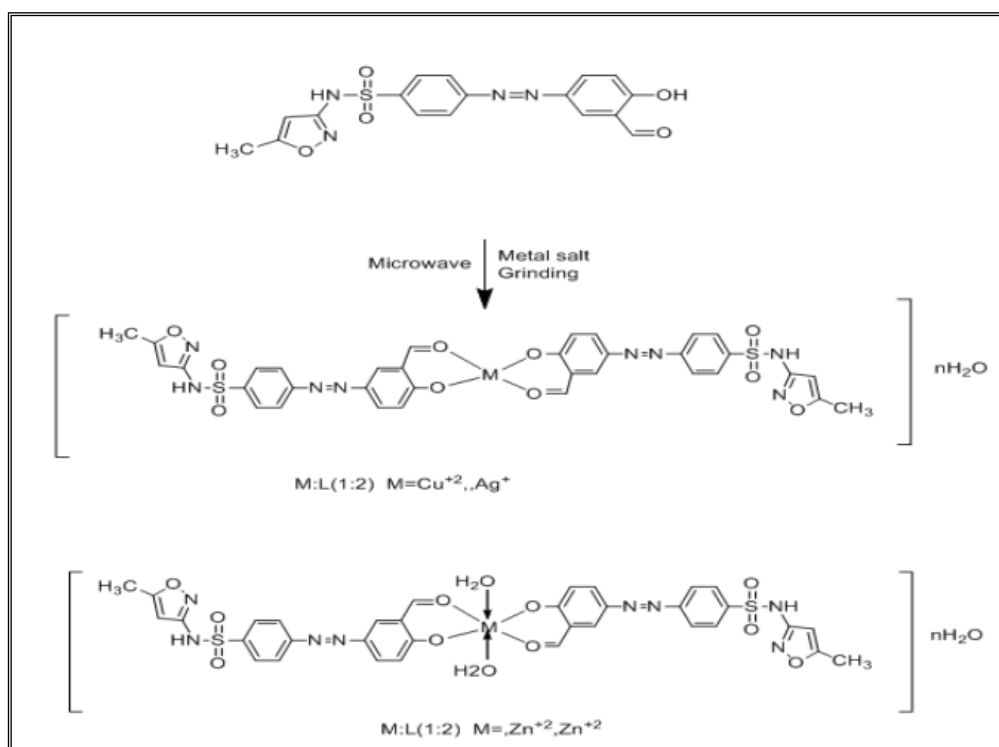


Figure (1-12) : (SMZ) - (2-hydroxypropyl) beta-cyclodextrin

Hany et al 2018 <sup>[39]</sup> have been reported microwave method synthesis 1-4, metals of azo-dye- sulfonamide complexes of Cu(II), derived from sulfamethoxazole Scheme (1-1), results observed that the reaction completed in a high yield with short time .



Scheme (1-1): Synthesis 1-4. metal of azo-dye- sulfonamide complexes n= number of crystalline H<sub>2</sub>O

Rostamizadeh et al 2019 <sup>[40]</sup> have reported Synthesis of Sulfabenzamide (SBZ) and (SMZ) as ligands with Zn(II). Spectroscopic methods <sup>1</sup>H NMR, UV-Vis, FT-IR spectroscopy and XRD confirmed the coordination of (SBZ) and (SMZ) ligands to metals through the (O and N) atoms of the sulfonamide group. Both (SBZ) and (SMZ) metal complexes were active against Gram-positive(+) and negative(-) bacterial strains.

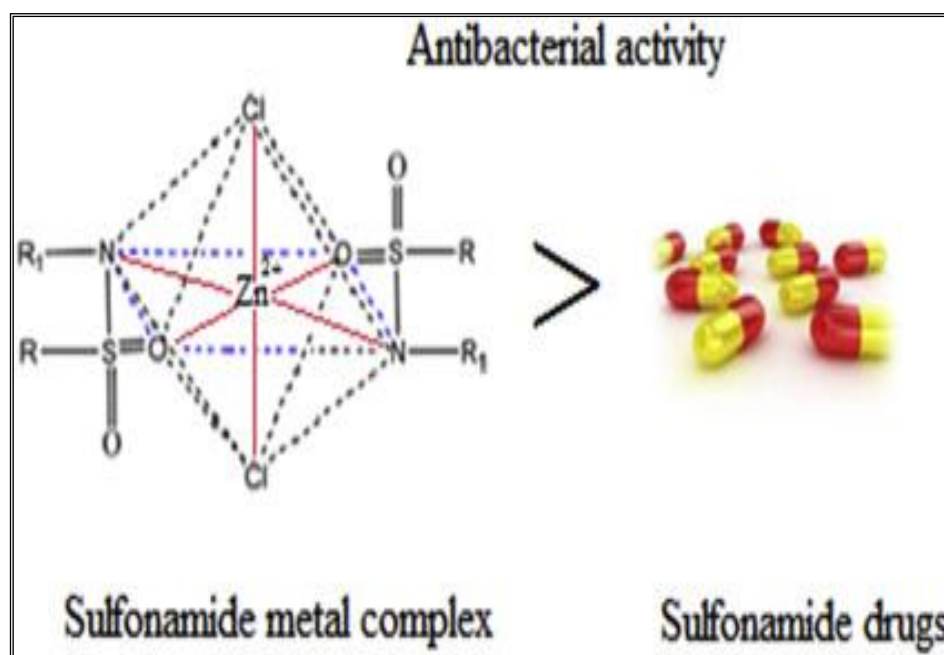


Figure (1-13) : Sulfabenzamide –Zn complexes

### 1.3. Amino acids

#### 1.3.1. Structure, classification and biochemical role

Only 20 amino acids Figure (1-14) generic formula:  $H_2NCHR\text{COOH}$  are found in the human peptides and proteins. These naturally occurring amino acids are used by cells to synthesize peptides and proteins. [41]. Amino acids are biochemical low molecular weight compounds as ligands with mixed operation as containing a carboxyl functional group ( $-\text{COOH}$ ) and amine functional group ( $-\text{NH}_2$ ), both grafted to the same carbon atom in  $\alpha$  position [41] are important in humans and other bio systems [42].

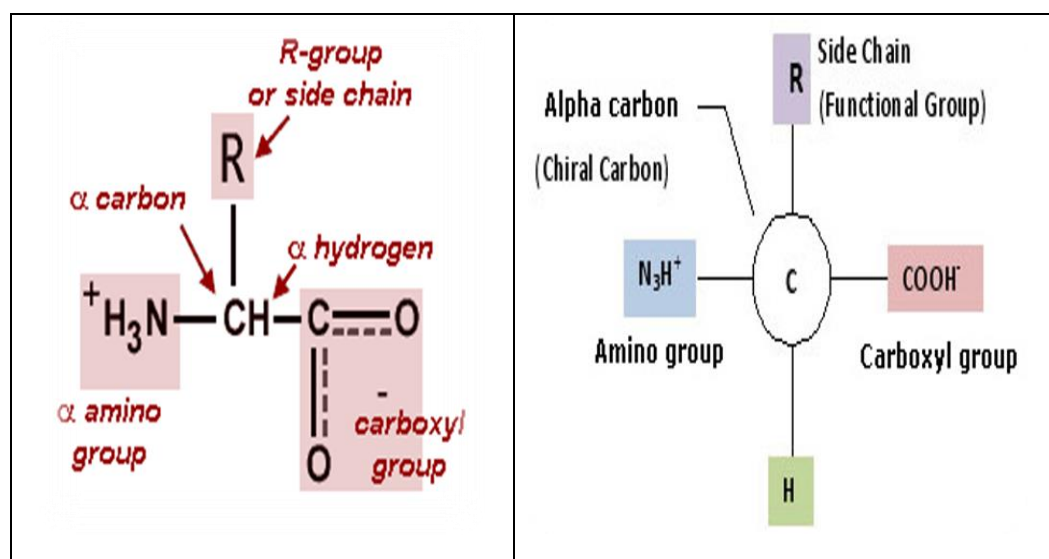


Figure (1-14): The basic structure of an amino acid

Depending on the structural Tables (1-2) to (1-4) features of side chain (R) amino acids (AA) are classified as follows: <sup>[42]</sup> .

1. Aliphatic amino acids include:

(Gly), (Ala), (Val), (Leu) and (Ile) .

2. Amino acids containing (OH), group or ( s) atom:

(Ser), (Thr), (Cys), and (Met).

3. Aromatic amino acids include:

(Phe), (Tyr) and (Trp)

4. Basic Amino acids:

(Lys), (Arg) and (His)

5. Acidic Amino acids:

(Asp), and (Glu).

6. Neutral Amino acids  $\Rightarrow$  (Asn), and (Gln).

7. Aliphatic cyclic side chain  $\Rightarrow$  (Pro).

Table (1-2) : Structural of Amino acids

$\begin{array}{c} \text{H} \\   \\ \text{H}_3\text{N}^+ - \alpha\text{C} - \text{C} \begin{array}{l} \diagup \text{O} \\ \diagdown \text{O}^- \end{array} \\   \\ (\text{CH}_2)_3 \\   \\ \text{NH} \\   \\ \text{C}=\text{NH}_2 \\   \\ \text{NH}_2 \end{array}$ <p>Arginine (Arg / R)</p>	$\begin{array}{c} \text{H} \\   \\ \text{H}_3\text{N}^+ - \alpha\text{C} - \text{C} \begin{array}{l} \diagup \text{O} \\ \diagdown \text{O}^- \end{array} \\   \\ \text{CH}_2 \\   \\ \text{CH}_2 \\   \\ \text{C}=\text{O} \\   \\ \text{NH}_2 \end{array}$ <p>Glutamine (Gln / Q)</p>	$\begin{array}{c} \text{H} \\   \\ \text{H}_3\text{N}^+ - \alpha\text{C} - \text{C} \begin{array}{l} \diagup \text{O} \\ \diagdown \text{O}^- \end{array} \\   \\ \text{CH}_2 \\   \\ \text{C}_6\text{H}_5 \end{array}$ <p>Phenylalanine (Phe / F)</p>	$\begin{array}{c} \text{H} \\   \\ \text{H}_3\text{N}^+ - \alpha\text{C} - \text{C} \begin{array}{l} \diagup \text{O} \\ \diagdown \text{O}^- \end{array} \\   \\ \text{CH}_2 \\   \\ \text{C}_6\text{H}_4 \\   \\ \text{OH} \end{array}$ <p>Tyrosine (Tyr / Y)</p>	$\begin{array}{c} \text{H} \\   \\ \text{H}_3\text{N}^+ - \alpha\text{C} - \text{C} \begin{array}{l} \diagup \text{O} \\ \diagdown \text{O}^- \end{array} \\   \\ \text{CH}_2 \\   \\ \text{C}_8\text{H}_6\text{N}_2 \end{array}$ <p>Tryptophan (Trp, W)</p>
$\begin{array}{c} \text{H} \\   \\ \text{H}_3\text{N}^+ - \alpha\text{C} - \text{C} \begin{array}{l} \diagup \text{O} \\ \diagdown \text{O}^- \end{array} \\   \\ (\text{CH}_2)_4 \\   \\ \text{NH}_2 \end{array}$ <p>Lysine (Lys / K)</p>	$\begin{array}{c} \text{H} \\   \\ \text{H}_3\text{N}^+ - \alpha\text{C} - \text{C} \begin{array}{l} \diagup \text{O} \\ \diagdown \text{O}^- \end{array} \\   \\ \text{H} \end{array}$ <p>Glycine (Gly / G)</p>	$\begin{array}{c} \text{H} \\   \\ \text{H}_3\text{N}^+ - \alpha\text{C} - \text{C} \begin{array}{l} \diagup \text{O} \\ \diagdown \text{O}^- \end{array} \\   \\ \text{CH}_3 \end{array}$ <p>Alanine (Ala / A)</p>	$\begin{array}{c} \text{H} \\   \\ \text{H}_3\text{N}^+ - \alpha\text{C} - \text{C} \begin{array}{l} \diagup \text{O} \\ \diagdown \text{O}^- \end{array} \\   \\ \text{CH}_2 \\   \\ \text{C}_4\text{H}_3\text{N}_2 \end{array}$ <p>Histidine (His / H)</p>	$\begin{array}{c} \text{H} \\   \\ \text{H}_3\text{N}^+ - \alpha\text{C} - \text{C} \begin{array}{l} \diagup \text{O} \\ \diagdown \text{O}^- \end{array} \\   \\ \text{CH}_2 \\   \\ \text{OH} \end{array}$ <p>Serine (Ser / S)</p>
$\begin{array}{c} \text{H}_2 \\   \\ \text{C} \\ / \quad \backslash \\ \text{H}_2\text{C} \quad \text{CH}_2 \\   \quad \quad   \\ \text{H}_2\text{N}^+ - \alpha\text{C} - \text{C} \begin{array}{l} \diagup \text{O} \\ \diagdown \text{O}^- \end{array} \end{array}$ <p>Proline (Pro / P)</p>	$\begin{array}{c} \text{H} \\   \\ \text{H}_3\text{N}^+ - \alpha\text{C} - \text{C} \begin{array}{l} \diagup \text{O} \\ \diagdown \text{O}^- \end{array} \\   \\ \text{CH}_2 \\   \\ \text{CH}_2 \\   \\ \text{COOH} \end{array}$ <p>Glutamic Acid (Glu / E)</p>	$\begin{array}{c} \text{H} \\   \\ \text{H}_3\text{N}^+ - \alpha\text{C} - \text{C} \begin{array}{l} \diagup \text{O} \\ \diagdown \text{O}^- \end{array} \\   \\ \text{CH}_2 \\   \\ \text{COOH} \end{array}$ <p>Aspartic Acid (Asp / D)</p>	$\begin{array}{c} \text{H} \\   \\ \text{H}_3\text{N}^+ - \alpha\text{C} - \text{C} \begin{array}{l} \diagup \text{O} \\ \diagdown \text{O}^- \end{array} \\   \\ \text{H} - \text{C} - \text{OH} \\   \\ \text{CH}_3 \end{array}$ <p>Threonine (Thr / T)</p>	$\begin{array}{c} \text{H} \\   \\ \text{H}_3\text{N}^+ - \alpha\text{C} - \text{C} \begin{array}{l} \diagup \text{O} \\ \diagdown \text{O}^- \end{array} \\   \\ \text{CH}_2 \\   \\ \text{SH} \end{array}$ <p>Cysteine (Cys / C)</p>
$\begin{array}{c} \text{H} \\   \\ \text{H}_3\text{N}^+ - \alpha\text{C} - \text{C} \begin{array}{l} \diagup \text{O} \\ \diagdown \text{O}^- \end{array} \\   \\ \text{CH}_2 \\   \\ \text{CH}_2 \\   \\ \text{S} \\   \\ \text{CH}_3 \end{array}$ <p>Methionine (Met / M)</p>	$\begin{array}{c} \text{H} \\   \\ \text{H}_3\text{N}^+ - \alpha\text{C} - \text{C} \begin{array}{l} \diagup \text{O} \\ \diagdown \text{O}^- \end{array} \\   \\ \text{CH}_2 \\   \\ \text{CH} \\ / \quad \backslash \\ \text{CH}_3 \quad \text{CH}_3 \end{array}$ <p>Leucine (Leu / L)</p>	$\begin{array}{c} \text{H} \\   \\ \text{H}_3\text{N}^+ - \alpha\text{C} - \text{C} \begin{array}{l} \diagup \text{O} \\ \diagdown \text{O}^- \end{array} \\   \\ \text{CH}_2 \\   \\ \text{C}=\text{O} \\   \\ \text{NH}_2 \end{array}$ <p>Asparagine (Asn / N)</p>	$\begin{array}{c} \text{H} \\   \\ \text{H}_3\text{N}^+ - \alpha\text{C} - \text{C} \begin{array}{l} \diagup \text{O} \\ \diagdown \text{O}^- \end{array} \\   \\ \text{HC} - \text{CH}_3 \\   \\ \text{CH}_2 \\   \\ \text{CH}_3 \end{array}$ <p>Isoleucine (Ile / I)</p>	$\begin{array}{c} \text{H} \\   \\ \text{H}_3\text{N}^+ - \alpha\text{C} - \text{C} \begin{array}{l} \diagup \text{O} \\ \diagdown \text{O}^- \end{array} \\   \\ \text{CH} \\ / \quad \backslash \\ \text{CH}_3 \quad \text{CH}_3 \end{array}$ <p>Valine (Val / V)</p>

Table (1-3): Common amino acid abbreviations

<b>Name</b>	<b>Three letter code</b>	<b>Molecular Weight</b>	<b>Molecular Formula</b>
Alanine	Ala	89.10	C <sub>3</sub> H <sub>7</sub> NO <sub>2</sub>
Arginine	Arg	174.20	C <sub>6</sub> H <sub>14</sub> N <sub>4</sub> O <sub>2</sub>
Asparagine	Asn	132.12	C <sub>4</sub> H <sub>8</sub> N <sub>2</sub> O <sub>3</sub>
Aspartic acid	Asp	133.11	C <sub>4</sub> H <sub>7</sub> NO <sub>4</sub>
Cysteine	Cys	121.16	C <sub>3</sub> H <sub>7</sub> NO <sub>2</sub> S
Glutamic acid	Glu	147.13	C <sub>5</sub> H <sub>9</sub> NO <sub>4</sub>
Glutamine	Gln	146.15	C <sub>5</sub> H <sub>10</sub> N <sub>2</sub> O <sub>3</sub>
Glycine	Gly	75.07	C <sub>2</sub> H <sub>5</sub> NO <sub>2</sub>
Histidine	His	155.16	C <sub>6</sub> H <sub>9</sub> N <sub>3</sub> O <sub>2</sub>
Hydroxyproline	Hyp	131.13	C <sub>5</sub> H <sub>9</sub> NO <sub>3</sub>
Isoleucine	Ile	131.18	C <sub>6</sub> H <sub>13</sub> NO <sub>2</sub>
Leucine	Leu	131.18	C <sub>6</sub> H <sub>13</sub> NO <sub>2</sub>
Lysine	Lys	146.19	C <sub>6</sub> H <sub>14</sub> N <sub>2</sub> O <sub>2</sub>
Methionine	Met	149.21	C <sub>5</sub> H <sub>11</sub> NO <sub>2</sub> S
Phenylalanine	Phe	165.19	C <sub>9</sub> H <sub>11</sub> NO <sub>2</sub>
Proline	Pro	115.13	C <sub>5</sub> H <sub>9</sub> NO <sub>2</sub>
Pyroglutamic	Glp	139.11	C <sub>5</sub> H <sub>7</sub> NO <sub>3</sub>
Serine	Ser	105.09	C <sub>3</sub> H <sub>7</sub> NO <sub>3</sub>
Threonine	Thr	119.12	C <sub>4</sub> H <sub>9</sub> NO <sub>3</sub>
Tryptophan	Trp	204.23	C <sub>11</sub> H <sub>12</sub> N <sub>2</sub> O <sub>2</sub>
Tyrosine	Tyr	181.19	C <sub>9</sub> H <sub>11</sub> NO <sub>3</sub>
Valine	Val	117.15	C <sub>5</sub> H <sub>11</sub> NO <sub>2</sub>



Table (1-4) : Classification of Amino Acids According to Biological value (Essential and Non – Essential ) Amino Acids

Essential Amino Acids			Non Essential Amino Acids		
1-	Arginine	Arg	1-	Alanine	Ala
2-	Histidine	His	2-	Aspartic acid	Asp
3-	Isoleucine	Ile	3-	Asparagine	Asn
4-	Leucine	Leu	4-	Cysteine	Cys
5-	Lysin	Lys	5-	Glutamine	Gln
6-	Methionine	Met	6-	Glycin	Gly
7-	Phenylalanine	Phe	7-	Proline	Pro
8-	Threonine	Thr	8-	Serine	Ser
9-	Tryptophan	Try	9-	Glutamic acid	Glu
10-	Valine	Val	10-	Thyrosine	Tyr

### 1.3.2 Basicity of Nitrogen L- $\alpha$ -amino-acid

Amino acids are molecules containing both acidic and alkaline functional groups. They show chirality Except for glycine, and their properties vary with attached side chains. Table 1 and 2 The N atom in amines unshared pair of electrons. a substantial difference in the chemistry of this classes of compounds. In nature for metalloproteinase, amino acids are excellent complexes for metal ions. all proteins are thought to need metals such as Zn, Fe , Cu, Co, Ni, Mg, and Ca as co-factors [43-44]. Metallo proteins and -enzymes, the metals are bonded via the nitrogen, oxygen or sulfur atoms of the amino acid side chains. amino acids are mostly bidentate (N,O)-complexes, or tridentate in the presence of suitable side chains [43]. Sakiyan et t al 2004 ,have reported the vitro antibacterial antifungal activities of 5 amino acid - Schiff bases derived from the reaction of 2-hydroxy-1-naphthaldehyde  $C_{11}H_8O_2$  with L-[His, Ala, Try, Phe] and complexes of these bases were studied, Figure (1-15) for Mn(III) -Schiff base [45].

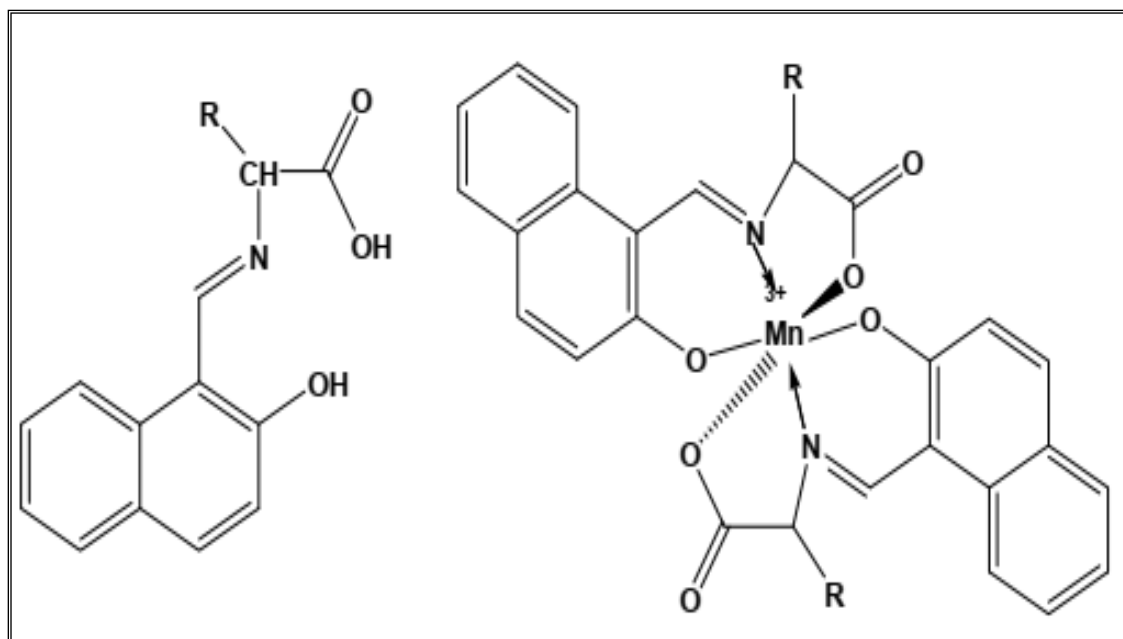


Figure (1-15): Structure of the Schiff base and Mn(III) -Schiff base

Wujec et al 2007 <sup>[46]</sup> have reported the relationship between antimicrobial activities and the formation constants ( $K_f$ ) of amino acid-Schiff bases prepared from DL- (glycine, alanine) and 5-bromo- or chloro (2-hydroxybenzaldehyde), and their Nickel (II) and Copper (II) complexes Figure (1-16) <sup>[46]</sup>. The complexes were determined potentiometrically in a water-dioxane (1:1) solution at 25°C. Antimicrobial activities of the complexes were estimated for six bacteria. The role of halogen (Cl and Br) substitution on the (2-hydroxybenzaldehyde  $C_7H_6O_2$ ), effect of the metal ion.

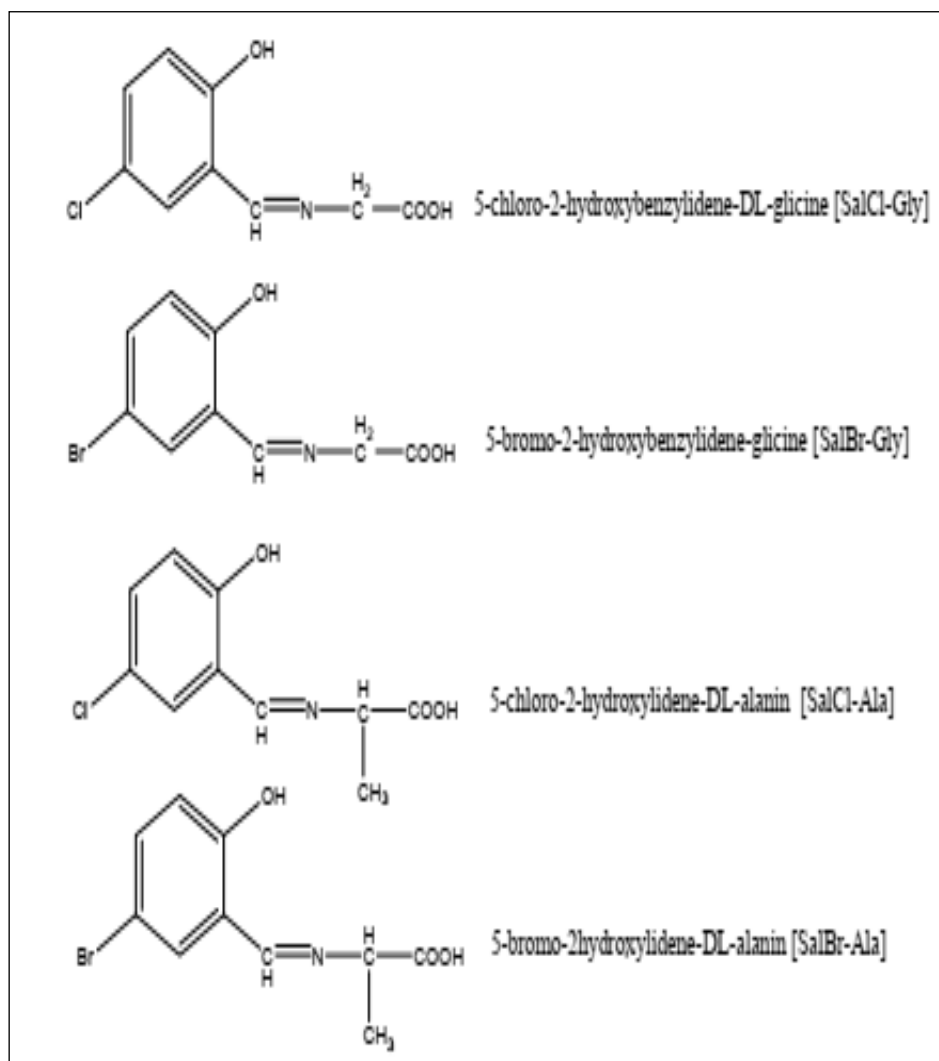


Figure (1-16) Structure of Amino Acid-Schiff bases

Sutha et al (2015) have been reported synthesis of nine mixed ligand complexes from 5-fluorouracil (5-FU) and via (L-Gly), (ala) and (L-Val) with Ni(II), Cu(II) and Zn(II) ions <sup>[47]</sup>. These complexes were characterized by physico-chemical and spectral studies and tested for their biological and antioxidant activities, structure of all the complexes are given in Figure (1-17).

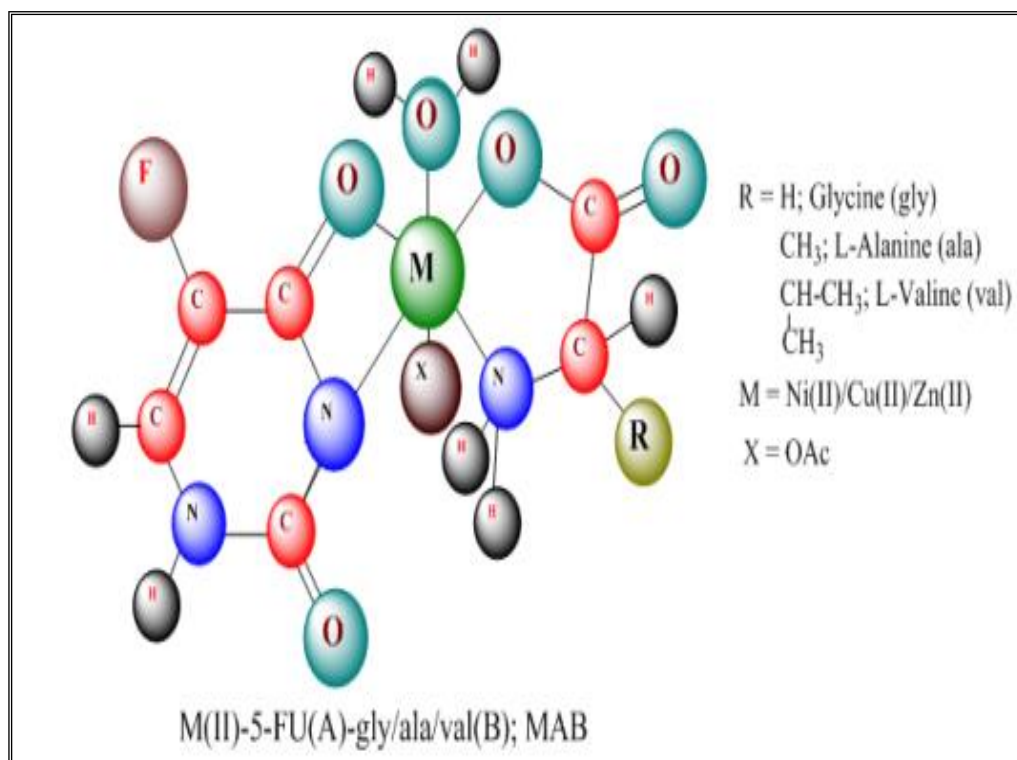


Figure (1-17) :General structure of (5-FU) - amino acids .

One of the most interesting features of metal coordinated systems is the concerted spatial arrangement of the amino acid - metal ions <sup>[47-48]</sup> In this thesis we use L-Valine is an essential branched-chain amino acid. and L-proline is essential amino acid as binds natural amino acids Bioactive Ligands . Here we show that a rationally designed metal complex formed from a trivalent ion , divalent ions. Proline can cause a number of problems in the human body and in plants <sup>[49]</sup>, For example, this can lead to multiple strains. also it can be liable for slower than normal healing and it is responsible for the creation of collagen . This ability of the amino acid (AA) is useful for maintaining the appropriate pressure levels throughout the body <sup>[49-50]</sup>, used to treat urinary tract infections. and it used as part of a synergistic combination with in a 5 trimethoprim:1 Trimoxazole ratio .

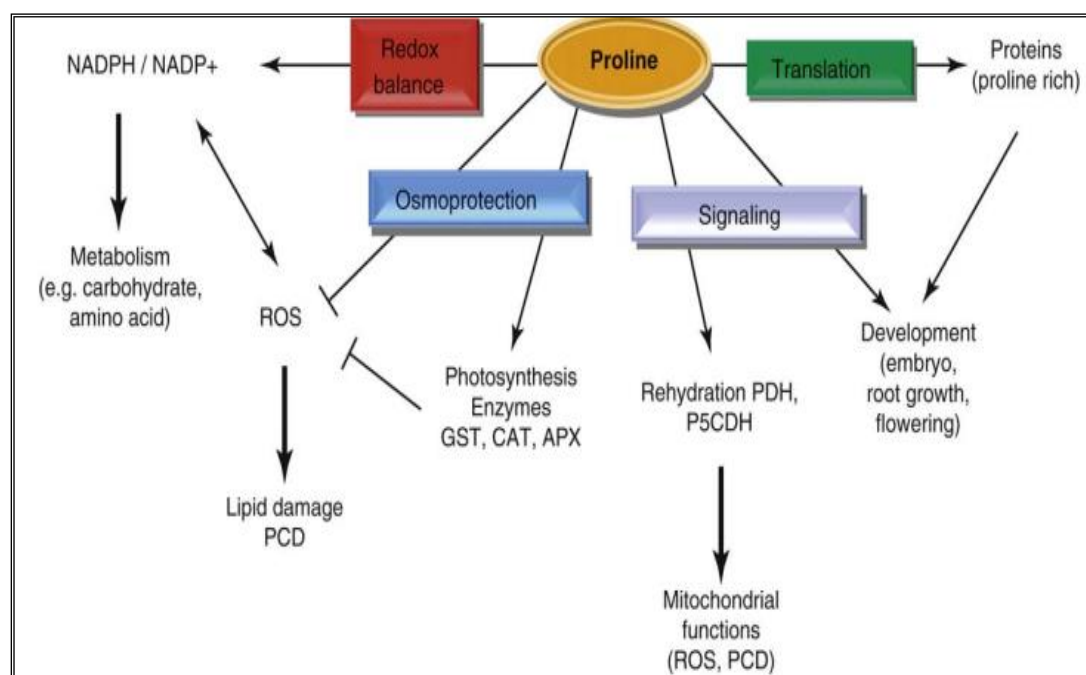
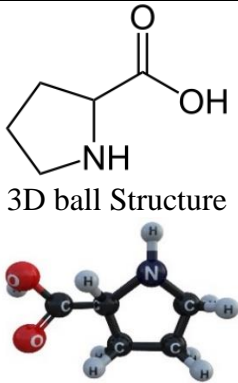
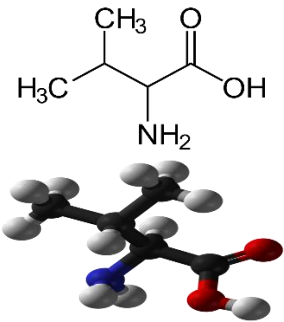
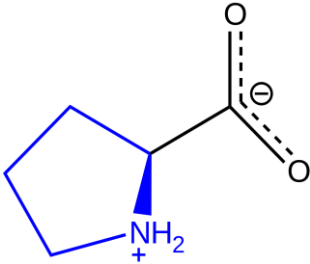
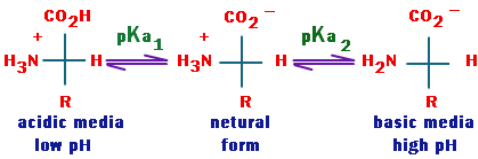


Figure (1-18) : Multiple functions of proline in plants.

L-Valine branched chain amino acid important for smooth nervous system and cognitive functioning. L-Valine with L-Isoleucine and L-Leucine use to promote muscle growth . It is a non-polar, acts as a bidentate ligand and has wide applications in the field of food industry and pharmaceutical studies of L-Valine with transition metal ions have been an active field of research [51-52] .

Table (1-5) : UPAC names and some physical properties of L- Proline and L- Valine

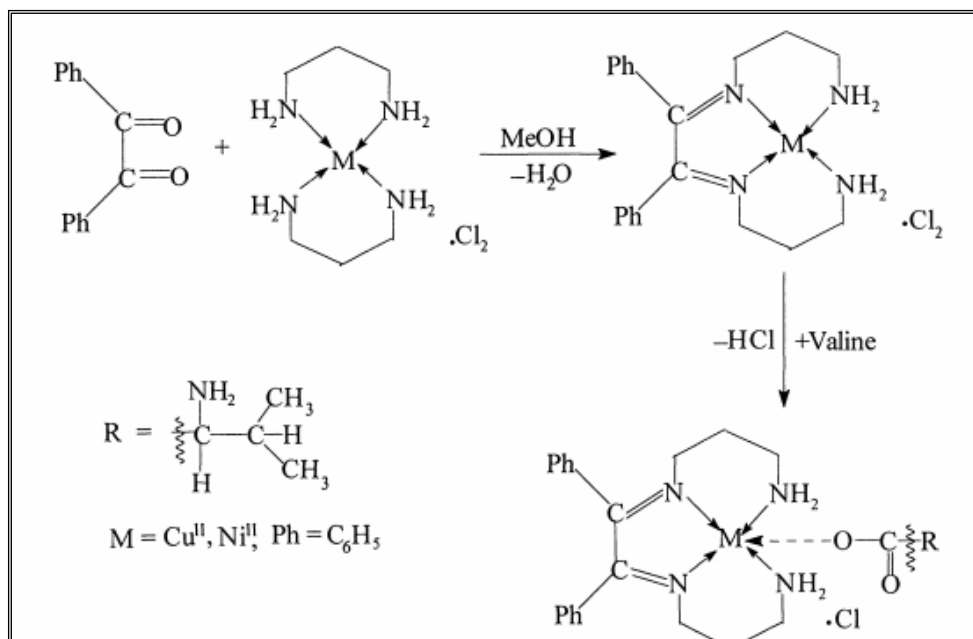
Synonyms name	<b>L-Proline</b> Pyrrolidine-2-carboxylic acid	<b>L-Valine</b> 2-Amino-3-methylbutanoic acid
Molecular formula	C <sub>5</sub> H <sub>9</sub> NO <sub>2</sub>	C <sub>5</sub> H <sub>11</sub> NO <sub>2</sub>
Structure formula	 <p>3D ball Structure</p>	
Molar mass	115.132 g.mol <sup>-1</sup>	117.148 g.mol <sup>-1</sup>
Meltingpoint (M.P)	205 to 228 °C	298 °C (decomposition)
Zwitter ionic		 <p>acidic media low pH      neutral form      basic media high pH</p>
History	1900 by Richard Willstätter	1901 by Hermann Emil Fischer

Both L- proline and L-valine are bidentate ligands with high affinity to metals .We selected L- proline and L-Valine as ligands to study the effect of imino group and cyclic side chain of L-proline on the stability of complexes with metal ions and amino and carboxyl groups in L-Valine .

#### 1.4. L- Valine complexes

Aijaz et al 2002 have synthesized 5 coordinated of Ni and Cu of L-Valine from benzyl C<sub>14</sub>H<sub>10</sub> O<sub>2</sub> and 1,3- diaminopropene-Cu/Ni complex and kinetic study. The  $k^{obs}$  values calculated under pseudo-

first order conditions. spectral data, proposed the coordination of the complexes as given in Scheme (1-2) [51].



Scheme (1-2): synthesis nickel (II) and copper (II) complexes of L-valine from benzyl

Nursen *et al.* (2003) [52] reported the synthesis and derivatives of characterization Schiff Base (N-indoladene-DL-Glycine, N-indalidiene-DL Alanine, and N-indoladene-DL-Valine complexes). The antibacterial screening of the Schiff bases ind- DL -Gly, ind- DL- Ala, and ind- DL- Val, against four different microorganisms.

Ammar *et al.* (2011). [53] used MINIQUAD75 to calculate stability constants of Ni(II) complexes. Aliyu and Naaliya calculated the stability constant of ternary system of Fe(II), Ni(II), Co(II), Zn(II), Cu(II), Cr(II) and Mn(II) complexes with amino acids such as [Ala, Arg, Asp, Gly, His, Lys, Met, pha, pro, Thre, Trp and Val. The protonation constants of amino acid (AA) and steps wise formation constants of metals complexes were determined potentiometrically.

Fayad *et al.* (2013),<sup>[54]</sup> have synthesized and characterized mixed-ligand complexes of M (II) ions with Saccharin (SacH) as a primary ligand and (L-Val) as a secondary ligand have general formula  $[M(\text{Val})_2(\text{SacH})_2]$ . L-Val H= (C<sub>5</sub>H<sub>11</sub>NO<sub>2</sub>) , SacH =C<sub>7</sub>H<sub>5</sub>NO<sub>3</sub>S. All the synthesized complexes were characterized by molar conductance, magnetic susceptibility (infrared and electronic) spectra, (C.H.N) and (A.A.S).

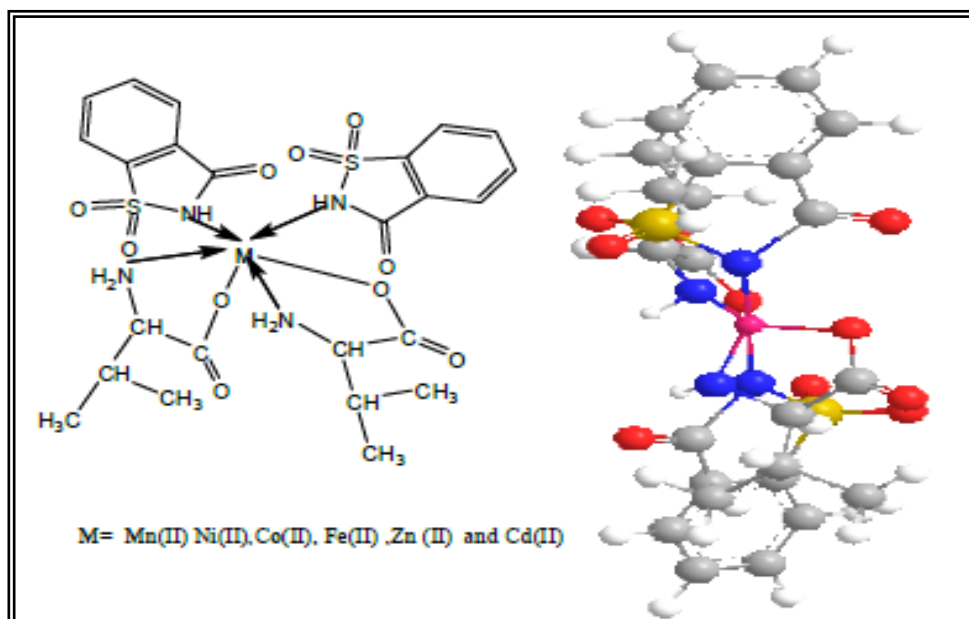


Figure (1-19) - structure 3D-geometrical  $[M(\text{Val})_2(\text{SacH})_2]$

Peketi & Gollapalli (2013)<sup>[55]</sup> were reported biomimetic and modelling studies of Co(II), Ni(II) and Cu(II) complexes with L-Valine in water– acetonitrile mixtures.

Shilpi *et al* (2014),<sup>[56]</sup> have been reported physicochemical investigations of the complexes L-valine with M(II). All Ni(II), Cu (II) and Zn(II) ions complexes are characterized by C.H.N, EDAX-SEM , molar conductance, TEM, mass spectroscopy , FT –IR , UV. Vis , TG/DTA, and fluorescence. Quantum chemical - computational geometrical parameters



carried out in (aqueous and gas) phase . Analysis suggests the molecular structure of L-valine as a result of metal binding, as Figure (1-20).

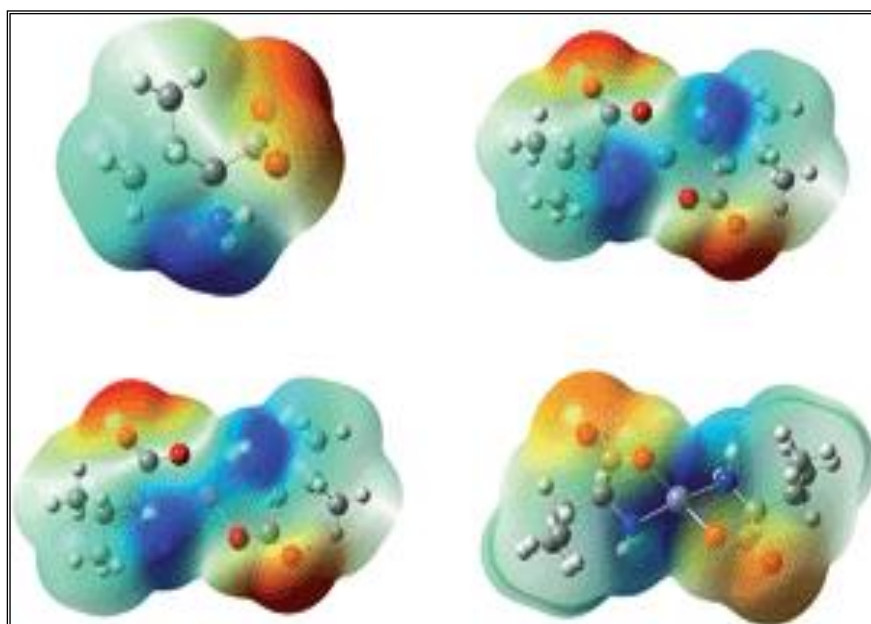


Figure (1-20) : Metal binding with L-valine

Takeshita et al. 2015<sup>[57]</sup> synthesized the mixed ligand complexes Cu(II) of L-Valine as primary ligand and imidazole as a secondary ligand. Under (N<sub>2</sub>) atmosphere Cyclic Voltammetry (C.V) were carried out reduction of Cu (II) ion species to Cu (I) ones, after UV light irradiation. At the fourth coordination sites and examined their photo-induced reactions with (TiO<sub>2</sub>), Figure (1-21).

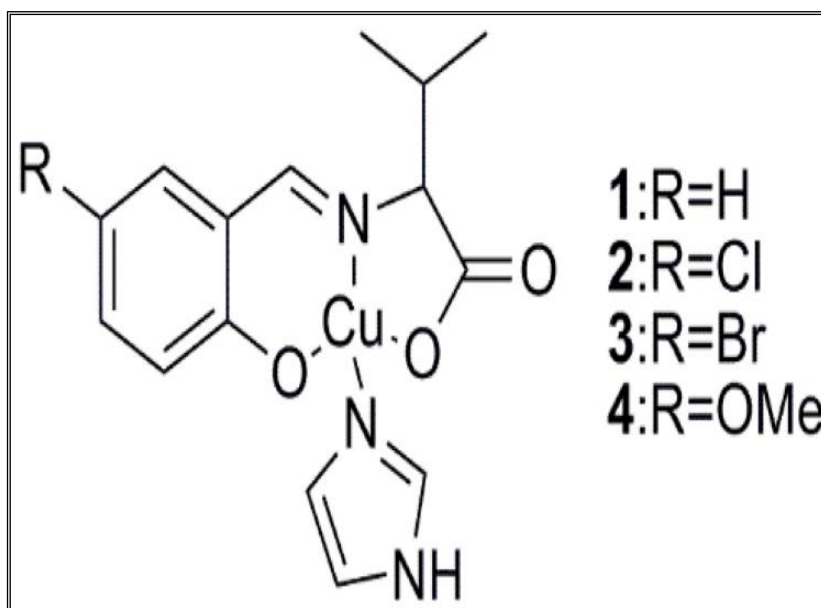


Figure (1-21) : Four Molecular structures of Cu(II) complexes

Nanami et al 2016 <sup>[58]</sup> report L-Valine - derivative – A chiral Schiff base Zn(II) –complexes, Figure (1-22)., ( $X^- = H^-$ ,  $Cl^-$ , and  $CH_3O^-$ ; L= imidazole)

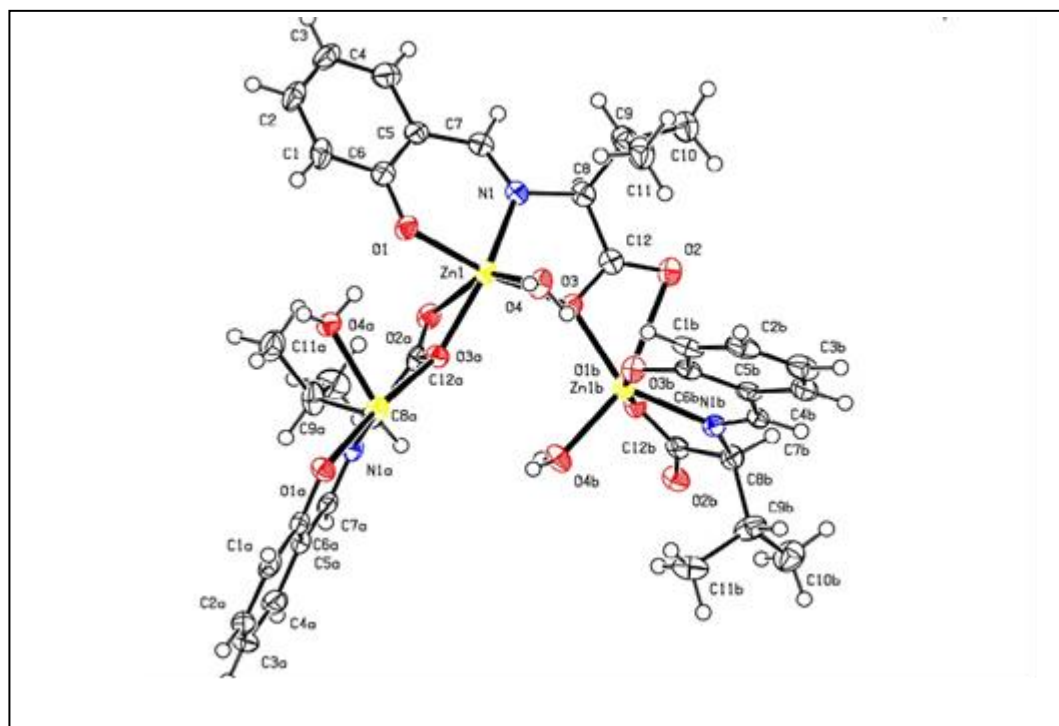


Figure (1-22): A chiral Schiff base Zn(II)

Saravanan et al (2017), <sup>[59]</sup> have synthesized and characterized ternary complexes of Cu (II) - 1,10-phenanthroline ,2,2'-bipyridyl, L-Valine and Urea .Figure (1-23) as formula :

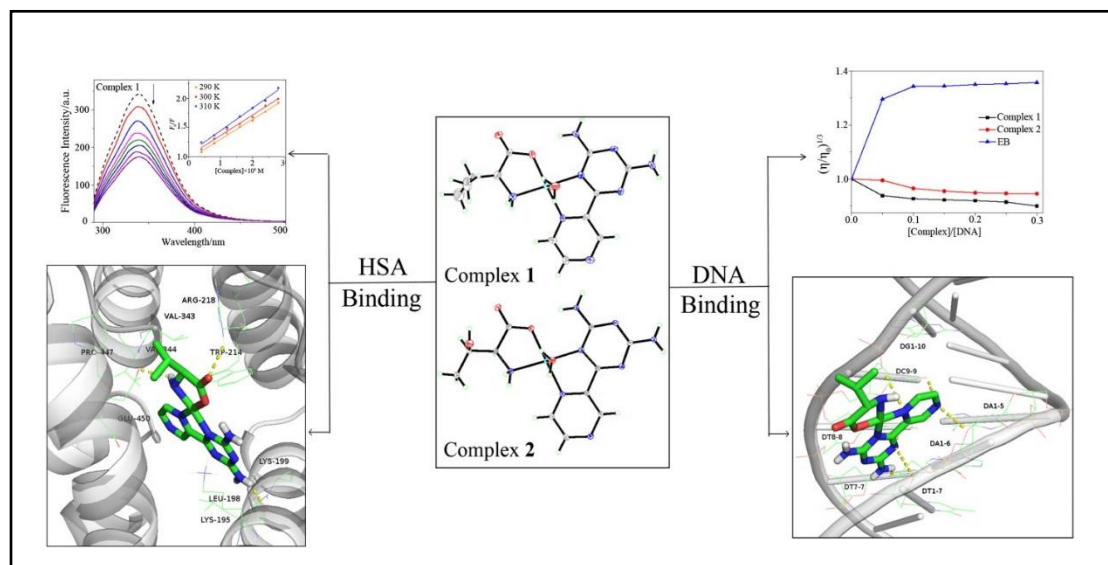
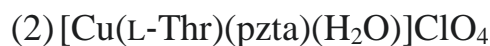
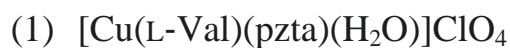


Figure (1-23) mixed ligand complex of  $[\text{Cu}(\text{L-Val})(\text{pzta})(\text{H}_2\text{O})]\text{ClO}_4$  and  $[\text{Cu}(\text{L-Thr})(\text{pzta})(\text{H}_2\text{O})]\text{ClO}_4$ .

Thakur et al (2018) <sup>[60]</sup>, have synthesized ternary complexes of Ce(III) general formula  $[\text{Ce}(\text{Aa})(1\text{N}2\text{N})22\text{H}_2\text{O}]$ , Figure (1-24) Aa= Amino acid = (a) (L-Val), (b) (Ser), (c) (Iso), 1N2N = 1-Nitroso-2-Naphthol /and characterized by elemental analysis, UV-Vis, IR spectroscopy, Tg, DTA and molar conductance studies.

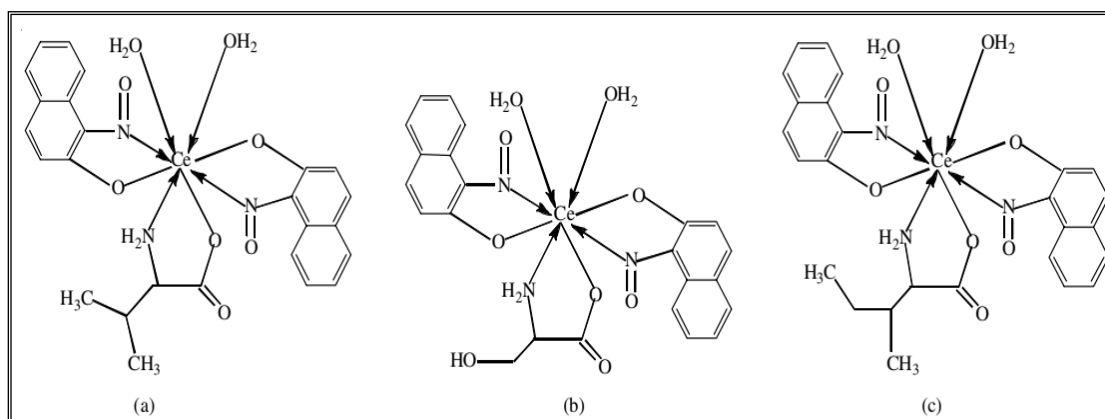


Figure (1-24) : Structures of  $[\text{Ce}(\text{1N2N})_2(\text{AA}) 2\text{H}_2\text{O}]$

(AA) = (a) (L-Val), (b) (Ser), (c) (Iso)

Saravanan et al (2019), <sup>[61]</sup> have synthesized and characterized DNA binding and biological activities of :

complex 1  $[\text{Cu}(\text{phen})(\text{L-valine})\text{TU}]\text{NO}_3$

complex 2  $[\text{Cu}(\text{bpy})(\text{L-Val})\text{U}]\text{NO}_3$

U= Urea and TU= thiourea

Results suggest that the complex 1 can bind to CT-DNA through intercalation and complex 2 binds through partial intercalation.

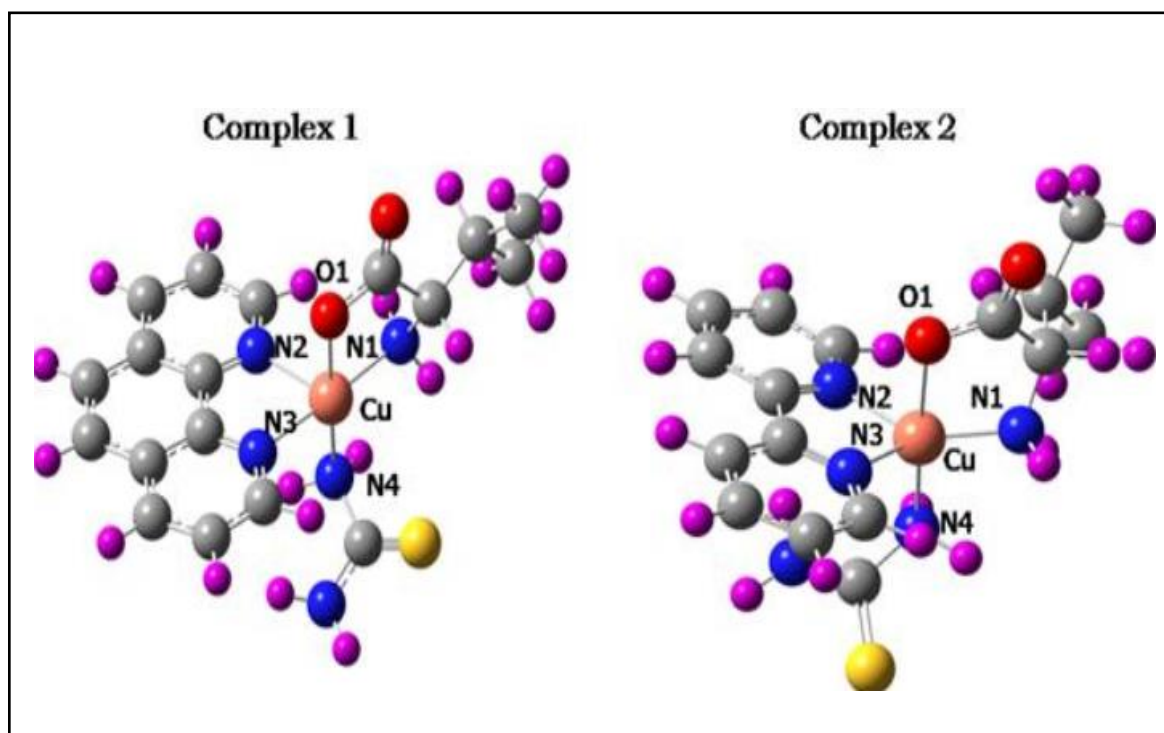


Figure (1-25) Structures of Cu (II) complex 1 and 2

## 1.5. L- Proline complexe

The molecular formula of L- proline has the secondary amino group known as imino group which belongs to a [5-member ring] in a molecule. major application L- Proline complexes in blood pressure maintenance, collagen formation, arteriosclerosis prevention and tissue repair. [55]

Teo, et al (1995), [62]. have synthesized and characterized copper (II) - methyleneda(4-hydroxy-L-proline), Figure (1-26) proline.

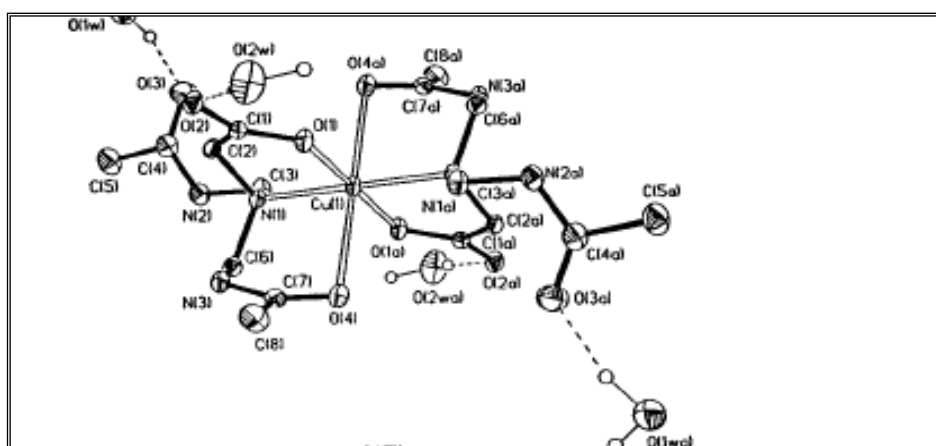


Figure (1-26) Structure of Copper (II) - methyleneda(4-hydroxy-L-proline)

Yamaguchi, et al (1996), [63] have synthesized and characterized [(L-proline)-Pt(II)], Figure (1-27).

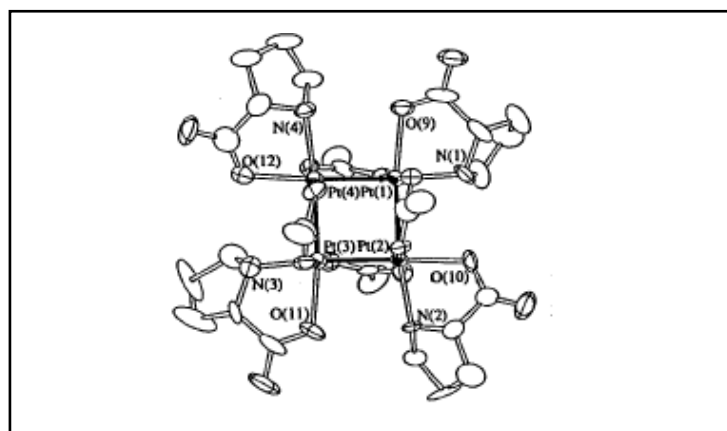


Figure (1-27) : Structure of [(L-proline)-Pt(II)]

Ramakrishna et al (2007) <sup>[64]</sup> have synthesized characterized and their DNA binding and cleavage activity studied mixed ligand Copper (II) complexes having N,O-donor amino acid L-proline and N,N-donor heterocyclic bases  $[\text{Cu}(\text{L-pro})(\text{B})(\text{H}_2\text{O})](\text{NO}_3)$  (1, 2) where L-pro = L-proline, B is a N,N-donor heterocyclic base, viz. 2,20 - bipyridine (bpy, 1), 1,10-phenanthroline (phen, 2), Figure (1-28) .

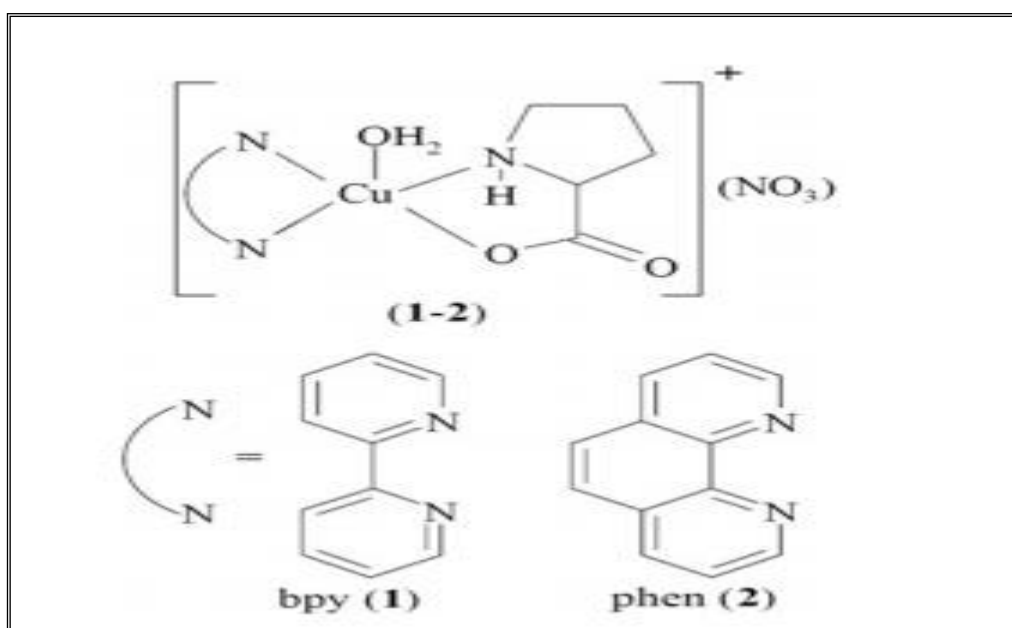


Figure (1-28): Structure of Complexes 1 and 2 and the heterocyclic bases

Rao et al 2006 <sup>[65]</sup> have been reported thermal study in controlled atmosphere carried out to understand stages of temperature range of decomposition on molecular formulae  $[\text{Th}(\text{Q})_2(\text{L-Pro})\text{NO}_3\cdot\text{H}_2\text{O}]$  and  $[\text{Th}(\text{Q})_2(\text{H-L-Pro})\text{NO}_3\cdot\text{H}_2\text{O}]$  complexes . The mixed ligand complexes contained 8-hydroxy quinoline as a primary ligand, L-proline and L-4-hydroxy proline containing N- and O- donor atoms as a secondary ligand. The, respectively. The TG study of the complexes shows that the deauration of both the complexes takes place in the temperature range

130-200 deg C and the anhydrous form is stable up to 500 deg C. The complexes show mass loss corresponding to loss of water molecule, amino acid moiety, nitrate and 8-hydroxy quinoline moiety. The complexes display endothermic DTA peak attributed to release of water molecule and a broad exothermic peak corresponding to elimination of ligand fragments. It has been observed that reaction is completed at 760 deg C yielding a fine powder of metal oxide (ThO<sub>2</sub>) confirmed by X-ray diffraction study. [66]

Fintan Kelleher et al (2007) [66] have synthesized starting from L-proline a series of homochiral [4.4]-spirodiamines and its metal complexation in particular been studied for their use in constraining peptides with L-proline residues to mimic the  $\beta$ -turn ,

Boddu et al (2014), [67] have been reported chemical speciation of mixed ligand L-proline and L-valine with of Ca(II), Zn(II) and Mn(II) complexes in various concentrations (0–60% v/v) of acetonitrile–water mixtures. Stability constants of mixed ligand complexes were calculated from the modelling studies. Reactions of [Ru(NO)Cl<sub>5</sub>]<sup>2-</sup> with glycine (Gly), L-alanine (L-Ala), L-valine (L-Val), L-proline (L-Pro), D-proline (D-Pro), L-serine (L-Ser), L-threonine (L-Thr), and L-tyrosine (L-Tyr) in *n*-butanol or *n*-propanol afforded eight new complexes (1–8) of the general formula [RuCl<sub>3</sub>(AA–H)(NO)]<sup>-</sup>, where AA = Gly, L-Ala, L-Val, L-Pro, D-Pro, L-Ser, L-Thr, and L-Tyr, respectively. The compounds were characterized by elemental analysis, electrospray ionization mass spectrometry (ESI-MS), <sup>1</sup>H NMR, UV–visible and ATR IR spectroscopy, cyclic voltammetry, and X-ray crystallography [68].

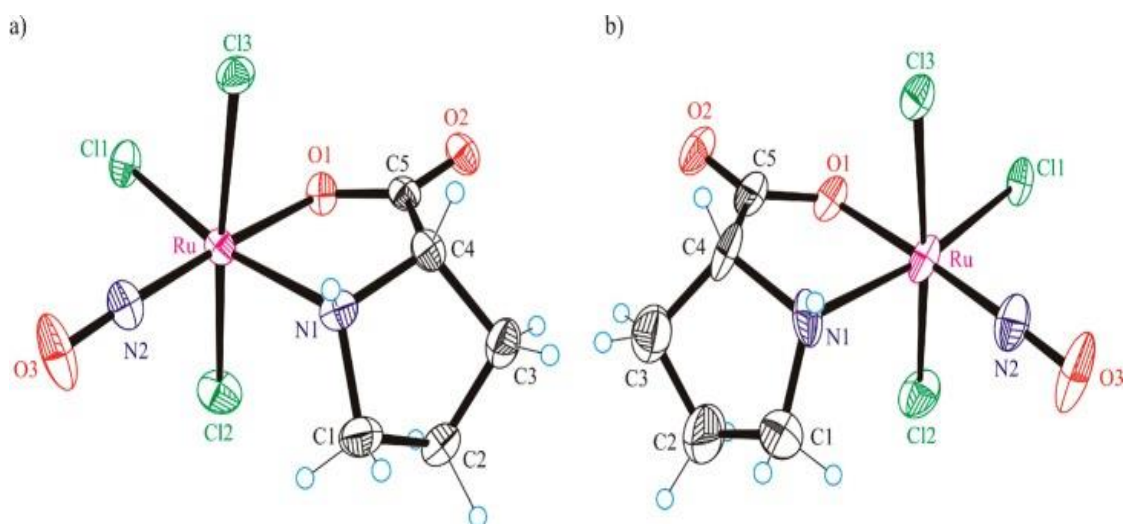
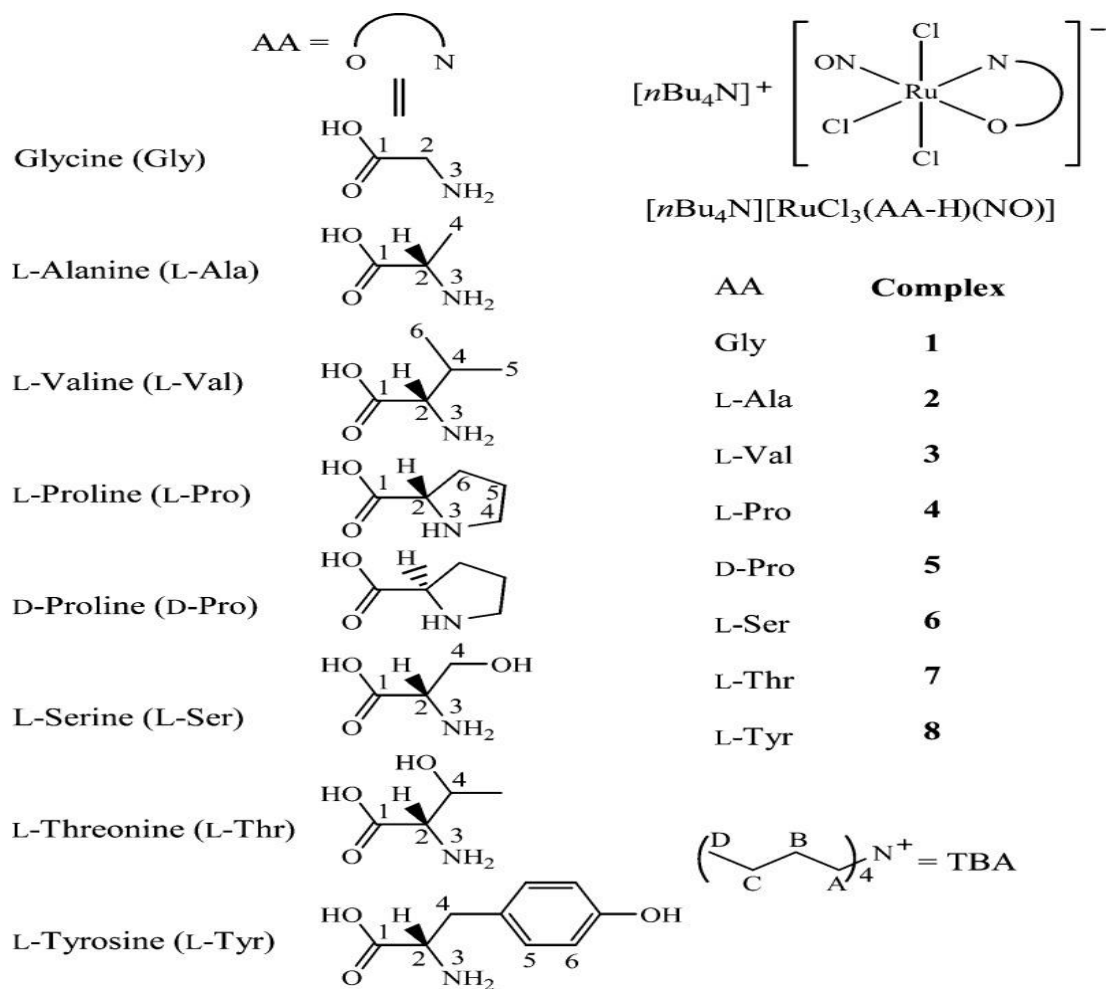


Figure (1-29) :(a)  $[\text{RuCl}_3(\text{L-Pro-H})(\text{NO})]^-$  (b)  $[\text{RuCl}_3(\text{D-Pro-H})(\text{NO})]^-$



Junyi Du, <sup>[69]</sup> reported a novel nonheme chiral Fe(IV)–oxo complex bearing an L-proline-derived aminopyridine was synthesized and spectroscopically characterized by UV-vis, CSI-TOF MS and EPR. The appropriate half-life of about 1 h at 0 °C allows us to study its reactivity in the C–H activation of various hydrocarbons in detail. In addition, its reactivity in asymmetric sulfoxidation and C–H hydroxylation was also investigated.

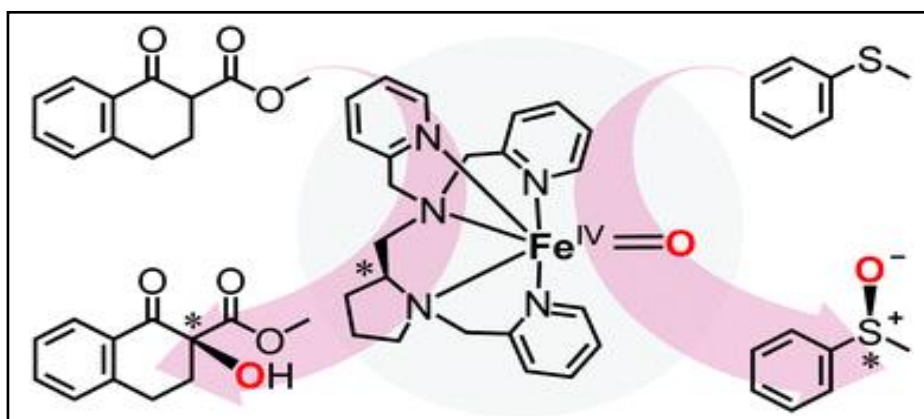


Figure (1-30) : Fe(IV)–oxo complex bearing an L-proline-derived aminopyridine

Mosarrat Parveen et al 2018 <sup>[70]</sup> reported the inhibition effect of L-proline (LPr) and LPr mixed with sodium benzoate (LPr+NaBenz) for mild steel (MS) corrosion in 1M HC in different temperature and concentration of LPr was varied between (100–600ppm, )were test by spectroscopic measurements, scanning electron microscopy technique) and theoretical (DFT) approach are in good agreement and correlate well with theoretical quantum chemical descriptors.

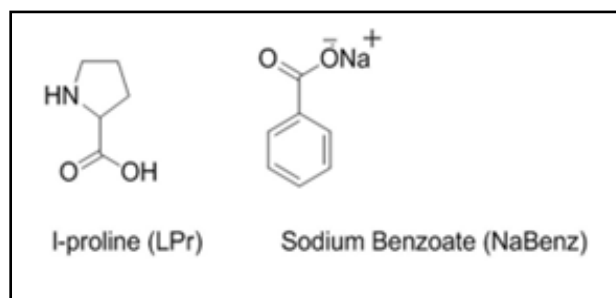


Figure (1-31): Molecular structure of studied inhibitors

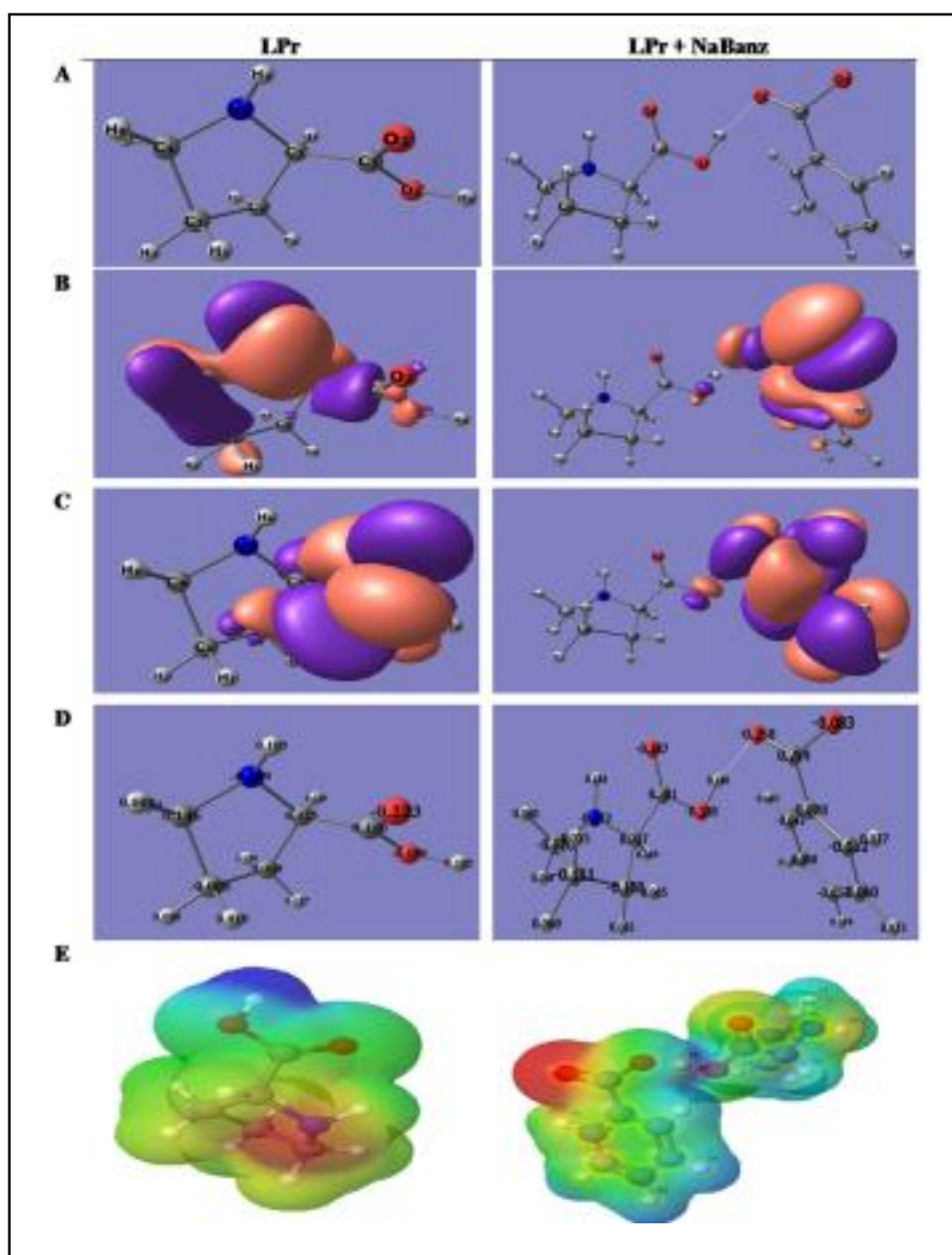


Figure (1-32): Quantum chemical results of Proline in the absence and presence of NaBenz calculated by the ORCA Programme: (A) optimized molecular structure, (B) HOMO; (C) LUMO (D) Mulliken charges (E) MEP.

When LPr is combined with NaBenz, the corrosion inhibition rate was improved greatly. Corrosion mitigating efficacy of LPr or LPr mixed with NaBenz obtained by different techniques are in good agreement and correlate well with theoretical quantum chemical descriptors.

Mala et al <sup>[71]</sup> have been reported relationship structure-cytotoxicity of di-/tri-organotin(IV) derivatives of mandelic acid - , L-proline and mixed ligand complexes of latter with 1,10-phenanthroline , having enhanced cytotoxicity. Various biophysical experiments such as DNA fragmentation. The observed results indicated that the cause of cancer cell death is apoptosis, and the number and nature of organic groups bonded to organotin(IV) as well as the nature of counter anions play an important role in determining the cytotoxicity of organotin(IV) derivatives compounds.

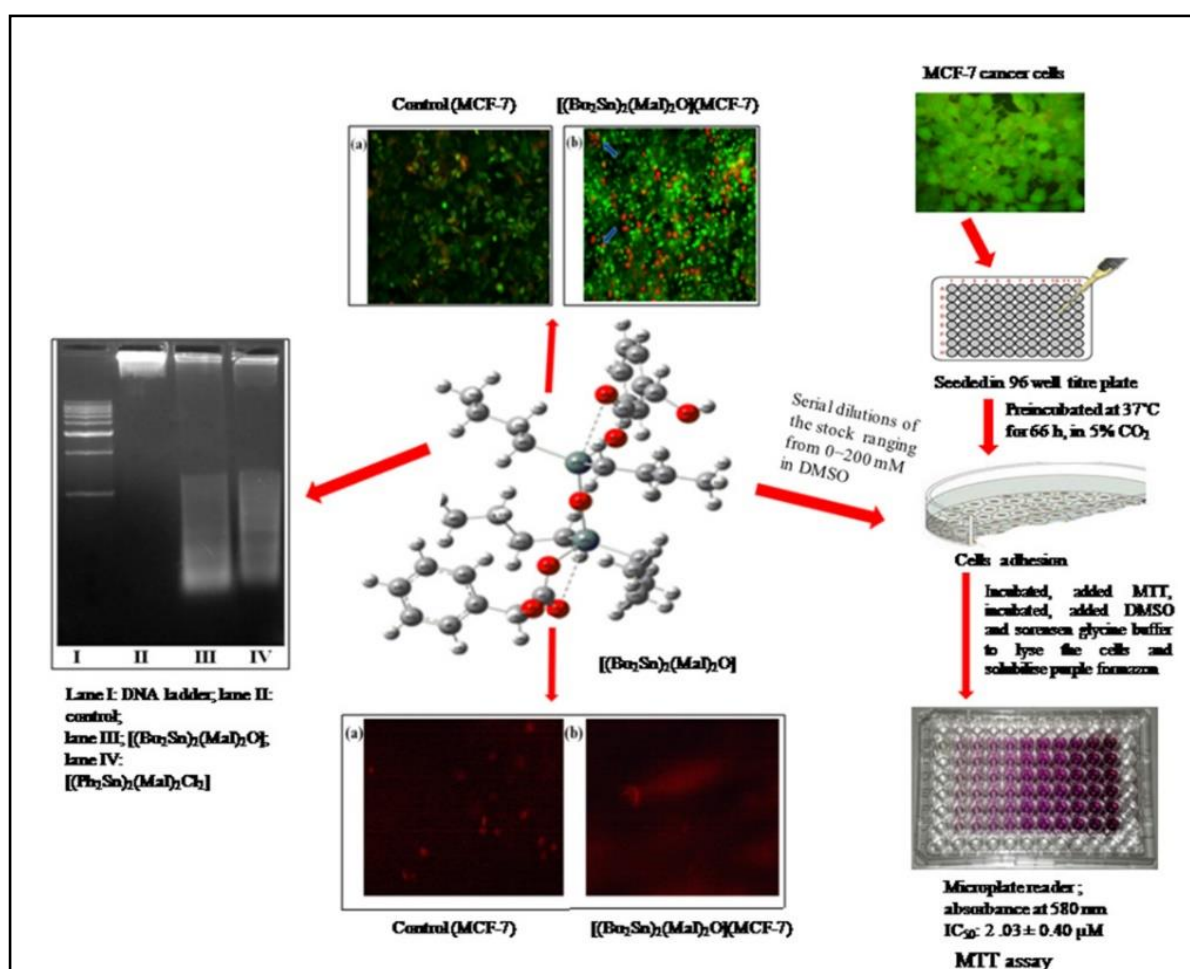


Figure (1-33): di-/tri-organotin(IV) derivatives of mandelic acid - , L-proline and mixed ligand complexes of 1,10 phenanthroline

## 1.6 Aim of The Present Work

Mixed ligands, and their coordination compounds which have played a great importance in medicine, bioinorganic chemistry and industry/ Due to these facts, aim of the present work deals with :

1. The synthesis of some mixed ligand sulfamethoxazole and L= Valine and L-proline then react with metal chloride of  $[\text{Cr}^{\text{III}}, \text{Fe}^{\text{II}}, \text{Al}^{\text{III}}, \text{Mn}^{\text{II}}, \text{Fe}^{\text{III}}, \text{Co}^{\text{II}}, \text{Ni}^{\text{II}}, \text{Cu}^{\text{II}}, \text{Zn}^{\text{II}}, \text{Cd}^{\text{II}}, \text{Hg}^{\text{II}}$  and  $\text{Sn}^{\text{II}}$ ] complexes.
2. To determine structure of the products using different spectroscopic techniques such as : FTIR , Electronic spectra , Magnetic moment measurement, and molar conductance for complexes.
3. The ligands and their metal complexes have been tested against gram positive and gram negative bacteria and pathogenic fungi.

Chapter  
Two

Experimental

## 2. The Experimental

### 2.1. Chemicals

The chemicals used in this work and their suppliers are listed in Table (2-1). All these chemicals were used without further purification.

No.	Chemicals	Company	Purity%
1	Absolute ethanol	Scharlau	99.90%
2	Acetone	Merck	%99
3	Aluminum(III) Chloride	Merck	%98
4	Benzen	Merck	%99
5	Cadmium(II) Chloride dehydrate	Merck	%99
6	Chromium (III) chloride hexahydrate	Merck	%99
7	Cobalt(II) chloride hexahydrate	Riedial – Dehaen	%99
8	Copper (II) chloride dihydrate	Merck	%99
9	Dimethy sulfoxoamide	Merck	%99.80
10	Dimethyl formamide	BDH	%99.90
11	Dimethyl sulfoxide (DMSO)	CDH	%99.5
12	Hexane	Merck	%99
13	Hexanol	Merck	%99
14	Hydrochloric acid	BDH	%98
15	Iron(III) chloride	Merck	%99
16	Manganese(II) chloride tetrahydrate	Merck	%99
17	Mercury (II) chloride	Merck	%99
18	Nickel (II) chloride hexahydrate	Merck	%99
19	Potassium hydroxide	BDH	%99.90
20	proline	PDH	%99
21	Silver Nitrate	BDH	98%
22	sulfamethoxazole	PDH	%99
23	Tin(II) Chloride dehydrate	Merck	%98
24	Iron(II) chloride	Merck	%99
25	Valine	PDH	%99

### 2.2. Instruments and apparatus

#### 2.2.1. The Melting point measurements

The Melting points of the all compounds in this study were determined by using (Gallenkamp) (USA) melting point apparatus.

### 2.2.2. Electrical conductivity measurements

The measurements for complexes were recorded at laboratory temperature for ( $10^{-3}$  molar) solution of the samples in DMSO by using an a Multi 740, Tram (Germany).

$$\Lambda_m = \frac{1000L}{C}$$

L Specific - conductivity = ( $\Omega^{-1} \text{ cm}^{-1}$ )

$\Lambda_m$  Molar - conductance of the metal = ( $\Omega^{-1} \text{ cm}^2 \text{ mol}^{-1}$ )

C Concentration = (mole/ $\text{cm}^3$ ). [72]

### 2.2.3. Metal determination

The metal contents of the complexes were determined by atomic absorption (A.A) technique, using a Phoenix -986 AA spectrophotometer, at Ibn Sina [73]

### 2.2.4. Chloride contents

Chloride contents were determined by standard methods [Vogel 1962] To the resultant solution of the complexes, aqueous solution of  $\text{AgNO}_3$  was added, white precipitate of  $\text{AgCl}$  was formed in the case of metals complexes have Chloride content [73].

### 2.2.5. Electronic (U.V-Vis) spectra

The electronic spectra of the compounds were obtained at range (200-900) nm, with quartz cell of (1.0 cm) length by using (*SHIMADZU* UV-Vis 160A) and the concentration of ( $1 \times 10^{-3}$  Molar), in Ibn Sena company

### 2.2.6. Magnetic susceptibility

The magnetic susceptibility of the complexes was obtained by using Balance magnetic susceptibility, Model (MSB-Mk1) at the College of Science, Al-Nahrain University. The effective magnetic moment ( $\mu_{\text{eff}}$ ) values obtained using the following Eqs. [74-75]

$$X_g = \frac{C_{Bal} L (R - R_0)}{10^9 M}$$

Where:

$R_0 \Rightarrow$  reading of empty tube,

$L \Rightarrow$  sample length cm.

$M \Rightarrow$  sample mass (g),

$R \Rightarrow$  reading for tube

sample,  $C_{Bal} = 2.84. \Rightarrow$  balance calibration constant

$\chi_M = \chi_g \times M.Wt.$  where,  $\chi_M =$  molar magnetic susceptibility

$\chi_g =$  gram magnetic susceptibility

The  $\chi_M$  diamagnetic correction  $\Rightarrow$  Pascal constants to obtain corrected magnetic susceptibility ( $\chi_M \text{ corr}$ ) .<sup>[75]</sup>

Magnetic moment  $\mu_{\text{eff}} = 2.828 \sqrt{X_A} \cdot T \Rightarrow T = t (^{\circ}\text{C}) + 273$

### 2.2.7. Elemental micro analysis

Elemental micro analysis for some complexes performed from (C.H.N.S.) analyzer EURO EA (EA3000) elemental analyzer at the College of Science, Al-Mustansiriyah University.

### 2.2.8. The infrared spectra

The infrared spectra were recorded on a *SHIMADZU* 8300 Fourier Transform Infrared Spectrophotometer (F.T.IR) by (4000-400)  $\text{cm}^{-1}$ .

## 2.3 Procedures For (Biological ) Evaluation

Antibacterial & antifungal- activities of the all compounds in this study were using disc diffusion method( cultivated on neutral agar medium) tested in vitro against ( 1- fungi and 2- bacterial) species. The degree of biological activities was determined by measuring [(IZ) diameter of the inhibition zone] and compared with the Dimethyl sulfoxamide (DMSO) as Control <sup>[76]</sup>.The test solution ( $3 \times 10^{-3}$  M) was



prepared by dissolving the compounds in DMSO. The dishes were incubated at 37 C for 2-days where clear or inhibition zones were detected around each hole. 0.1 mL DMSO alone under the same condition for each organism and by subtracting the (IZ) resulting with DMSO from that obtained in each case [76].

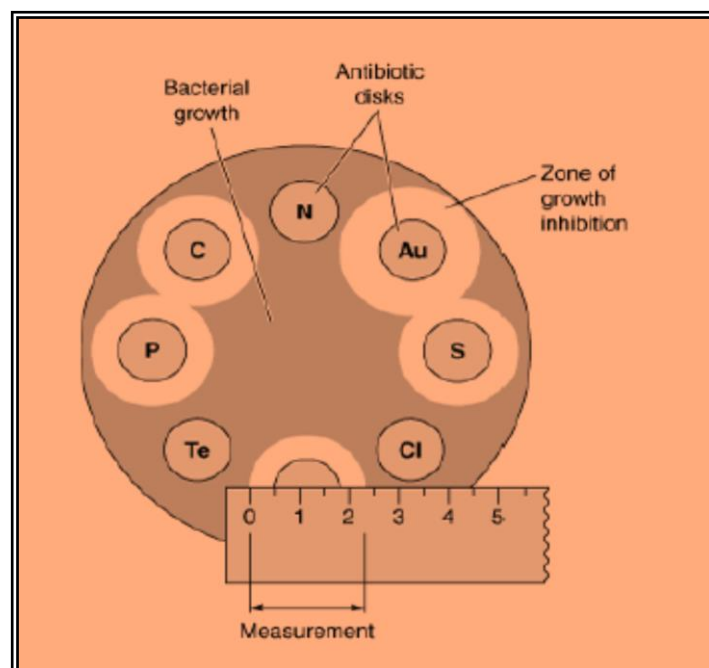


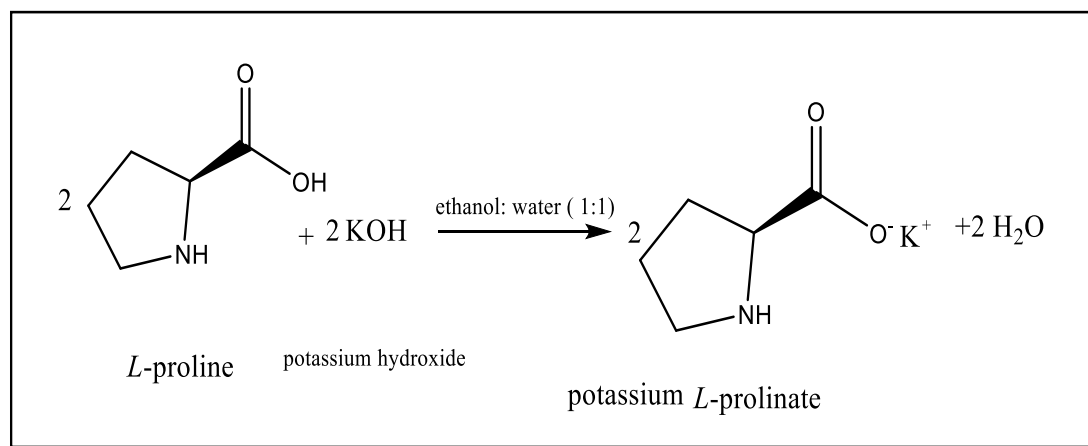
**Figure (2-1) : Antibiotic sensitivity testing**

## 2.4 General Preparation of Mixed- ligand Metal Complexes with some metal ions

All the complexes were prepared by a similar procedure: [77-79] using all salts as metal chlorides. Table (3.2) weights metals chloride

### 2.4.1 preparation of potassium L-prolinate

Potassium L- prolinate ( $K + proH$ ) was prepared by neutralization A solution in ethanol: water ( 1:1) of ( 2 mmol, 0.22) gm ) of L-proline acid with (2 mmole ,0.11 gm) of KOH according to the following reaction.



**Scheme (2-1): preparation of potassium L-prolinate**

### 2.4.2 preparation of $[M(SMZ)(L-Pro)_2]$ and $[M'(SMZ)(L-pro)_2] Cl$ complexes .

Set of metal chloride solution  $MCl_2 \cdot nH_2O$  [ $n=0 \dots 6$ ] and  $M'Cl_3 \cdot 6H_2O$  .

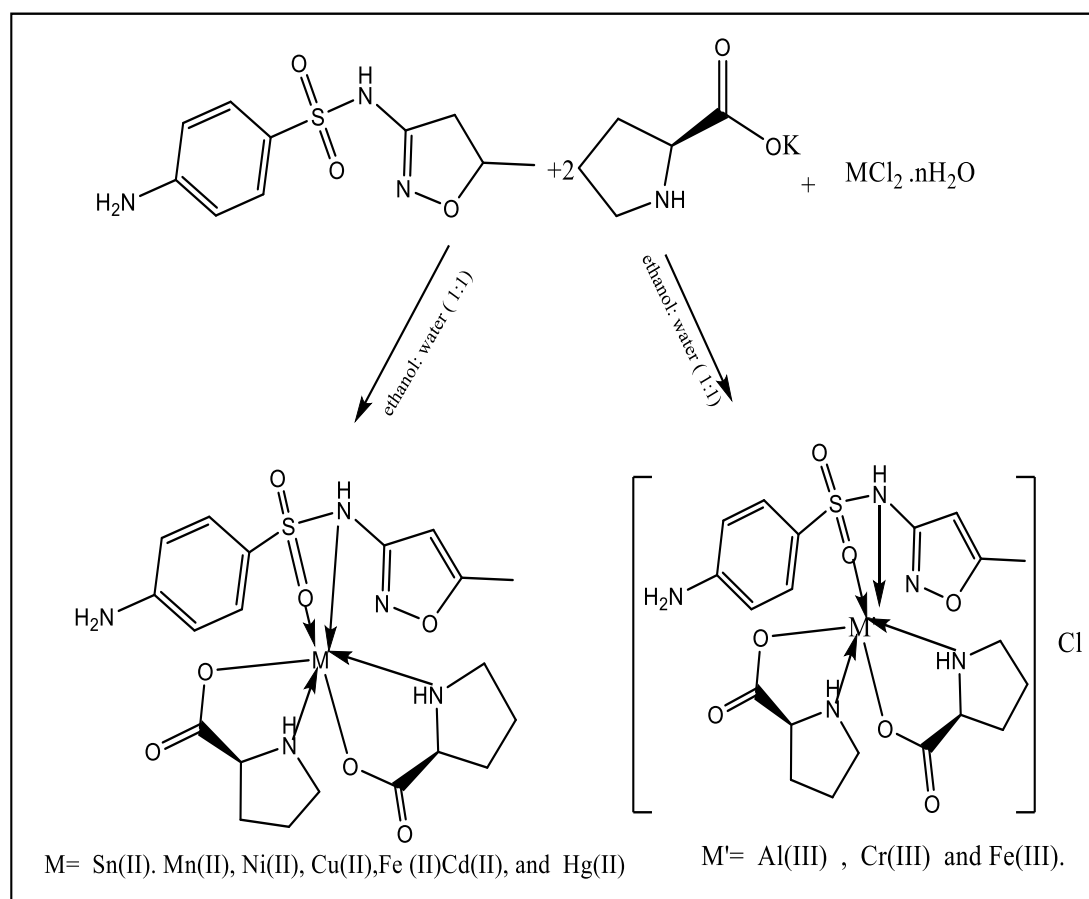
$M = Sn(II), Mn(II), Ni(II), Cu(II), Fe(II), Cd(II),$  and  $Hg(II)$

$M' = Al(III), Cr(III)$  and  $Fe(III)$ . ( 1 mmol ,10 mL) of metal chloride was prepared by dissolving (Weight of metal chloride (gm.1mmole) showed in Table (2-2) and reaction mixture to raise the pH up to  $\sim 6.0$

**Table (2-2): Weights metals Chloride**

<b>Metal Salts</b>	<b>of metal Weight chloride (gm) (1mmole)</b>
SnCl <sub>2</sub> .2H <sub>2</sub> O	0.225
MnCl <sub>2</sub> .4H <sub>2</sub> O	0.197
FeCl <sub>2</sub>	0.126
CoCl <sub>2</sub> .6H <sub>2</sub> O	0.238
NiCl <sub>2</sub> .6H <sub>2</sub> O	0.237
CuCl <sub>2</sub> .2H <sub>2</sub> O	0.170
CdCl <sub>2</sub> .2H <sub>2</sub> O	0.219
CrCl <sub>3</sub> .6H <sub>2</sub> O	0.266
FeCl <sub>3</sub>	0.161
AlCl <sub>3</sub>	0.133

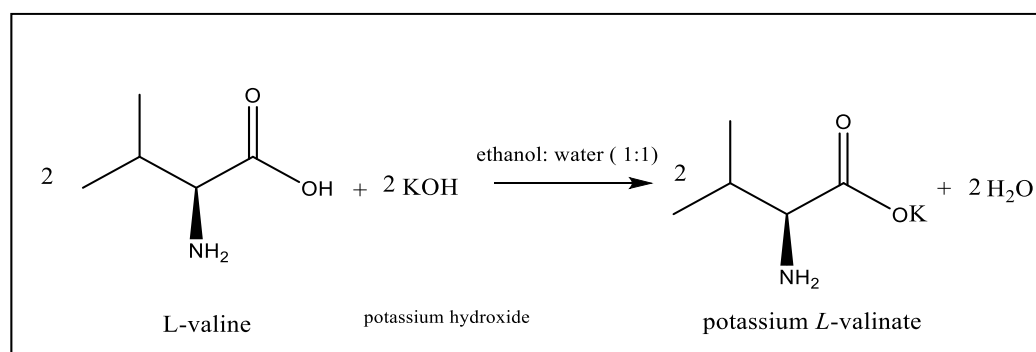
A solution of sulfamethoxazole (0.252 gm , 1 mmole , 10 mL ) ethanol: water 1:1 and 10 mL solution of potassium L-prolinate method that mentioned in 2.7.2 were added simultaneously to stirred for 1 hour solution of metal chloride in the stoichiometric ratio. [SMZ: M: 2(K<sup>+</sup> L-Pro<sup>-</sup>)] (Scheme 2.2). The solution was stirred for (20-60 ) minute and allowed to stand for over night . The product formed was filtered off , washed with aqueous ethanol (1:1) dried in air ,and analyzed employing standard method according to the following reaction Scheme (2-2).



Scheme (2-2) : preparation of  $[M(\text{SMZ})(\text{L-Pro})_2]$  and  $[M'(\text{SMZ})(\text{L-pro})_2] \text{Cl}$ .

### 2.4.3 Preparation of potassium L-Valinate

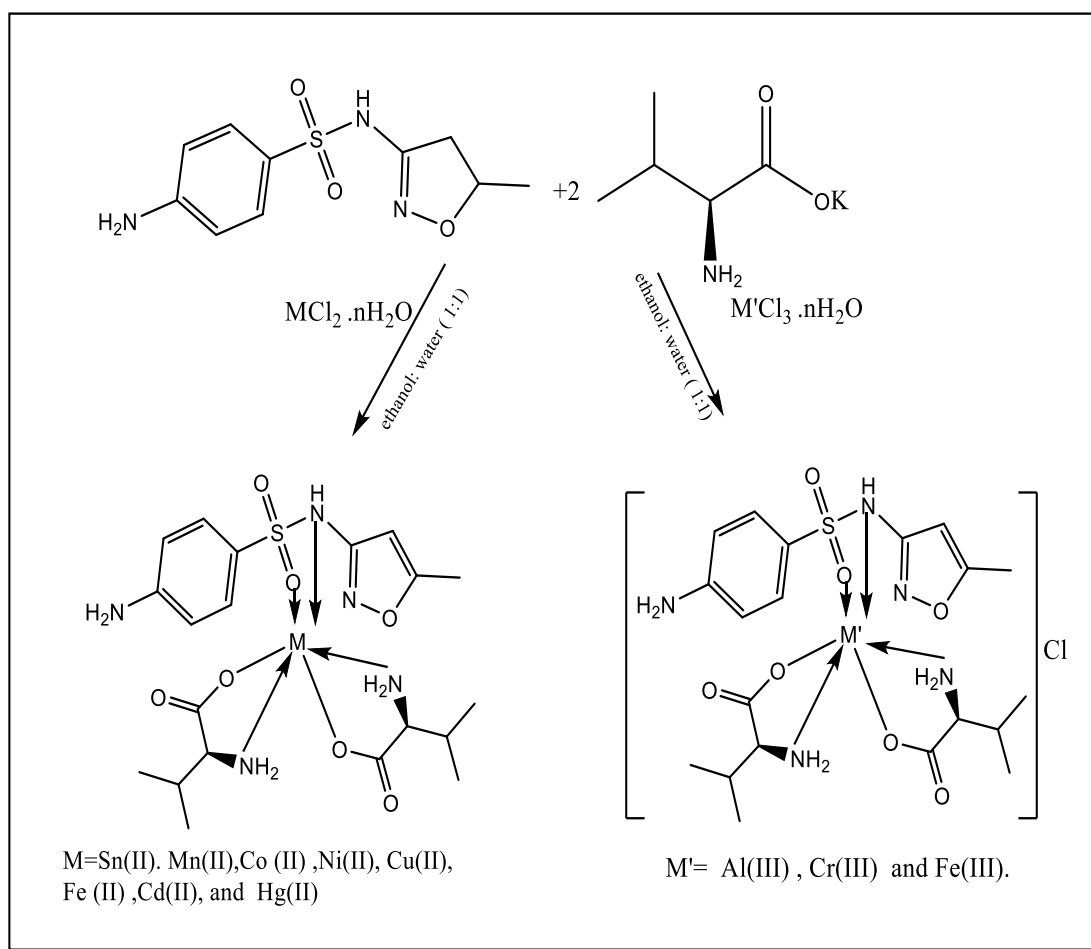
potassium L- Valinate ( $\text{K}^+ \text{L-Val}^-$ ) was prepared by neutralization of 2mmol ( 0.22 gm ) of L-Valine acid with (2 mmole ,0.11 gm)of KOH in a flask and stirred at room temperature according to the Scheme (2-3)



Scheme (2-3): Preparation of Potassium L- Valinate

### 2.4.4 Preparation of $[M(\text{SMZ})(\text{L-Val})_2]$ and $[M'(\text{SMZ})(\text{L-Val})_2]\text{Cl}$ complexes

The same procedure as described under 2.5.2 was employed, except use potassium L-Valinate method that mentioned in 2.5.3 were added simultaneously to a stirred for 1 hour solution of metal chloride in the stoichiometric ratio  $[\text{SMZ}: \text{M}: 2(\text{K}^+ \text{L-Val}^-)]$  according to the reaction Scheme (2-4).

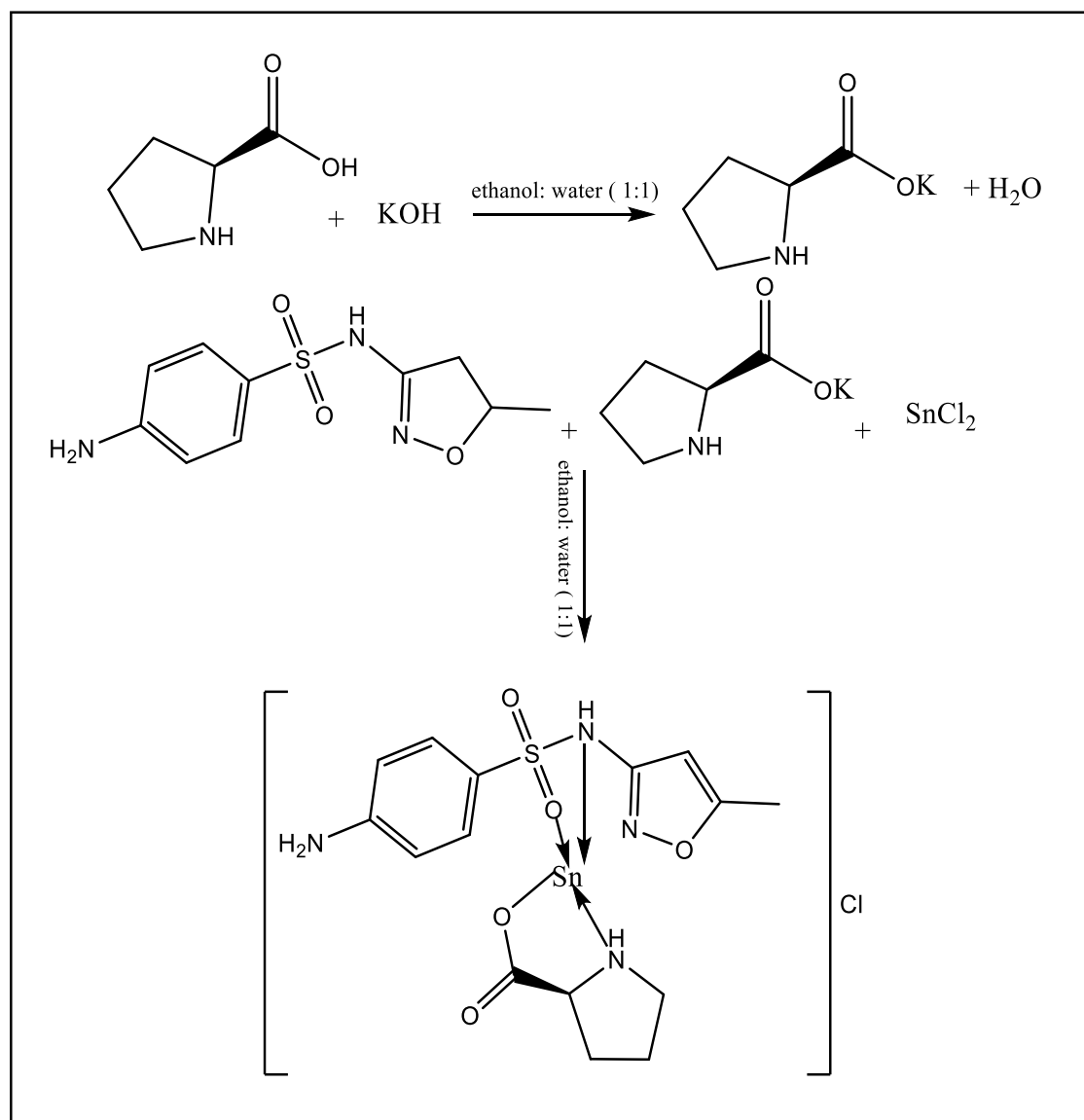


Scheme (2-4): Preparation of  $[M(\text{SMZ})(\text{L-Val})_2]$  and  $[M'(\text{SMZ})(\text{L-Val})_2]\text{Cl}$

### 2.4.5 Preparation of $[\text{Sn}(\text{SMZ})(\text{L-Pro})]\text{Cl}$

A solution of sulfamethoxazole (0.252 gm, 1 mmole, 10 mL) ethanol: water (1:1) and 10 mL solution of potassium L-prolinate

method that mentioned in 2.5.2 were added simultaneously to a stirring for (1 hour) solution of Sn (II) chloride (0.22 gm,1 mmole) in the stoichiometric ratio.[SMZ: Sn: (K<sup>+</sup> L-Pro<sup>-</sup>) Scheme (2-5) .



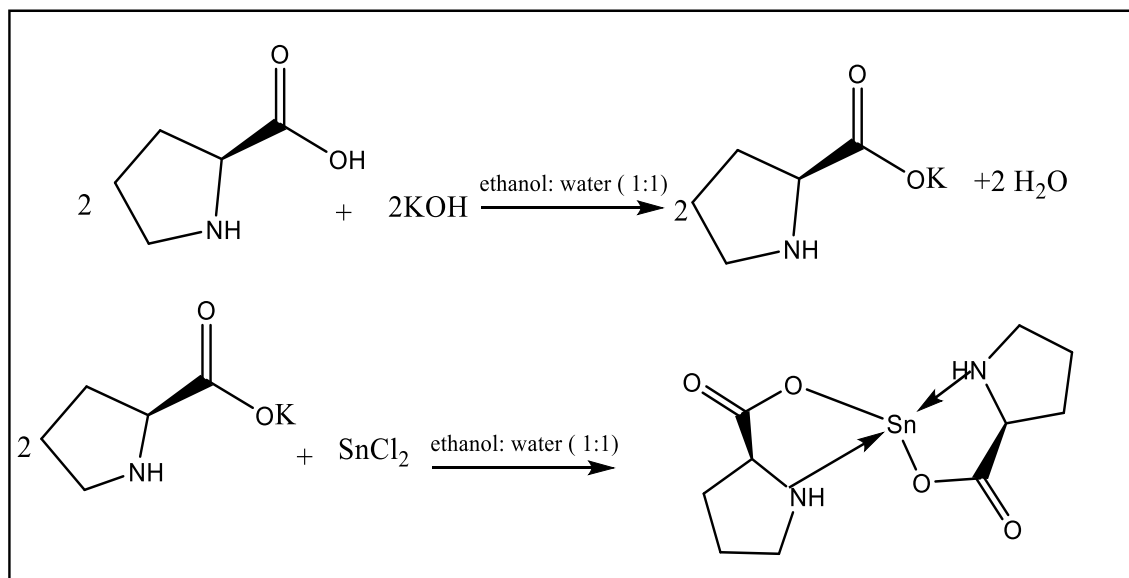
Scheme (2-5) : Preparation of [ Sn(SMZ)( L-Pro)]Cl

## 2.5 Preparation of mono - ligand Metal Complexes

### 2.5.1 Preparation of [Sn(L-Pro)<sub>2</sub>]

A solution of potassium L-prolinate (2mmol, 0.22 gm ) , 10 mL) in (1/1) ethanol-water (20 mL) was added with stirring to Sn (II) chloride

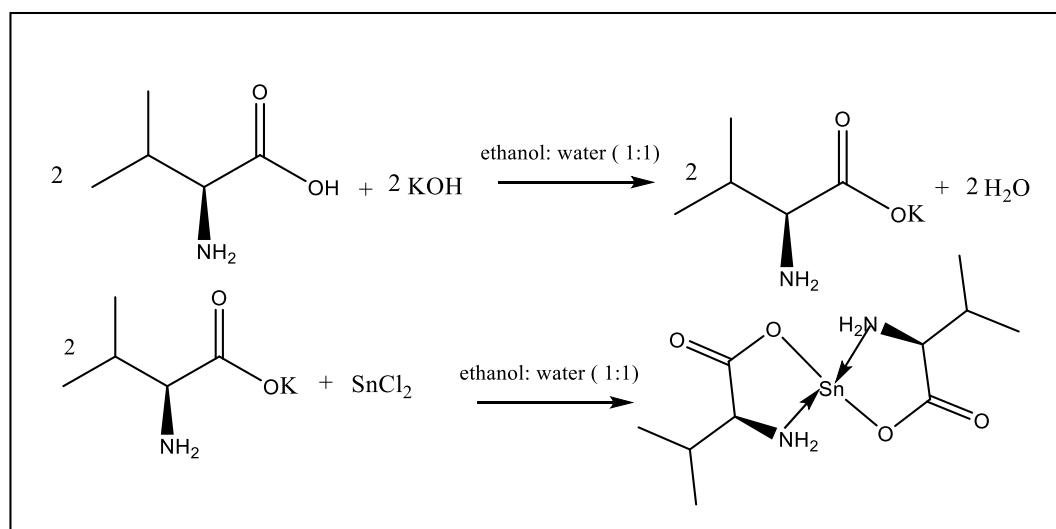
(0.22 gm, 1 mmole) dissolved in ethanol: water 50 % 20mL in a flask and stirred at room temperature by using stoichiometric amount (1:2) Metal : ligand molar ratios, the mixture was stirred for (30 mint) . The solid precipitate obtained collected by the filtration and recrystallized from H<sub>2</sub>O/ethanol as light yellow powder .



Scheme (2-6) : Preparation of [Sn(L-Pro)<sub>2</sub>]

### 2.5.2 Preparation of [Sn(L-Val)<sub>2</sub>]

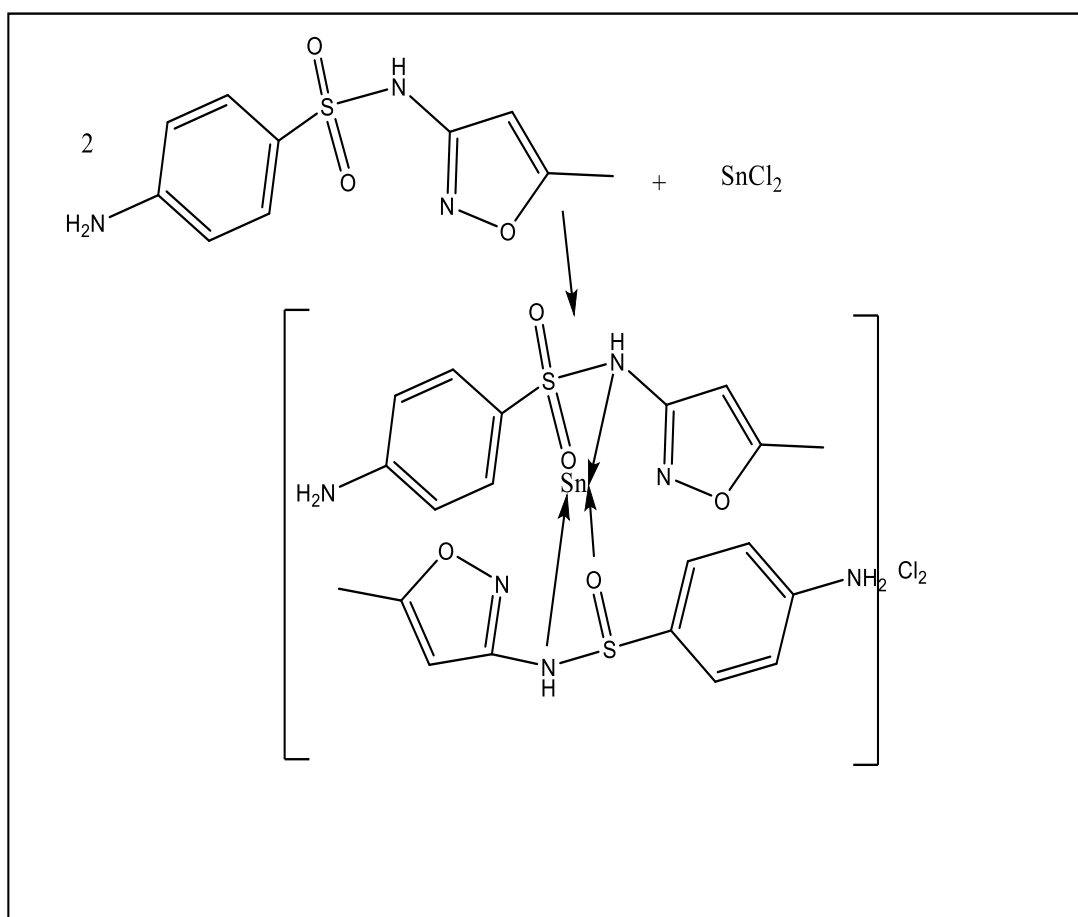
A solution of potassium L-Valinate (K<sup>+</sup> L-Val<sup>-</sup>) (2mmol) , 10 mL) in (1/1) ethanol-water was add with stirring to Sn (II) chloride (0.22 gm, 1 mmole) dissolved in ethanol: water 50 % 20mL in a flask and stirred at room temperature by using stoichiometric amount (1:2) metal : ligand molar ratios, the above reaction mixture to raise the pH up to ~ six and the mixture was stirred for (30 min) , The solid precipitate obtained collected by the filtration and recrystallized from H<sub>2</sub>O/ethanol , Scheme (2-7).

Scheme (2-7) : Preparation of [Sn(L-Val)<sub>2</sub>]

### 2.5.3 Preparation of [Sn(SMZ)<sub>2</sub>]Cl<sub>2</sub>

A solution of sulfamethoxazole (0.5 gm, 2 mmole) in (1/1) ethanol-water (20 mL) was added with stirring to Sn (II) chloride (0.22 gm, 1 mmole) dissolved in ethanol: water 50 % 20mL in a flask and stirred at room temperature by using stoichiometric amount (1:2) metal : ligand molar ratios, the mixture was stirred for (30mint). The solid precipitate obtained collected by the filtration and recrystallized from H<sub>2</sub>O/ethanol as light yellow powder .





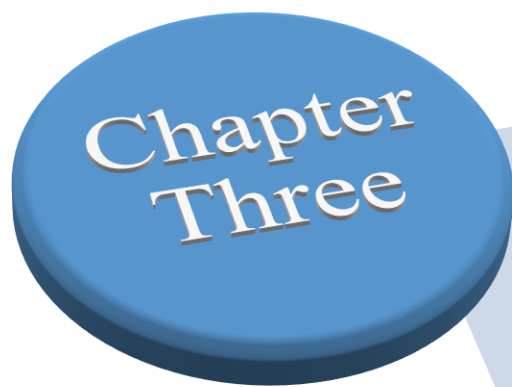
Scheme (2-8) : Preparation of  $[\text{Sn}(\text{SMZ})_2]\text{Cl}_2$

Stoichiometry of the  $[\text{Sn}(\text{SMZ})_2]\text{Cl}_2$  complex formed by Sn (II) chloride and sulfamethoxazole is determined using the Job's (CVM), spectrophotometry is based on the measurement of a series of different solutions such as those shown in Table 2 in which the molar concentrations of two reactants differ but their sum is constant ( $1 \times 10^{-3}$  M). Ten clean 100-mL volumetric flasks were labeled 1 to 10. The mole fraction of SMZ and Sn in the solution at a suitable wave length (408 nm) was calculated using distilled water as reference. Table (2-3). After (5 minutes) the absorbance (A) of each solution was measured at 408 nm. The mole fraction of each component in the solution was calculated and plotted against absorbance using distilled  $\text{H}_2\text{O}$  as reference. <sup>[79]</sup>

Table (2-3): Data for (CVM)of Determining Stoichiometry of Complex

<b>Volumes of Flask 1 mL sulfamethoxazole sol'n ligand 1x10<sup>-3</sup> M</b>	<b>Flask 2 mL Sn sol'n metal 1x10<sup>-3</sup> M</b>
10	0
9	1
8	2
7	3
6	4
5	5
4	6
3	7
2	8
1	9
0	10

The mole fraction in which the number of moles of Sn<sup>2+</sup> and SMZ are in the stoichiometric ratio. Since the sum of mole fractions in a mixture always =1.



Results  
&  
Discussion

### 3.1. General Methodology

Many biologically important reactions take place with the aid of drugs and amino acids in which transition-metal atoms play an important roles. [80-81] The effects of M(II) and M' (III) metal ions on the catalase-like activities. One types of antibiotics including Sulfamethoxazole and two amino acids including (L-Proline, and L-Valine ) have been selected to synthesis and characterization of the five style of complexes as below:

#### A: Mixed-Ligand metal complexes

#### B: Mono Ligand metal complexes

A: Sulphamethoxazole (*antibiotics*) are used as primary ligands and/or

L-Proline, and L-Valine respectively as secondary ligands with M(II) and M' (III) complexes as shown in the Table (3-1).

**Table (3-1): Compositions of synthesised Mixed- Ligand Metals Complexesc**

Ttype Mixed ligand complexes	Primary ligand	Secondary Ligand amino acid	Compositions
Style 1 L-ProH M SMZ. 2.1.1 1.1.1	Sulfamethoxazole (SMZ)	L-Proline (L-ProH)	$[(L-Pro)_2 M (SMZ)]$ M= Mn(II), Fe (II),Ni(II), Cu(II),Cd(II), Hg(II) and Sn(II)
	Sulfamethoxazole (SMZ)	L-Proline (L-ProH)	$[(L-Pro)_2 M' (SMZ)]Cl$ M' = Al(III) ,Cr(III) and Fe(III)
	Sulfamethoxazole (SMZ)	L-Proline (L-ProH)	$[Sn(SMZ)(L-Pro)]Cl$
Style 2 L-Val M. SMZ. 2.1.1	Sulfamethoxazole (SMZ)	L-Valine (L-ValH)	$[(L-Val)_2 M (SMZ)]Cl$ M= Mn (II), Fe (II), Co(II),Ni(II), Cu(II), ,Cd(II), Hg(II) and Sn(II)
	Sulfamethoxazole (SMZ)	L-Valine (L-ValH)	$[(L-Val)_2 M' (SMZ)]Cl$ M' = Fe(III) ,Cr(III) and Al(III)

## B : Mono Ligand Complexes

Sulphamethoxazole (*antibiotics*) L-Proline, and L-Valine are used as mono ligand complexes as shown in the Table (3-2)

Table (3-2): Compositions of synthesised Mono ligand Metals Complexes

Type	ligands	Compositions
Style 1	Sulfamethoxazole (SMZ)	$[\text{Sn}(\text{SMZ})_2]\text{Cl}_2$
Style 2	amino acid L-Proline ( L-ProH)	$[\text{Sn}(\text{L-Pro})_2]$
Style 3	amino acid L-Valine ( L-ValH)	$[\text{Sn}(\text{L-Val})_2]$
Style 4	Sulfamethoxazole (SMZ)	$[ \text{M}'(\text{SMZ})_3]\text{Cl}_3$ $\text{M}'=\text{Fe}(\text{III}),\text{Cr}(\text{III})$ and $\text{Al}(\text{III})$

### 3.2. (U.V-Vis) Spectra of the Ligands

The electronic spectral studies of ligands Table (3-3) were carried out in DMSO ( $10^{-3}\text{M}$ ) solution <sup>[77,78]</sup>.

Table (3-3) : Electronic data of starting materials and ligands

Symbol	nm $\lambda$	$\epsilon$ max molar <sup>-1</sup> .cm <sup>-1</sup>	$\nu'$ cm <sup>-1</sup>	Assignment
SMZ	275	1951	36363	$\pi \rightarrow \pi^*$
L-proH C <sub>5</sub> H <sub>9</sub> NO <sub>2</sub>	240	312	41666	$\pi \rightarrow \pi^*$
	284	131	35211	$n \rightarrow \pi^*$
	349	40	28653	$n \rightarrow \pi^*$
L-ValH C <sub>5</sub> H <sub>11</sub> NO <sub>2</sub>	279	36900	38314	$\pi \rightarrow \pi^*$
	342	885	3250	$n \rightarrow \pi^*$

#### 3.2.1 (U.V-Vis) Spectrum of the (SMZ)

The UV -Vis spectrum of the (SMZ)in (DMSO) solvent appeared a high intense absorption band due to the C=N chromophore at 275 nm ( $36363 \text{ cm}^{-1}$ ) ( $\epsilon_{\text{max}}=1951 \text{ molar}^{-1}.\text{cm}^{-1}$ ) ( $\pi-\pi^*$  transition) within the organic ligand. <sup>[82-83]</sup>

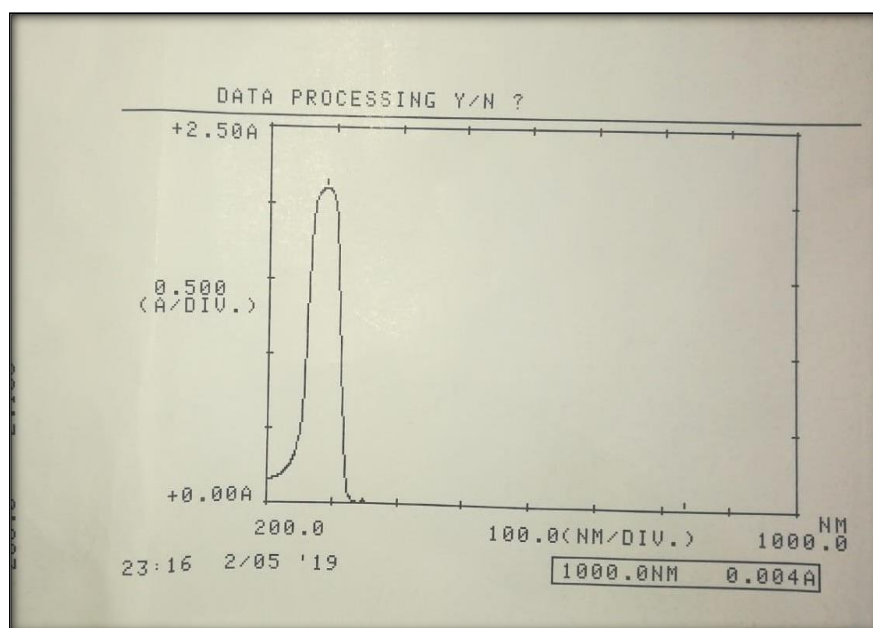


Figure (3-1) : U.V-Vis- Spectrum of the (SMZ)

### 3.2.2 (U.V-Vis) Spectrum of the (proH )

The (U.V-Vis) spectrum of the (L-proH ), Figure (3-2) and Table (3-7), exhibits three band at 240 ,284 and 349 nm. The first one may be assigned to intraligand ( $\pi \rightarrow \pi^*$ ) transition, where as the second and third band may be assigned to the ( $n \rightarrow \pi^*$ ) transition of the heterocyclic and COO-groups [nnn]. It is found that these bands were shifted to lower energy on complexation, [83]

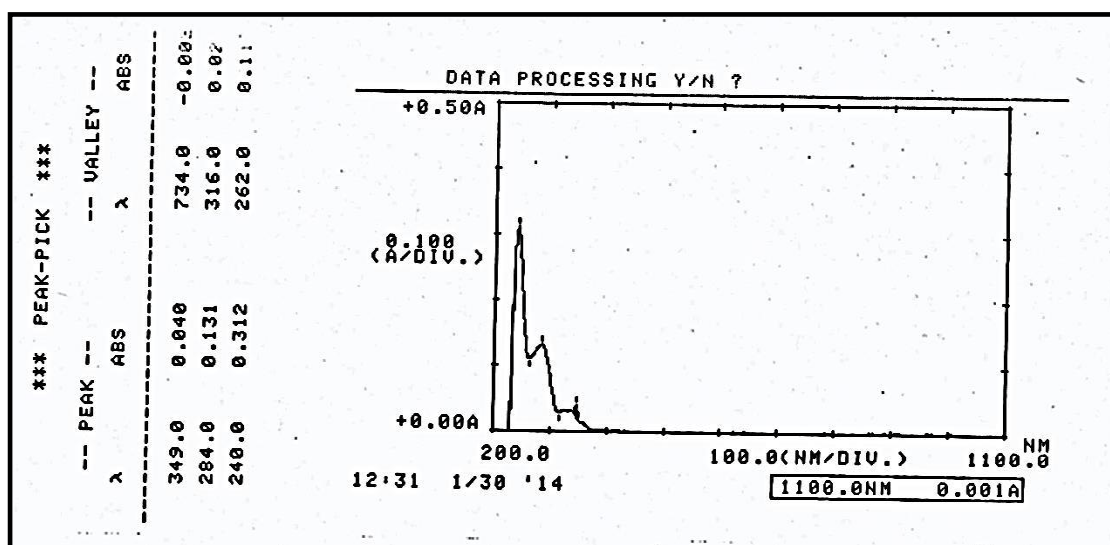


Figure (3-2) U.V-Vis- Spectrum of the (L-proH )

### 3.2.3. (U.V-Vis) Spectrum of the (L-ValH)

The (U.V-Vis) spectrum for the L-Valine, Figure (3-3), exhibits absorption peak at (279 nm)( 36900  $\text{cm}^{-1}$ ) and an intense peak at 342 nm ( $3250\text{cm}^{-1}$ ), assigned to ( $\pi \rightarrow \pi^*$ ), and ( $n \rightarrow \pi^*$ ) transition respectively [84-85]

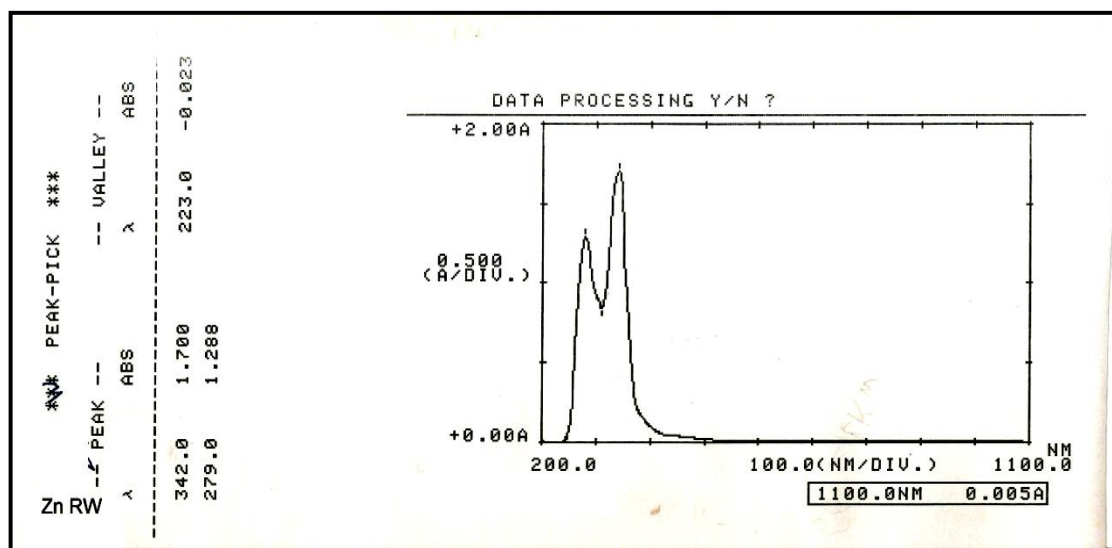


Figure (3-3): U.V-Vis- Spectrum of the (L-ValH)

## 3.3. FT-IR Spectra of the Ligands

### 3.3.1. FT-IR Spectrum of (SMZ)

The FTIR spectrum of the sulfamethoxazole. Table (3-4) and Figure(3-4) showed bands at (3468,3379)  $\text{cm}^{-1}$  and (3300)  $\text{cm}^{-1}$  were assigned to stretching vibrations of  $-\text{NH}_2$  and  $-\text{NH}$  respectively of free (SMX) , (C=N) of isoxazol ring at (1622)  $\text{cm}^{-1}$ . Sulfoxide ( $\text{SO}_2$ ) stretching occurs at 1365  $\text{cm}^{-1}$  [ $\nu_{\text{asym.}}(\text{SO}_2)$ ] and 1148  $\text{cm}^{-1}$  [ $\nu_{\text{sym.}}(\text{SO}_2)$ ]. The stretching band  $\nu$  of aromatic (C=C) showed at 1504  $\text{cm}^{-1}$ . [86]

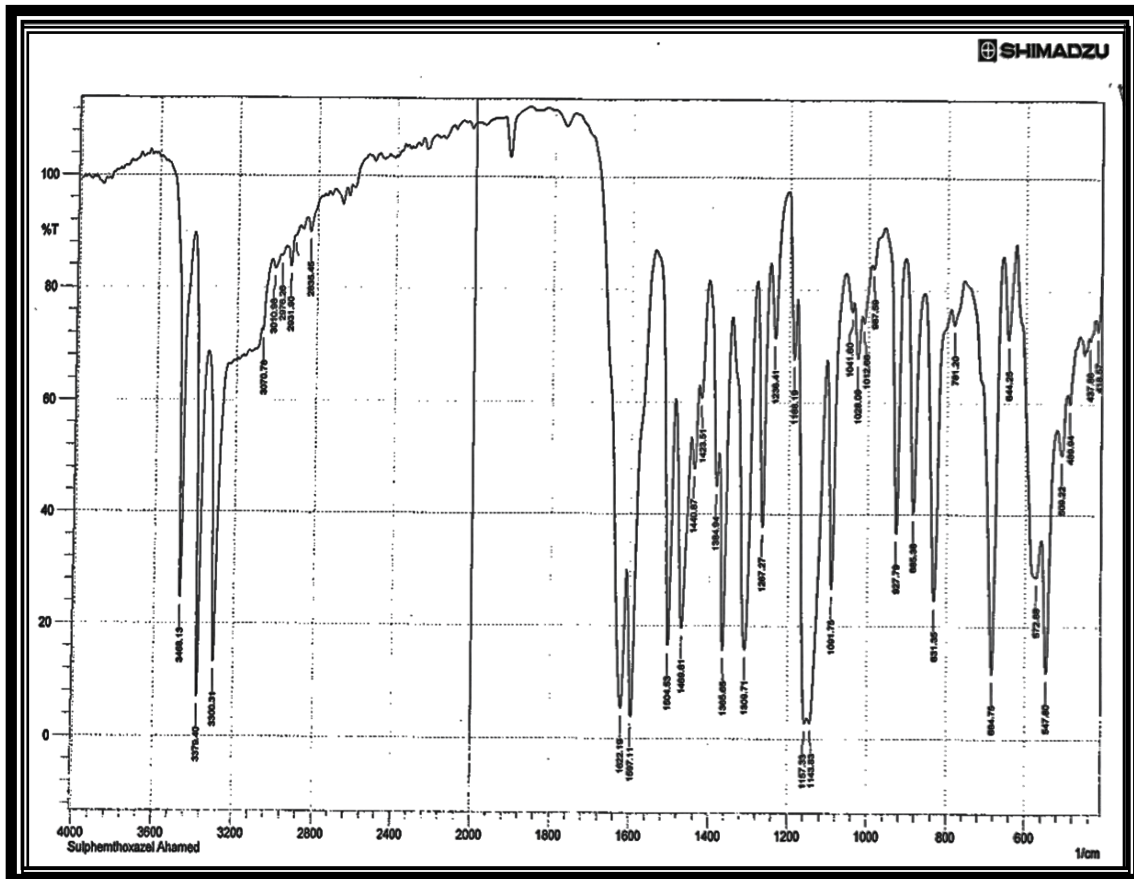


Figure (3-4) : FT- IR spectrum of (SMZ)



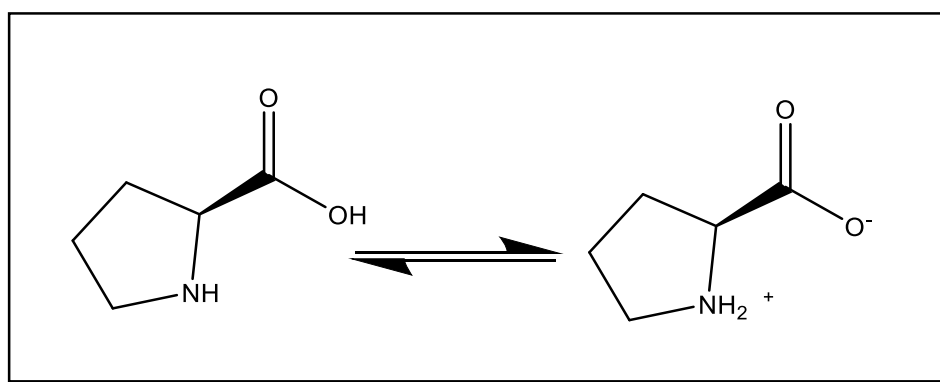
Table ( 3 -4 ) : FT-R spectral data (  $\nu$  )  $\text{cm}^{-1}$  for the SMZ

	( $\nu$ as $\text{NH}_2$ , $\nu$ s $\text{NH}_2$ ) amine – & –NH amide	as (NH): And $\nu$ s (NH): sulfonam ide	(C–H) Aliph and Arom.	$\delta(\text{NH}_2)$	$\nu(\text{C}=\text{C})$ : phenyl ring	$\nu\text{SO}_2$ asy	$\nu(\text{C}=\text{N})$ isoxazol ring	$\nu(\text{C}-\text{O})$	$\nu(\text{SO}_2)$ sy	$\nu(\text{S}-\text{N})$	$\nu(\text{C}-\text{S})$	$\nu(\text{N}-\text{O})$
SMZ	3468 s 78s33	3070	2929 w 2831	1620 vs	1597 vs 1504	1365 s	1622	1267 ms	1157 1143	987 w	831 Vs	1309

$\nu$ s = very strong , s = strong , m= medium , w = weak

### 3.3.2. FT-IR Spectrum of L- proline

The FT- IR spectrum of free ligand amino acid such as (L- proline) {  $\nu$  NH<sub>2</sub><sup>+</sup> and  $\nu$  COO<sup>-</sup> } regions free amino acids exist as zwitterions. <sup>[85]</sup> .The chelation of L- proline (ProH) was evidently present in its (zwitterionic form) therefore, the N-H moiety must be protonated, generating a (NH<sub>2</sub><sup>+</sup>) group whereas the acid group remains in the anionic (COO<sup>-</sup>) group form , Scheme (3-1) .



Scheme (3-1): Zwitter ion of L-proline

FT-IR spectrum for the (L- proline ) summarized in Table (3-5) , Figure (3-5) exhibited a band around  $\nu(3417)\text{cm}^{-1}$  that corresponds to the stretching vibration of  $\nu(\text{N-H})$  ,  $\nu(\text{O-H})$ , strong absorption band at  $\nu(3080)\text{cm}^{-1}$  is due to the  $\nu(\text{N-H})_{\text{sym}}$  while the very strong bands at  $1650\text{cm}^{-1}$  ,  $\nu(\text{COO})_{\text{asy}}$  1415 -1360  $\text{cm}^{-1}$  ,  $\nu(-\text{COO})_{\text{sym}}$  and.  $\nu(\text{C-N})$  1242  $\text{cm}^{-1}$  respectively.

Table (3-5): FT-IR Spectrum of L- proline

L-proH	$\nu(\text{N-H}) + \nu(\text{O-H})$	$\nu(\text{C-H})$	$\nu(-\text{COO})_{\text{asy}}$	$\nu(-\text{COO})_{\text{sym}}$	$\nu\text{C-N}$
C <sub>5</sub> H <sub>9</sub> NO <sub>2</sub>	3417s-br	2958 s 2874m	1650 vs	1415-1360 vs	1242 vs

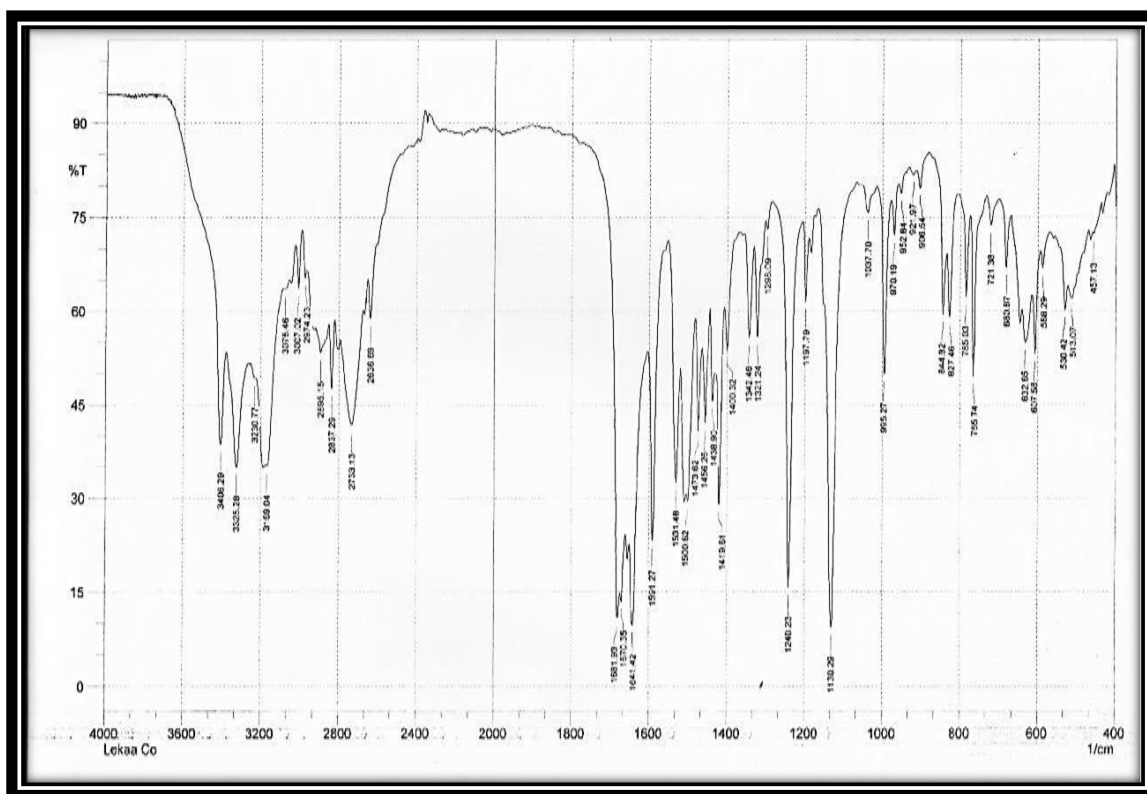
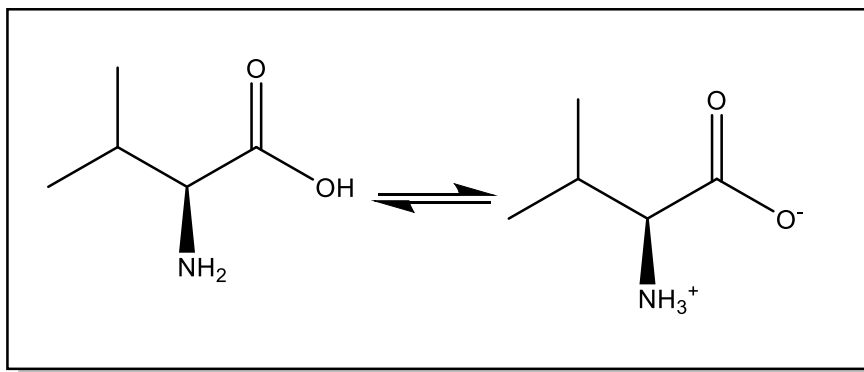


Figure (3-5) : FT- IR spectrum of L- proline

### 3.3.3. FT-IR Spectrum of L- Valine

The FT- IR spectrum of free amino acid ligand such as (L-Valin) {  $\nu$   $\text{NH}_3^+$  and  $\nu$   $\text{COO}^-$  } regions free amino acids exist as zwitterions. [98] Scheme (3-2), exhibited a strong band around (3382)  $\text{cm}^{-1}$  that corresponds to the  $\nu$  (N-H) +  $\nu$  (O-H), strong absorption band at (1597)  $\text{cm}^{-1}$  is appeared which could explained as  $\nu$  (OCO)<sub>asym</sub> where the  $\nu$  (OCO)<sub>sym</sub> was noticed at (1300)  $\text{cm}^{-1}$  [14]. A broad band at 2927  $\text{cm}^{-1}$  is due to asymmetric stretch of  $\nu$   $\text{CH}_2$  group, three peaks at (2880, 2865, 2835) and 2810  $\text{cm}^{-1}$  due to Asymmetric  $\nu$   $\text{CH}_2$  group, A broad band is seen at 2104  $\text{cm}^{-1}$  in IR spectrum of valine molecule. This is due to combination  $\text{CH}_3$  bend and the rocking vibration of amine ( $\text{NH}_2$ ) group (1065+1032). Table (3-6) and Figure (3-6).



Scheme (3-2): Zwitter ion of L-Valine

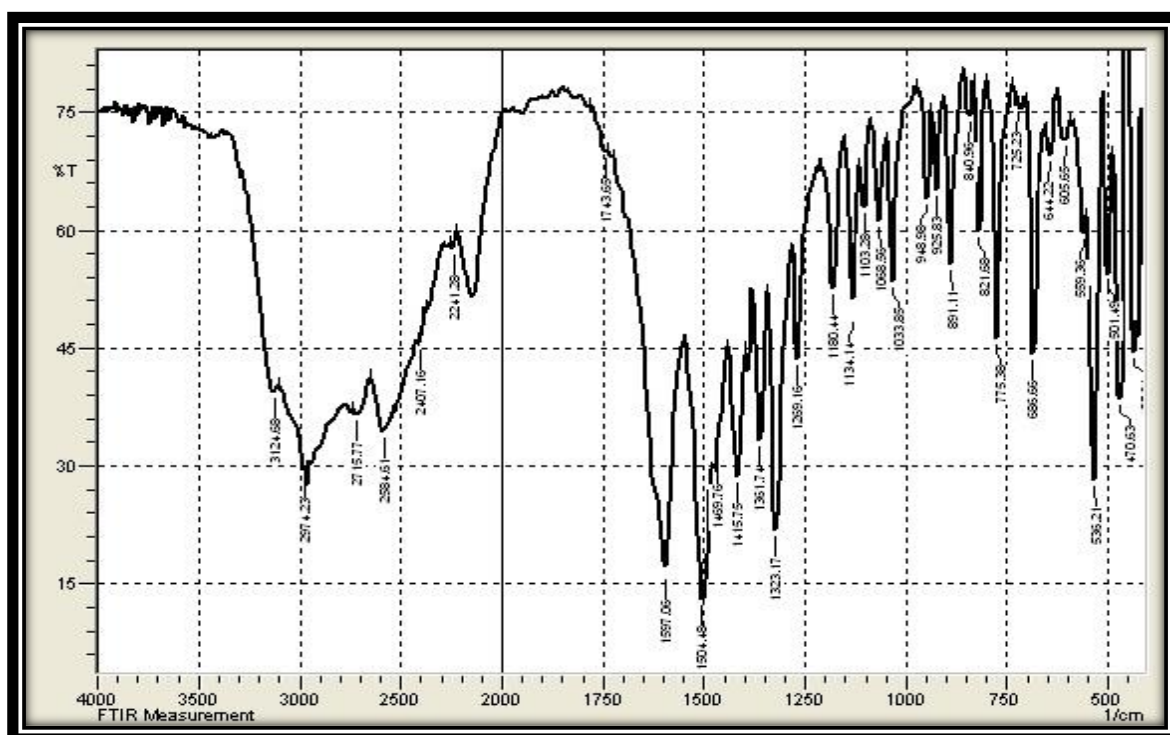


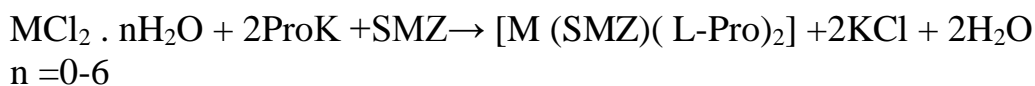
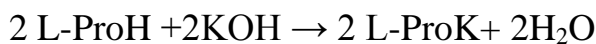
Figure (3- 6) FT-IR spectrum of (L-Valine)

**Table (3-6): Infrared Spectrum Data (wave number  $\nu$ ) cm<sup>-1</sup> for the L- Valine**

L- Valine	$\nu$ (N-H <sub>2</sub> ) + $\nu$ (O-H),	$\nu$ (C-H <sub>2</sub> )	$\nu$ (-COO)asy	$\nu$ (-COO)sym	$\Delta\nu$ (-COO) asy-sym
C <sub>5</sub> H <sub>11</sub> NO <sub>2</sub>	3382 br	2927 s 2880 2865m	1597vs	1457vs	140

### 3.4. Physico-Chemical Characterization of Mixed – ligand (L-prolin -Metal - SMZ) Complexes

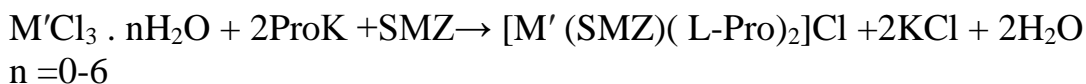
Generally, the metal chloride reacted with the mixed ligands according to the following proposed general equation:



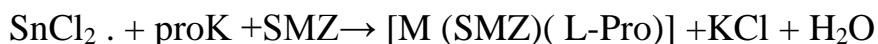
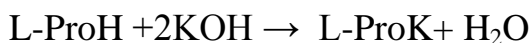
where; L-Pro = deprotonated L-proline symbolized as L-ProH (primary ligand).

Sulfamethoxazole = SMZ (secondary ligand).

M = Sn(II), Mn(II), Fe(II), Ni(II), Cu(II), Cd(II), and Hg(II)



M' = Al(III), Cr(III) and Fe(III) as Scheme (2-2)



As in Scheme (2-5).

All the synthesized complexes were stable in air with varying colors and found to be nonhygroscopic solids, and have higher melting points of the ligand than that of their corresponding complexes reveals that the complexes were much more stable than SMZ and L-ProH ligands. The physical and analytical data of complexes are presented in Table (3-7). The results of elemental analysis were found a direct correlation between the experimentally and the calculated found values indicating the formation of the complexes as shown in Table (3-8). The  $[\text{M}(\text{SMZ})(\text{L-Pro})_2]$  complexes were prepared by reacting the respective with the ligands using 1:1:2 mole ratios. [Metal : (SMZ): (L-proK)<sub>2</sub>], and i.e., one mole of metal chloride : one mole of (SMZ), and two moles of potassium L-proline. while  $[\text{Sn}(\text{SMZ})(\text{Pro})]\text{Cl}$  uses one mole of potassium L-proline. <sup>[87-90]</sup> Atomic

Absorption Spectroscopy (AAS) analysis of the complexes was carried out by the direct method which gave total metal content <sup>[73]</sup>. The calculated and experimental values of metal percentage M % in each complex are in fair agreement. some complexe are not soluble in ethanol, benzene or water , but are soluble in DMF and are more soluble in in dimethyl sulfoxide (DMSO) Table (3-9). All complexes soluble in HCl except [Sn(SMZ)(L-Pro)<sub>2</sub>]. The important of determining Cl ion estimation in the complex is to confirm whether the Cl ion is present in the complex or not. The test for chloride ion for [M(SMZ)(Pro)<sub>2</sub>],[Sn(SMZ)(Pro)]Cl and [M'(SMZ)(Pro)<sub>2</sub>]Cl with AgNO<sub>3</sub> solution was positive (+) for [Sn(SMZ)(Pro)]Cl and [M'(SMZ)(Pro)<sub>2</sub>]Cl indicating that chloride ion is outside of coordination sphere but negative (-) for all [M(SMZ)(Pro)<sub>2</sub>] which in depicted in Table (3-7) n supports of molar conductance measurements. Conductivity measurements of the synthesis complexes in the appropriate solvent are used to decide whether a complex is electrolyte or neutral<sup>(91,92)</sup> Table (3-10).

Table (3-7) : The Physical Properties & Atomic Absorption Results of the [M-SMZ - L-ProH] and [ M'-SMZ - L-ProH] Complexes.

Chemical Formula	Color	M.P °c (de) °c	Yield %	Metal analysis (% found) (% cal)	Λ <sub>m</sub> Ω <sup>-1</sup> cm <sup>2</sup> mol <sup>-1</sup> In DMSO
<b>[SMZ -M-L-ProH]</b>					
[Sn(SMZ)( L-Pro) <sub>2</sub> ]	Pale yellow		85	(23.91) 25	9
[Mn(SMZ)( L-Pro) <sub>2</sub> ]	Gray	235	80	(10.32) 11	7
[Fe(SMZ)( L-Pro) <sub>2</sub> ]	Brown	>260	82	(10.47) 11	11

[Ni(SMZ)( L-Pro) <sub>2</sub> ]	Green	>260	72	(10.95) 12	10
[Cu(SMZ)( L-Pro) <sub>2</sub> ]	Blue	>260	77	(11.74) 12.5	8
[Cd(SMZ)( L-Pro) <sub>2</sub> ]	White	>260	89	(19.05) 20	14
[Hg(SMZ)(Pro) <sub>2</sub> ]	White	230d	82	(26.58) 25	16
<b>[M-SMZ –L-ProH]</b>					
[Al (SMZ)( L-Pro) <sub>2</sub> ]Cl	White	>260	77	5.35	32
[Cr (SMZ)( L-Pro) <sub>2</sub> ]Cl	Green	>260	88	9.82 10.2	32
[Fe(SMZ)( L-Pro) <sub>2</sub> ]Cl	Orange	>260	78	10.47 10.90	34
<b>[Sn(SMZ)( L-Pro)]</b>					
[Sn(SMZ)(Pro)] Cl	White off	>260	66	27.57 28	32

M.wt = Molecular Weight,  $\Lambda_m$ =Molar Conductivity, d = decomposition

Table (3-8): Microanalysis results

Chemical Formula	Elemental analysis Found%			Elemental analysis calculate %		
	C	H	N	C	H	N
[Mn(SMZ)( L-Pro) <sub>2</sub> ]	47.37	5.11	13.15	47.37	5.11	5.91
[Ni(SMZ)( L-Pro) <sub>2</sub> ]	47.04	5.08	13.06	47.04	5.08	13.39
[Cu(SMZ)( L-Pro) <sub>2</sub> ]	46.62	5.03	12.94	46.00	5.03	13.31
[Cd(SMZ)( L-Pro) <sub>2</sub> ]	42.75	4.61	11.87	42.00	4.61.	11.11
Chemical Formula: C <sub>21</sub> H <sub>27</sub> MN <sub>5</sub> O <sub>6</sub> S						

Table (3-9): Solubility of all complexes in different solvents

Chemical Formula	C <sub>3</sub> H <sub>6</sub> O	C <sub>6</sub> H <sub>6</sub>	DMF	DMSO	EtOH	H <sub>2</sub> O	Hexanol	HCl
[Sn(SMZ)(L-Pro) <sub>2</sub> ]	-	-	-	+	-	-	-	--
[Mn(SMZ)(L-Pro) <sub>2</sub> ]	-	-	+	+	-	-	-	+
[Fe(SMZ)(L-Pro) <sub>2</sub> ]	-	-	-	+	-	-	-	+
[Ni(SMZ)(L-Pro) <sub>2</sub> ]	+	--	+	+	-	+	+	+
[Cu(SMZ)(L-Pro) <sub>2</sub> ]	+	+	+	+	+	+	+	+
[Cd(SMZ)(L-Pro) <sub>2</sub> ]	-	+	+	+	--	-	+	+
[Hg(SMZ)(L-Pro) <sub>2</sub> ]	-	-	--	+	+	-	-	+
[Al(SMZ)(L-Pro) <sub>2</sub> ]	+	-	+	+	-	+	-	+
[Cr(SMZ)(L-Pro) <sub>2</sub> ]	-	--	-	+	-	-	-	+
[Fe(SMZ)(L-Pro) <sub>2</sub> ]	+	--	+	+	+	+	-	+
[Sn(SMZ)(L-Pro)]Cl	--	--	--	+	+	-	-	+
(+ ) Soluble, (-) Insoluble, (---) Sparingly								



Table (3-10): Molar Conductivity ( $\Omega^{-1}\text{cm}^2\text{mol}^{-1}$ ) in water and some organic solvents

No.	Solvent	Non Electrolyte	Electrolyte Type			
			1:1	1:2	1:3	1:4
1	Water	0	120	240	360	480
2	Ethanol	0-20	35-45	70-90	120 $\approx$	$\approx$ 160
3	Nitromethane	0-20	75-95	150-180	220-260	290-330
4	Methyl cyanide	0-30	120-160	220-300	340-420	$\approx$ 500
5	Dimethyl formamide	0-35	65-90	130-170	200-240	$\approx$ 300
6	Dimethyl sulfoxide	0-20	30-40	70-80	-	-

### 3.4.1. FT-IR spectra of [M-SMZ - L-ProH] and [M'-SMZ - L-ProH] complexes

In order to determine the coordination sites of the ligand in the complexes, FT-IR spectrum of the ligand was compared with the spectra of the complexes. The relevant vibration bands of the all compounds were recorded in KBr disc in the region 400–4000  $\text{cm}^{-1}$ . The assignment of the characteristic bands FT-IR spectrum of the free ligand L-ProH, Figure (3-2) and SMZ Figure (3-1) are summarized in Table (3-6) and (3-4). The characteristic frequencies of the all complexes are given in Tables (3-11) and (3-12) and shown in Figures (3-7) to (3-17) were supported by comparison with the vibrational frequencies of the free L-ProH. ligands and other related complexes. [28] In all amino acids the stretching vibration of  $\nu(\text{NH}_3^+)$  appears at (3030-3130)  $\text{cm}^{-1}$  region, in the spectrum of L-proline it appears at (3080)  $\text{cm}^{-1}$ . In complexation this band was vanished in all complexes with appearance bands of coordinated ( $\text{NH}_2$ ) within the range (3141-3471)  $\text{cm}^{-1}$ . [13,14,109] The bands at (1650)  $\text{cm}^{-1}$  and (1400)  $\text{cm}^{-1}$  were assigned to the  $\nu(-\text{COO})_{\text{asy}}$  and  $\nu(-\text{COO})_{\text{sym}}$  respectively. in L-proline reveals to

difference between asymmetric ( $\nu_{\text{asym}}$ ) symmetric ( $\nu_{\text{sym}}$ ),  $\Delta\nu(-\text{COO})_{\text{asym-sym}}=200\text{cm}^{-1}$  [8,13,73]. was appeared in the prepared complexes within the range (214-239)  $\text{cm}^{-1}$  Table (3-11) indicating of participate the ( $\text{COO}^-$ ) group as a mono dentate donor in the coordination process with the metal ion . IR all spectra demonstrate that the L-proline act as bidentate ligand in coordination with metal ion involving (  $-\text{COO} \rightarrow \text{M}$  Oxygen carboxylate) a bands due to  $\nu(\text{N-S})$  in all group and  $\text{M} \leftarrow \text{NH-}$  nitrogen imine group The IR spectrum of the free (SMX) ligand Figure (3-4) showed the stretching vibration band at (1622)  $\text{cm}^{-1}$  is due to the  $\nu(\text{C}=\text{N})$  of isoxazol ring, this band was shifted to lower frequencies within the rang (1588-1614)  $\text{cm}^{-1}$ , Table (3-11) proving the involvement C=N group of isoxazol ring in the complexes formation with metal ions [35,38]. The band appears at (1365)  $\text{cm}^{-1}$  is due to the asymmetrical streaching vibration of  $\nu(\text{SO}_2)$  group which is shifted in complexation to higher frequencies within the rang (1367-1394)  $\text{cm}^{-1}$  while the band which appears at (1148)  $\text{cm}^{-1}$  attributed to symmetrical stretching vibration band of  $\nu(\text{SO}_2)$  group, on complexation this band was shifted to lower frequencies within the range (1026-1136)  $\text{cm}^{-1}$ .

Table (3-11) : Infrared spectral data(wave number  $\hat{\nu}$ )  $\text{cm}^{-1}$  for [SMZ – M – L-ProH]

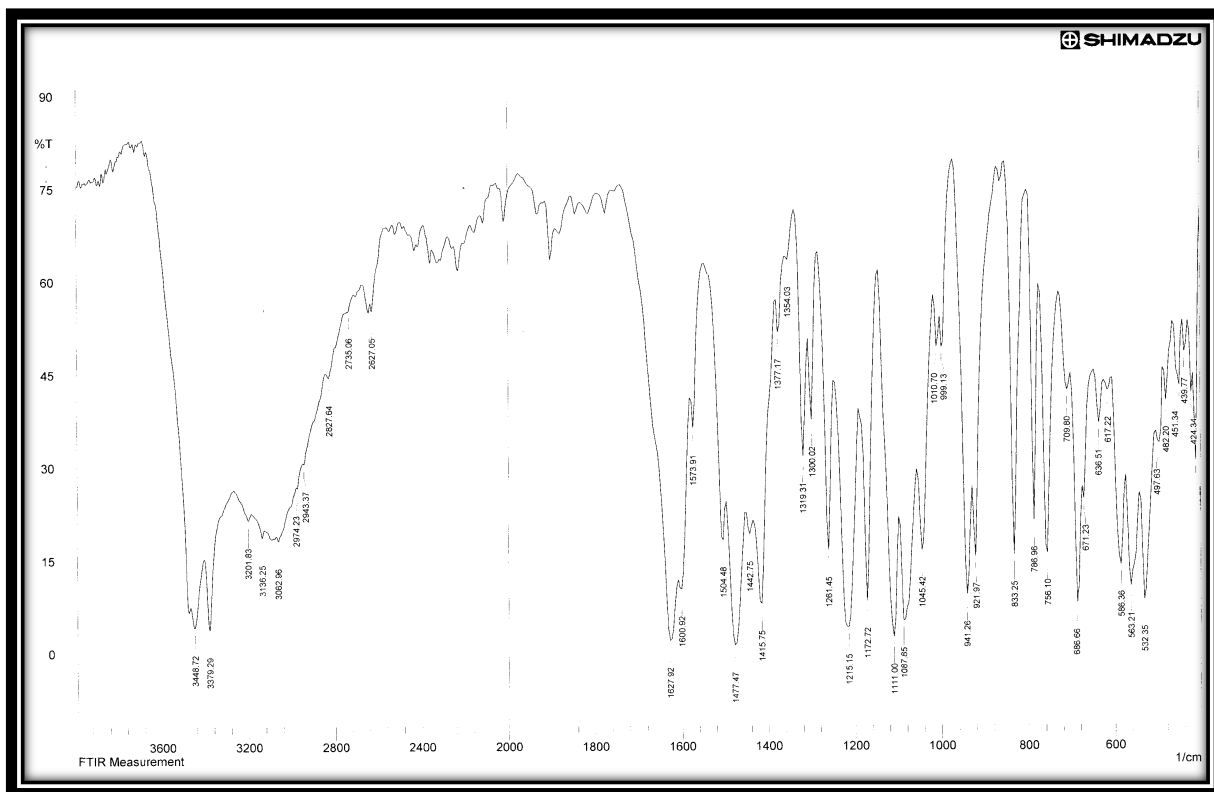
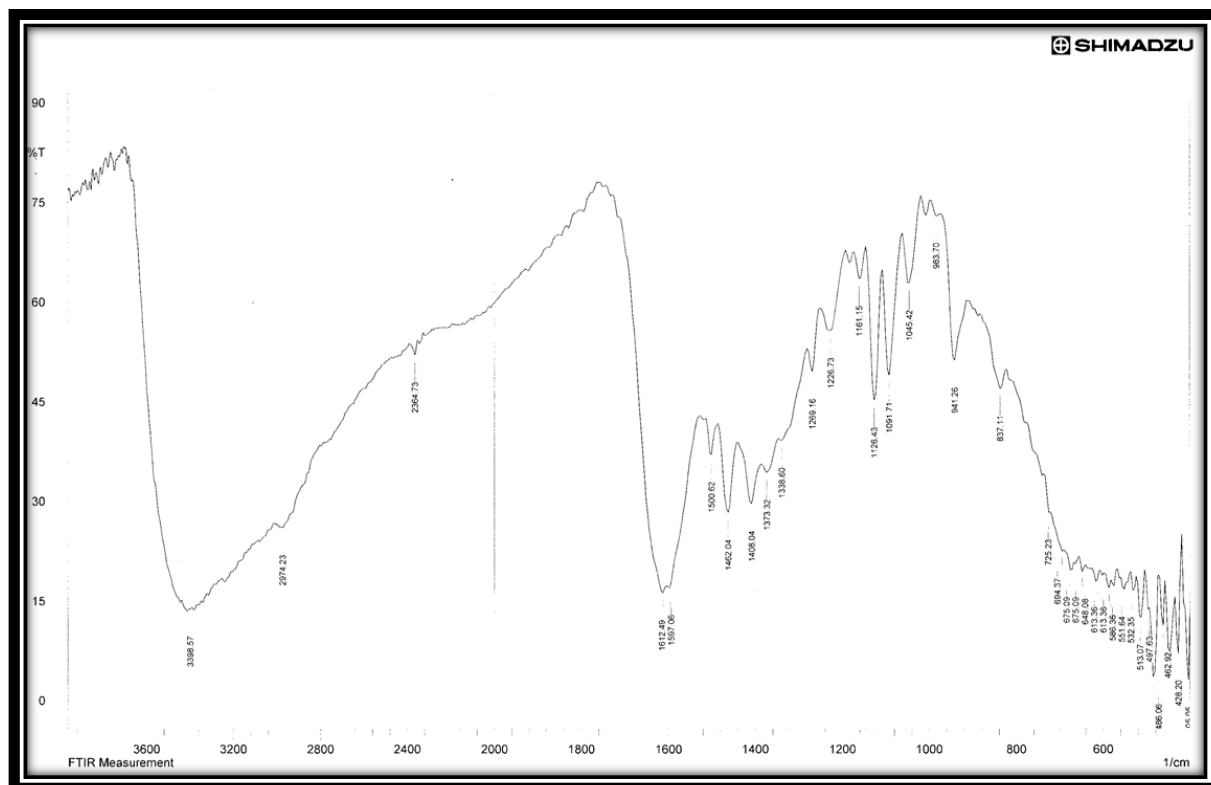
Compounds	NH <sub>2</sub> NH	$\nu$ (C-H)	C=C Ar.	(SO <sub>2</sub> ) <sub>asy</sub>	(-COO) <sub>asy</sub> (C-N)	(-COO) <sub>sym</sub>	$\nu\Delta$ (-COO) asy-sym	(C=N) SMZ) Isoxazol in ring	(SO <sub>2</sub> ) sy	(S-N)	(M-N)	(M-O)
[Mn (SMZ)(L-pro) <sub>2</sub> ]	3448, 3161	2974 s, 2943m	1415	1367 s	1627 1600	1377	250	1504 m	1045	941	563	482
[ Fe (SMZ)(L-pro) <sub>2</sub> ]	3398 vs -br	2974vs	1475 m	1373	1597	1373 s	224	1612	1126m	941	551	467 w
[ Ni (SMZ)(L-pro) <sub>2</sub> ]	3468 3209 3136	2981vs	1597	1365m	1620 1597 vs	1365 s	255	1500 vs	1138 vs	929	547	451w
[ Cu (SMZ)(L-pro) <sub>2</sub> ]	3471 3205 3140	2981m ,2855m	1597	1365 vs	1620 1597 vs	1354 vs	266	1604	1116 vs	929	547	459
[ Cd (SMZ)(L-pro) <sub>2</sub> ]	3265 3236	2962 w 2818	1556	1388 vs	1591 vs	1388 1352	239	1597	1153 vs	933	577m	462
[ Hg (SMZ)(L-pro) <sub>2</sub> ]	3352 3170	2981 m	1502	1379	1549 s	1319	230	1597vs	1153 vs	933	547	

Some new bands observed in the regions around  $(507-559) \text{ cm}^{-1}$  and  $(437-474) \text{ cm}^{-1}$  may be ascribed to M-N and M-O vibrations, respectively [76, 91]. It may be noted that, these vibrational bands are absent in the spectra of the ligands.

The FTIR spectral data of  $[\text{Sn}(\text{SMZ})(\text{L-pro})_2]$  such  $[\text{Sn}(\text{SMZ})(\text{L-pro})]$ . All free amino acids show a strong carboxyl asymmetric stretching band at  $(1560-1680) \text{ cm}^{-1}$  and weaker symmetric stretching band at  $\sim (1380-14000) \text{ cm}^{-1}$  [35-38] in the spectrum of L- L-proH it appears at  $(1506-1650) \text{ cm}^{-1}$  and respectively. The asymmetric stretching band of  $\nu(\text{COO}^-)$  was shifted to a higher frequency metal complexes, whereas the  $\nu(-\text{COO})_{\text{sym}}$  band was shifted to a lower frequency at  $(1379-1393) \text{ cm}^{-1}$ , these values are quite agreeable with the values reported earlier [91, 92]. The large difference between  $\nu(\text{COO}^- \text{ carboxylato})_{\text{asy-sym}}$  value of  $\sim 200 \text{ cm}^{-1}$  indicates the monodentate binding nature of the  $\nu(\text{COO}^- \text{ carboxylato})$  group. Accordingly, one can deduce that the L-proH binds the Sn(II) on a bidentate fashion (NO). The bonding sites are the (Imine NH) nitrogen and the (COO- carboxylato) oxygen atoms. L-prolin acts as mononegative bidentate ligand and forms M-N and M-O bonds.

Table (3-12) Infrared spectral data(wave number  $\nu$ )  $\text{cm}^{-1}$  for [M -SMZ -L-ProH]

Compounds	$\nu_{\text{as}}$ (NH):NH <sub>2</sub> vs (NH): sulfonamide group vs (NH): sulfonamide group	(C-H)	C=C Arom.	(SO <sub>2</sub> ) asy	(-COO) asy (C-N)	(-COO) sym	$\nu_{\Delta}$ (-COO) asy-sym	(C=N) Isoxazol ring in (SMX)	(SO <sub>2</sub> ) sym	(S-N)	(M-N)	(M-O)
[Al(SMZ)(L-pro) <sub>2</sub> ]Cl	3471 3209br	2981 s 2858m	1465 vs	1367 s	1620 1597	1365	232	1500	1141	929	551	459
[Cr(SMZ)(L-pro) <sub>2</sub> ]Cl	3417vs br	2981 s, 2904m	1516 m	1377 w	1620 1597vs	1365	232	1635	1130	804	540	447
[Fe(SMZ)(L-pro) <sub>2</sub> ]Cl	3468, 3379 vs	2981 s 2858m	1465 v	1311	1624 1597	1365	232	1500	1145	925	547	451
[Sn(SMZ)(L-pro) <sub>2</sub> ]	3468, 3394 vs	2985 vs, 2858br	1465 vs	1377	1624 1597	1365	232	1500	1141	929	551	455
[Sn(SMZ)(L-pro)]	3471 3360 vs	2985 vs, br	1465 vs	1377	1620 1597	1365	232	1500	1141	929	547	455

Figure (3-7) FT-IR Spectrum of  $[\text{Mn}(\text{SMZ})(\text{L-Pro})_2]$ Figure (3-8) FT-IR Spectrum of  $[\text{Fe}(\text{SMZ})(\text{L-Pro})_2]$

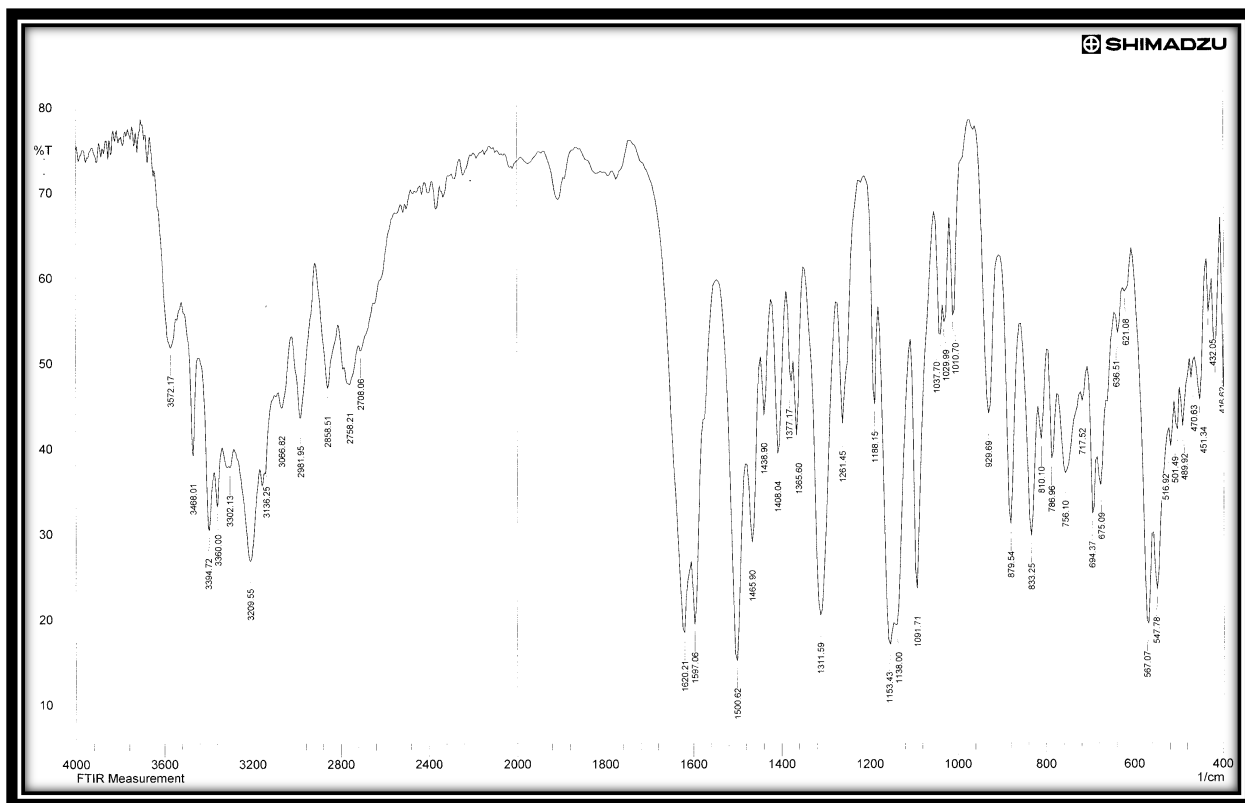


Figure (3-9) FT-IR Spectrum of [Ni(SMZ)(L-Pro)<sub>2</sub>]

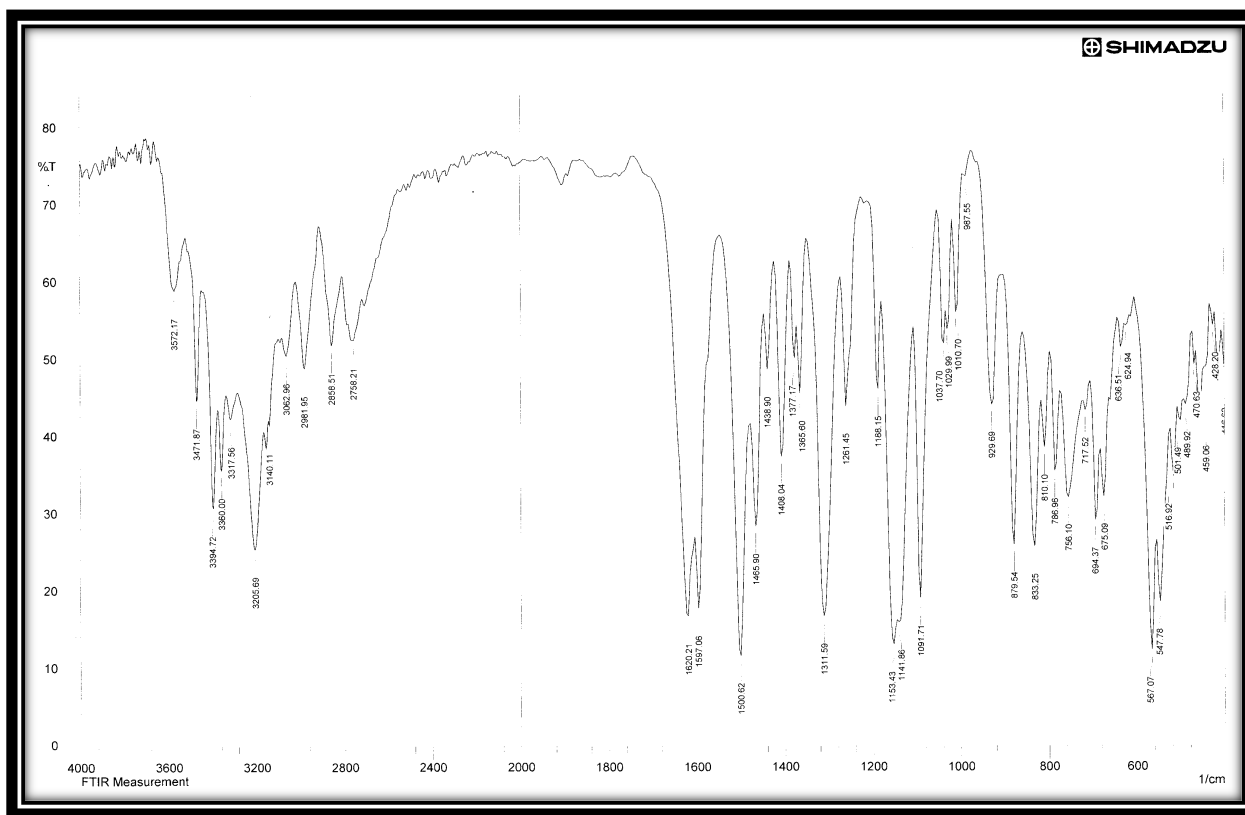
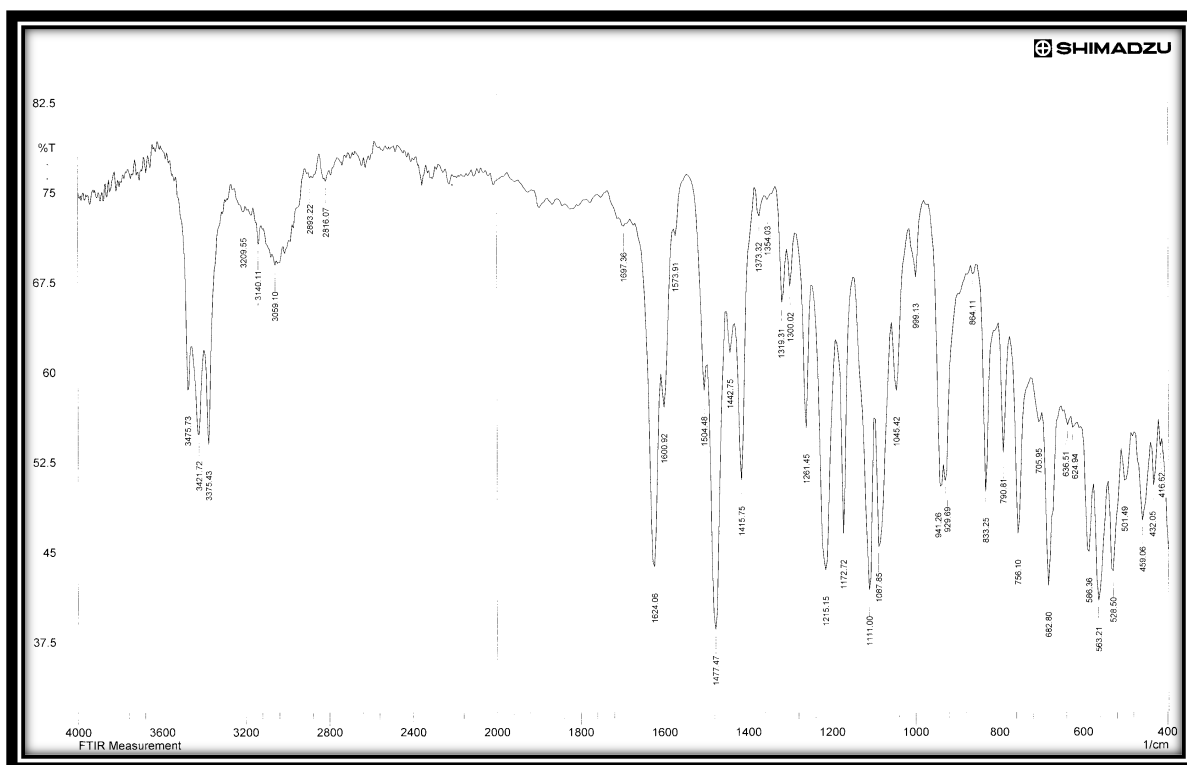
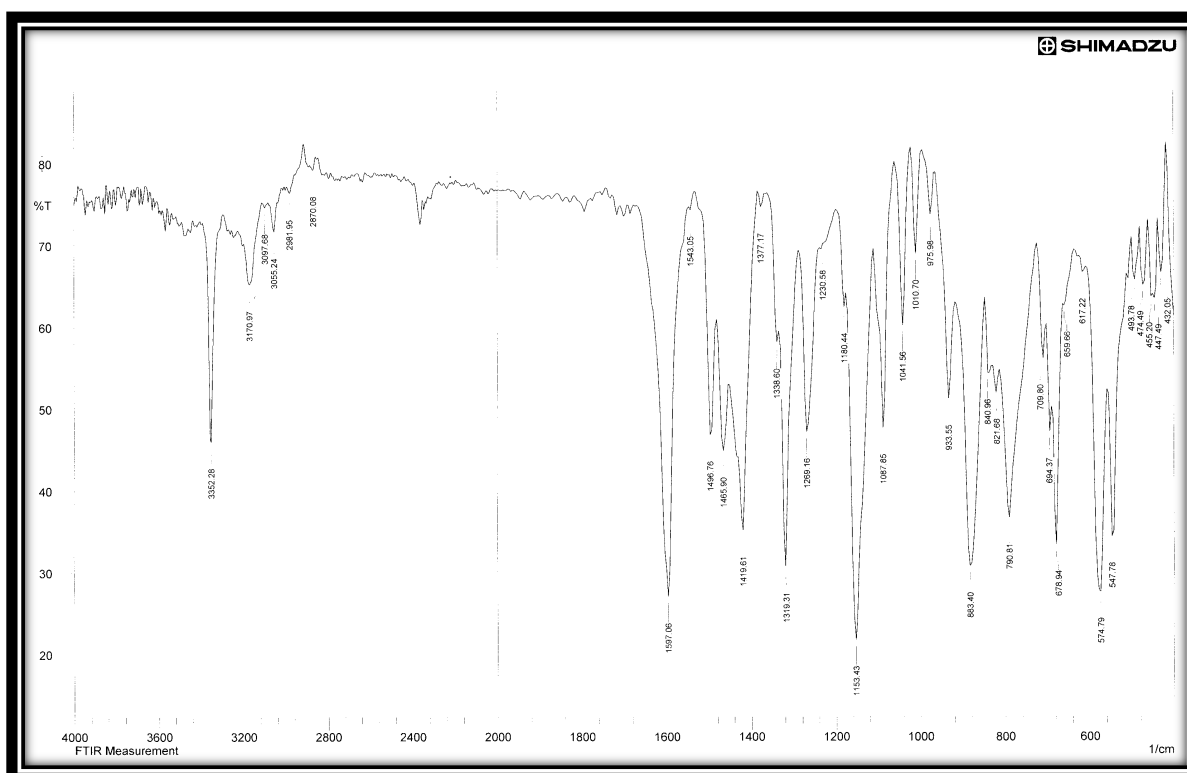


Figure (3-10) FT-IR Spectrum of [Cu(SMZ)(L-Pro)<sub>2</sub>]

Figure (3-11) FT-IR Spectrum of  $[\text{Cd}(\text{SMZ})(\text{L-Pro})_2]$ Figure (3-12) FT-IR Spectrum of  $[\text{Hg}(\text{SMZ})(\text{L-Pro})_2]$



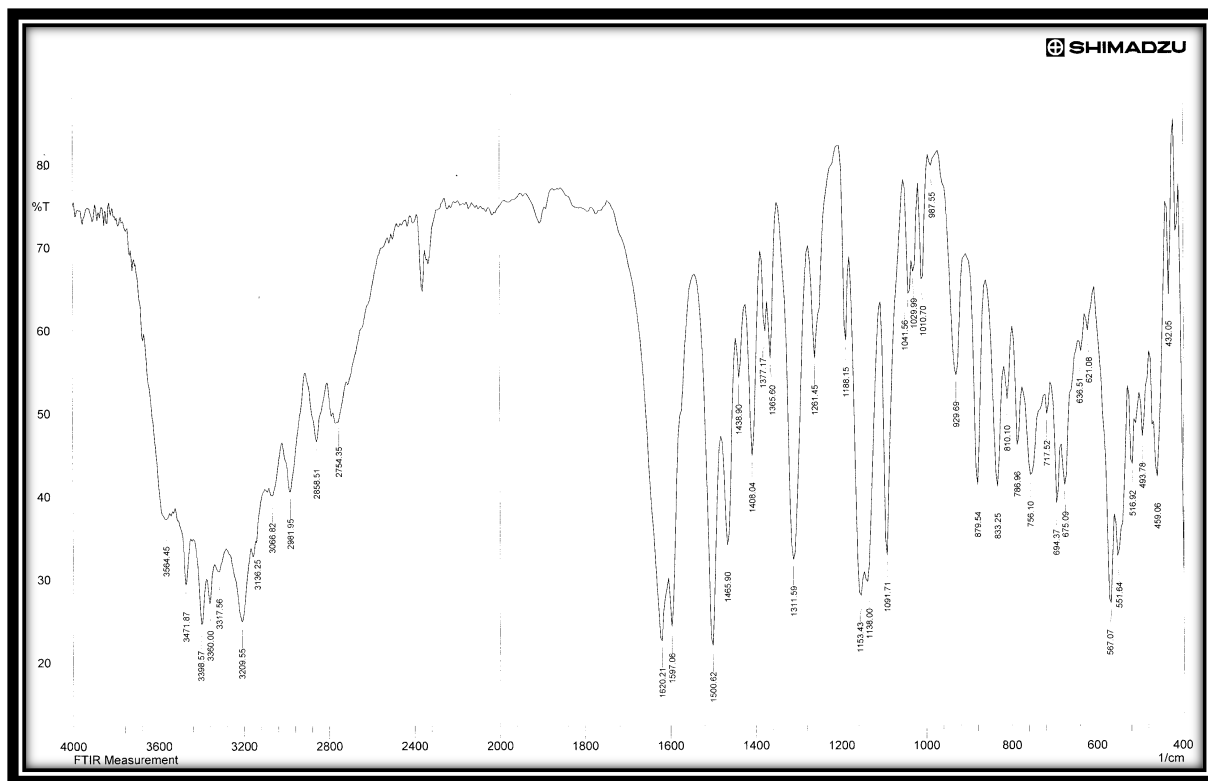


Figure (3-13) : FT-IR Spectrum of  $[Al (SMZ)(L-pro)_2]Cl$

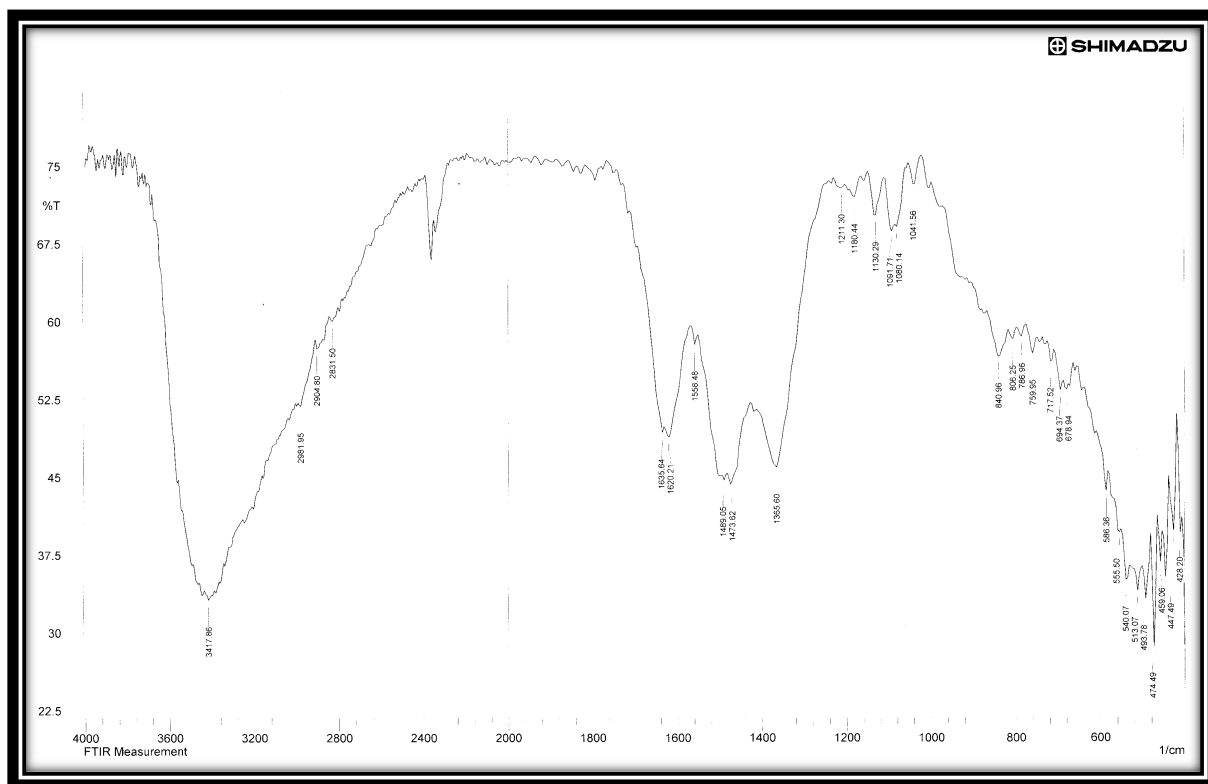
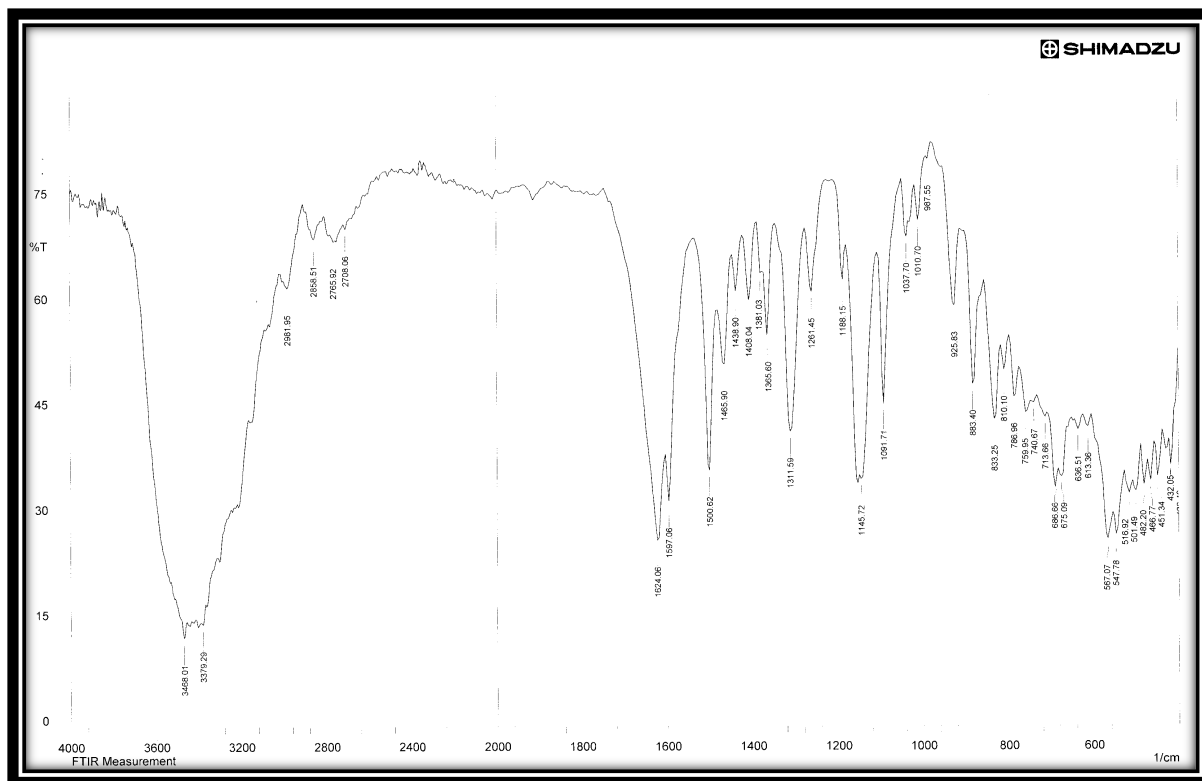
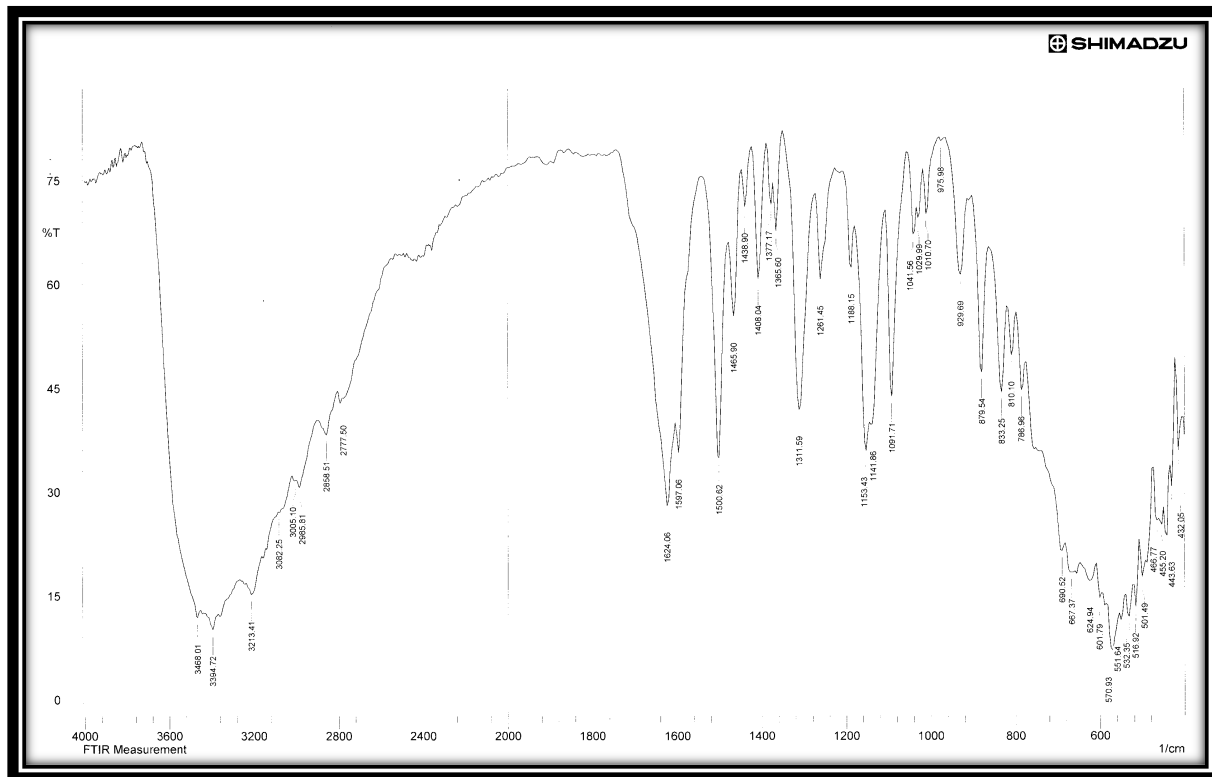


Figure (3-14) : FT-IR Spectrum of  $[Cr (SMZ)(L-pro)_2]Cl$

Figure (3-15) : FT-IR Spectrum of  $[\text{Fe}(\text{SMZ})(\text{L-pro})_2]\text{Cl}$ Figure (3-16) : FT-IR Spectrum of  $[\text{Sn}(\text{SMZ})(\text{L-Pro})_2]$

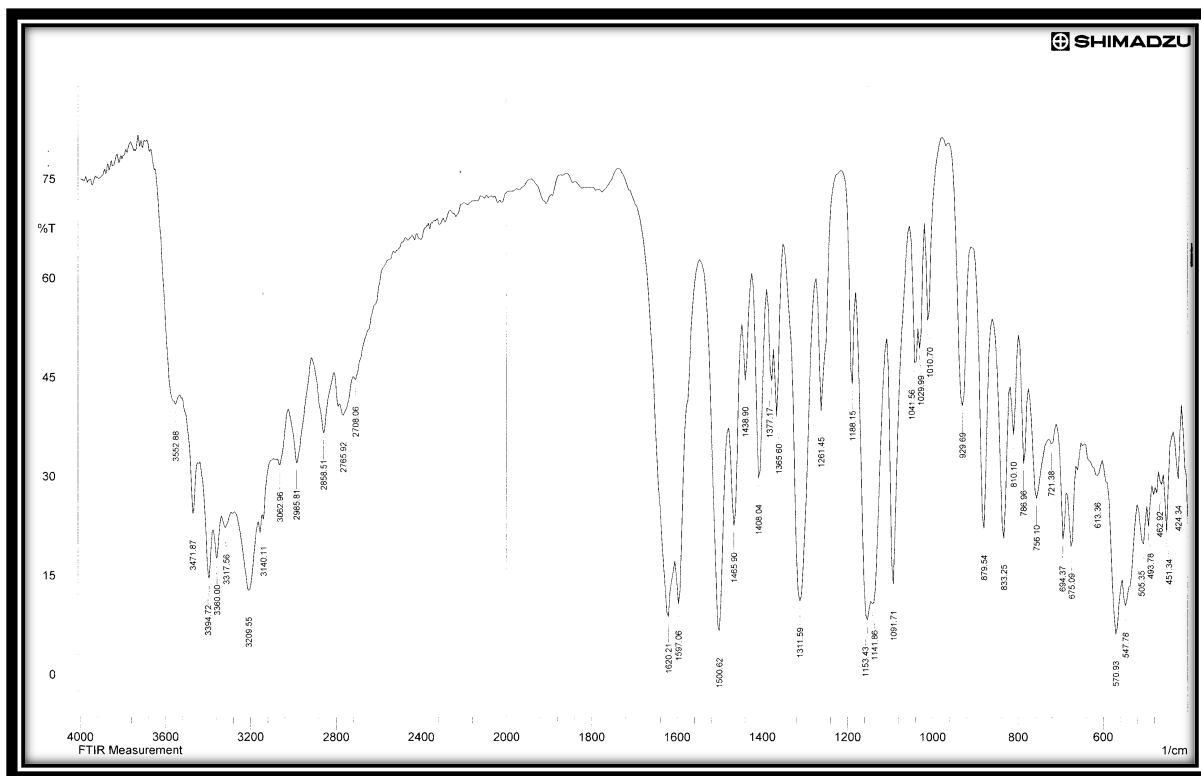


Figure (3-17) FT-IR Spectrum of  $[Sn(SMZ)(L-Pro)]Cl$

### 3.4.2 UV/Vis spectra , magnetic properties of compounds

Magnetic properties <sup>[74]</sup> and electronic absorption spectra of transition metal complexes are usually attributed to the partially filled d-orbital of the metal. The energy required for such transitions is that of the near U.V and visible region. are due to absorption bands due to the ligand, Charge transfer (CT) transitions between ligand (L) and metal (M), d – d transitions and Ion pair, Figures (3-18) to (3-21) .The d–d transitions are forbidden due to (Laporte law Forbidden) appeared in the visible region at lower energy with low intensity.

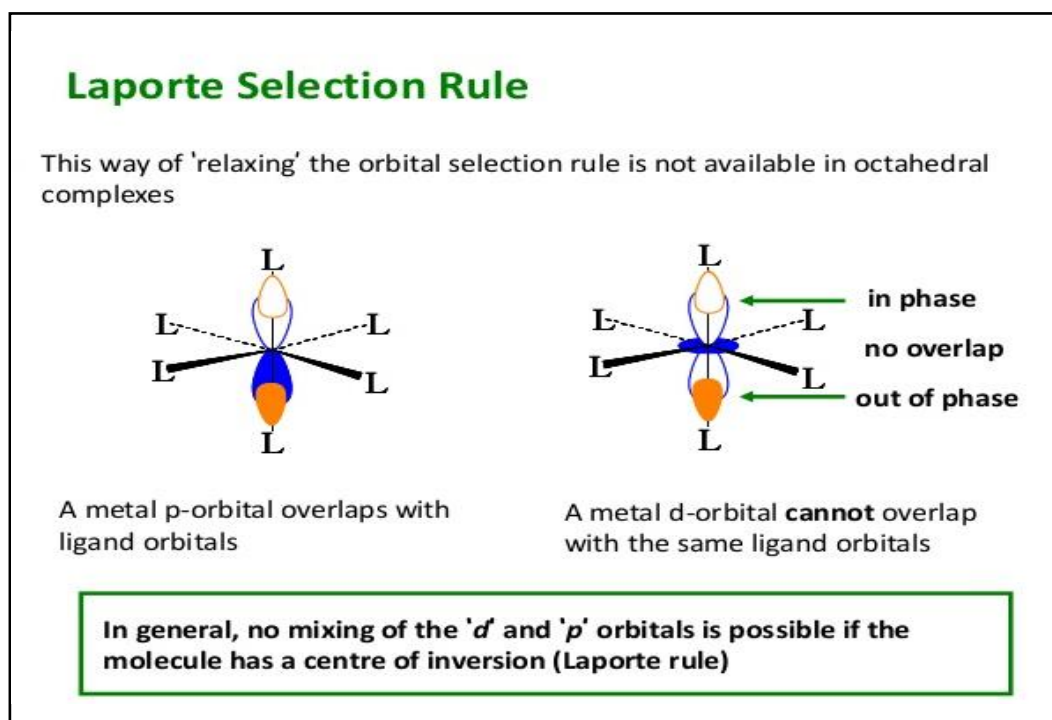


Figure (3-18) :Laport Selection rule

The Orgel- and Tanabe-Sugano diagrams Figure (3-19) are now universally used for the interpretation of the spectra of transition metal complexes.

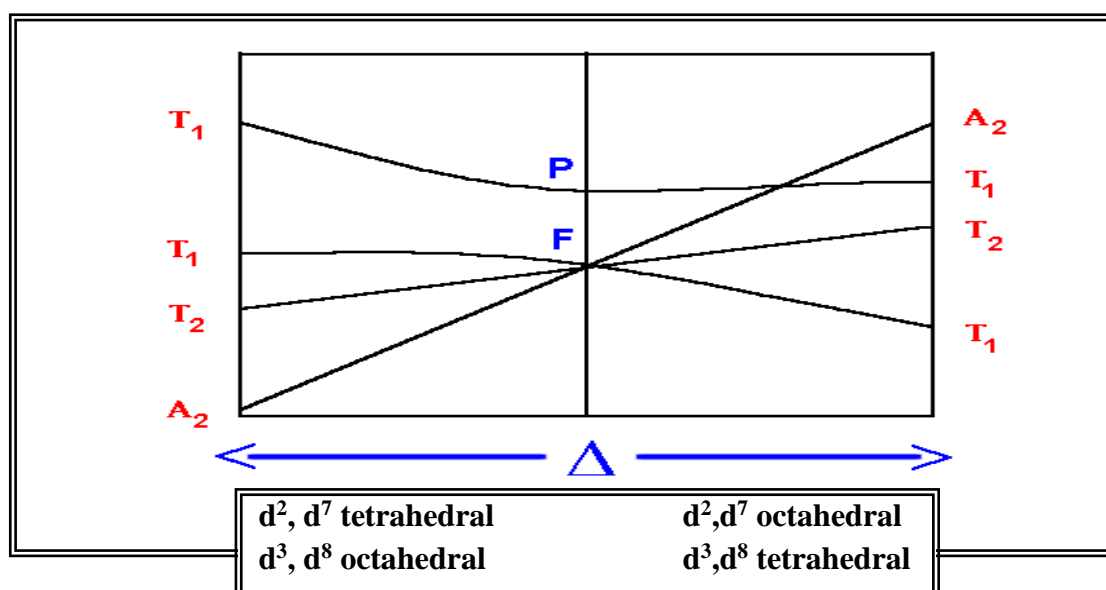


Figure (3-19):The Orgel- diagrams

Charge transfer spectra are due to transitions between metal and ligand. Study of electronic spectra of complexes help in the determination of structure of the complexes through the electronic interaction of the metal d-orbital and ligand orbital.

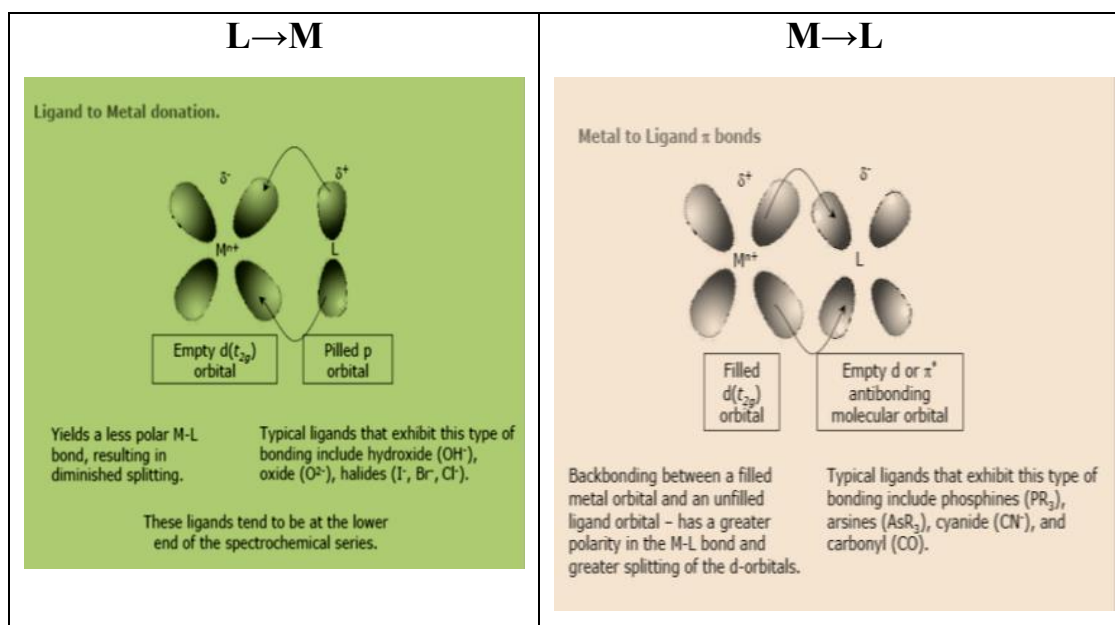


Figure (3-20) : Types Of Charge transfer (CT) transition

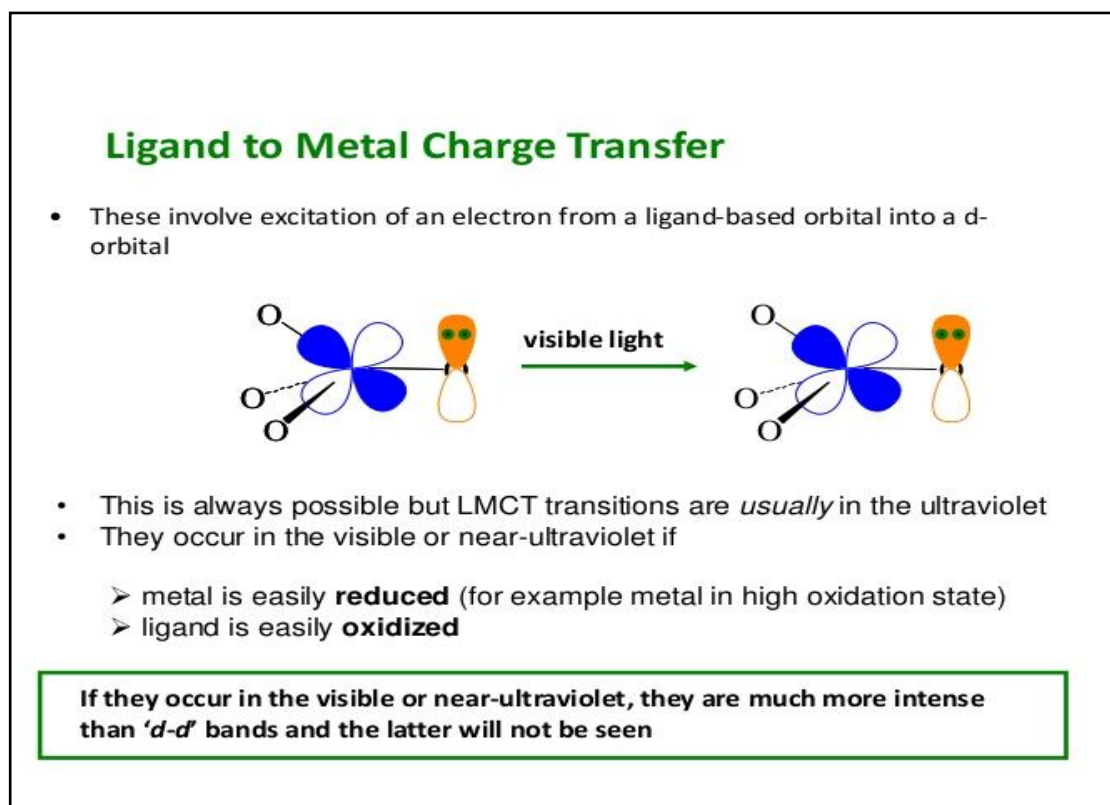


Figure (3-21) : Involve Electron from Ligand based orbital

In the electronic spectral studies the ligand field parameters such as ligand field splitting energy (10 Dq), Racah's interelectronic repulsion parameter (B) and nephelauxetic ratio ( $\beta$ ) have been determined by using the following relationships:

(a) **Ligand Field Splitting Energy (10 Dq)**

$$10 Dq = v_2 - v_1$$

$$10 Dq = v_1$$

$$10 Dq = v_3 - 1/2 v_1 - 1/3 (v_3 - v_2)$$

(b) **Racah's Interelectronic Repulsion Parameters (B')**

$$B' = \frac{v_2 + v_3 - 3v_1}{15}$$

$$B' = \frac{v_3 - 2v_1 + 10Dq}{15}$$

(c) **Nephelauxetic Ratio ( $\beta$ )**

$$\beta = \frac{B}{B'} = (\text{B complex} / B')$$

Table (3-13): Racah's (B') values for some Ions (Cm<sup>-1</sup>)

Free ion	(Cm <sup>-1</sup> ) (B')
Mn <sup>II</sup>	960
Cr <sup>III</sup>	1030
Fe <sup>II</sup>	9010
Co <sup>II</sup>	970
Ni <sup>II</sup>	1080
Cu <sup>II</sup>	1240
Nephelauxetic Series order for donor atom as F <sup>-</sup> > O > N > Cl > Br > S > I	

The spectral region where these occur spans the near infrared, visible and U.V. region as listed in Table (3-14).

Table (3-14): Visible and U.V. region

Ultraviolet (Uv)	Visible (Vis)	Near infrared (NIR)	Unit
50,000 – 26300	26300 -12800	12800 -5000	cm <sup>-1</sup>
200 – 380	380 -780	780 - 2000	nm

Charge transfer spectra are due to transitions between metal and ligand. Study of electronic spectra of complexes help in the determination of structure of the complexes through the electronic interaction of the metal d-orbital and ligand orbital. In our work the spectra were recorded in the range (200-1100) nm, using dimethyl sulfoxide (DMSO) as a solvent of values magnetic moment  $\mu_{\text{eff}}$  were corrected for diamagnetic effects using the relationship monated in Chapter 2 [74]. The results obtained from the equation were compared with the actual values obtained through magnetic measurements. Table (3-15) show the positions of electronic absorption bands and their transitions and also include show the magnetic moment measurements  $\mu_{\text{eff}}$  for prepared complexes and the suggested structure for each complex.

Table (3-15) : Electronic Spectral Data of the [M-SMZ - L-ProH] complexes

Complexes	$\lambda$ nm	$\nu$ cm <sup>-1</sup>	$\epsilon$ max mol <sup>-1</sup> .L.cm <sup>-1</sup>	Assignments	$\mu_{\text{eff}}$ (BM)
[Mn(SMZ)(Pro) <sub>2</sub> ]	279	35842	2027	CT	5.79
	742	13477	12	6A <sub>1g</sub> → 4T <sub>1g</sub> ,	
	803	12453	11	6A <sub>1g</sub> → 4T <sub>2g</sub> (G)	
[Fe(SMZ)(Pro) <sub>2</sub> ]	265	37735	1919	CT	-
	345	28985	1670	CT	
[Ni(SMZ)(Pro) <sub>2</sub> ]	296	33783	2259	L.f	2.28
	962	10395	6	3A <sub>2g</sub> (F)→3T <sub>1g</sub> (P) $\nu_3$	
[Cu(SMZ)(Pro) <sub>2</sub> ]	295	33898	2206	C.T	1.83
	410	24390	12	<sup>2</sup> B <sub>1g</sub> → <sup>2</sup> B <sub>2g</sub>	
	532	18796	9		
	804	12437	7	<sup>2</sup> B <sub>1g</sub> → <sup>2</sup> E <sub>g</sub>	
[Cd(SMZ)(Pro) <sub>2</sub> ]	274	36496	1845	C.T	0 Dima,
	805	12422	1		
[Hg(SMZ)(Pro) <sub>2</sub> ]	285	35087	2103	C.T	0 Dima.
	807	12391	1		

Table (3-16): Electronic Spectral Data of the [M'-SMZ - L-ProH] Complexes

Complexes	$\lambda$ nm	$\nu'$ cm <sup>-1</sup>	$\epsilon$ max (molar <sup>-1</sup> .cm <sup>-1</sup> )	Assignments	$\mu_{\text{eff}}$ (BM)
[Al(SMZ)(Pro) <sub>2</sub> ]Cl	283	35335	2052	CT	Dima
[Cr(SMZ)(Pro) <sub>2</sub> ]Cl	270	37037	257	CT	1.91
	861	11614	25	<sup>4</sup> A <sub>2g</sub> → <sup>4</sup> T <sub>1g</sub> (v3),	
	989	10111	32	<sup>4</sup> A <sub>2g</sub> → <sup>4</sup> T <sub>1g</sub> (v2)	
[Fe(SMZ)(Pro) <sub>2</sub> ]Cl	286	34965	2138	CT	5.22
	815	11750	3	6A <sub>1g</sub> →4T <sub>2g</sub> (4G)	
[Sn(SMZ)(Pro) <sub>2</sub> ]	285	35087	1935	$\pi \rightarrow \pi^*$	0 Dima.
	885	11299	46	CT	
	994	10060	61	CT	
[Sn(SMZ)(Pro)]Cl	279	35842	1984	$\pi \rightarrow \pi^*$	0 Dima.
	818	12224	4	CT	

### 3.4.3 Ultraviolet / Visible [UV/Vis] spectra of [M-SMZ - L-ProH] and [M'-SMZ - L-ProH] complexes

#### 3.4.3.1 UV/Vis spectrum of [Mn(SMZ)(Pro)<sub>2</sub>]

The UV/Vis of Mn(II) (d<sup>5</sup>) spectrum gave one essential symbol in the free ion, (<sup>6</sup>S) as shown in Figure (3-22), if any transition between the crystal field to being spin-forbidden, <sup>6</sup>S term give one symbol, <sup>6</sup>A<sub>1g</sub>, in the octahedral field therefore the electronic spectra and the colors of (d<sup>5</sup>) ions were very weak (which unoccupied from charge transfer observations).



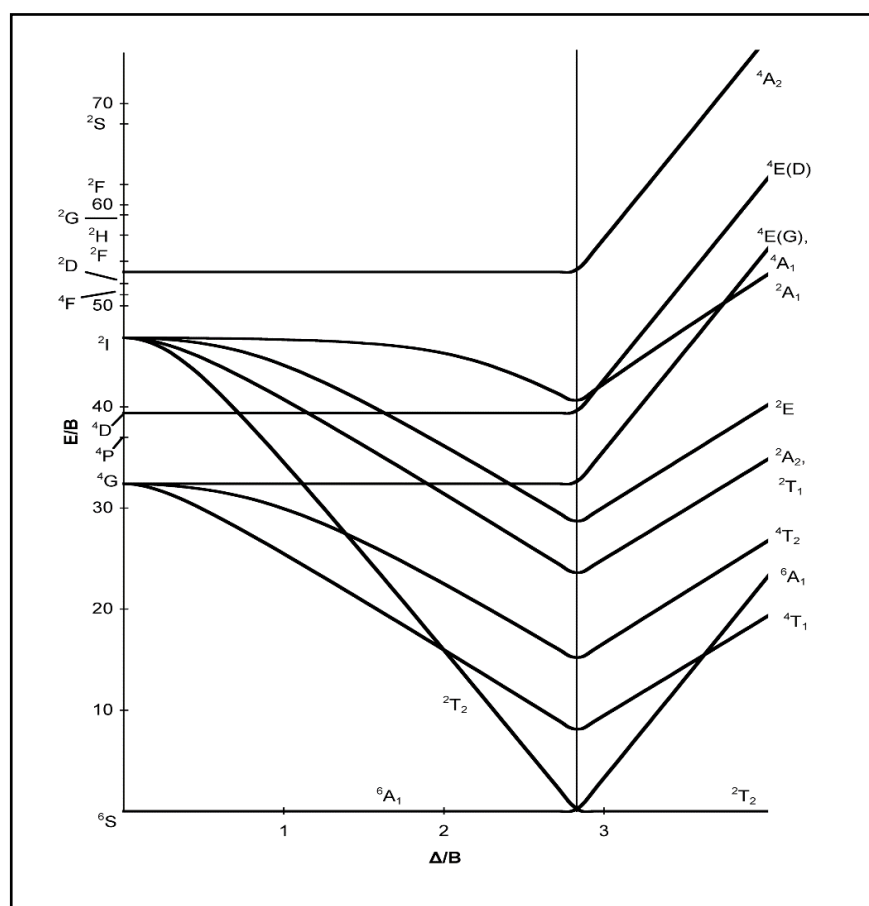
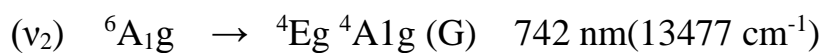


Figure (3-22): Tanabe-Sugano diagram for  $d^5$  system for Mn(II)

The UV/Vis of  $[\text{Mn}(\text{SMZ})(\text{Pro})_2]$  exhibits three peaks, Figure (3-23) and Table (3-15). First high intense peaks at 279 nm (35842) is due to the (Charg-Transfer) and two bands in the d-d transition region can be assigned to the following transitions:



These results reveal the octahedral geometry, for this complex. The value of the  $\mu_{\text{eff}}$  is (5.79 B.M.) in accordance with the presumption of high-spin  $d^5$  Mn(II) ion in (Oh) geometry <sup>(87)</sup>

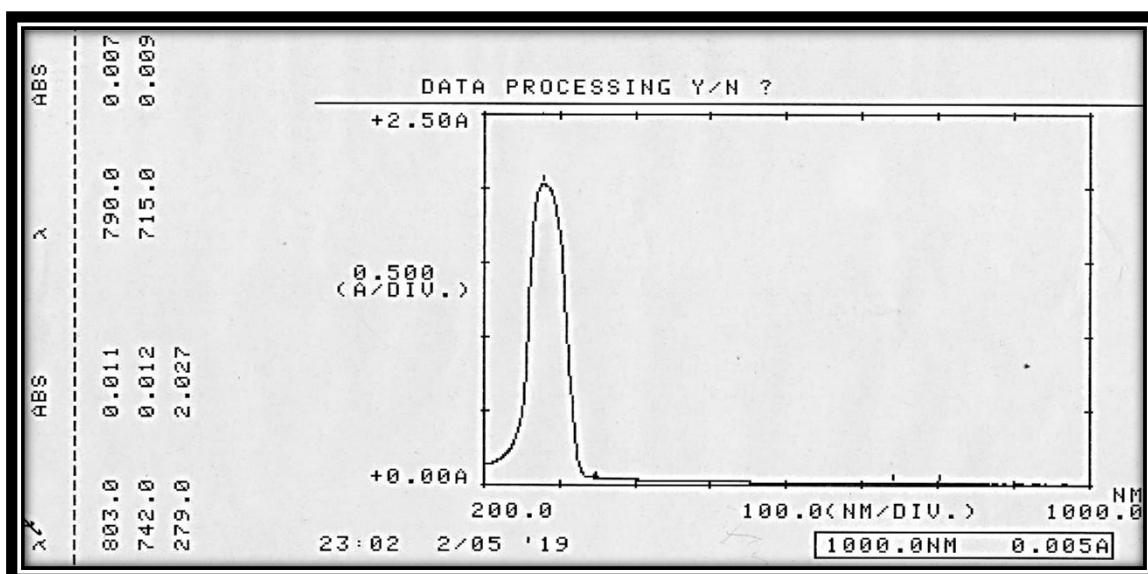


Figure (3-23) Electronic Spectrum of  $[\text{Mn}(\text{SMZ})(\text{L-Pro})_2]$

### 3.4.3.2. UV/Vis Spectrum of $[\text{Fe}(\text{SMZ})(\text{L-Pro})_2]$

Electronic spectrum of  $[\text{Fe}(\text{SMZ})(\text{L-Pro})_2]$  shows two bands high intense peaks Figure (3-24), at 265 nm ( $37735 \text{ cm}^{-1}$ ) and 345 nm ( $28985 \text{ cm}^{-1}$ ) are to the (Charg-Transfer (CT)–ligand to metal) because they occur near ultraviolet and high intense peaks than d-d bands and the latter not, see Figure (3-21).

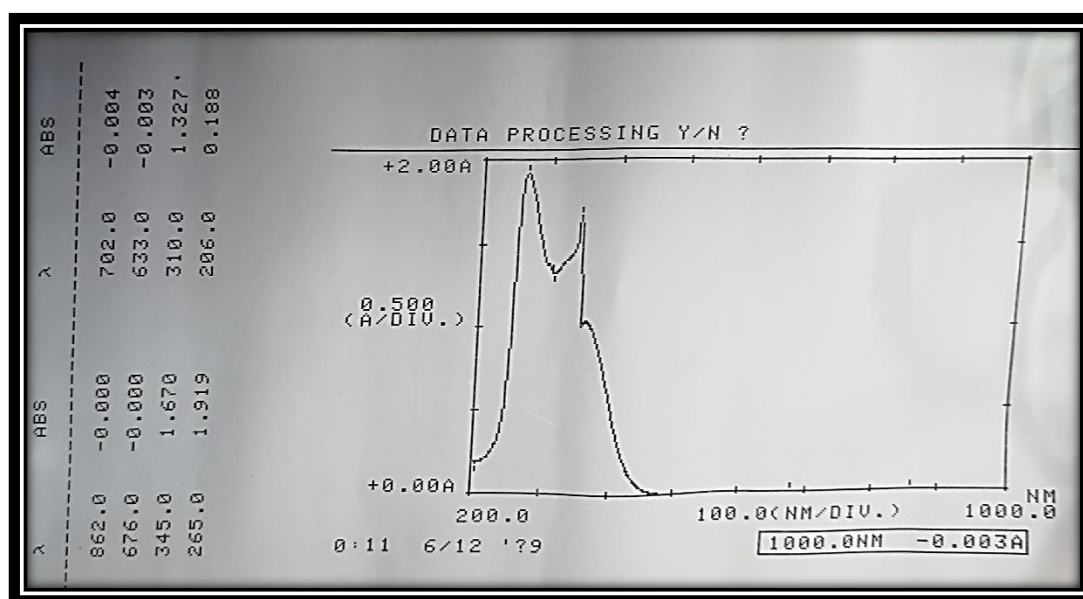


Figure (3-24): UV/Vis Spectrum of  $[\text{Fe}(\text{SMZ})(\text{L-Pro})_2]$

### 3.4.3.3 UV/Vis Spectrum of [Ni (SMZ)( L-Pro)<sub>2</sub>]

Ni(II) d<sup>8</sup> (Term <sup>3</sup>F) complex is paramagnetic at room temperature with  $\mu_{\text{eff}}$  equal to 2.28 B.M. which is consistent with an (Oh) field and correspond to two unpaired electrons as expected for (six coordinated) spin free Ni(II) species. In the electronic spectrum of the Ni(II) complex Figure (3-25): shows two distinct bands appears at (296 nm)33783cm<sup>-1</sup> and (962 nm)10395cm<sup>-1</sup> which may be assigned to ligand field and d-d  ${}^3A_{2g}^{(F)} \rightarrow {}^3T_{1g}^{(P)} \nu_3$  transitions

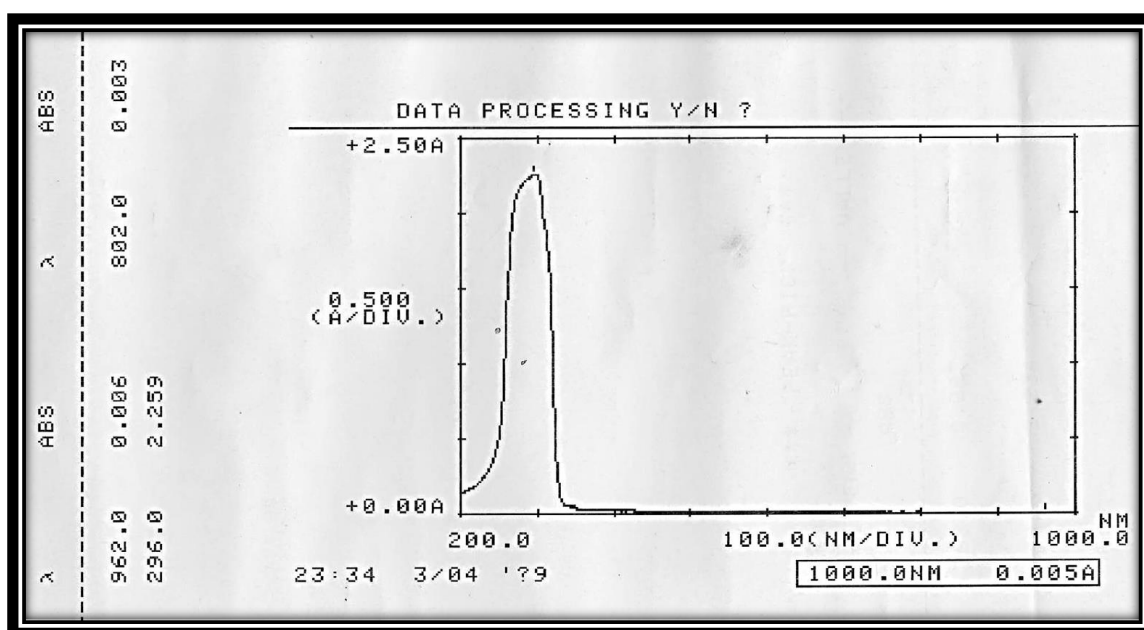


Figure (3-25): Electronic Spectrum of [Ni(SMZ)( L-Pro)<sub>2</sub>]

### 3.4.3. 4. UV/Vis Spectrum of [Cu(SMZ)( L-Pro)<sub>2</sub>] Complex

The value of ( $\mu_{\text{eff}}$ ) that have been measured for [Cu(SMZ)(Pro)<sub>2</sub>] d<sup>9</sup> (Term <sup>2</sup>D), complex was (1.83 B.M.). This value is in the range of mononuclear octahedral geometry which is in agreement with data reported by several research workers which indicates the presence in (Oh) structure [28 , 93] The Cu (II)ion is characterized by large distortion from octahedral symmetry and the bond is unsymmetrical, being the result of a number of transitions, according to the diagram in Figure (3-26) [82].

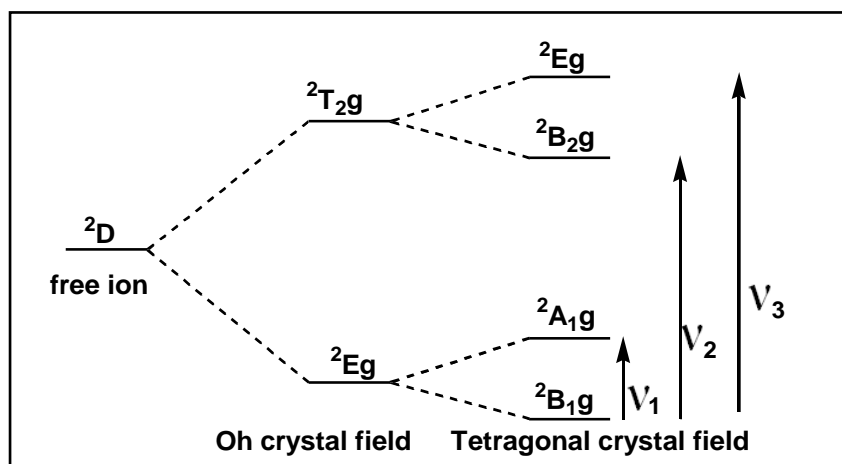


Figure (3-26) : overlapping of bands which occurs in the case of Cu(II).

[Cu(SMZ)( L-Pro)<sub>2</sub>] complex spectrum showed four bands in the region [(295nm)35898cm<sup>-1</sup> may be due, to LMCT, which is a characteristic of copper(II) complexes with amines , <sup>[94-95]</sup> and show a broad band at (24390-12437 cm<sup>-1</sup>) which can be assigned to  $2B_{1g} \rightarrow 2B_{2g}$  and  $2B_{1g} \rightarrow 2E_g$  transitions, Figure (3-27) which also compatible with complexes have (Oh) structure <sup>[85]</sup>.

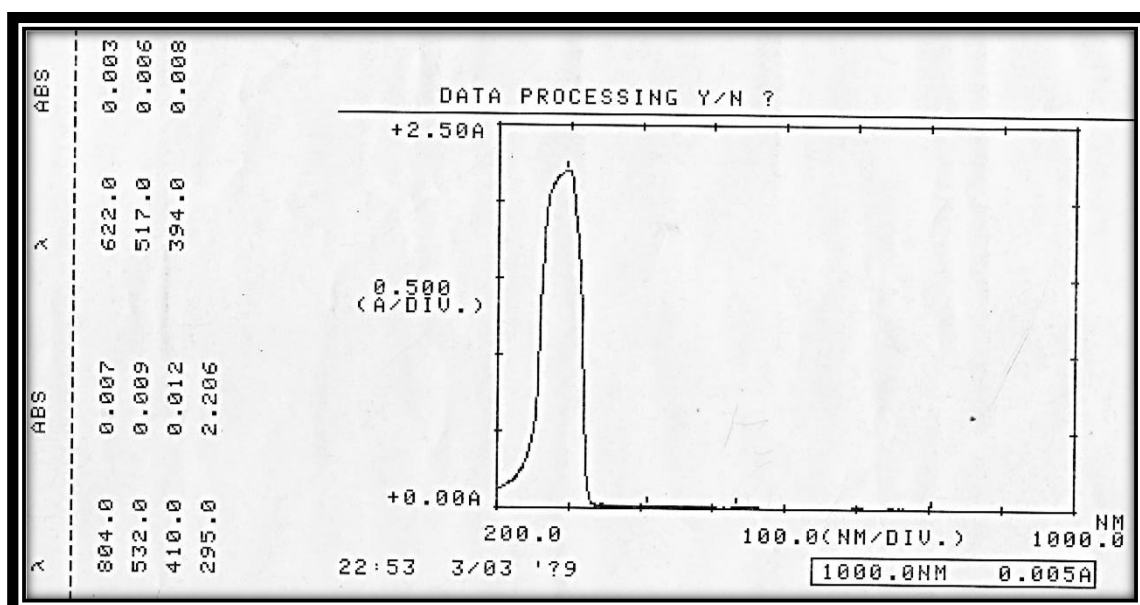


Figure (3-27) : UV/Vis Spectrum of [Cu(SMZ)( L-Pro)<sub>2</sub>]

### 3.4.3.5 UV/Vis Spectrum of [Cd(SMZ)(L-Pro)<sub>2</sub>]

The Cd(II) complex showed diamagnetic properties as expected from their electronic configuration. The electronic spectrum of [Cd(SMZ)(L-Pro)<sub>2</sub>], d<sup>10</sup> complex show two transitions Table (1-15). The high intensity band in the (274 nm (36496 cm<sup>-1</sup>) assigned to  $\pi \rightarrow \pi^*$  transitions due to conjugated  $\pi$  system The low intensity second band was observed at wavelength. 805 nm (12422 cm<sup>-1</sup>) ascribed to L-M (C.T) transitions. Figure (3-28) which also compatible with complexes have a (Oh) structure [26,95].

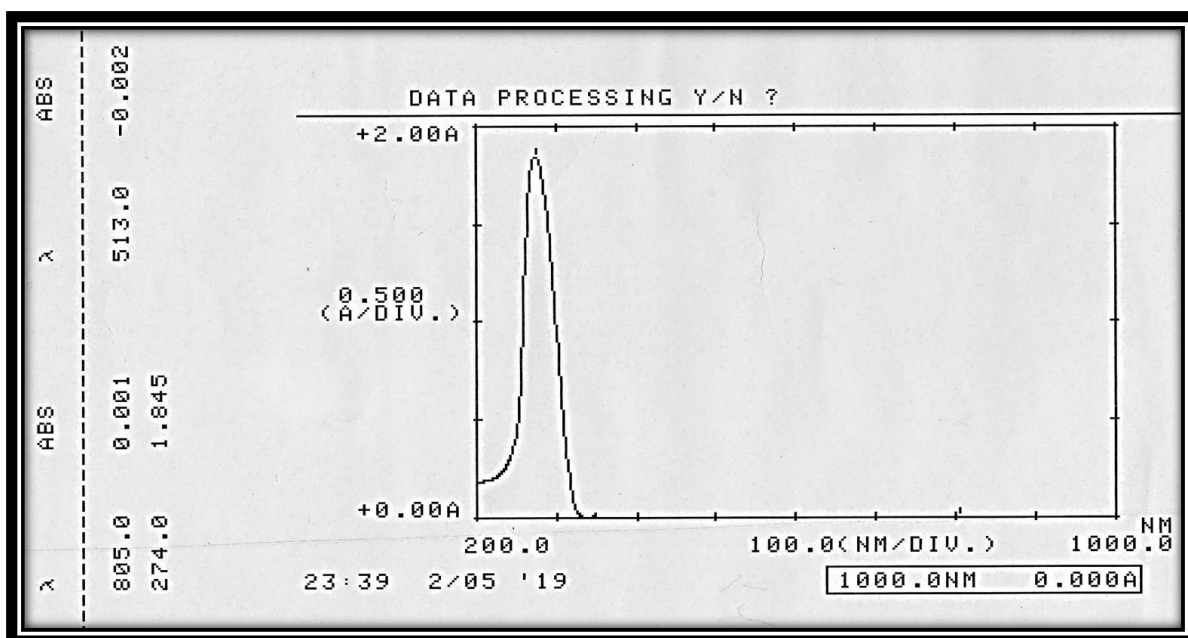


Figure (3-28) : UV/Vis Spectrum of [Cd(SMZ)(L-Pro)<sub>2</sub>]

### 3.4.3.6 . UV/Vis Spectrum of [Hg(SMZ)(L-Pro)<sub>2</sub>]

The [Hg(SMZ)(Pro)<sub>2</sub>] complex showed diamagnetic properties as expected from their electronic configuration. The electronic spectrum of Hg (II) , d<sup>10</sup> , complex show two transitions Table (1-15).The high intensity band in the 285 nm (35087 cm<sup>-1</sup>) due to  $\pi \rightarrow \pi^*$  transitions due to conjugated  $\pi$  system The low intensity second band was observed at wavelength. 807 nm (12391 cm<sup>-1</sup>) ascribed to L-M charge transfer (C.T)

transitions. Figure (3-29) which also compatible with complexes have (Oh) structure [26,57,95].

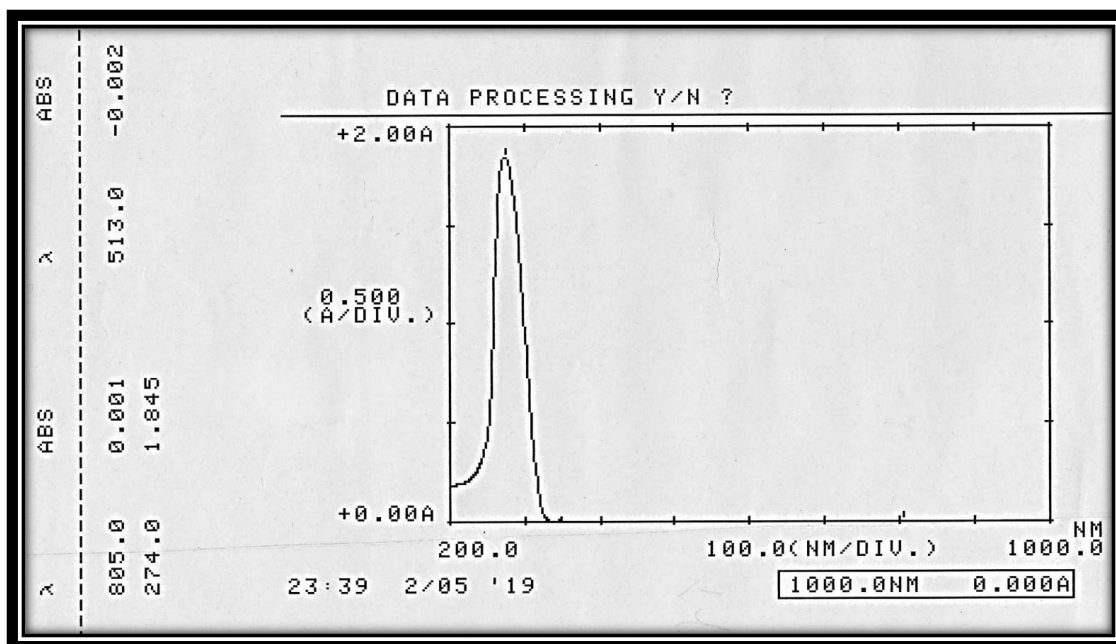


Figure (3-29) UV/Vis Spectrum of  $[\text{Hg}(\text{SMZ})(\text{L-Pro})_2]$

### 3.4.3.7 UV/Vis Spectrum of $[\text{Al}(\text{SMZ})(\text{L-pro})_2]\text{Cl}$

The (U.V-Vis)  $[\text{Al}(\text{SMZ})(\text{Pro})_2]\text{Cl}$  complex spectrum Figure (3-30) and Table (1-16). exhibits one high intense peak at 283 nm ( $35335\text{cm}^{-1}$ ), due to the intra ligand charge transfer (INCT). The Al (III) complex showed diamagnetic properties [74,100].

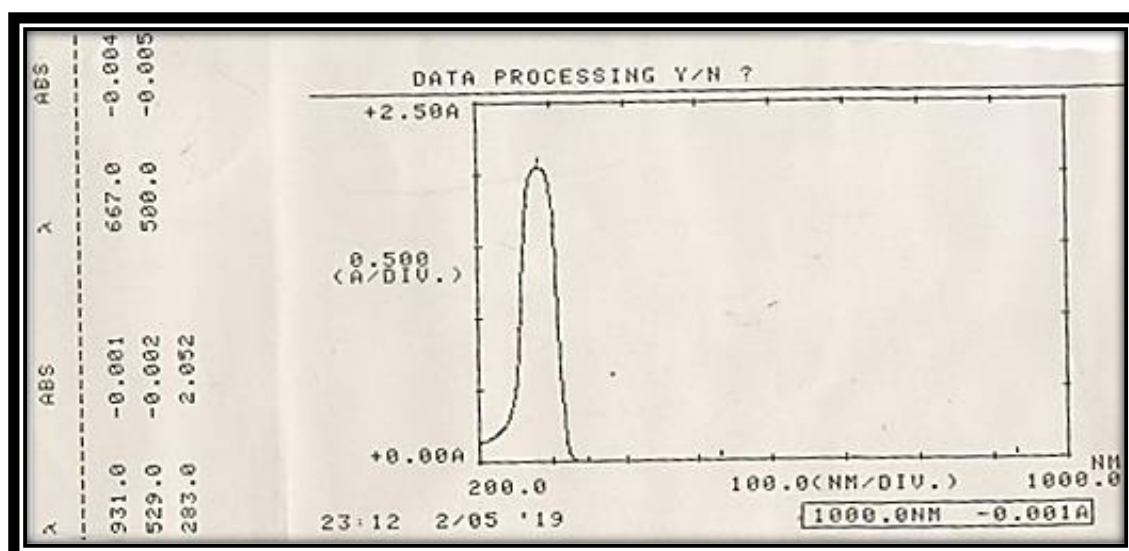


Figure (3-30) : UV/Vis Spectrum of  $[\text{Al}(\text{SMZ})(\text{L-pro})_2]\text{Cl}$

### 3.4.3.8 UV/Vis Spectrum of [Cr (SMZ)(L-pro)<sub>2</sub>]Cl

The UV/Vis [Cr (SMZ)(L-pro)<sub>2</sub>]Cl complex spectrum Figure (3-31) and Table (1-16). exhibits three transitions. The first high intense peak at 270 nm (37037cm<sup>-1</sup>), due to the intra ligand charge transfer(INCT) and second and third bands at 861nm(11614 cm<sup>-1</sup>), 989nm (10111cm<sup>-1</sup>) Table 3-8 which are assignable to <sup>4</sup>A<sub>2g</sub>→<sup>4</sup>T<sub>1g</sub> (ν<sub>3</sub>), <sup>4</sup>A<sub>2g</sub>→<sup>4</sup>T<sub>1g</sub> (ν<sub>2</sub>) respectively [82,83]. The magnetic moment of the [Cr(SMZ)(Pro)<sub>2</sub>]Cl is (1.91 B.M.) Table (3-16), therefore an octahedral geometry was assume[Cr (SMZ)(L-pro)<sub>2</sub>]Cl for Cr (III) complex.

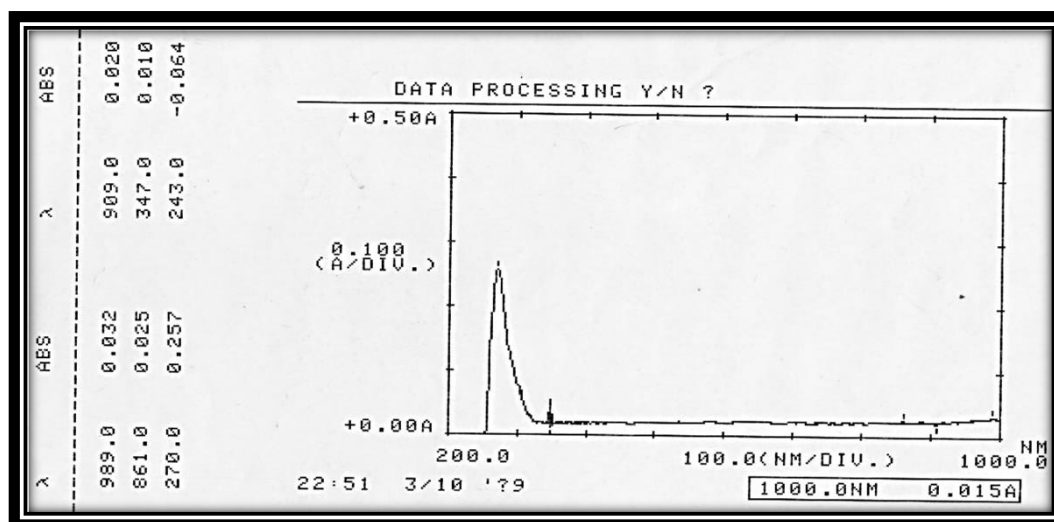


Figure (3-31) : UV/Vis Spectrum of [Cr (SMZ)(L-pro)<sub>2</sub>]Cl

### 3.4.3.9 UV/Vis Spectrum of [Fe (SMZ)(L-pro)<sub>2</sub>]Cl

The UV/Vis spectrum of the [Fe (SMZ)(L-pro)<sub>2</sub>]Cl complex Figure (3-32) showed two bands in the d-d transition assigned to the <sup>6</sup>A<sub>1g</sub> → <sup>4</sup>T<sub>1g</sub> (20366cm<sup>-1</sup>) and <sup>6</sup>A<sub>1g</sub> → <sup>4</sup>T<sub>2g</sub>(12195cm<sup>-1</sup>) and one obscured by the intense charge-transfer band observed at 294 nm (34013 cm<sup>-1</sup>) these assignments are to the other earlier report made for Fe(III) complexes<sup>(96)</sup>. The higher energy ligand field bands were The value of the measured magnetic moment is (5.22 B.M.) in accordance with the presumption high-spin d<sup>5</sup> ferric ion in octahedral geometry .

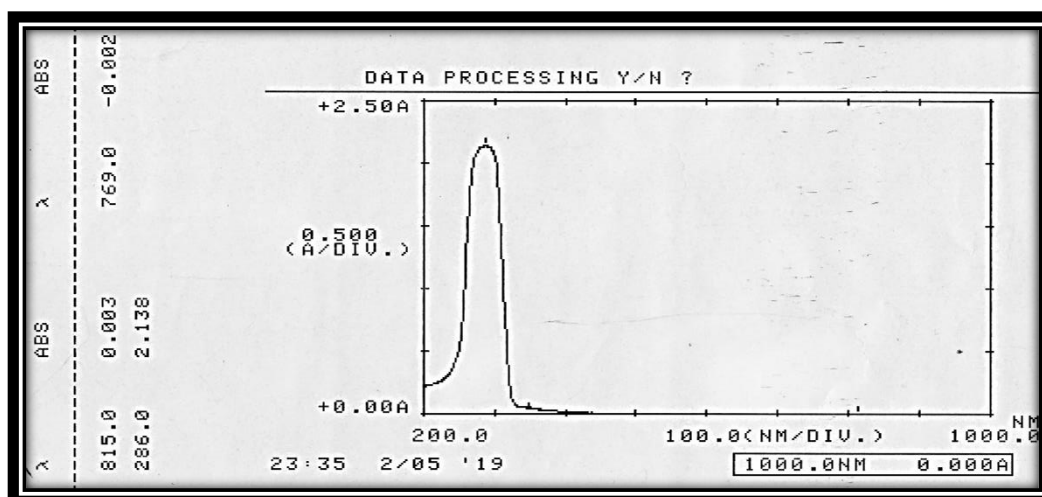


Figure (3-32) : UV/Vis Spectrum of  $[\text{Fe}(\text{SMZ})(\text{L-pro})_2]\text{Cl}$

### 3.4.3.10 UV/Vis Spectrum of $[\text{Sn}(\text{SMZ})(\text{L-Pro})_2]$

The  $[\text{Sn}(\text{SMZ})(\text{L-Pro})_2]\text{Cl}$  complex showed diamagnetic properties as expected from their electronic configuration. The electronic spectrum of Sn (II) complex, Figure (3-33), in the 285 nm - 35087  $\text{cm}^{-1}$  assigned to  $\pi \rightarrow \pi^*$  transitions due to conjugated  $\pi$  system and a two bands were observed at wavelength 885 nm, nm ( $11299\text{cm}^{-1}$ ) and 994 nm, nm ( $10060\text{cm}^{-1}$ ) ascribed to L-M charge transfer (C.T) transitions of the heterocyclic and  $\text{COO}^-$  groups.

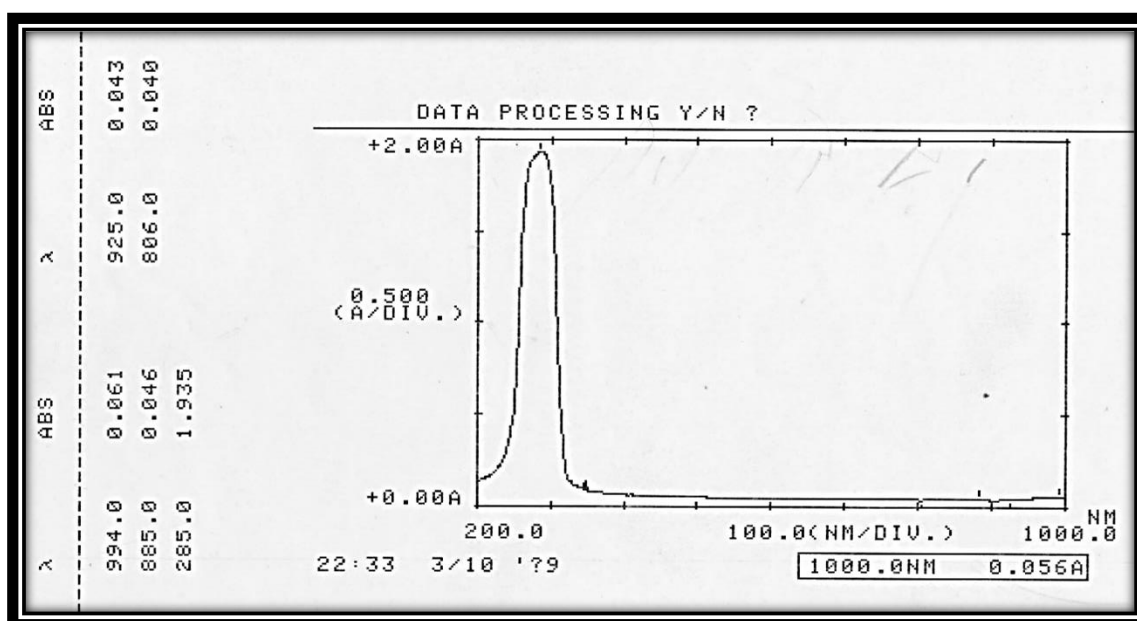


Figure (3-33) : UV/Vis Spectrum of  $[\text{Sn}(\text{SMZ})(\text{L-pro})_2]$



### 3.4.3.11 UV/Vis Spectrum of [Sn(SMZ)(L-Pro)] Cl

The [Sn(SMZ)(L-Pro)] Cl complex showed diamagnetic properties as expected from their electronic configuration. The electronic spectrum of Sn (II) complex in the 279 nm  $35842\text{ cm}^{-1}$  assigned to  $\pi \rightarrow \pi^*$  transitions due to conjugated  $\pi$  system and a second band was observed at wavelength, 818nm ( $12224\text{ cm}^{-1}$ ) ascribed to L-M charge transfer (C.T) transitions. of the heterocyclic and COO- groups, Figure (3-34)

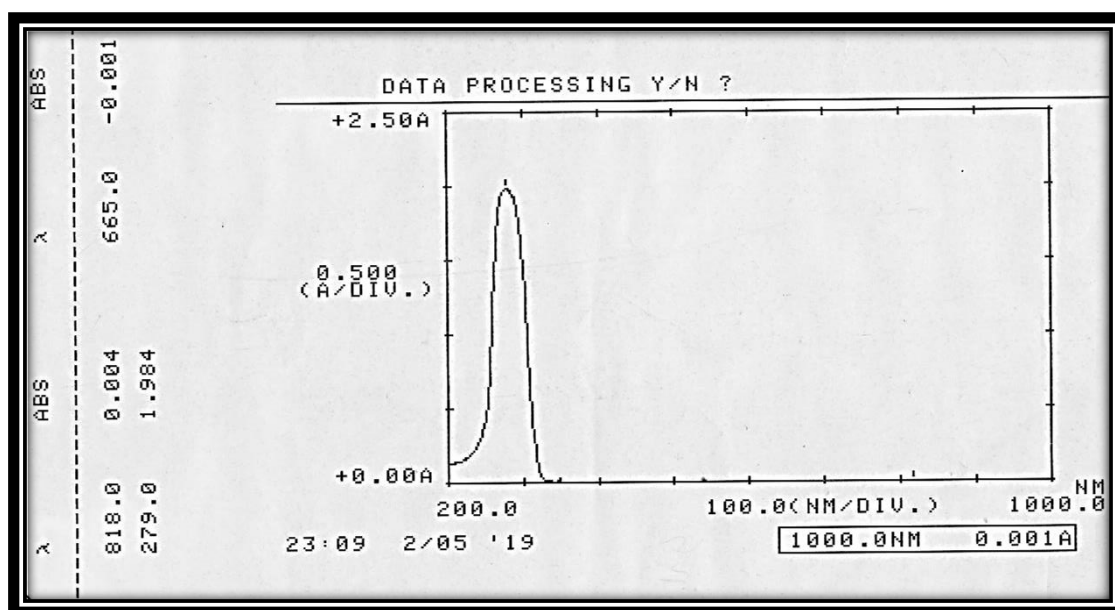


Figure (3-34) : UV/Vis Spectrum of [Sn(SMZ)(L-Pro)] Cl

### 3.4.4 The Proposed Molecular Structure for [L-pro H- Metal - (SMZ)] Complexes M-(II), M'-(III)

Studying complexes on bases of the above, spectral observations suggest the octahedral (Oh) geometry for all synthesized complexes which exhibited coordination number six and may be formulated as  $[M(\text{SMZ})(\text{L-pro})_2]$  for M-(II) and  $[M'(\text{SMZ})(\text{L-pro})_2]\text{Cl}$  for M'-(III). And coordination number four [Sn(SMZ)(L-pro)] Cl complex. The general structure of the complexes are 3D as shown in Figures (3-35), (3-36) and (3-37).

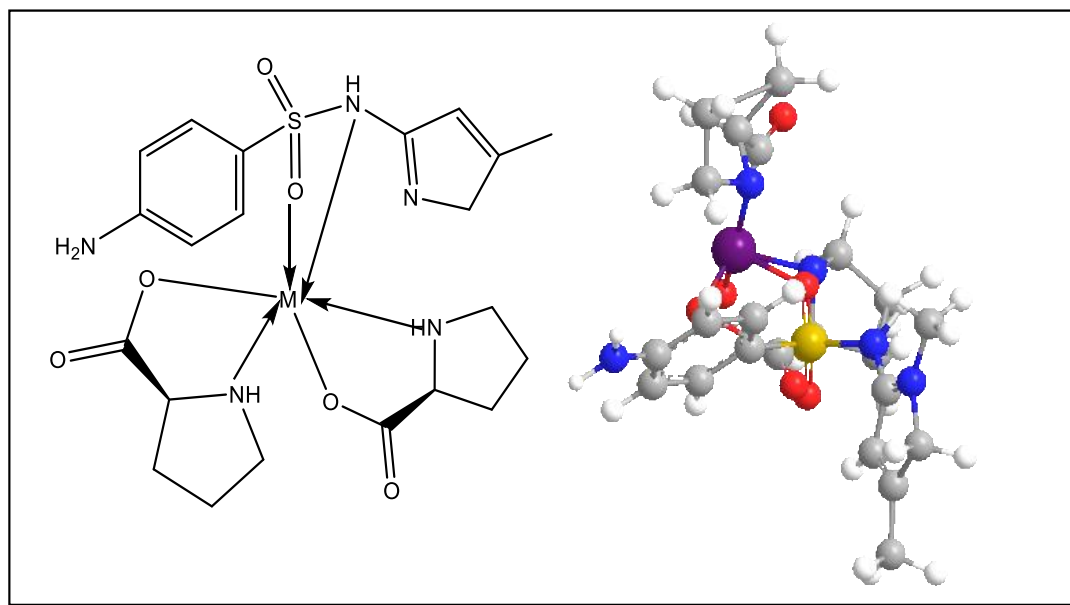
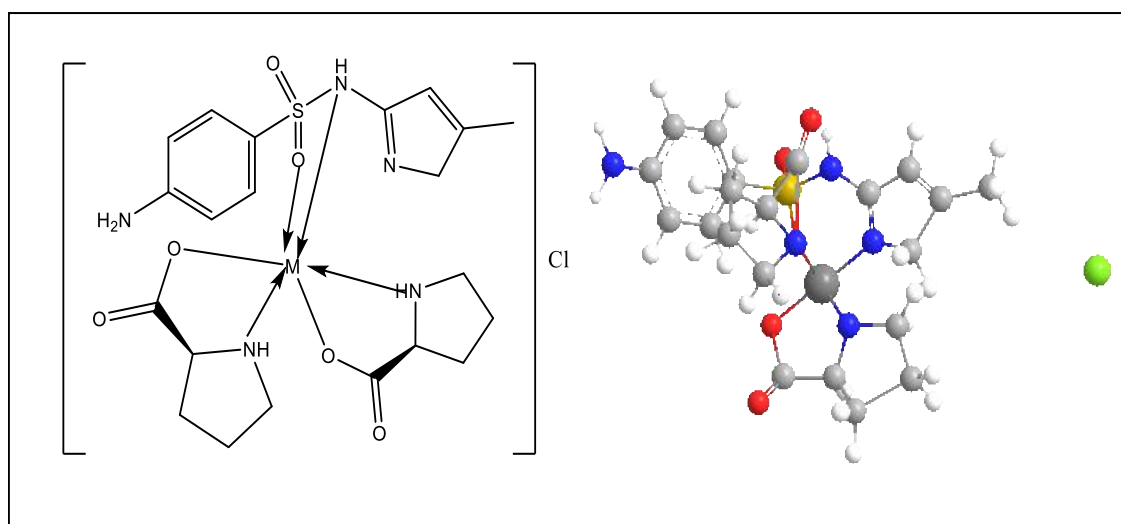
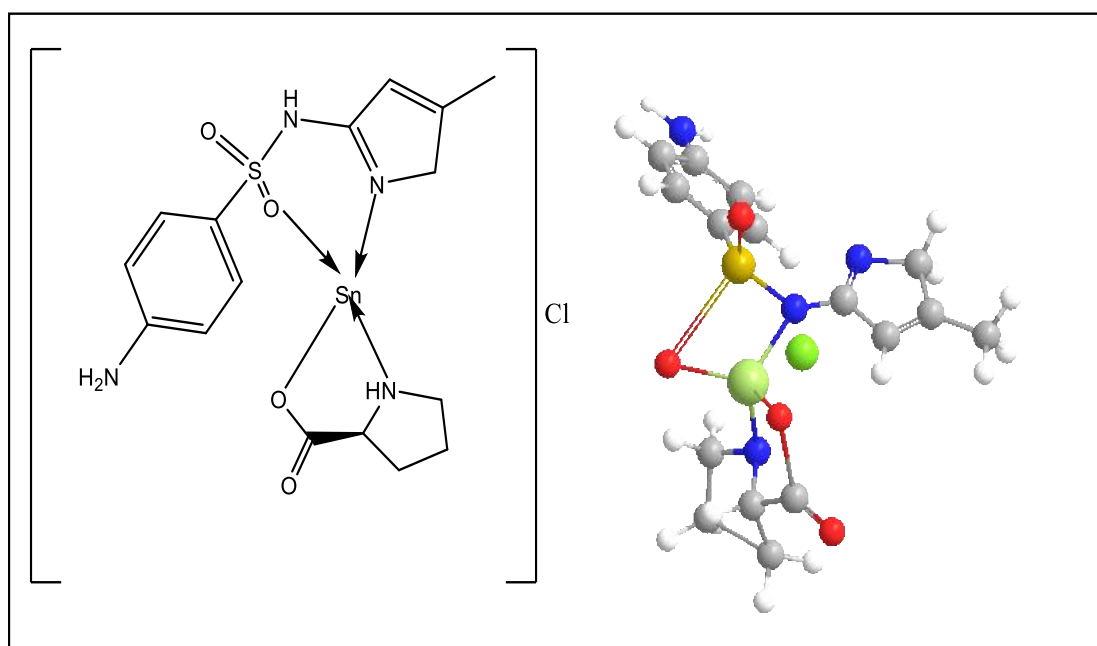


Figure (3-35) : 3D Molecular Modeling Proposed  $[M(SMZ)(L-pro)_2]$ .



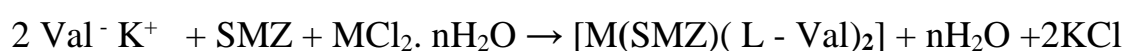
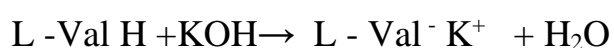
Figure(3-36) : 3D Molecular Modeling Proposed  $[M'(SMZ)(L-pro)_2]$ .



Figure(3-37) : 3D Molecular Modeling Proposed  $[Sn(SMZ)(L-pro)]Cl$

### 3. 5 Physico-Chemical Characterization of Mixed – ligand (L-Valine -Metal-SMZ) Complexes.

Generally, the complexes were prepared by reacting the respective metal salts with the ligands using 1:2:1 mole ratio, i.e., one mole of metal chloride, one mole of (SMZ) and two moles of potassium L -Val inate (L -Val K). The synthesis of mixed ligand metal complexes may be according to the following proposed general equation:



where; L-Valine symbolized as L-ValH

(primary ligand). L-Valinate ion  $L-Val^-$  = deprotonated L-ValH

Sulfamethoxazole = SMZ (secondary ligand).

M= Sn (II) ,Mn(II), Co(II), Ni(II), Cu(II), Cd(II) and Hg(II).

See Scheme (2-7) .



n =0-6

M' = Al(III) Cr (III) and Fe (III)

The physicochemical based on formula weights characteristics are given in (Table 3-17). The complexes are soluble in dimethyl sulfoxide (DMSO) while insoluble in common solvents, Table (3-18) [73]. The calculated and experimental values of metal percentage in each complex are in fair agreement. The test for chloride ion content with  $\text{AgNO}_3$  solution was negative ( $\text{Cl} \% = \text{Nil}$ ) for  $[\text{M}(\text{SMZ})(\text{L} - \text{Val})_2]$  indicating that no chloride ion outside of the coordination sphere [64] while positive for  $[\text{M}'(\text{SMZ})(\text{Val})_2]\text{Cl}$  indicating that chloride ion outside of the coordination sphere, the molar conductance's values ( $\Lambda_m$ ) of  $10^{-3}$  solutions of the complexes in DMSO lie in very low range (7-16)  $\Omega^{-1}\text{cm}^2\text{mol}^{-1}$  which are located in the range of non-electrolytes for  $\text{M}(\text{II})$ . and they proposed to have the general formulae  $[\text{M}(\text{SMZ})(\text{L} - \text{Val})_2]$ , . While the  $[\text{M}'(\text{SMZ})(\text{Val})_2]\text{Cl}$  complexes, they behave as 1:1 electrolytes .

Table (3-17) : The Physical Properties &amp; Atomic Absorption Results of the [M-SMZ - L-ValH] and [M'-SMZ - L-ValH] Complexes

Chemical Formula	Color	M.P °c (de) °c	Yield %	Metal analysis (%found) % cal	$\Delta m$ $\Omega^{-1} \text{ cm}^2 \text{ mol}^{-1}$ In DMSO
<b>[ M-SMZ - L- Val H]</b>					
[Sn(SMZ)( L-Val) <sub>2</sub> ]	Pale yellow	>260	85	(20.7) (19.16)	9
[Mn(SMZ)( L-Val) <sub>2</sub> ]	Gray	235	80	(11.1) (9.61)	7
[Fe(SMZ)( L-Val) <sub>2</sub> ]	Brown	>260	82	(11.7) (10.30)	11
[Ni(SMZ)( L- Val) <sub>2</sub> ]	Green	>260	72	(10.18) (10.20)	10
[Cu(SMZ)( L- Val) <sub>2</sub> ]	Blue	>260	77	(11.62) (11.55)	8
[Cd(SMZ)( L-Val) <sub>2</sub> ]	White	>260	89	(12.1) (18.00)	14
[Hg(SMZ)( Val) <sub>2</sub> ]	White	230d	82	- (27.92)	16
<b>[ M'-SMZ - L-ProH]</b>					
[Al (SMZ)( L- Val) <sub>2</sub> ]	White	>260	81	- (4.94)	10
[Cr (SMZ)( L- Val) <sub>2</sub> ]	Green	>260	81	(11.4) (9.12)	18
[Fe(SMZ)( L- Val) <sub>2</sub> ]	Orange	>260	81	(12.1) (9.25)	16

Table (3-18): The solubility of complexes

<b>Chemical Formula</b>	<b>C<sub>3</sub>H<sub>6</sub>O</b>	<b>C<sub>6</sub>H<sub>6</sub></b>	<b>DMF</b>	<b>DMSO</b>	<b>EtOH</b>	<b>H<sub>2</sub>O</b>	<b>Hexanol</b>	<b>HCl</b>
[Sn(SMZ)(Pro) <sub>2</sub> ]	-	-	-	+	-	-	--	-
[Mn(SMZ)(L-Val) <sub>2</sub> ]	-	-	+	+	-	-	-	+
[Fe(SMZ)( L-Val ) <sub>2</sub> ]	-	-	-	+	-	-	-	+
[Ni(SMZ)( L-Val ) <sub>2</sub> ]	+	--	+	+	-	+	+	+
[Cu(SMZ)( L-Val ) <sub>2</sub> ]	+	+	+	+	+	+	+	+
[Cd(SMZ)( L-Val ) <sub>2</sub> ]	-	+	+	+	--	-	+	+
[Hg(SMZ)( L-Val ) <sub>2</sub> ]	-	-	--	+	+	-	-	+
[Al (SMZ)( L-Val ) <sub>2</sub> ]	+	--	+	+	+	-	+	+
[Cr (SMZ)( L-Val ) <sub>2</sub> ]	+	--	+	+	+	+	+	+
[Fe(SMZ)( L-Val ) <sub>2</sub> ]	+	-	+	+	+	+	+	+
[Sn(SMZ)( L-Val )]	+	--	--	+	--	-	+	+
(+ ) Soluble, (-) Insoluble, (---) Sparingly								

Table (3-19) : Infrared spectral data (wave number  $\hat{\nu}$ )  $\text{cm}^{-1}$  for [SMZ – M – L-ValH] complexes

Complexes	$\nu_{\text{as}}$ (NH):NH <sub>2</sub> vs (NH): sulfonamide group vs (NH): sulfonamide group	$\nu$ (C-H)	(C=C) Ar.	(SO <sub>2</sub> ) asy	(-COO) asy (C-N)	(-COO) sym	$\nu_{\Delta}$ (-COO) asy-sym	(C=N) (SMZ) Isoxazol ring in	(SO <sub>2</sub> ) sy	(S-N)	(M-N)	(M-O)
[Mn (SMZ)(L-Val) <sub>2</sub> ]	3498 3379 3201	2943 s, 2889m	1419s	1319	1627s 1600	1377	250	1504 m	1111	941	566	482
[Co(SMZ)(L-Val) <sub>2</sub> ]	3456 3321 3209	2978 s, 2934 2881br	1477 m	1354	1612s 1585	1396	216	1508	1134	956	520	470
[Ni (SMZ)(L-Val) <sub>2</sub> ]	3468 3205	2958vs	1593 vs	1365m	1620 1593 vs	1365 s	255	1500 vs	1153 vs	929	547	466w
[Cu (SMZ)(L-Val) <sub>2</sub> ]	3471 3209 3140	2981m 2858m	1597	1365 vs	1620 1597 vs	1354 vs	266	1604	1111 vs	929	547	470
[Cd (SMZ)(L-Val) <sub>2</sub> ]	3468 3379 32055	2951m	1597	1315	1597 vs	1408 1315	189	1504	1122 vs	945 vs	551 m	482
[Hg (SMZ)(L-Val) <sub>2</sub> ]	3479 3205 3170	2970m	1502	1379	1543 s	1319	224	1597vs	1153 vs	933	547	474

Table (3-20): Infrared spectral data (wave number  $\hat{\nu}$ )  $\text{cm}^{-1}$  for  $[\text{SMZ} - \text{M} - \text{L-ValH}]$  complexes

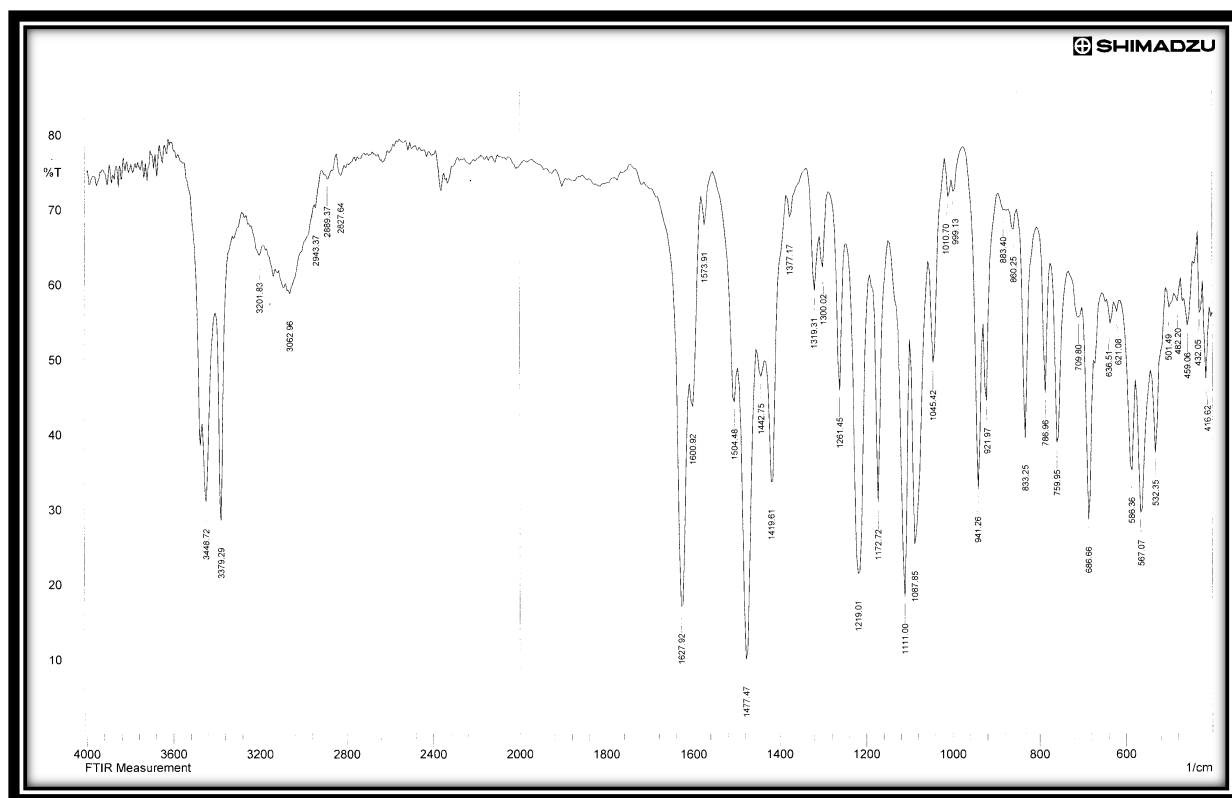
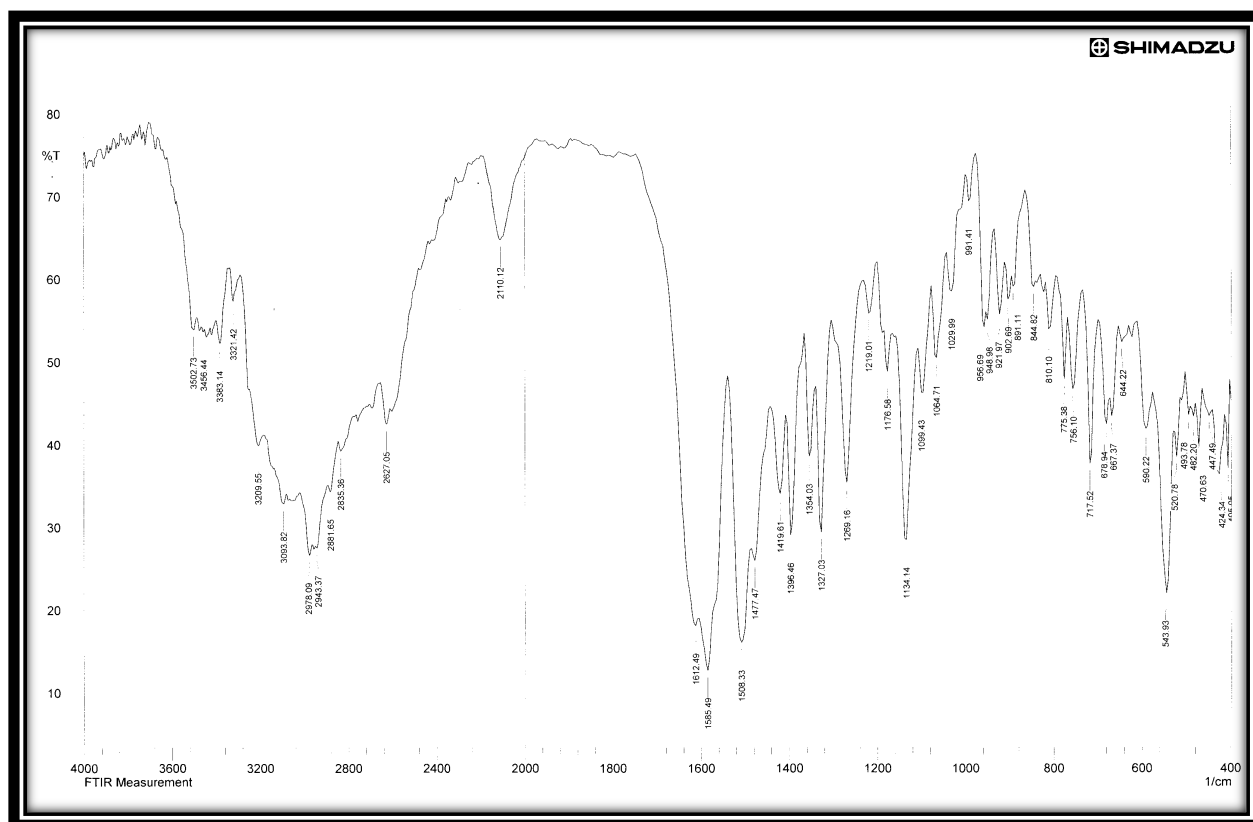
Compounds	$\nu_{\text{as}}(\text{NH}) : \text{NH}_2$ vs $\nu(\text{NH})$ : sulfonamide group vs $\nu(\text{NH})$ : sulfonamide group	$\nu(\text{C-H})$	(C=C) Ar.	(SO <sub>2</sub> ) asy	$\nu$ methaxazole ring.	(-COO) asy (C-N)	(-COO) sym	$\nu_{\text{A}}$ (-COO) asy-sym	(C=N) (SMZ) Isoxazol In ring	(SO <sub>2</sub> ) sy	(S-N)	(M-N)	(M-O)
$[\text{Al}(\text{SMZ})(\text{L-Val})_2]\text{Cl}$	3417 3360 3205	2981 2858 m	1455 s	1311	1624s	1597	1377	220	1500 vs	1141 vs	929	567	482
$[\text{Cr}(\text{SMZ})(\text{L-Val})_2]\text{Cl}$	3471 3394 vs -br3140	29812v s 2858w	1465	1365	1624s	1597	1365 s	232	1620 vs	1141 vs	929	547	478 w
$[\text{Fe}(\text{SMZ})(\text{L-Val})_2]\text{Cl}$	3468, 3360 3205	2981 s, 2858 br	1465	1365	1620	1597 vs	1365	232	1500 vs	1153	929	547	478
$[\text{Sn}(\text{SMZ})(\text{L-Val})_2]$	3468 3205	2958vs	1593 vs	1365 m	1620	1593 vs	1365 s	228	1500 vs	1153 vs	929	547	459w
$[\text{Sn}(\text{SMZ})(\text{L-Val})]$	3471 3209 3140	2981m ,2858m	1597	1365 vs	1620	1597 vs	1354 vs	243	1604	1111 vs	929	547	470



### 3. 5. 1. FT-IR spectra of [SMZ -M-L-ValH] and [SMZ - M'-L-ValH] complexes

The assignment of the characteristic bands (FT-IR) spectrum of the free ligand L-ValH, Figure (3-3), and, SMZ Figure (3-1) are summarized in Table (3-6) and (3-4). The characteristic frequencies of the all complexes are given in Tables (3-19) and (3-20) and shown in Figures (3-38) to (3-49) were supported by comparison with the vibrational frequencies of the free L-ValH. ligand and other related complexes.

The asymmetric stretching band of  $\nu$  ( $\text{COO}^-$ ) were shifted to a higher frequency in metal complexes at  $(1543-1672) \text{ cm}^{-1}$ , whereas the  $\nu$  ( $-\text{COO}$ )<sub>sym</sub> band were shifted to a lower frequency at  $(1315-1396) \text{ cm}^{-1}$ , these values are quite agreeable with the values reported earlier <sup>[57,86]</sup>. The coordination mode of (SMZ) with metal ions is predicted as a bidentate through the O,N atoms of sulfonylamid group for all complexes, more evidence new bands which appeared in the range  $(520-567) \text{ cm}^{-1}$  and  $(466-482) \text{ cm}^{-1}$  due to the stretching frequencies of (M-O), (M-N). The bands appeared at  $(1111-1153 \text{ cm}^{-1})$  and  $(1311 - 1278 \text{ cm}^{-1})$  may be assigned to the bending of  $(\text{SO}_2)$  sym and  $(\text{SO}_2)$  sy groups <sup>[38]</sup>. The medium and strong bands like bands which mentioned in 3. 4. 1 for most .Function groups . The multiband and shifting of sulfonamide  $-\text{NH}$  in the spectra of the all complexes indicating the involvement of  $-\text{NH}$  in chomplexation with central metal ion by nitrogen of sulfonamide  $-\text{NH}$  according to the data reported in literature <sup>[47-48]</sup> . The value of  $\Delta\nu = [\nu (\text{COO}^-)]_{\text{asym}} - [\nu (\text{COO}^-)]_{\text{sym}}$  is ranging from  $(201-294) \text{ cm}^{-1}$ , indicating a monodentate bonding of carboxylate ( $\text{COO}^-$ ) group. Thus, (L-Val) acts as bidentate monobasic ligand through Oxygen ( $\text{COO}^-$ ) group, and Nitrogen primary amine  $-\text{NH}_2$  group.

Figure (3-38) : FT-IR Spectrum of  $[\text{Mn}(\text{SMZ}) (\text{L-Val})_2]$ Figure (3-39) : FT-IR Spectrum of  $[\text{Co}(\text{SMZ}) (\text{L-Val})_2]$

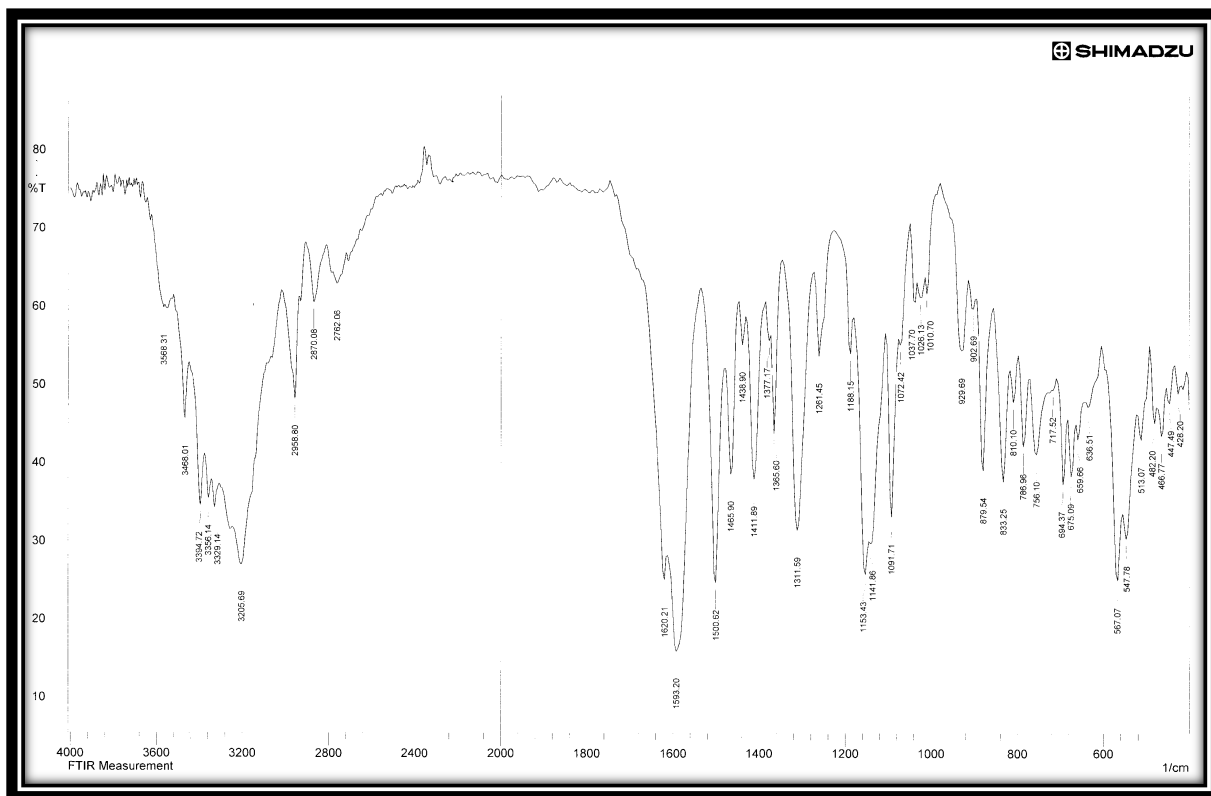


Figure (3-40): FT-IR Spectrum of [Ni(SMZ) (L-Val)<sub>2</sub>]

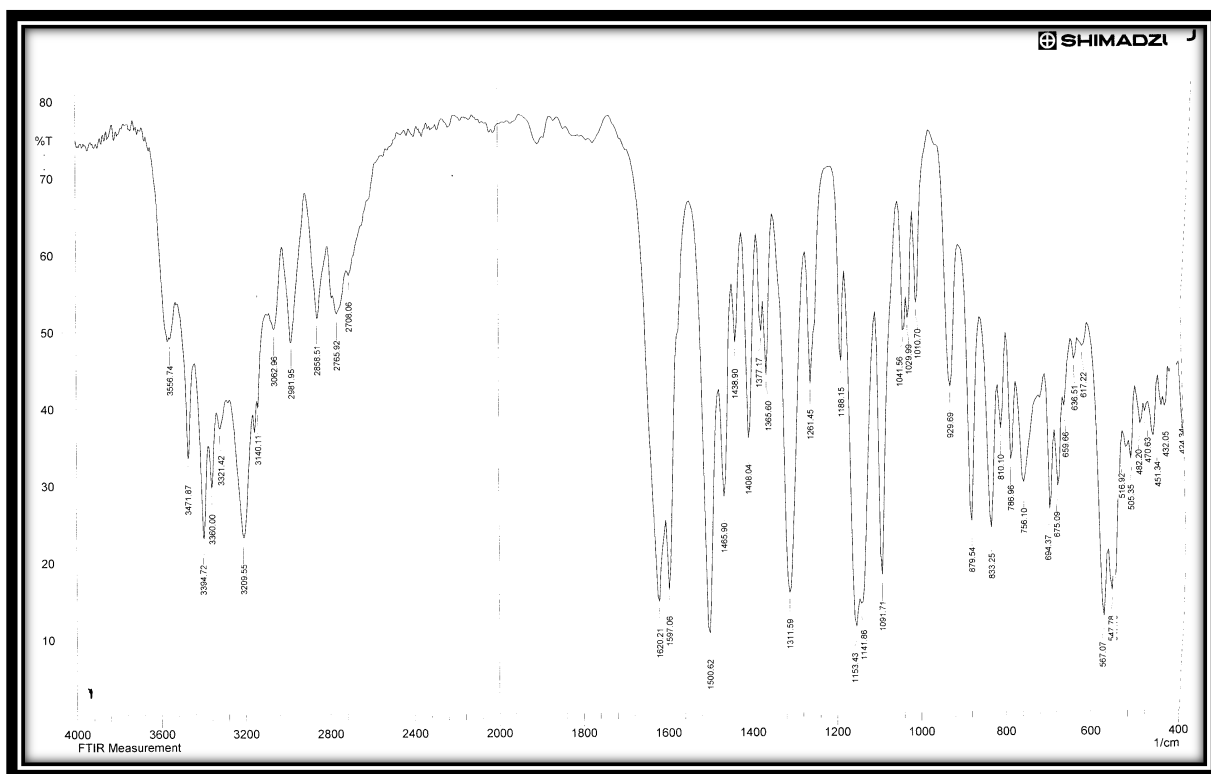
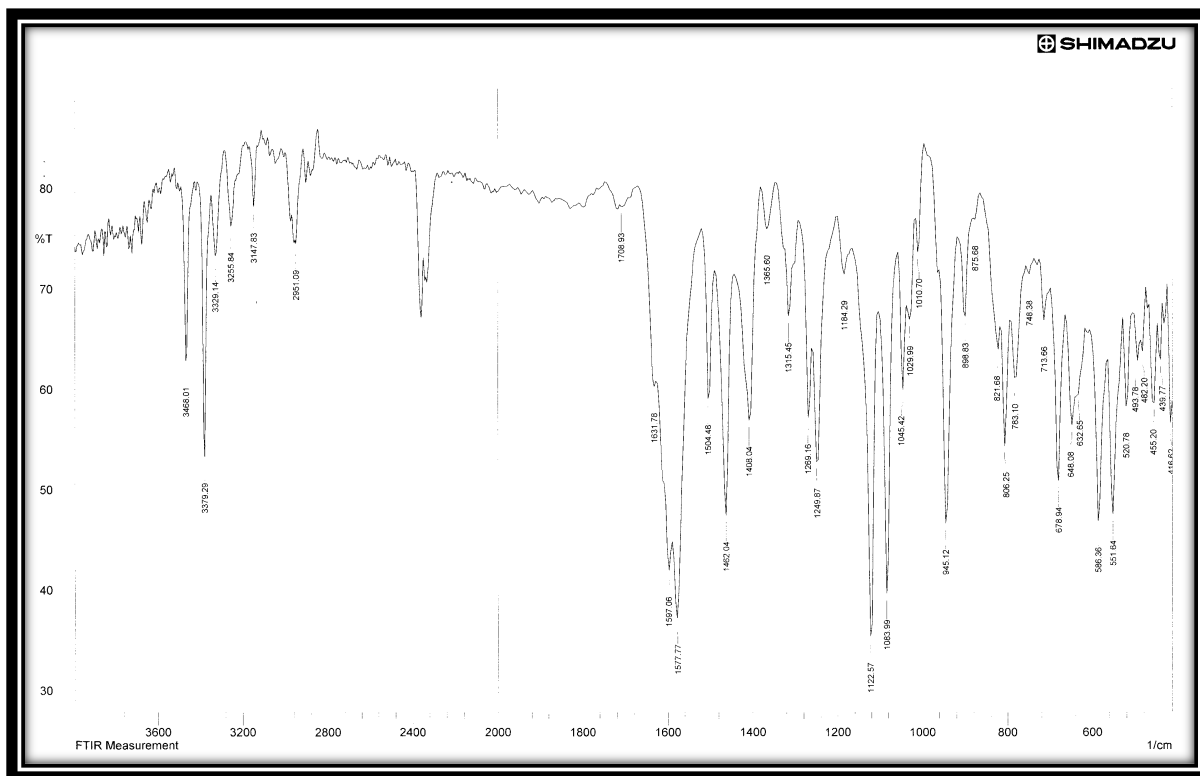
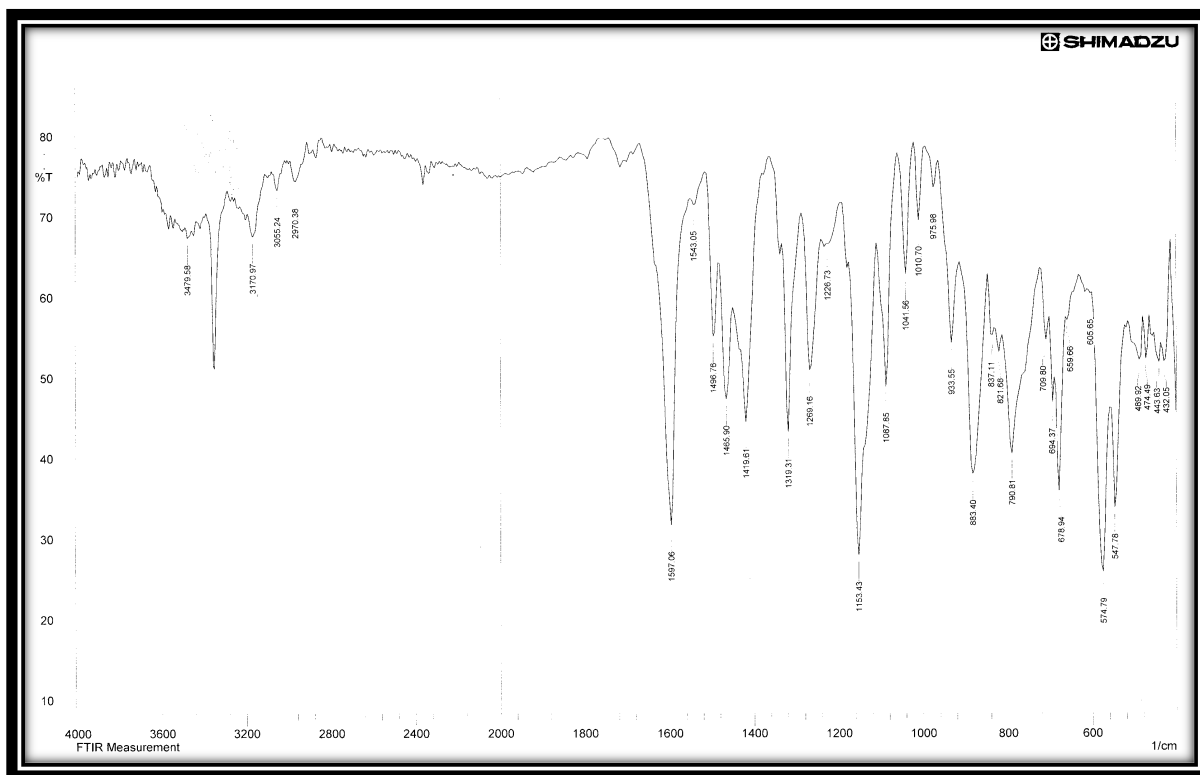
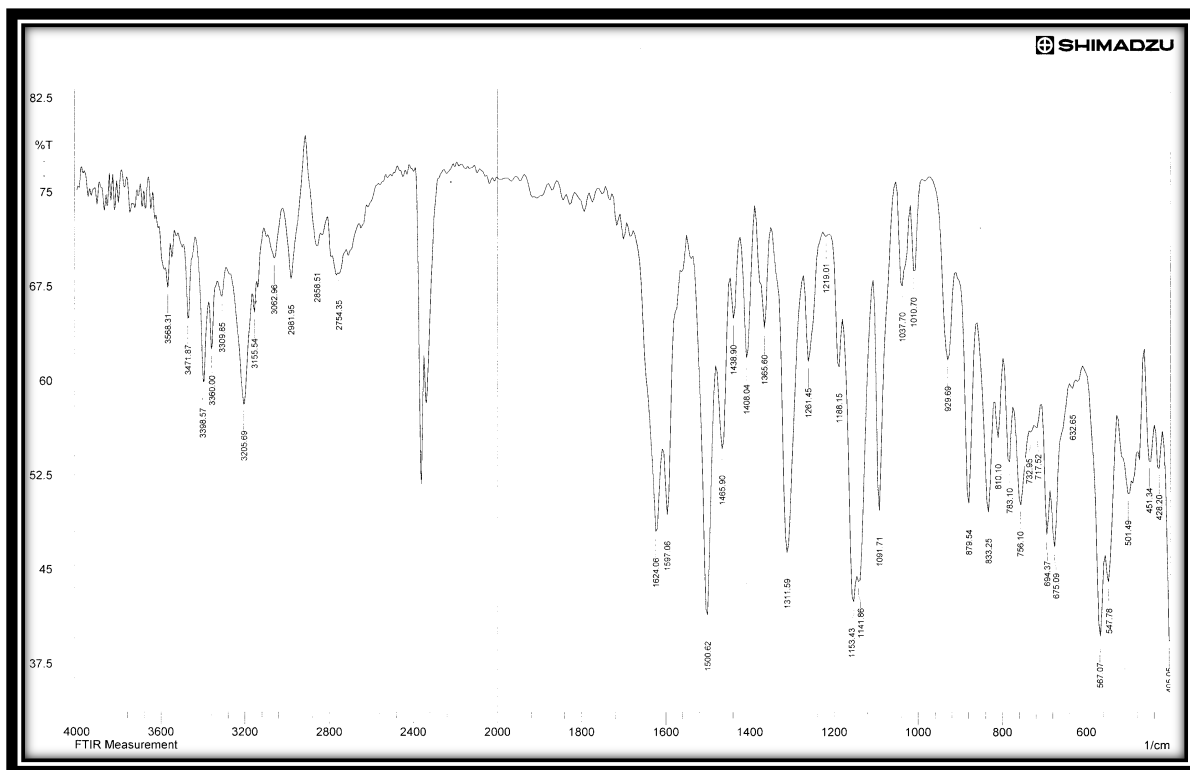
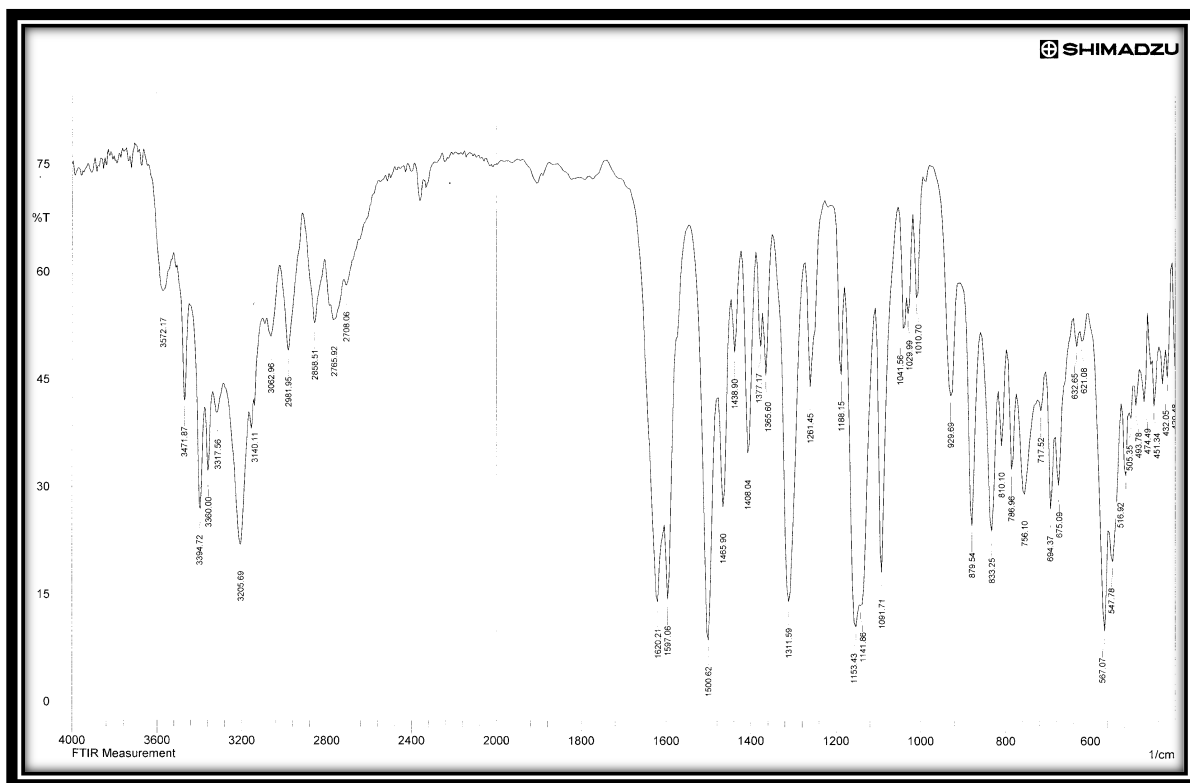
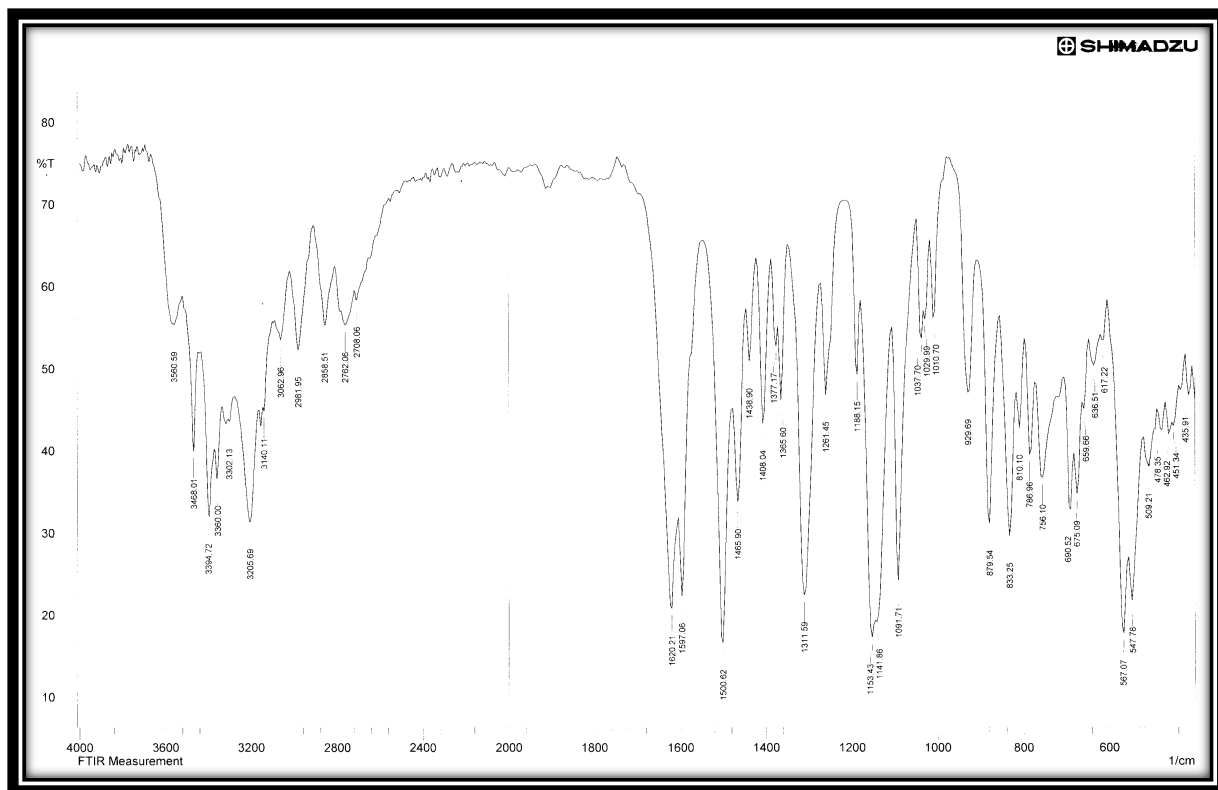
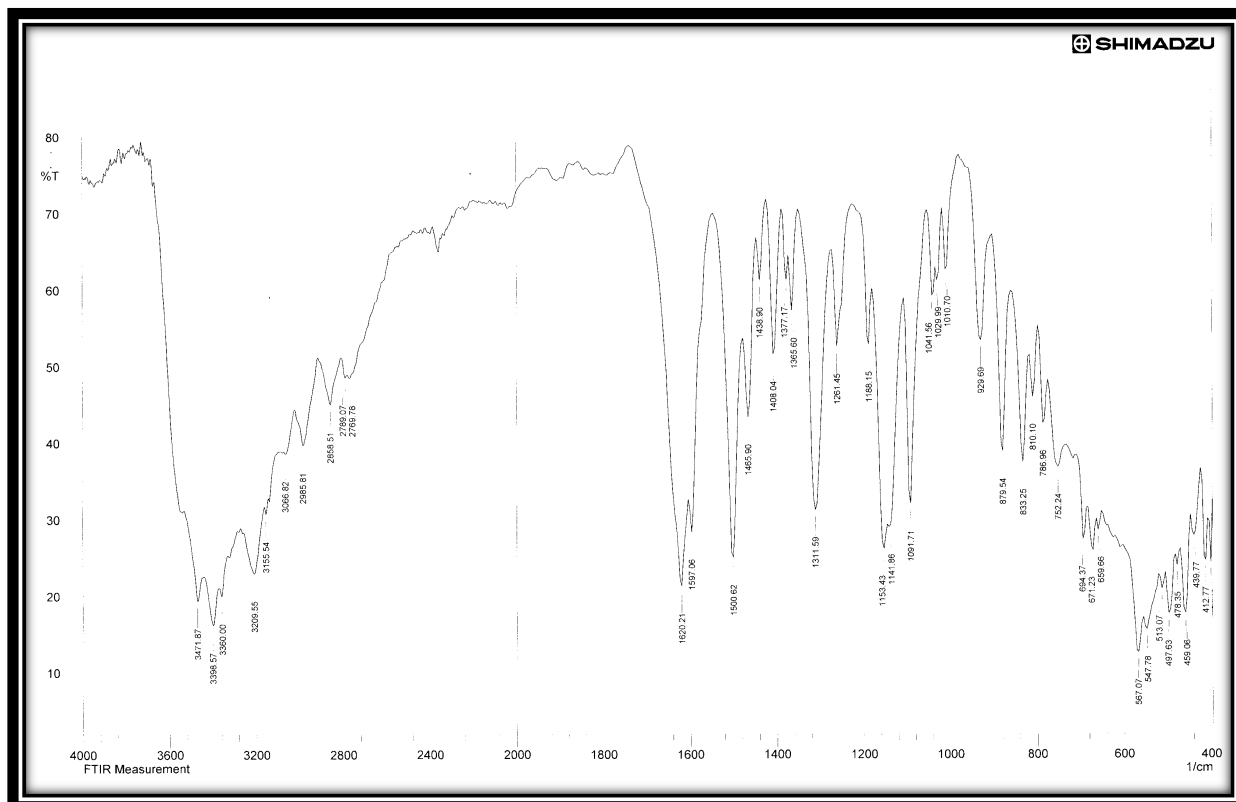


Figure (3-41): FT-IR Spectrum of [Cu(SMZ) (L-Val)<sub>2</sub>]

Figure (3-42) FT-IR Spectrum of  $[\text{Cd}(\text{SMZ}) (\text{L-Val})_2]$ Figure (3-43) : FT-IR Spectrum of  $[\text{Hg}(\text{SMZ}) (\text{L-Val})_2]$

Figure (3-44) FT-IR Spectrum of  $[Al (SMZ) (L-Val)_2]Cl$ Figure (3-45) : FT-IR Spectrum of  $[Cr (SMZ) (L-Val)_2]Cl$

Figure (3-46) : FT-IR Spectrum of  $[\text{Fe}(\text{SMZ})(\text{L-Val})_2]\text{Cl}$ Figure (3-47) : FT-IR Spectrum of  $[\text{Sn}(\text{SMZ})(\text{L-Val})_2]$

### 3.5.2. Ultraviolet / Visible [UV/Vis]

Spectra of [M-SMZ -L-ValH] and [M'-SMZ - L-ProH] complexes Tables (3-21) and (3-22) show the positions of electronic absorption bands and their transitions and  $\mu_{eff}$  .

Table (3-21): Electronic Spectral Data of the Mixed- Ligand (L-Valin - Metal(II) -(SMZ) Complexes

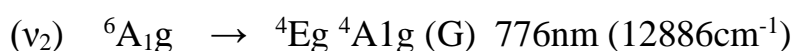
Complexes	$\lambda$ nm	$\nu'$ cm <sup>-1</sup>	$\epsilon$ max Mol <sup>-1</sup> .L. cm <sup>-1</sup>	Assignments	$\mu_{eff}$ B.M
[Mn(SMZ)( L-Val) <sub>2</sub> ]	295 675 776 802	33898 14814 12886 12468	2297 84 68 65	C.T 6A <sub>1g</sub> → 4T <sub>2g</sub> v <sub>3</sub> 6A <sub>1g</sub> → 4T <sub>1g</sub> v <sub>2</sub> 6A <sub>1g</sub> → 4T <sub>1g</sub> (G v <sub>2</sub> )	5.61
[Co(SMZ)( L- Val) <sub>2</sub> ]	271 499 899	36900 20040 11123	1591 15 3	C.T 3A <sub>2g</sub> (F) → 3T <sub>1g</sub> (P) 3A <sub>2g</sub> (F) → 3T <sub>2g</sub> (F)	5.67
[Ni(SMZ)( L. Val) <sub>2</sub> ]	297 373 803	33670 26809 12453	2240 34 16	C.T <sup>3</sup> A <sub>2g</sub> ( <sup>F</sup> ) → <sup>3</sup> T <sub>1g</sub> ( <sup>f</sup> ) v <sub>2</sub> <sup>3</sup> A <sub>2g</sub> ( <sup>F</sup> ) → <sup>3</sup> T <sub>1g</sub> ( <sup>p</sup> ) v <sub>3</sub>	2.14
[Cu(SMZ)( Val) <sub>2</sub> ]	298 816 950	33557 12254 10526	2259 3 2	C.T <sup>2</sup> B <sub>1g</sub> → <sup>2</sup> B <sub>2g</sub> <sup>2</sup> B <sub>1g</sub> → <sup>2</sup> E <sub>g</sub>	1.62
[Cd(SMZ)( L-Val) <sub>2</sub> ]	275 812	36363 12315	1910 2	C.T C.T	Diamagnetic
[Hg(SMZ)( L.Val) <sub>2</sub> ]	290 823	34482 12150	2193 4	C.T C.T	Diamagnetic

Table (3-22): Electronic Spectral Data of the Mixed- Ligand (L-Valin -  
Metal(III) -(SMZ) Complexes

Complexes	$\lambda$ nm	$\nu$ 'cm <sup>-1</sup>	$\epsilon$ max (molar <sup>-1</sup> .cm <sup>-1</sup> )	Assignments	$\mu_{\text{eff}}$ (BM)
[Al(SMZ)( L-Val) <sub>2</sub> ]Cl	289 848	34602 11792	2138 3	c.t The 3d ← 3p transitions in the Al-N	Dima
[Cr(SMZ)( L-Val ) <sub>2</sub> ]Cl	300 845	33333 11834	2370 22	INCT <sup>4</sup> A <sub>2g</sub> → <sup>4</sup> T <sub>1g</sub> (v <sub>3</sub> )	1.85
[Fe(SMZ)( L-Val ) <sub>2</sub> ]Cl	295 723	33898 13831	2206 9	CT 6A <sub>1g</sub> →4T <sub>2g</sub> (4G)	5.13
[Sn(SMZ)( L- Val) <sub>2</sub> ]	295 850 984	33893 11764 10162	2262 175 180	$\pi$ - $\pi^*$ C.T C.T	0 Diana
[Sn(SMZ)( L- Val )]Cl	279 818	35842 12224	1984 4	$\pi$ → $\pi^*$ CT	0 Diana

### 3.5.2.1 UV/Vis Spectrum of [Mn(SMZ)(L- Val)<sub>2</sub>]

The magnetic moment shown in Table (3-21) of the brown Mn(II) d<sup>5</sup> (Term <sup>6</sup>S) complex is 5,61 B.M. corresponding to five unpaired electrons. However, UV-Vis spectrum, Figure (3-48), of the [Mn(SMZ)(Val)<sub>2</sub>] complex showed four bands one in 295nm (33898cm<sup>-1</sup>) assigned to the charge transfer transition and three bands in the d-d transition region at 12468 cm<sup>-1</sup>, 12886 cm<sup>-1</sup> and 14814 cm<sup>-1</sup> and can be assigned to the following transitions:



In the (d<sup>5</sup>) system the octahedral splitting equal to tetrahedral yellow and green colors but the O.h geometry are characterize by the pale pink or without color [82] as the present complex .The value of the measured



magnetic moment is (5,61 B.M.) in accordance with the presumption of high-spin  $d^5$  Mn(II) ion in octahedral geometry<sup>(87)</sup>,  $10 Dq = \nu_1 = 12468 \text{ cm}^{-1}$ .  
 1. The value which is the ratio of B complex / B-ion shows a value of 0.39.  $B'$  value of ( $971 \text{ cm}^{-1}$ ) for the free Mn(II) ion,  $\nu_2 / \nu_1 = 0.59$ ,  $\nu_1 / \nu_2 = 1.69$ , first spin-allowed transition  $\Delta_o = \Delta E = 12468 \times 0.01196 = 149.1172 \text{ kJ/mol}$ ,  $\Delta E = \Delta_o = 12468 \times 1.24 \times 10^{-4} = 1.546032 \text{ eV}$

Table (3-23) : Electronic Spectral Data of the  $[\text{Mn}(\text{SMZ})(\text{L-Val})_2]$

Absorption Band ( $\text{cm}^{-1}$ )	transitions	B	Dq / B'	B'	$\beta$	10Dq	15 B'
12.468	${}^6\text{A}_{1g} \rightarrow \text{T}_{1g}(\nu_1)$						
21,077	${}^6\text{A}_{1g} \rightarrow {}^4\text{E}_{1g} {}^4\text{A}_{1g}(\nu_2)$	960	1.9	589	0.39	12.468	8835
22.222	${}^6\text{A}_{1g} \rightarrow {}^4\text{T}_{2g}(\nu_3)$						

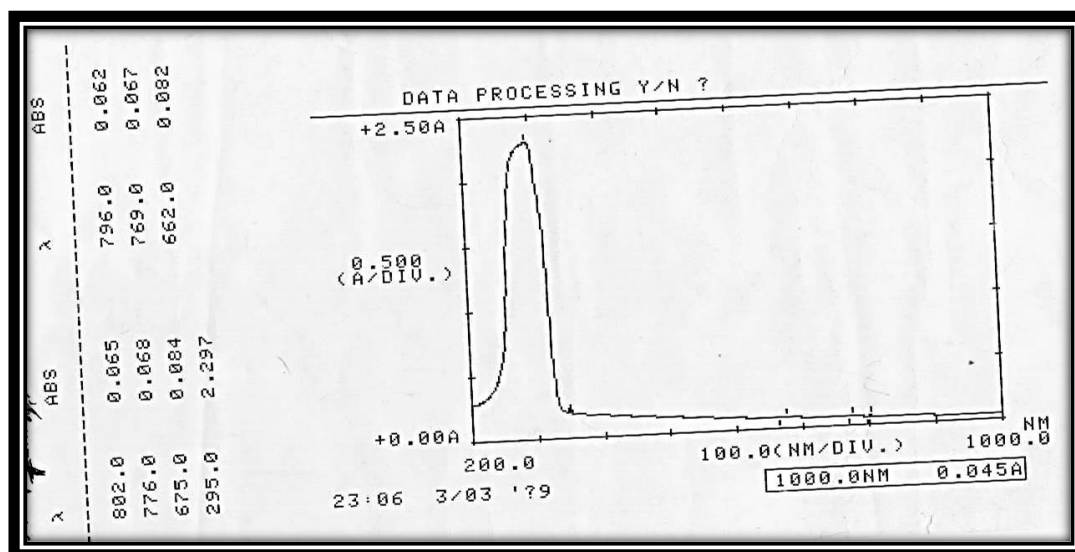


Figure (3-48) : UV/Vis Spectrum of  $[\text{Mn}(\text{SMZ})(\text{L-Val})_2]$

The relatively high value of 10Dq and low value of ( $\beta$ ) (0.39) indicate the participation of the nitrogen in the coordination with Mn (II) ion through a

bond of high covalent character. The low ratio of  $\nu_2/\nu_1$  (1.69) indicates the octahedral geometry .

### 3.5.2.2 UV/Vis Spectrum of [Co (SMZ)(L- Val)2]

The magnetic moment shown in Table (3-21) of the brown Co (II)  $d^7$  complex is 5,67 B.M. corresponding to (five unpaired ) electrons. Electronic spectrum of Cobalt (II) complex Figure (3-49) show three transitions, but these transitions can not be assigned because of the greater overlapping of them <sup>(97,98)</sup>. Octahedral complex of Co (II) consists of two bands one in the (15,400-15,500)  $\text{cm}^{-1}$  and the other in the (20,000-20,830)  $\text{cm}^{-1}$  regions <sup>(99)</sup>.

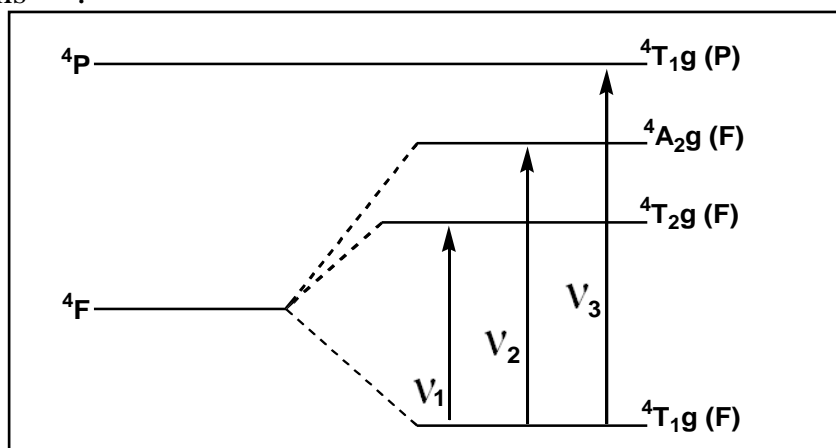


Figure (3-49) : Electronic transition for  $d^7$  system for Co(II).

The UV-Vis spectrum of the [Co(SMZ)(Val)<sub>2</sub>] Figure (3-50) three bands appear; one at (15,382  $\text{cm}^{-1}$ ) and the other two d-d transition at (20040  $\text{cm}^{-1}$ ) and (11123  $\text{cm}^{-1}$ ) which were assigned to the transitions  $\nu_3$  and  $\nu_2$  respectively. The value of  $\nu_1$  were calculated using Tanabe-Sugano diagram for  $d^7$  system, Figure (3-51) and found to be (22,724  $\text{cm}^{-1}$ ) which refer to  $4T_{1g}(F) \rightarrow 4T_{2g}(P)$  transition.

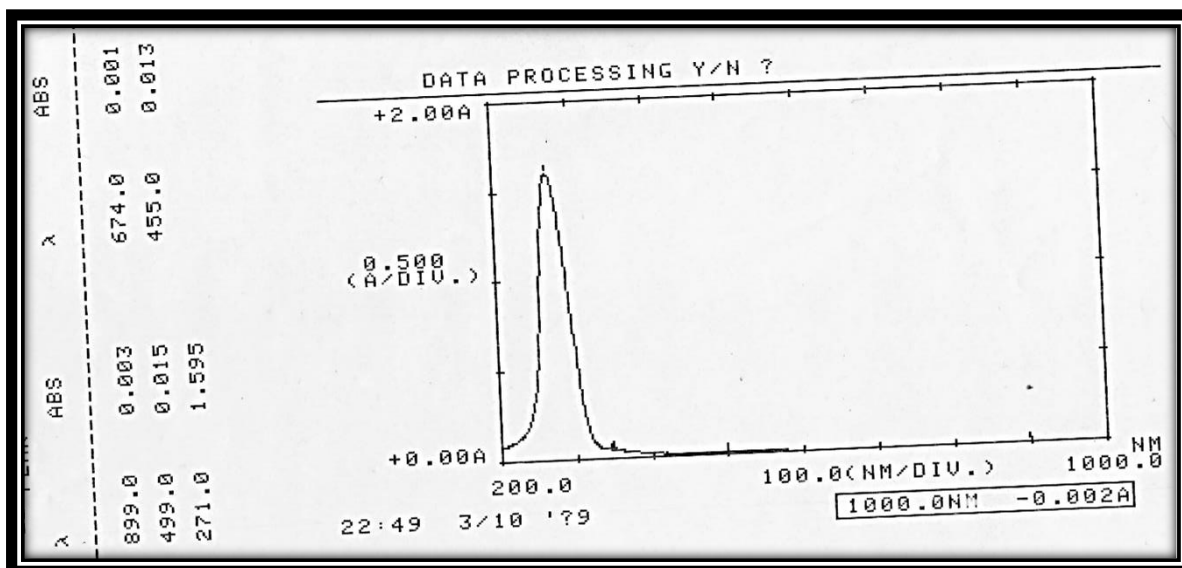


Figure (3-50) : Electronic Spectrum of  $[\text{Co}(\text{SMZ})(\text{L-Val})_2]$

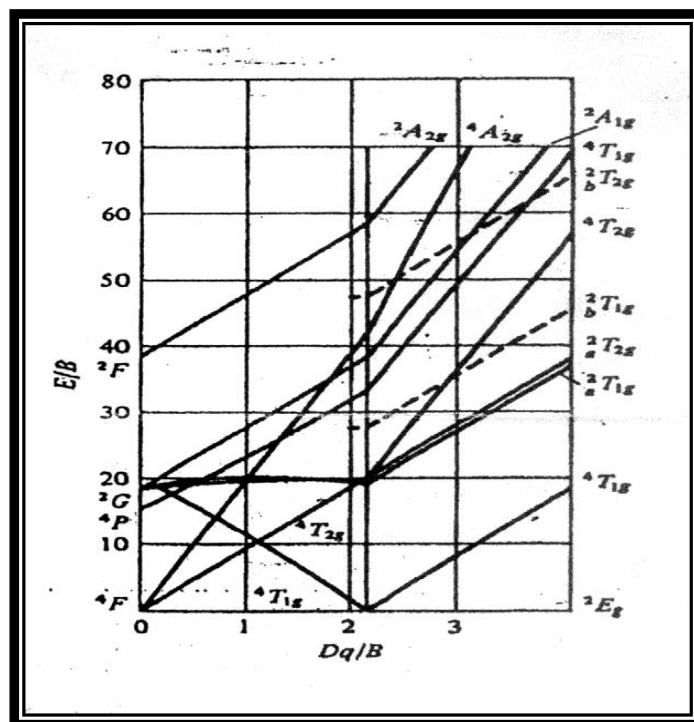


Figure (3-51): Tanabe-Sugano diagram for  $d^7$  system.

From appendix Figure. (3-49) and Figure (3-50) as

$$499 + 899 = 1390 \text{ nm}$$

$$1390 \div 2 = 695 \text{ nm}$$

$$3495 \text{ nm} = 28612 \text{ cm}^{-1}, \quad {}^4T_{1g}(\text{F}) \rightarrow {}^4T_{2g}(\text{P}) (\nu_2).$$

$$1390 \text{ nm} = 71942 \text{ cm}^{-1}, \quad {}^4A_{2g} \leftarrow {}^4T_{1g}. (\nu_1).$$

$$\frac{\nu_1}{\nu_2} = \frac{71942}{28612} \cong 2.51$$

$$E = \frac{(\nu_3)}{B} = 27$$

$$B = \frac{20240}{27} = 749$$

$$\frac{\Delta_0}{B} = 18$$

$$\Delta_0 = 18 \times 749 = 13482 \text{ cm}^{-1}$$

$$\beta = \frac{B \text{ complex}}{B} = \frac{749}{971} = 0.77$$

On the basis of analytical, conductance and spectral data, octahedral geometry is assigned to Cobalt complex.

### 3.5.2.3 UV/Vis Spectrum of [Ni (SMZ)(L- Val)<sub>2</sub>]

The magnetic moment of the Ni(II) d<sup>8</sup> (Term <sup>3</sup>F) complex is 2.14 B.M, indicating the octahedral configuration of this complex <sup>[94]</sup>. The electronic spectrum of the [Ni(SMZ)( L-Val)<sub>2</sub>] complex shows three bands at (297 nm) 35842 cm<sup>-1</sup>, <sup>1</sup> which may be assigned to charge transfer transitions and show other two d-d transition bands at (373nm) 26809 cm<sup>-1</sup> and (803nm) 12453 cm<sup>-1</sup>, (Table 3-21) which are assignable to A<sub>2g</sub><sup>(F)</sup>→<sup>3</sup>T<sub>1g</sub><sup>(p)</sup> (ν<sub>3</sub>) and <sup>3</sup>A<sub>2g</sub><sup>(F)</sup> →<sup>3</sup>T<sub>1g</sub><sup>(f)</sup> ν<sub>2</sub>.

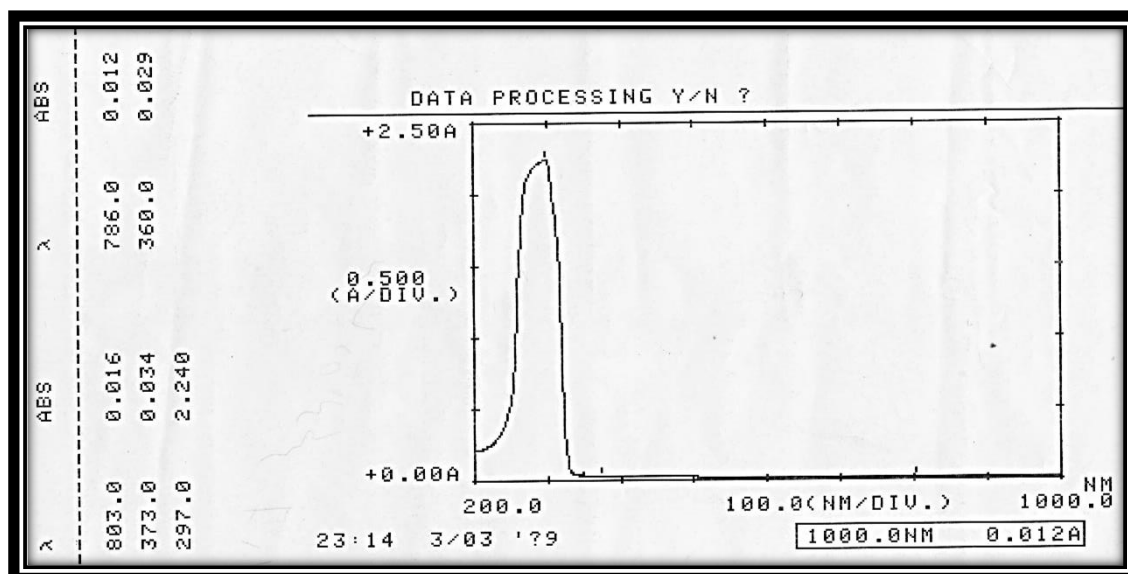


Figure (3-52) : Electronic Spectrum of [Ni (SMZ)(L-Val)<sub>2</sub>]

### 3.5.2.4 UV/Vis Spectrum of [Cu (SMZ)(L-Val)<sub>2</sub>]

Cu(II) compounds are blue or green because of single broad absorption band in the region (11,000-16,000)  $\text{cm}^{-1}$ <sup>(101)</sup>. The  $d^9$  ion is characterized by large distortion from Oh symmetry and the bond is unsymmetrical, being the result of a number of transitions, for free ion ground  $^2D$  term.

according to the diagram in Figure (3-53)

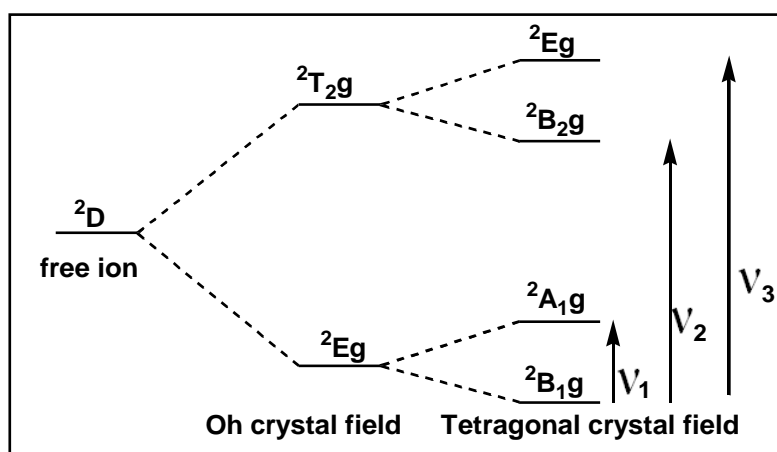


Figure (3-53): Diagram transition of Cu(II)

The value of ( $\mu_{\text{eff}}$ ) that have been measured for [Cu(MZ)(Val)<sub>2</sub>] complex was (1.62 B.M.) this value is in the range of mononuclear octahedral geometry<sup>(102,103)</sup>. The electronic spectrum of the [Cu(SMZ)(L-Val)<sub>2</sub>] complex, Figure (3-54) shows three bands at (298 nm)  $33557 \text{ cm}^{-1}$  assigned

to charge transfer transitions and show other two d-d transition bands at (816nm)  $12254 \text{ cm}^{-1}$  and (950nm)  $10526 \text{ cm}^{-1}$ , Table 3-22 which are assignable to  ${}^2B_{1g} \rightarrow {}^2B_{2g}$  and ( $\nu_3$ ) and  ${}^2B_{1g} \rightarrow {}^2E_g$   $\nu_2$ .

No spectral bands were found below ( $10000 \text{ cm}^{-1}$ ) which supports (Oh) geometry.

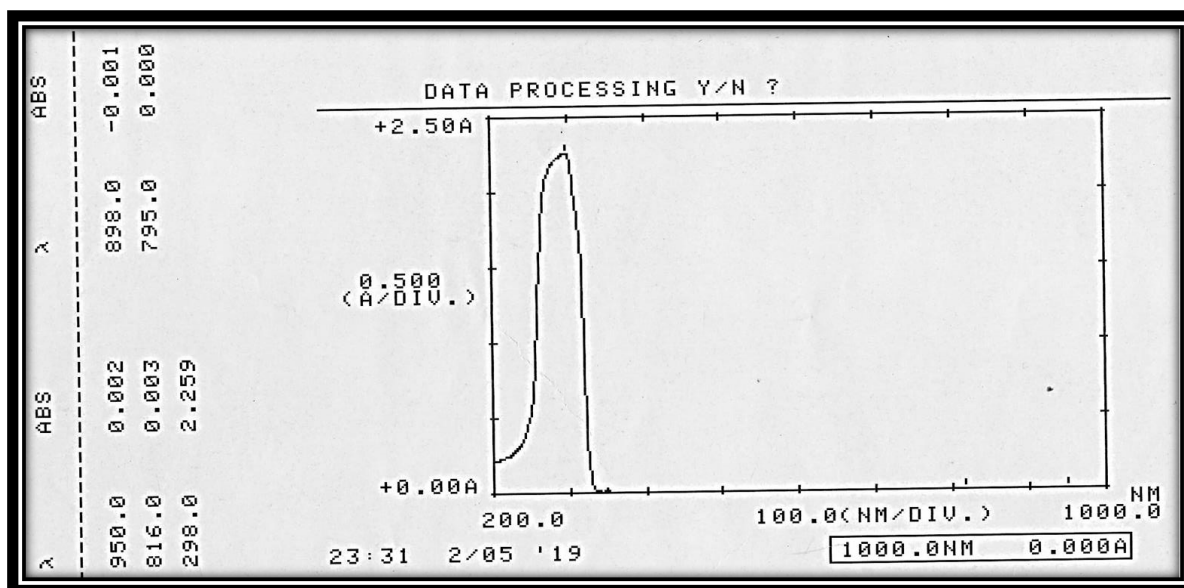


Figure (3-54) : Electronic Spectrum of  $[\text{Cu}(\text{SMZ})(\text{L-Val})_2]$

### 3.5.2.5 UV/Vis Spectrum of $[\text{Cd}(\text{SMZ})(\text{L-Val})_2]$

The  $[\text{Cd}(\text{SMZ})(\text{L-Val})_2]$   $d^{10}$  complex showed diamagnetic properties as expected from their electronic configuration. The electronic spectrum of Cd (II), complex show two transitions (Table 3-21). The high intensity band in the 275 nm ( $36363 \text{ cm}^{-1}$ ) assigned to  $\pi \rightarrow \pi^*$  transitions due to conjugated  $\pi$  system. The low intensity second band was observed at wavelength. 812 nm ( $12315 \text{ cm}^{-1}$ ) ascribed to L-M charge transfer (C.T) transitions. which also compatible with complexes have (Oh) structure [84].

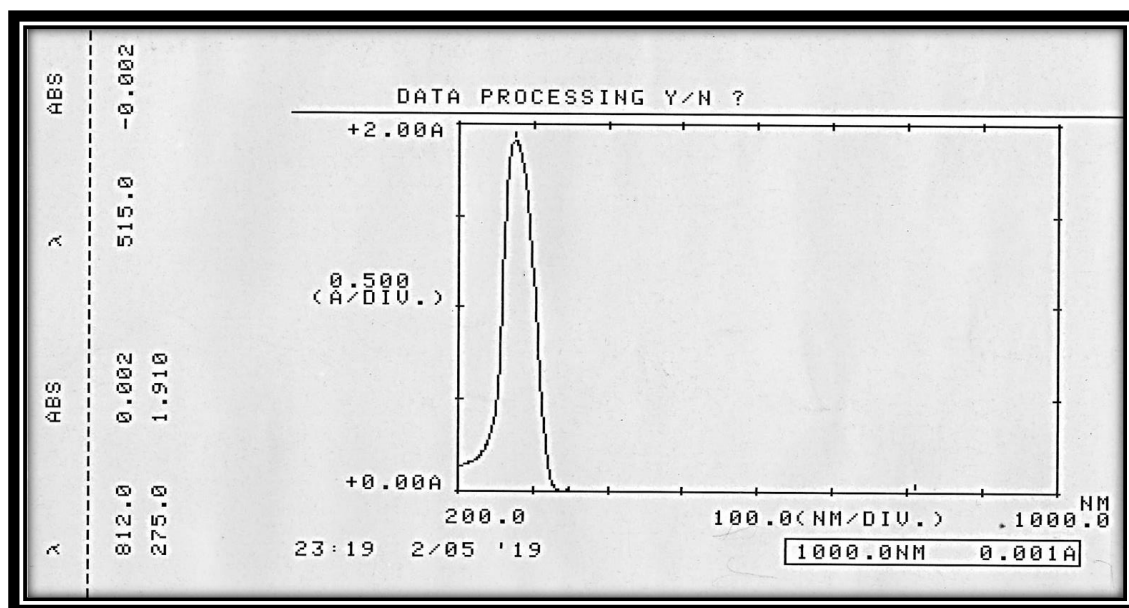


Figure (3-55) : Electronic Spectrum of [Cd (SMZ)( L-Val)<sub>2</sub>]

### 3.5.2.6 UV/Vis Spectrum of [Hg(SMZ)( L- Val)<sub>2</sub>]

The [Hg(SMZ)( L-Val)<sub>2</sub>] complex, Figure (3-56), showed diamagnetic properties as expected from their electronic configuration. The electronic spectrum of Hg (II) , d<sup>10</sup>, complex show two transitions Table (3-21). The high intensity band in the 290 nm (34482 cm<sup>-1</sup>) assigned to  $\pi \rightarrow \pi^*$  transitions due to conjugated  $\pi$  system .The low intensity second band was observed at wavelength. 823 nm (12150 cm<sup>-1</sup>) ascribed to L-M charge transfer (C.T) transitions. which also compatible with complexes have a (Oh) structure [82,85].

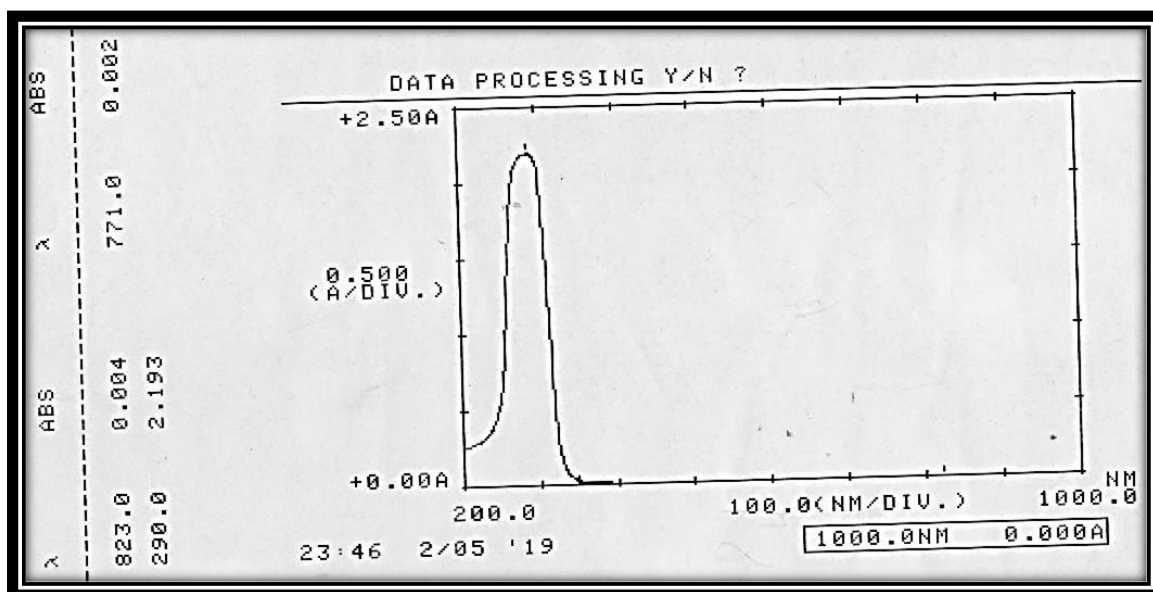


Figure (3-56) : Electronic Spectrum of  $[\text{Hg}(\text{SMZ})(\text{L-Val})_2]$

### 3.5.2.7 UV/Vis Spectrum of $[\text{Sn}(\text{SMZ})(\text{L-Val})_2]$

The electron configuration of  $[\text{Sn}(\text{SMZ})(\text{L-Val})_2]$  complex such Sn is  $[\text{Kr}] 4d^{10}5s^2 5p^0$  whose all electrons are paired., there are no unpaired electrons and no permanent magnetic moment per atom that reported in literature .The UV -Vis spectrum of the (SMZ)in (DMSO) solvent appeared a high intense absorption band due to the C=N chromophore at 279 nm ( $36900 \text{ cm}^{-1}$ ) ( $\pi\text{-}\pi^*$  transition) shifts to a higher wave length in the spectrum of  $[\text{Sn}(\text{SMZ})(\text{L-Val})_2]$  complex and appears at 295 nm ( $33893 \text{ cm}^{-1}$ ) in the complex <sup>[26,85]</sup> .This indicates the coordination of C=N nitrogen to metal atom. The complex also show two weak band 850 nm ( $11764 \text{ cm}^{-1}$ ) and 984 nm ( $10162 \text{ cm}^{-1}$ ), Figure (3-57), may be assigned as charge transfer bands. It has been reported that the metal is capable of forming  $d\pi\text{-}\pi^*$  bonds with ligands containing nitrogen or oxygen as the donor atom. The Tin atom has its d orbital completely vacant, and hence  $\nu(\text{N}\rightarrow\text{Sn})$  or  $\nu(\text{O}\rightarrow\text{Sn})$  bonding can take place by the acceptance of the lone pair of electrons from the nitrogen or oxygen of the (SMZ). <sup>[26,67,71]</sup>



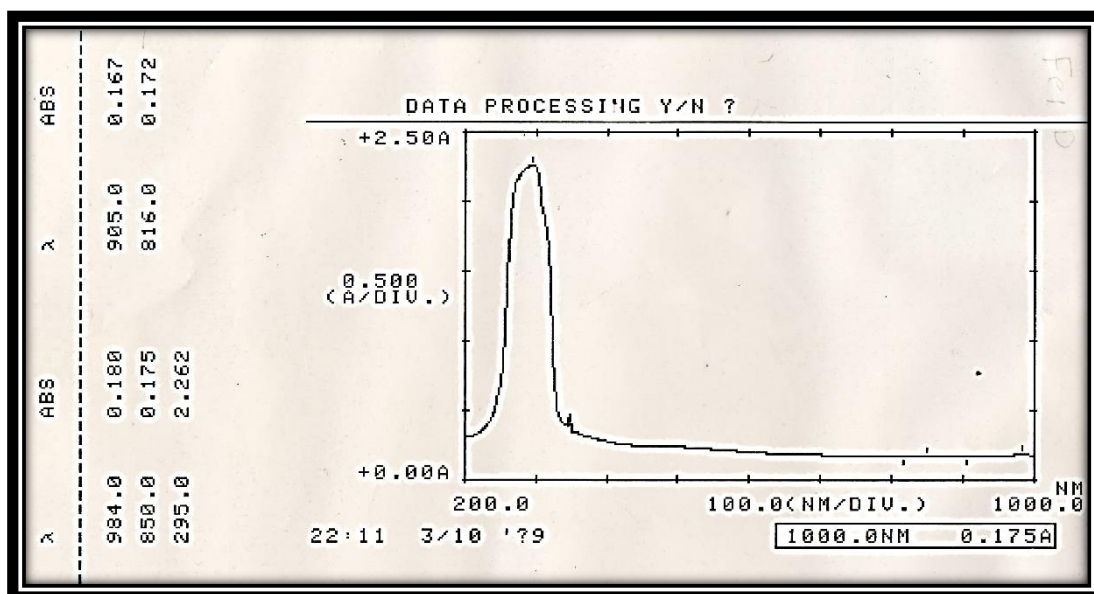


Figure (3-57) : Electronic Spectrum of  $[\text{Sn}(\text{SMZ})(\text{L-Val})_2]$

### 3.5.2.8 UV/Vis Spectrum of $[\text{Al}(\text{SMZ})(\text{L-Val})_2]\text{Cl}$

The (U.V- Vis) spectrum of  $[\text{Al}(\text{SMZ})(\text{L-Val})_2]\text{Cl}$  complex in DMSO, Figure (3-58), exhibits two transitions. The first high intense peak at  $289 \text{ nm cm}^{-1}$  due to the intra ligand charge transfer (INCT) and second band at  $34602 \text{ } 848 \text{ nm} (11792 \text{ cm}^{-1})$  due to the  $3p$  transitions in the  $\text{Al} \rightarrow$  ligand were observed by monitoring  $4s \rightarrow 3p$  emission from  $\text{Al}(4s)$  atoms produced by pre dissociation of the excited complex. <sup>[100]</sup>

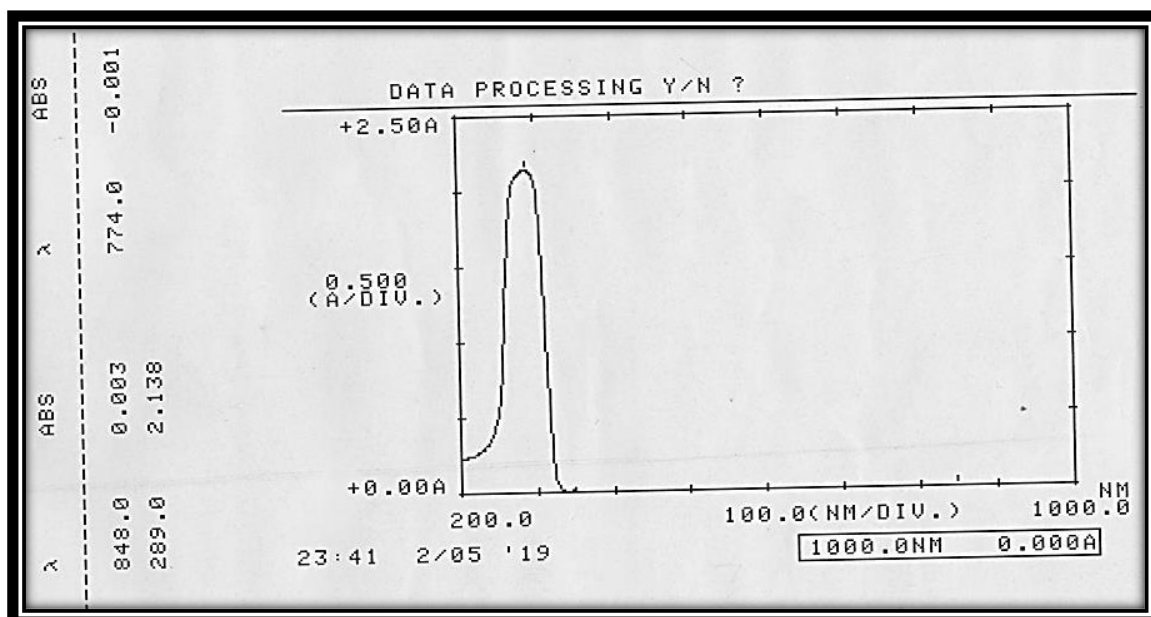


Figure (3-58) : Electronic Spectrum of  $[Al(SMZ)(L-Val)_2]Cl$

### 3.5.2.9. UV/Vis Spectrum of $[Cr(SMZ)(L-Val)_2]Cl$

The (U.V- Vis)  $[Cr(SMZ)(Val)_2] Cl$  complex spectrum in DMSO, Figure (3-59) exhibits two transitions. The first high intense peak at 300 nm ( $33333cm^{-1}$ ) due to the intra ligand charge transfer(INCT) and second band at 845 nm( $11834 cm^{-1}$ ) Table (3-22) which are assignable to  $^4A_{2g} \rightarrow ^4T_{1g} (v_3)$ , <sup>[103,105]</sup>. The magnetic moment of the  $[Cr(SMZ)(Val)_2] Cl$  is (1.85 B.M.), therefore an octahedral geometry was assume  $[Cr(SMZ)(Val)_2] Cl$  stereochemistry

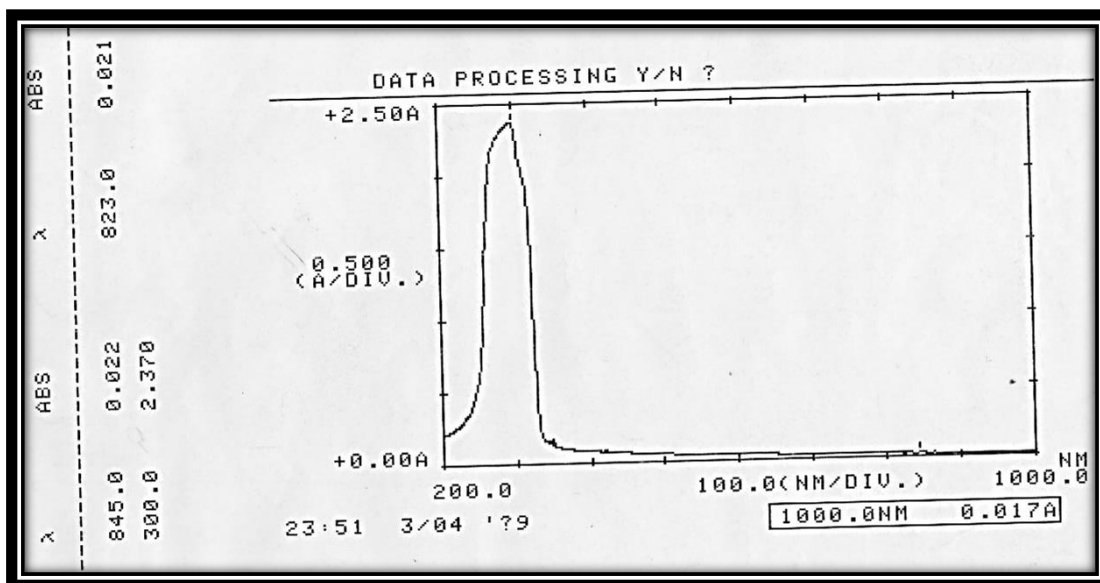


Figure (3-59) : Electronic Spectrum of  $[\text{Cr}(\text{SMZ})(\text{L-Val})_2]\text{Cl}$

### 3.5.2.10 UV/Vis Spectrum of $[\text{Fe}(\text{SMZ})(\text{L-Val})_2]\text{Cl}$

The UV-Vis spectrum of the  $[\text{Fe}(\text{SMZ})(\text{Val})_2]$  complex Figure (3-60), showed one bands in the d-d transition can be assigned to the  ${}^6\text{A}_{1g} \rightarrow {}^4\text{T}_{1g}$ , 723nm ( $13831\text{cm}^{-1}$ ) and one obscured by the intense charge-transfer band observed at 295nm ( $13831\text{cm}^{-1}$ ) these assignments are comparable to the other earlier report made for Fe. (III) complexes<sup>(94)</sup>.

The higher energy ligand field bands were The value of the measured magnetic moment is (5.13 B.M.) in accordance with the presumption of high-spin  $d^5$  ferric ion in octahedral geometry<sup>(97)</sup>.

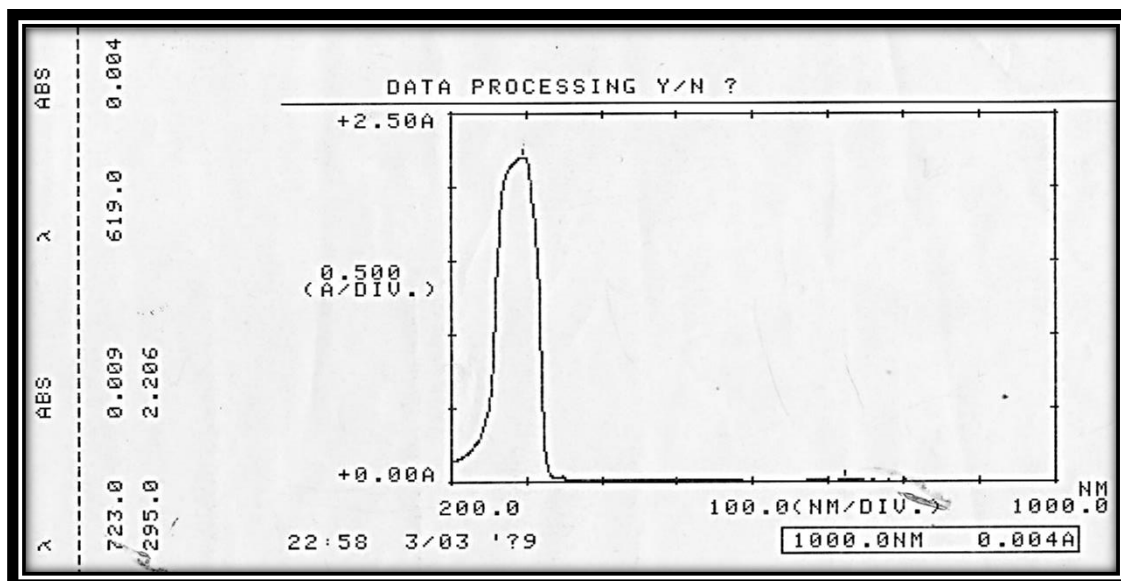


Figure (3-60) : Electronic Spectrum of [Fe (SMZ)(L-Val)<sub>2</sub>]Cl

### 3.5.3. The Proposed Molecular Structure for [L-Valin - Metal - (SMZ) ] Complexes

Studying complexes on bases of the above C.H.N , spectral observations suggest the octahedral geometry for all synthesized complexes which exhibited coordination number six and may be formulated as [M(SMZ)(L-Val)<sub>2</sub>] for M-(II) and [M' (SMZ)(L-Val)<sub>2</sub>] Cl for M'-(III). The general structure of the complexes are 3D as shown in Figures (3-61) and (3-62) .

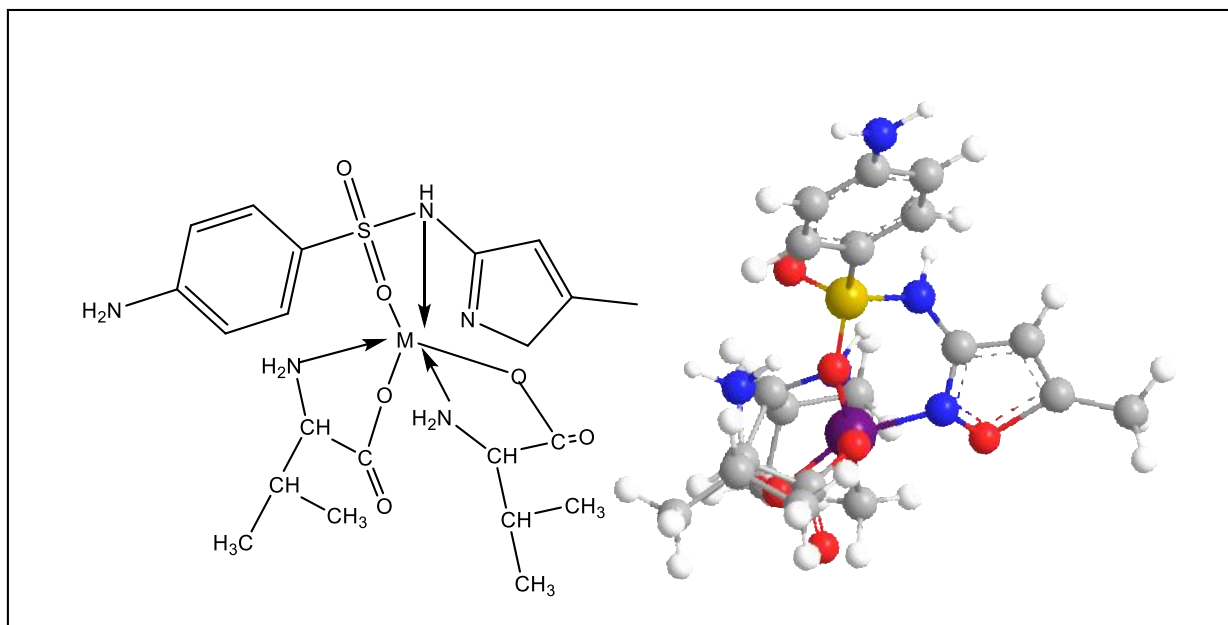


Figure (3-61) : 3D Molecular Modeling Proposed Complexes  $[M(\text{SMZ})(\text{L-Val})_2]$ .  $[\text{Sn}(\text{II}), \text{Mn}(\text{II}), \text{Co}(\text{II}), \text{Ni}(\text{II}), \text{Cu}(\text{II}), \text{Zn}(\text{II}), \text{Cd}(\text{II}) \text{ and } \text{Hg}(\text{II})]$

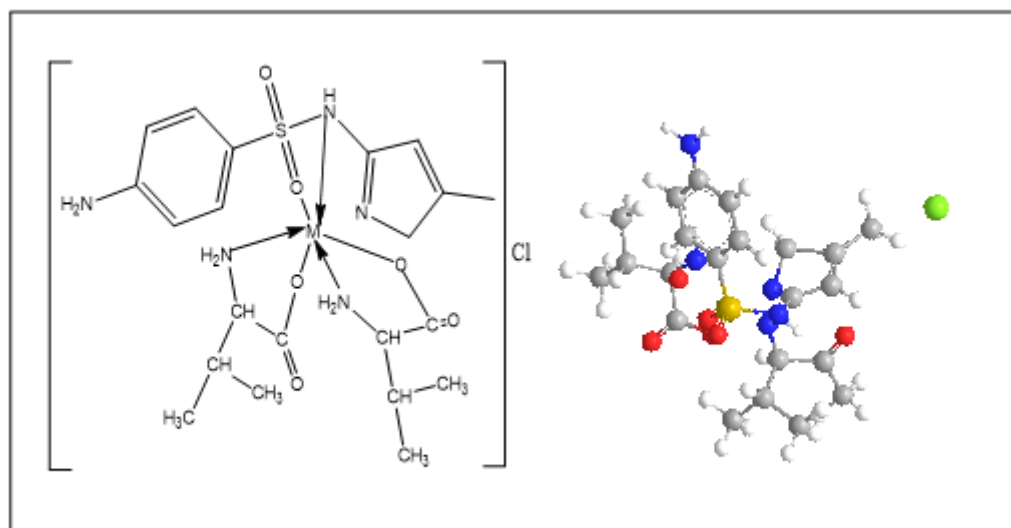


Figure (3-62) : 3D Molecular Modeling Proposed  $[M'(\text{SMZ})(\text{L-Val})_2] \text{Cl}$   
 $[\text{Al}(\text{III}), \text{Cr}(\text{III}), \text{ and } \text{Fe}(\text{III})]$

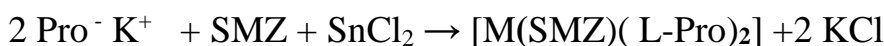
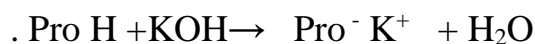
### 3.6. Synthesis and Characterization of Mono Ligand Complexes

#### 3.6.1 Sn (II) Complexes

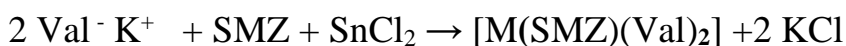
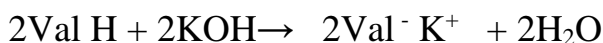
##### 3.6.1.1 Synthesis and Characterization of [Sn(L-pro)<sub>2</sub>], [Sn(L-Val)<sub>2</sub>] and [Sn(SMZ)<sub>2</sub>]Cl<sub>2</sub> Complexes

The two complex were prepared by reacting SnCl<sub>2</sub> with the Two amino acids [ L-Valinate and L-prolinate] using 1:2 mole ratios, [M : L-Valineate ],and [M : L-prolinate ] i.e. one mole of metal chloride and one mole of L-amino acids [37,50,]. The synthesis of mixed ligand metal complexes may be according to the following proposed general equation:

Set [Sn(L-pro)<sub>2</sub>]



Set [Sn(L- Val)<sub>2</sub>]



(primary ligand). SMZ = Sulfamethoxazole

(secondary ligand). Val H= L-Valine , Val<sup>-</sup> = L-Valinate ion

The suggested -molecular formula, and the results obtained from the physical proberities[color, M.P temperatures, conductivity ] and Sn% and are given in Table (3-24) , (3-25) .The test for chloride ion with AgNO<sub>3</sub> solution was negative indicating the no presence of chloride ion outside the coordination sphere [65] Microanalysis and analytical data for the Tin(II) complexes indicated 1:2 ( M: L).mole retio. The two complexes are non-hygroscopic, of white and yellow in colours and stable at room temperature. The lower value of molar conductance (Λ<sub>m</sub>) in low range 8-10. ohm<sup>-1</sup> cm<sup>2</sup> mol<sup>-1</sup>, in DMSO indicates non-electrolytic type . The low conductivity value is in agreement with low solubility of the complexes in water, ethanol, acetone and most organic solvents. On the other hand,

complexes are soluble in DMSO and HCl. Melting point at higher temperatures are listed Table (3-26).

Table (3-24): The Physical Properties & Atomic Absorption Results of the Tin (II) Complexes

Chemical Formula	Color	M.P °c (de) °c	Yield %	Metal analysis (% found) % cal	$\Lambda_m$ $\Omega^{-1} \text{ cm}^2 \text{ mol}^{-1}$ In DMSO
[Sn (L-Pro) <sub>2</sub> ]	Pale yellow	>260	85	33.82 34.21	8
[Sn (L-Val) <sub>2</sub> ]	White off	>260	82	34.21	10
[Sn(SMZ) <sub>2</sub> ]Cl <sub>2</sub>	White off	>260	82	19.48	73

Table (3-25): Microanalysis and analytical data for [Sn(SMZ)<sub>2</sub>]Cl<sub>2</sub>

Chemical Formula	Elemental analysis Found%			Elemental analysis calculate %		
	C	H	N	C	H	N
[Sn( L-Pro) <sub>2</sub> ]	34.80	4.79	8.80	34.62	4.65	8.07
[Sn(SMZ) <sub>2</sub> ]Cl <sub>2</sub>	39.95	3.64	13.79	39.43	3.86	14.67

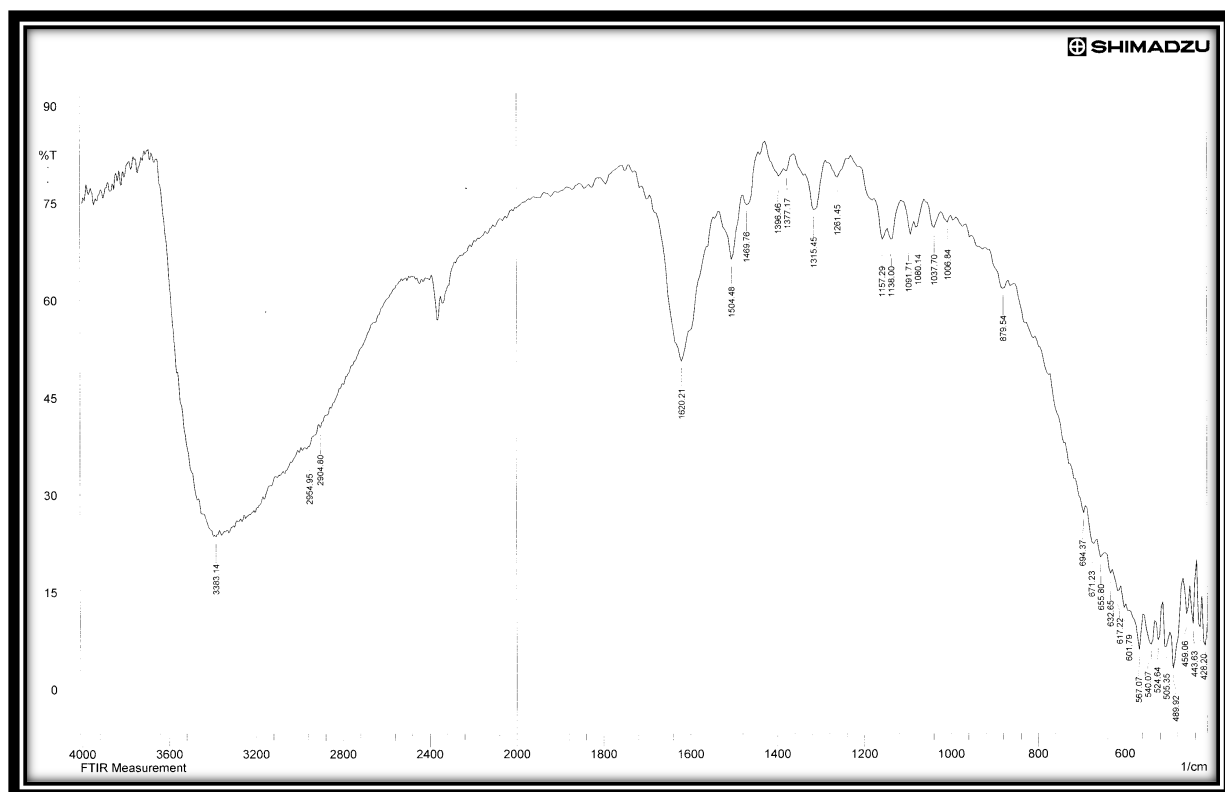
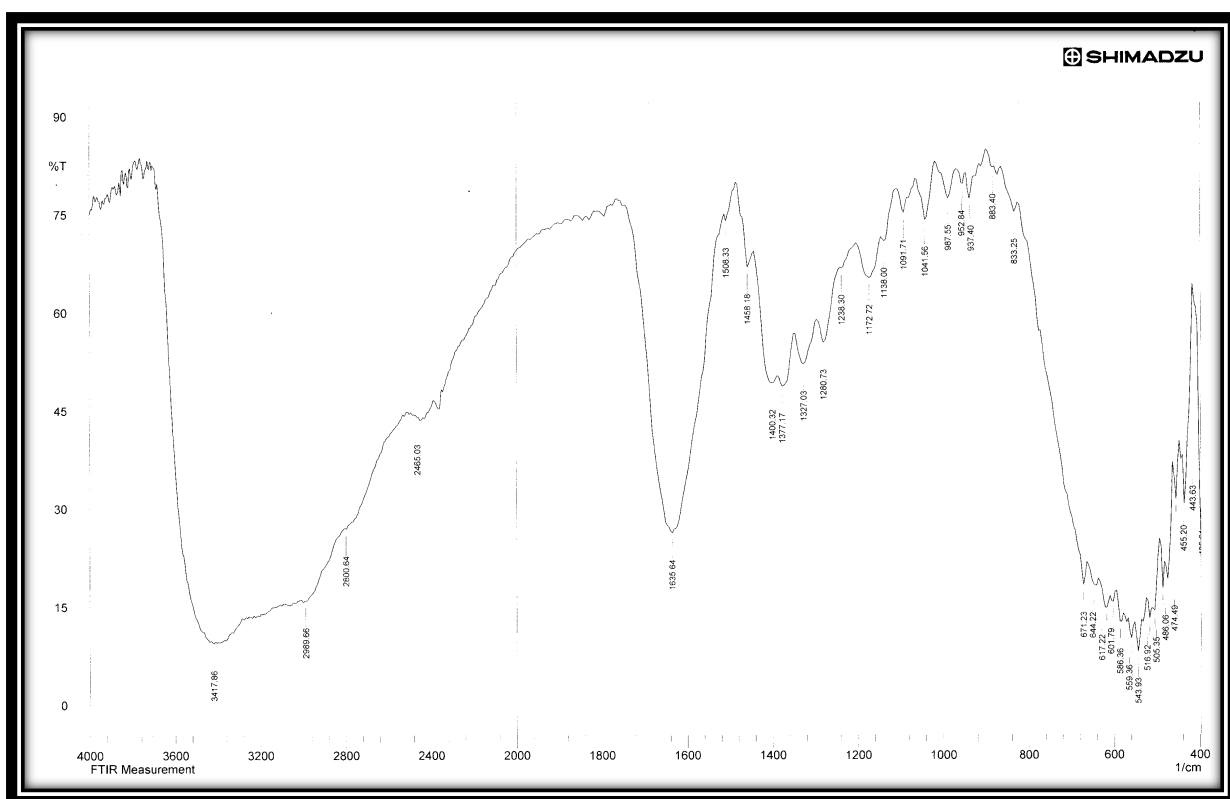
Table (3-26): Solubility of [Sn (II)] complexes in different solvents

Chemical Formula	C <sub>3</sub> H <sub>6</sub> O	C <sub>6</sub> H <sub>6</sub>	DMF	DMSO	EtOH	H <sub>2</sub> O	HCl
[Sn(Val) <sub>2</sub> ]	-	-	-	+	-	-	+
[Sn(Pro) <sub>2</sub> ]	-	-	-	+	-	+	+
[Sn(SMZ) <sub>2</sub> ] Cl <sub>2</sub>	--	--	--	+	+	+	+
(+ ) Soluble, (-) Insoluble, (---) Sparingly							

### 3.6.1.2 FT-IR spectra of [Sn(L-Val)<sub>2</sub>] and [Sn(L-pro)<sub>2</sub>] complexes

The assignment of the characteristic bands (FT-IR) spectra for the free ligand (L-ProH), Figure (3-5), are summarized in Table (3-5), and (L-ValH) Figure (3-6), are summarized in Tables (3-6) and . The important IR peaks of the complexes are given in Table (3-27) and shown in Figures (3-63) and (3-64). In all amino acids the stretching vibration of  $\nu(\text{NH}_3^+)$  appears at (3030-3130)  $\text{cm}^{-1}$  region<sup>[107-109]</sup>. The bands at (1635  $\text{cm}^{-1}$ ) and (1400  $\text{cm}^{-1}$ ) for [Sn(L-Val)<sub>2</sub>] and (1620  $\text{cm}^{-1}$ ) and (1396  $\text{cm}^{-1}$ ) for [Sn(L-Pro)<sub>2</sub>] were assigned to the  $\nu(-\text{COO}_{\text{asy}})$  and  $\nu(-\text{COO}_{\text{sym}})$ . And  $\Delta \nu(-\text{COO})_{\text{asy-sym}} = (224 \text{ and } 235) \text{ cm}^{-1}$  respectively<sup>[8,13,73]</sup>. The value of  $\Delta \nu(-\text{COO})_{\text{asy-sym}}$  were appeared in the two prepared complexes within the range (208-239)  $\text{cm}^{-1}$  Table (3-33) indicating of participate the (COO<sup>-</sup>) group as a mono dentate donor ligand in the coordination process with the metal ion<sup>[54]</sup>. Information about the ions coordination were obtained by comparing the IR frequencies of the [ two amino acids] free ligands with those of the Sn(II) complexes<sup>[68]</sup>. IR spectra demonstrate that the amino acid act as bidentate ligand in coordination with Sn (II) involving Nitrogen of (-NH<sub>2</sub>) group in L-Valin and Nitrogen of (-NH) group in L-proline , and oxygen (-COO) group .<sup>[54]</sup> The absorption bands at 543  $\text{cm}^{-1}$  and 559  $\text{cm}^{-1}$  corresponds to the stretching vibration of the Sn-O group, in good agreement with literature data for related complexes. a peak displayed at 1504 and 1508  $\text{cm}^{-1}$  for [Sn(L-Val)<sub>2</sub>] and [Sn(L-pro)<sub>2</sub>] ,assigned for  $\nu(\text{C}=\text{O})$  acid stretching respectively .New bands of weak intensity observed in the regions around (543-559)  $\text{cm}^{-1}$  and (474-489)  $\text{cm}^{-1}$  may be ascribed to SnN and Sn - O vibrations, respectively<sup>[37]</sup>. It may be noted that, these vibrational bands are absent in the spectra of the free two amino acids .



Figure (3-63) : FT-IR Spectrum of  $[\text{Sn}(\text{L-Val})_2]$ Figure (3-64) : FT-IR Spectrum of  $[\text{Sn}(\text{L-pro})_2]$

**Table (3-27): Infrared spectral data( $\nu$ )  $\text{cm}^{-1}$  for Tin -amino acids complexes**

Complexes	$\nu$ $\text{NH}_2$ $\nu$ Val $\nu$ NH pro	$\nu$ (C-H) + $\text{CH}_3$	(COO) asy	$\nu$ (C=O)	$\nu$ (-COO) sym	$\Delta \nu$ (-COO) asy-sym	$\nu$ (Sn -O)	$\nu$ (Sn-N)
[Sn(L-Val) $_2$ ]	3383	2954 s 2904	1620 vs	1504	1396	224	543	489
[Sn(L-pro) $_2$ ]	3417- 3149	2954m 2904	1635vs	1508	1400	235	559	474

### 3.6.1.3. UV/Vis Spectrum of [Sn(L-Val)<sub>2</sub>] and [Sn(L-pro)<sub>2</sub>] complexes

Sn [Kr] 4d<sup>10</sup>5S<sup>2</sup>5P<sup>0</sup> all electrons are paired therefore the magnetic moment values for Sn (II) are zero, Table (3-28), which indicate that they are diamagnetic. All transitions may be assigned as  $\pi$ - $\pi^*$  and charge transfer bands. It has been reported that the metal is capable of forming  $d\pi$ - $p\pi^*$  bonds with ligands containing nitrogen or oxygen as the donor atom. The Tin atom has its d orbital completely vacant, and hence  $\nu$  (N $\rightarrow$ Sn) or  $\nu$  (O $\rightarrow$ Sn) bonding can take place by the acceptance of the lone pair of electrons from the nitrogen or oxygen of the (L-Val) and (L-Pro) [54,86]. Figure (3-65) and (3-66).

**Table (3-28) : Electronic Spectral Data of the [Sn (L-Val)<sub>2</sub>] and [Sn (L-Pro)<sub>2</sub>]**

Comp.	$\lambda$ nm	$\nu$ cm <sup>-1</sup>	$\epsilon$ max (molar <sup>-1</sup> .cm <sup>-1</sup> )	Assignments	$\mu_{\text{eff}}$ (BM)
[Sn (L-Val) <sub>2</sub> ]	212	47169	687	$\pi$ - $\pi^*$ C.T C.T	0 Dima
	275	36363	224		
	305	32786	217		
	974	10266	164		
[Sn (L-Pro) <sub>2</sub> ]	265	37735	2155	$\pi$ - $\pi^*$ C.T $d\pi$ - $p\pi^*$	0 Dima
	676	14792	301		
[Sn(SMZ) <sub>2</sub> ]Cl <sub>2</sub>	286	34965	2103	$\pi$ - $\pi^*$ C.T	0 Dima
	834	11990	4		

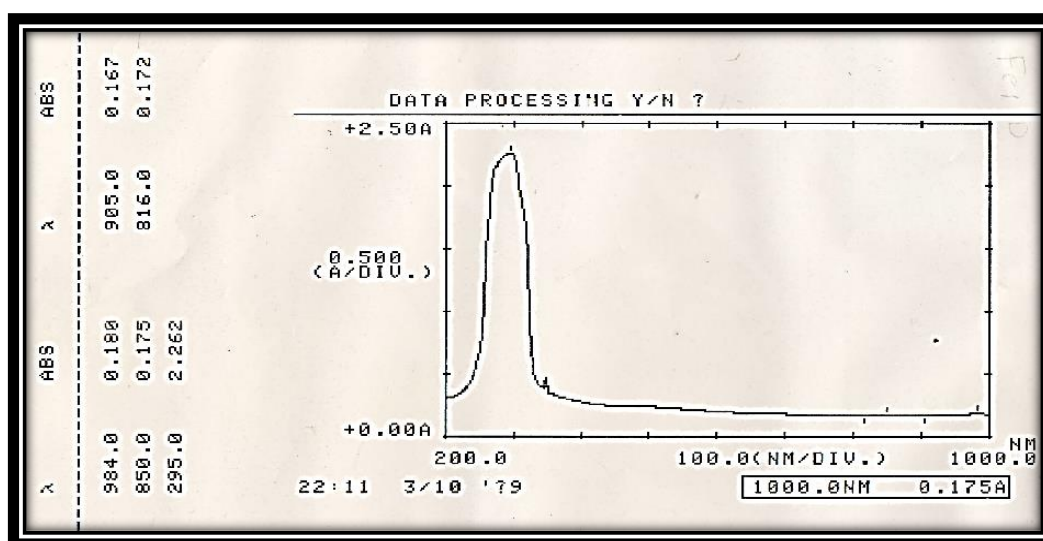


Figure (3-65) : Electronic Spectrum of [Sn (L-Val)<sub>2</sub>]

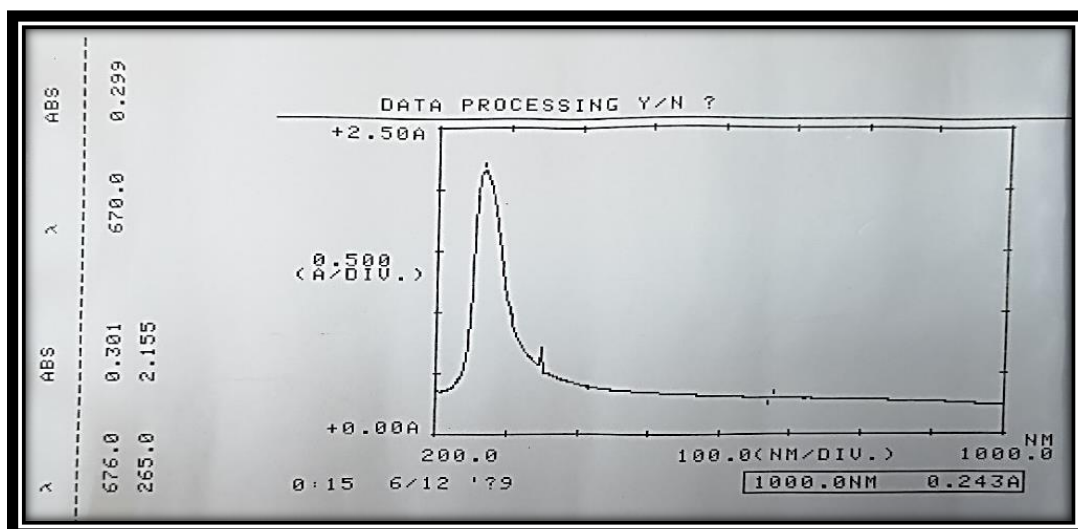


Figure (3-66) : Electronic Spectrum of [Sn ( L-Pro)<sub>2</sub>]

#### 3.6.1.4 The proposed molecular structure [Sn(L-Val)<sub>2</sub>] and [Sn(L-pro)<sub>2</sub>] complexes

The results obtained lead to the conclusion that (L-Val) and (L-pro) acts as a bidentate ligand complexing the Sn (II) ion through the involving oxygen (COO<sup>-</sup>) group in both amino acids and Nitrogen of NH<sub>2</sub> group in (L-ValH) and NH group in (L-proH). The Sn (II) acquires a coordination number of four. In conclusion, our investigation this suggest that the L-ValH and L-proH) coordinate with Sn (II) forming tetrahedral geometry. The general structure of the complexes is 3D as is shown in Figures (3-67) and (3-68).

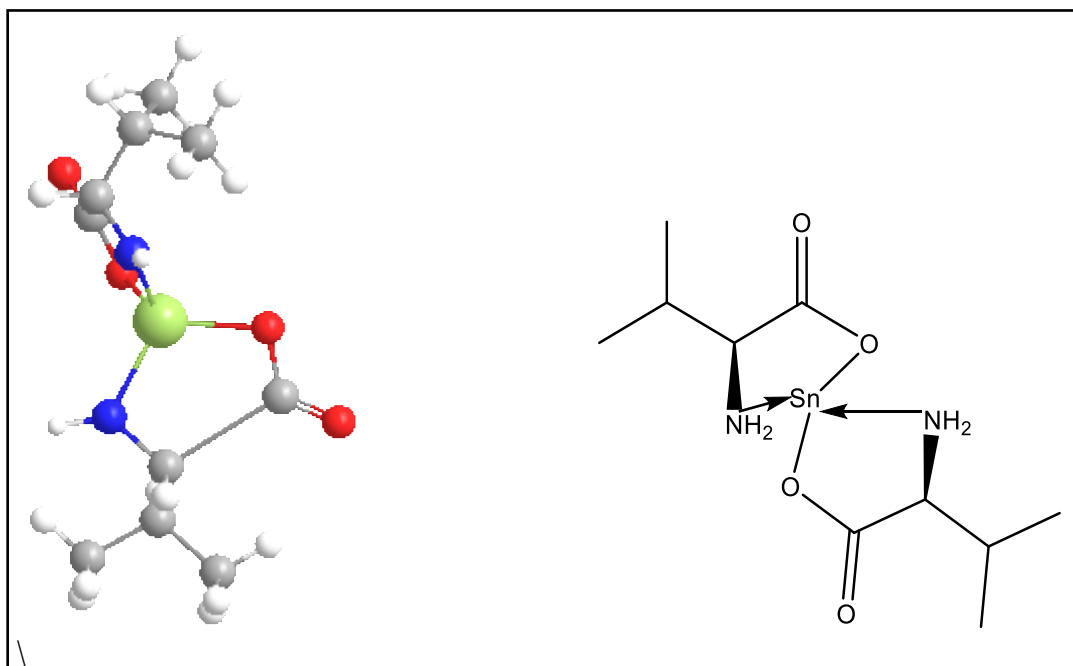


Figure (3-67) : The geometry structure , 3D of  $[\text{Sn}(\text{L-Val})_2]$   
 (3*S*,8*S*)-3,8-diisopropyl-1,6-dioxa-4,9-diaza-5-stannaspiro[4.4]nonane-  
 2,7-dione

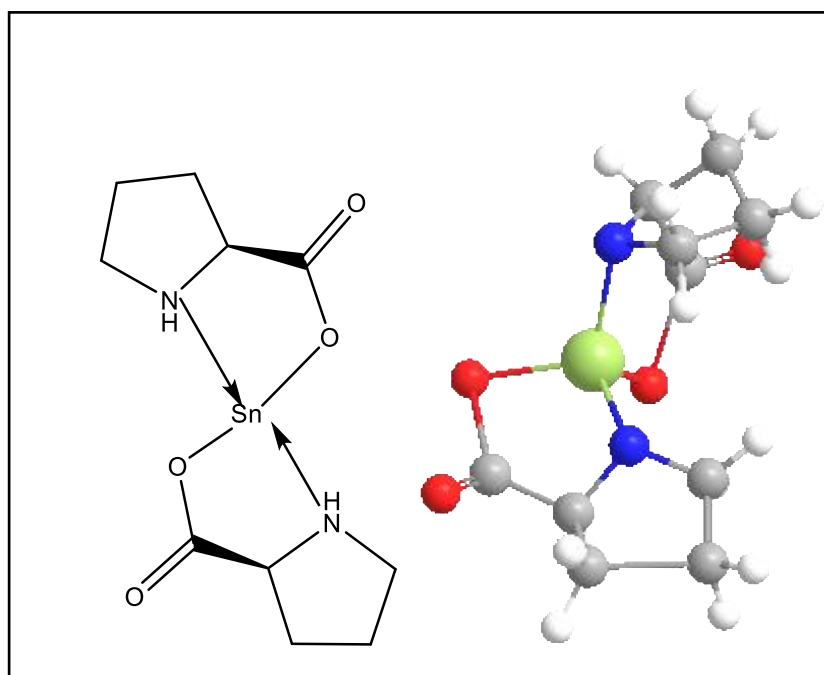


Figure (3-68) : The geometry structure , 3D of  $[\text{Sn}(\text{L-Pro})_2]$   
 (3*aS*,3*a'S*)-octahydro-3*H*,3'*H*-1,1'-spirobi[pyrrolo[1,2-  
 c][1,3,2]oxazastannole]-3,3'-dione

### 3.6.1.5 Synthesis and Characterization of $[\text{Sn}(\text{SMZ})_2]\text{Cl}_2$

The synthesis of complex may be according to the following proposed equation:  $2 \text{SMZ} + \text{SnCl}_2 \cdot 2\text{H}_2\text{O} \rightarrow [\text{Sn}(\text{SMZ})_2]\text{Cl}_2 + 2\text{H}_2\text{O}$

SMZ = Sulfamethoxazole.  $[\text{Sn}(\text{SMZ})_2]\text{Cl}_2$  complex was dissolved in various solvents and HCl.  $[\text{Sn}(\text{SMZ})_2]\text{Cl}_2$  complex. The complex was soluble in DMSO, DMF,  $\text{H}_2\text{O}$ , and HCl, while partially soluble in Benzene and acetone. Conductance data of Sn(II) complex refer that two of chloride ions presence outside of the coordination sphere. The obtained results were strongly matched with the (C.H.N) analysis data where  $\text{Cl}^-$  ions are detected after degradation of this complex by using nitric acid ( $\text{HNO}_3$ ) then precipitation of chloride ions using ( $\text{AgNO}_3$ ) solution. <sup>[82]</sup>. light yellow. The conductivity value  $73 \Omega^{-1} \text{cm}^2 \text{mol}^{-1}$  in DMSO Table( 3-24) imply the presence of electrolyte type 1.2 using FT-IR spectroscopy. Bands of IR spectra for selected ligand and its ion metal complexes are represented in Table (3-4) and Figure (3-4),  $\delta$  (N-H) vibrations (aromatic sec. amine) of  $-\text{NH}_2$  occur at  $[3468 \text{ and } 3378] \text{cm}^{-1}$  for free (SMZ) due to  $\nu$  [a symmetric and symmetric]  $\text{NH}_2$ , respectively. The hypochromic effect (decreasing in the intensity of  $\nu$  (NH) vibrations in case of complex rather than (SMZ) alone as well as the blue-shifted in the wavenumbers from  $3299 \text{cm}^{-1}$  more evidence new bands appeared in  $[(567) \text{ and } (451)] \text{cm}^{-1}$  due to the stretching frequencies of (Sn-O) and (Sn-N) bonds, respectively. The absorption band at  $567 \text{cm}^{-1}$  corresponds to the stretching vibration of the Sn-O group, in good agreement with literature data for related complexes <sup>[68, 82]</sup>

Table ( 3- 29 ) :FT-R spectral data (  $\nu$ )  $\text{cm}^{-1}$  for the SMZ

<b>complexes</b>	<b>SMZ</b>	<b>[Sn(SMZ)<sub>2</sub>]Cl<sub>2</sub></b>
<b>Sn-N</b>	-	451
<b>Sn-O</b>	-	567
<b><math>\nu(\text{C-S})</math></b>	831	833
<b><math>\nu(\text{SO}_2)</math> sy</b>	1157 1143	1153 1141
<b><math>\nu(\text{C-O})</math></b>	1267 ms	1261ms
<b><math>\nu\text{C-N}</math></b>	1311s	1309
<b><math>\nu\text{SO}_2</math> asy</b>	1365 s	1377s
<b><math>\nu(\text{C=C})</math>: phenyl ring</b>	1597 vs 1504	1597 vs 1504 vs
<b><math>\delta(\text{NH}_2)</math></b>	1622	1620
<b><math>\nu</math> (C-H) Aliph and Arom</b>	2929 2831	2981 w 2858
<b>as (NH): And <math>\nu\text{s}</math> (NH): sulfonamide group</b>	3372 3300	3360 3140
<b><math>\nu\text{as NH}</math>):NH<sub>2</sub> <math>\nu\text{s}</math> (NH):NH<sub>2</sub></b>	3468 s 78s33	3468 $\nu\text{as}$ 3384 $\nu\text{s}$

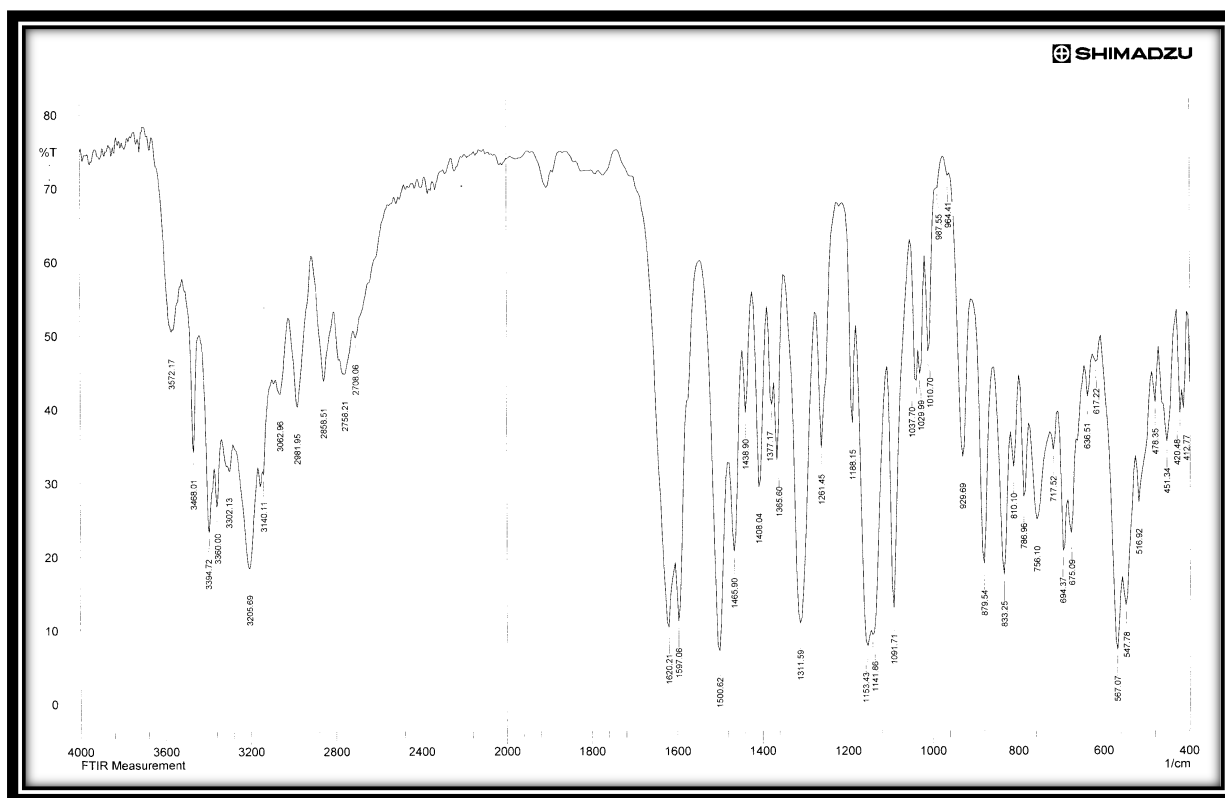


Figure (3-69) : FT-IR Spectrum of  $[\text{Sn}(\text{SMZ})_2]\text{Cl}_2$

The UV -Vis spectrum of the (SMZ) in (DMSO) solvent showed a high intense absorption band due to the C=N chromophore at 275 nm ( $36363 \text{ cm}^{-1}$ ) ( $\pi\text{-}\pi^*$  transition) shifts to a higher wavelength in the spectrum of  $[\text{Sn}(\text{SMZ})]\text{Cl}_2$  complex and appears at 286 nm ( $34965 \text{ cm}^{-1}$ ) in the complex. This indicates the coordination of C=N nitrogen to metal atom. The complex also show one weak <sup>[15-16]</sup> band 834 nm ( $11990 \text{ cm}^{-1}$ ) may be assigned as charge transfer bands. It has been reported that the metal is capable of forming  $d\pi\text{-}p\pi^*$  bonds with ligands containing nitrogen or oxygen as the donor atom. The Sn atom has its d orbital completely vacant, and hence  $\nu (\text{N} \rightarrow \text{Sn})$  or  $\nu (\text{O} \rightarrow \text{Sn})$  bonding can take place by the acceptance of the lone pair of electrons from the nitrogen or oxygen of the (SMZ). <sup>[37-38]</sup>.



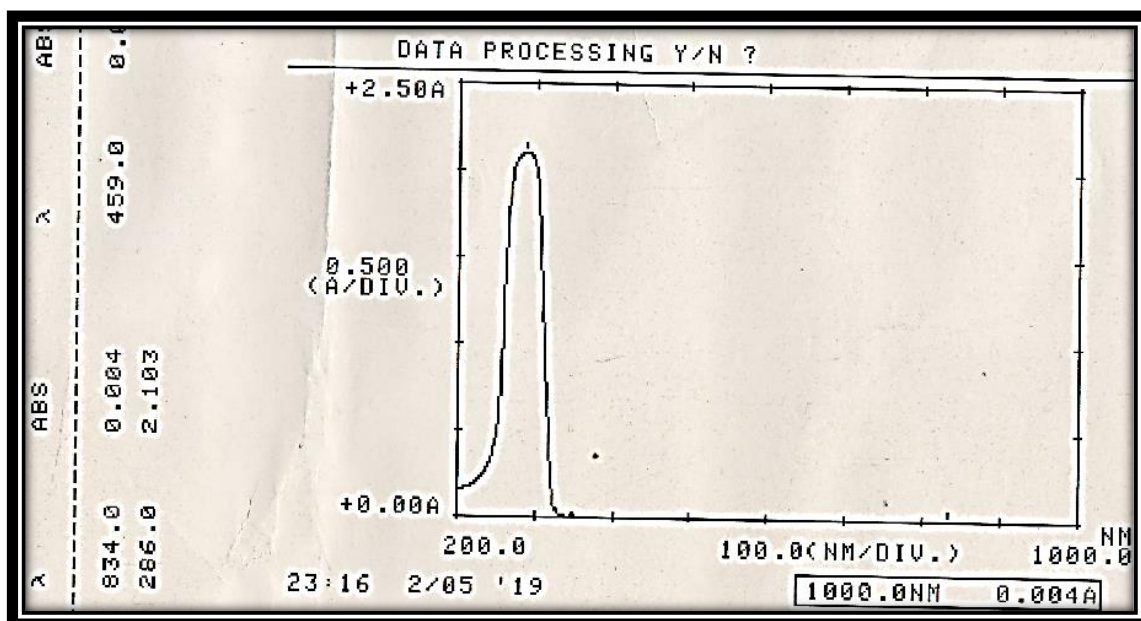


Figure (3-70) : UV -Vis spectrum of the  $[\text{Sn}(\text{SMZ})_2]\text{Cl}_2$

### CONTINUOUS-VARIATIONS METHOD (CVM)

When a colorless aqueous solution of  $\text{SnCl}_2$  is treated with SMZ solution color changes light yellow. Stoichiometry of the complex formed by  $\text{Sn}(\text{II})$  and sulfamethoxazole is determined using the Job's (CVM), spectrophotometry is based on the measurement of a series of different solutions such as those shown in Table (3-30) in which the molar concentrations of two reactants differ but their sum is constant ( $1 \times 10^{-3} \text{ M}$ ). Ten clean 100-mL volumetric flasks were labeled 1 to 10. The mole fraction of SMZ and Sn in the solution at a suitable wavelength (408 nm) was calculated using distilled water as a reference. Table (3-30) After (5 minutes) the absorbance (A) of each solution was measured at 408 nm. The mole fraction of each component in the solution was calculated and plotted against absorbance using distilled  $\text{H}_2\text{O}$  as reference. The experimental results of the stoichiometry Figure 3-71 of the complex of Sn (II) and sulfamethoxazole is 1:2 [105-106].

Table (3- 30):Data for (CVM) of Determining Stoichiometry of Complex

Volumes of Flask 1 mL sulfamethoxazole sol'n ligand $1 \times 10^{-3}$ M	Volumes of Flask 2 mL Sn sol'n metal $1 \times 10^{-3}$ M	Mole Fraction		
		Ligand	Metal	ABS
10	0	1.0	0	0
9	1	0.9	0.1	0.123
8	2	0.8	0.2	0.283
7	3	0.7	0.3	0.392
6	4	0.6	0.4	0.441
5	5	0.5	0.5	0.571
4	6	0.4	0.6	0.723
3	7	0.3	0.7	0.610
2	8	0.2	0.8	0.392
1	9	0.1	0.9	0.201
0	10	0	0.1	0

The mole a fraction in which the number of moles of  $\text{Sn}^{2+}$  and SMZ is in the stoichiometric ratio Since the sum of mole fractions in a mixture always =1

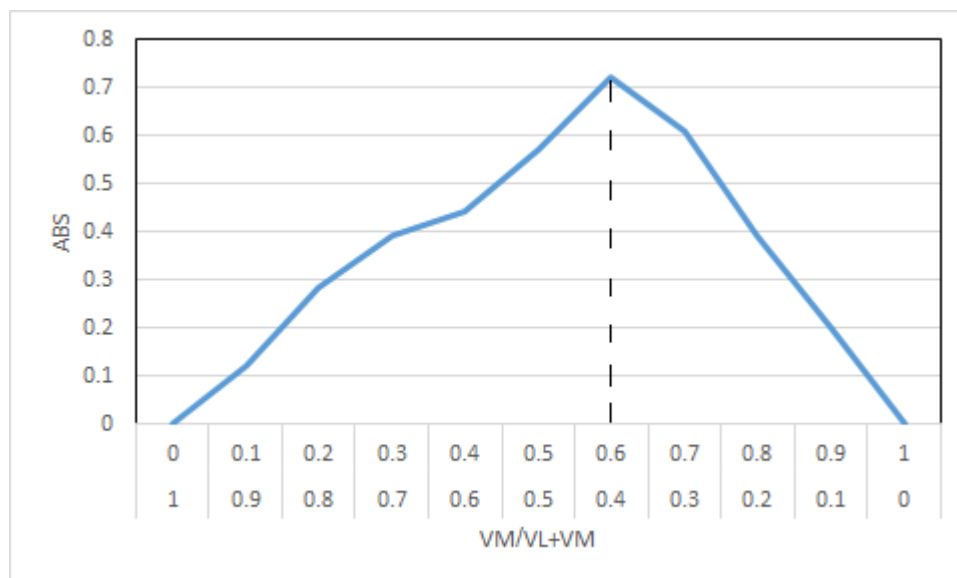
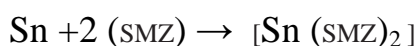
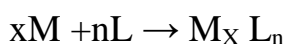


Figure (3-71): Mole ratio (M: L)(1:2) by continues variation method

The stability of the complex in solution was investigated by the evaluation of ( $K_f$ ) (stability formation constants or (stability Constant)(K) according to the following equation [107-108].



The stability constants of the complex containing SMZ were calculated from Eqs. Below  $Sn (SMZ) \leftrightarrow Sn(SMZ)$

The formation constant  $K_f$  (or equilibrium constant) for the reaction can be calculated once the equilibrium concentrations are known:

$$K_f = \frac{[M_x L_n]}{[M]^x \cdot [L]^n}$$

$$K_f = \frac{[Sn(SMZ)]}{[Sn] \cdot [SMZ]^2}$$

ligand concentration  $[L]$  = metal concentration  $[M] = 1 \times 10^{-3} M$

Beer's Law, gives the relationship between concentration:  $c^0$  and absorbance  $A$  using quartz cell of (1.0)cm length with concentration  $(1 \times 10^{-3})$  mole  $L^{-1}$  solution in concentration at  $25 \pm 1$  °C.

$$\Delta G = -2.3 R.T. \text{Log}K \quad (\text{Gibs free energy})$$

Table (3- 31): Results of continues variation method

ABS* low concentration for metal	ABS* low concentration for ligand	$\epsilon_1 \quad \epsilon_2 \quad \epsilon_{\text{ava}}$ metal ligand average			$C_0$ primary concentration for matel or ligand	Kf $L \cdot \text{mol}^{-1}$	Log Kf	$\Delta G$ Kcal/mol
		$\epsilon = \frac{ABS \cdot S}{bc}$ ( $L \cdot \text{mol}^{-1} \cdot \text{cm}^{-1}$ )						
0.123	0.201	1230	2010	1620	0.00026	$3.52 \times 10^5$	5.546	-7576

The composition and the stability constant evaluated the mole ratio methods (Figure 3 and Table 3). The method showed that the molar ratio of Sn(II) is 1:2, ( metal : ligand ). The stability constant is found to be  $(3.52 \times 10^5)$   $L \cdot \text{mol}^{-1}$ . and  $-7576$  Kcal/mol Gibbs free energy According to their results and discussed through different techniques the, tetrahedral geometry has been proposed for the resulting tin(II) complex, as shown in Figure 4. The

sulfamethoxazole ligand behaves as a bidentate ligand and coordinate to the metal ions (O-SO<sub>2</sub> and C=N) groups.

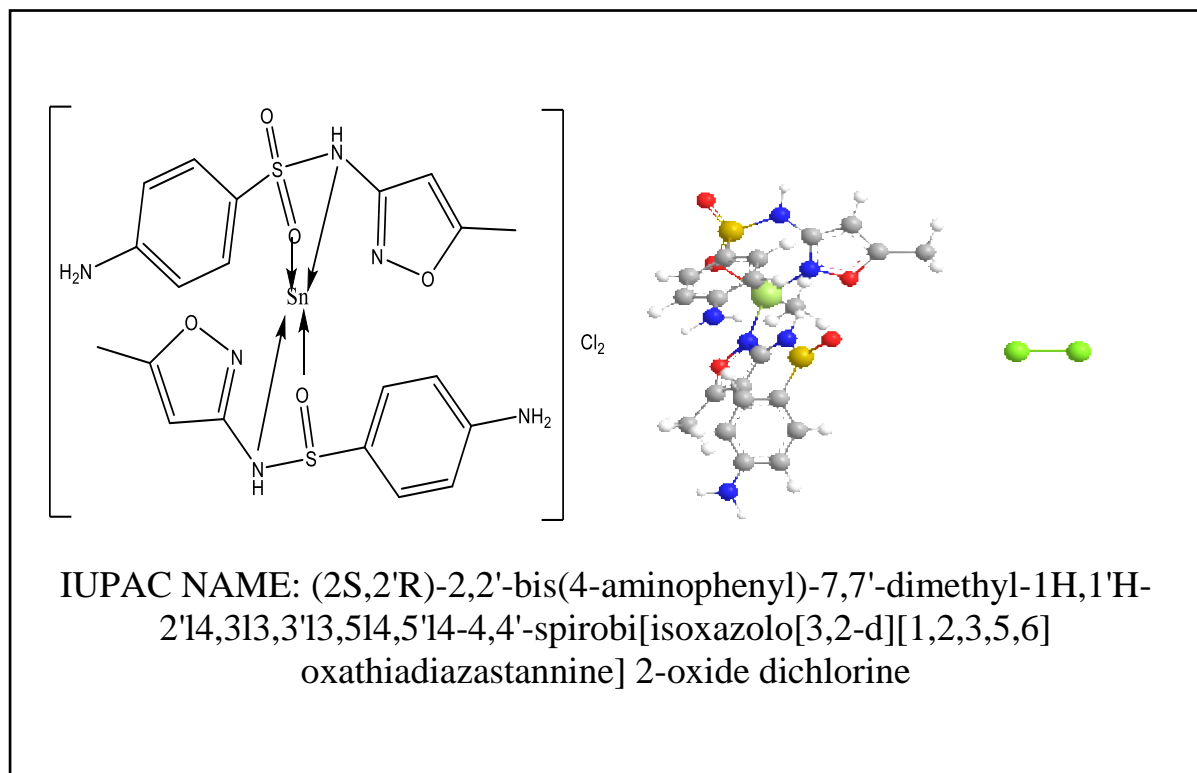


Figure (3-72) : Probable 3-D structure of the [Sn(SMZ)<sub>2</sub>]Cl<sub>2</sub>

### 3.6.2. Synthesis and Characterization of [M' (SMZ)<sub>3</sub>]Cl<sub>3</sub> Complexes

The three complex were prepared by reacting the metal chloride M' Cl<sub>3</sub> . nH<sub>2</sub>O with the (SMZ) using 1:3 mole ratios, i.e. one mole of metal chloride and three mole of (SMZ). The synthesis of complexes may be according to the following proposed general equation:



M' = Al(III) Cr (III) and Fe (II) , SMZ = Sulfamethoxazole

The suggested -molecular formula, and the results obtained from the physical properties [color, M.P temperatures, conductivity] and M'% and are (given in Table . (3-32) . Molar conductance's ( $\Lambda_m$ ) of 10<sup>-3</sup> solutions of the complexes in DMSO lie in very high range (76-97)  $\Omega^{-1}cm^2 mol^{-1}$  supporting their electrolytic behavior type 1:3 [74].

Table (3- 32) : The Physical Properties & Atomic Absorption Results of the [ [SMZ - M'-] Complexes

Chemical Formula	M.wt	Color	M.P °c (de) °c	Yield %	Metal analysis (% found) % cal	$\Delta m$ $\Omega$ -1 cm <sup>2</sup> mol <sup>-1</sup> In DMSO
[Al(SMZ) <sub>3</sub> ]Cl <sub>3</sub>	891	White	175	85	3.2	97
[Cr(SMZ) <sub>3</sub> ]Cl <sub>3</sub>	918,2	White	177	80	5.66	87
[Fe(SMZ) <sub>3</sub> ]Cl <sub>3</sub>	922	White	178	82	6.60	76

Table (3- 33): Solubility of [SMZ - M'-] Complexes in different solvents

Chemical Formula	C <sub>3</sub> H <sub>6</sub> O	C <sub>6</sub> H <sub>6</sub>	DMF	DMSO	EtOH	H <sub>2</sub> O	Hexanol	HCl
[Al(SMZ) <sub>3</sub> ]Cl <sub>3</sub>	+	--	+	+	+	-	+	+
[Cr(SMZ) <sub>3</sub> ]Cl <sub>3</sub>	+	--	+	+	+	+	+	+
[Fe(SMZ) <sub>3</sub> ]Cl <sub>3</sub>	+	-	+	+	+	+	+	+
(+ Soluble, (-) Insoluble, (---) Sparingly)								

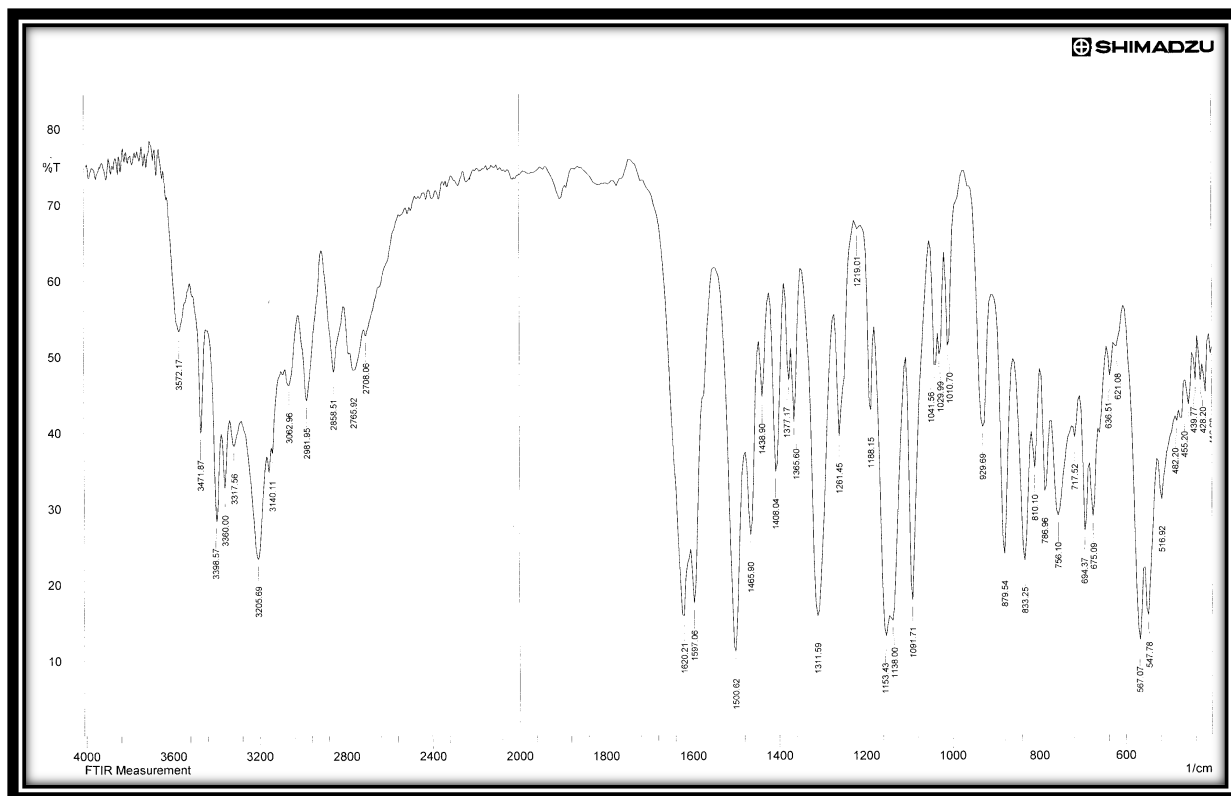
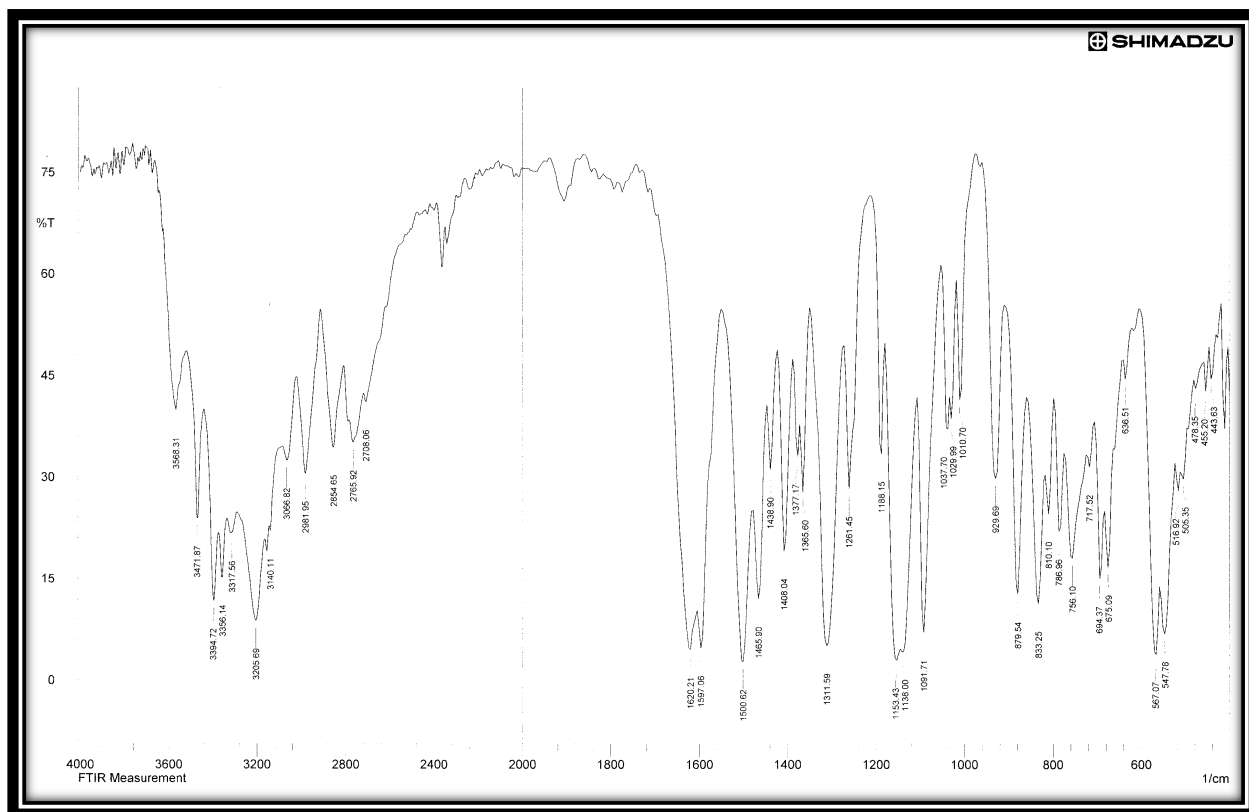
In three complexes. according to the results , the coordination mode of this SMZ with metal ions is clearly predicted as a bidentate through the N ,O atoms of sulfonylamid group, more evidence new bands which appeared in the range (447-567 )cm<sup>-1</sup> and (466-482) cm<sup>-1</sup> due to the stretching frequencies of (M-O), (M-N).

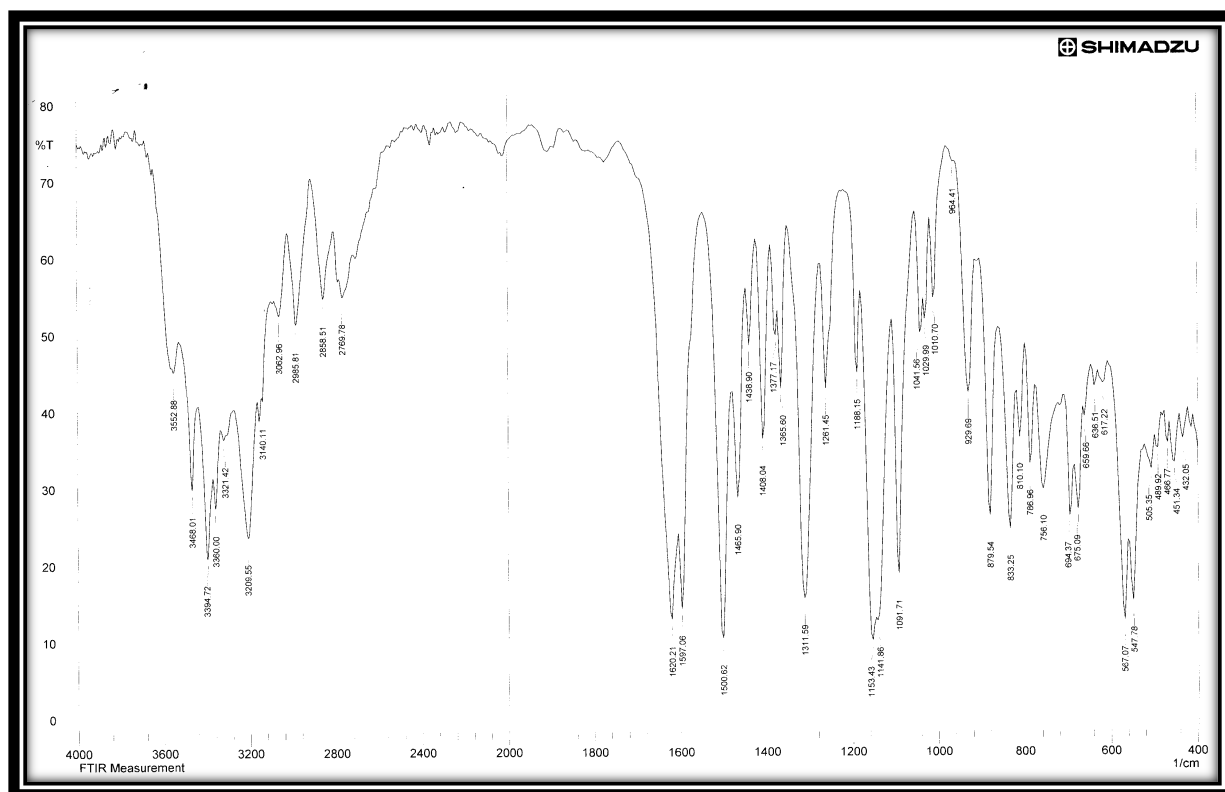
### 3.6.2.1 FT-IR spectra of [Al(SMZ)<sub>3</sub>]Cl<sub>3</sub>, [Cr(SMZ)<sub>3</sub>]Cl<sub>3</sub>, and [Fe(SMZ)<sub>3</sub>]Cl<sub>3</sub> complexes

The assignment of the characteristic bands (FT-IR) spectra for the free ligand (SMZ), Figure (3-4), are summarized in Table (3-4), and [SMZ - M'] complexes ( The important IR peaks of the complexes) are given in Tables (3-34) and shown in Figures (3-73) , (3-74) and (3-75).

Table (3-34) : Infrared spectral data(wave number  $\nu$ )  $\text{cm}^{-1}$  for [ M'-SMZ ]

Complexes	$\nu_{\text{as}}$ (NH):NH <sub>2</sub>	$\nu_{\text{vs}}$ (NH):NH <sub>2</sub>	$\nu_{\text{vs}}$ (NH): sulfonamide group	$\nu$ (C-H)	(C=C) Ar.	(SO <sub>2</sub> ) asy	(C-N)	(C=N) (SMZ) Isoxazol In ring	(SO <sub>2</sub> ) sy	(S-N)	(M-N)	(M-O)
[Al (SMZ) <sub>3</sub> ] Cl <sub>3</sub>	3471	3360	3205	2981 2858m	1465s	1311	1624s 1597	1500 vs	1138 vs	929	567	482
[Cr (SMZ) <sub>3</sub> ] Cl <sub>3</sub>	3471 vs -br	3394	3240	2981vs 2854	1465	1365	1620 1597 vs	1500 vs	1138 vs	929	547	478 w
[Fe (SMZ) <sub>3</sub> ] Cl <sub>3</sub>	3468 vs -br	3360	3205	2985s 2858br	1465	1365	1620 1597 vs	1500 vs	1153	929	547	466

Figure (3-73) :FT-IR Spectrum of  $[Al(SMZ)_3]Cl_3$ Figure (3-74) :FT-IR Spectrum of  $[Cr(SMZ)_3]Cl_3$

Figure (3-75) : FT-IR Spectrum of  $[\text{Fe}(\text{SMZ})_3]\text{Cl}_3$ Table (3-35) Electronic Spectral Data of  $[\text{Al}(\text{SMZ})_3]\text{Cl}_3$ ,  $[\text{Cr}(\text{SMZ})_3]\text{Cl}_3$  and  $[\text{Fe}(\text{SMZ})_3]\text{Cl}_3$  Complexes

Complexes	$\lambda$ nm	$\nu$ $\text{cm}^{-1}$	$\epsilon$ max ( $\text{molar}^{-1} \cdot \text{cm}^{-1}$ )	Assignments	$\mu_{\text{eff}}$ (BM)
$[\text{Al}(\text{SMZ})_3]\text{Cl}_3$	290 803	34482 12453	2151 1	C.T The 3d $\leftarrow$ 3p transitions in the Al-N	0 Dima
$[\text{Cr}(\text{SMZ})_3]\text{Cl}_3$	300 758 973	33333 13192 10277	2366 10 7	Charge transfer ${}^4\text{A}_{2g} \rightarrow {}^4\text{T}_{1g}(\text{P}) \nu_3$ ${}^4\text{A}_{2g} \rightarrow {}^4\text{T}_{1g} \nu_2$	1.97
$[\text{Fe}(\text{SMZ})_3]\text{Cl}_3$	294 491 820	34013 20366 12195	2182 2 2	CT $6\text{A}_{1g} \rightarrow 4\text{T}_{2g} (4\text{G})$ $6\text{A}_{1g} \rightarrow 4\text{T}_{1g} (4\text{G})$	5.14



### 3.6.2.2 .1 UV/Vis Spectrum of $[\text{Al}(\text{SMZ})_3]\text{Cl}_3$

The (U.V-Vis) of spectrum  $[\text{Al}(\text{SMZ})_3]\text{Cl}_3$  complex of (SMZ) spectrum in DMSO, Figure (3-76) , exhibits two transitions. The first high intense peak at 290 nm ( $34482\text{cm}^{-1}$ ), due to the intra ligand charge transfer(INCT) and second band at 803 nm( $12453\text{ cm}^{-1}$ ),The  $3d \leftarrow 3p$  transitions in the  $\text{Al} \rightarrow$  ligand were observed by monitoring  $4s \rightarrow 3p$  emission from Al(4s) atoms produced by pre dissociation of the excited complex. <sup>[100]</sup> , Figure (3-79)

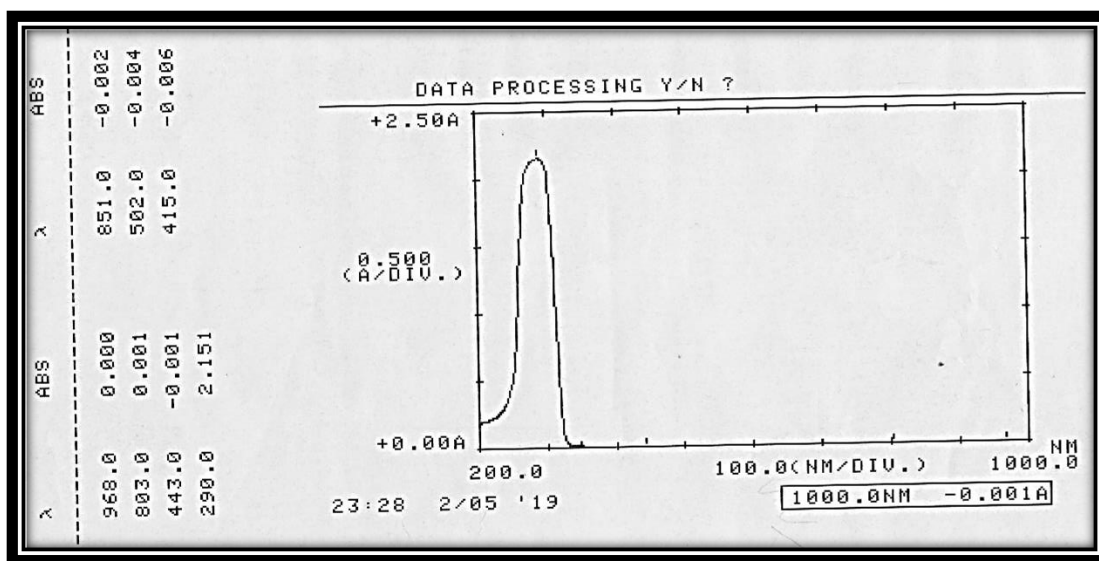


Figure (3-76) : Electronic Spectrum of  $[\text{Al}(\text{SMZ})_3]\text{Cl}_3$

### 3.6.2.2 .2 UV/Vis Spectrum of $[\text{Cr}(\text{SMZ})_3]\text{Cl}_3$

The (U.V- Vis), spectrum of  $[\text{Cr}(\text{SMZ})_3]\text{Cl}_3$  complex of (SMZ)spectrum in DMSO, Figure (3-77) , exhibits three transitions. The first high intense peak at 300 nm ( $33333\text{cm}^{-1}$ ), due to the intra ligand charge transfer(INCT) and second and third bands at 758 nm( $13192\text{ cm}^{-1}$ ), 973 m ( $10277\text{cm}^{-1}$ ) table 3-8 which are assignable to  ${}^4\text{A}_{2g} \rightarrow {}^4\text{T}_{1g} (\nu_3)$  ,  ${}^4\text{A}_{2g} \rightarrow {}^4\text{T}_{1g} (\nu_2)$  respectively <sup>[83,103,105]</sup>.The magnetic moment of the  $[\text{Cr}(\text{SMZ})_3]\text{Cl}_3$  is (1.97 B.M.) Table (3-35), therefore an octahedral geometry was assume  $[\text{Cr}(\text{SMZ})_3]\text{Cl}_3$  for Cr (III) complex. The following structure can be suggested as in Figure (3-79)

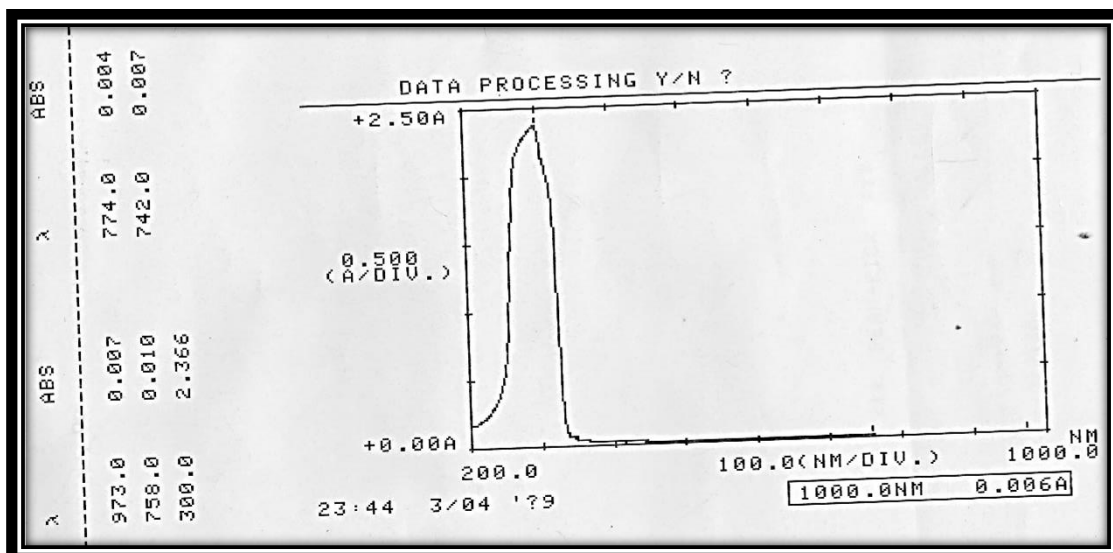


Figure (3-77) Electronic Spectrum of  $[\text{Cr}(\text{SMZ})_3]\text{Cl}_3$

### 3.6.2.2. 3 UV/Vis Spectrum of $[\text{Fe}(\text{SMZ})_3]\text{Cl}_3$

The UV-Vis spectrum of  $[\text{Fe}(\text{SMZ})_3]\text{Cl}_3$  complex, Figure (3-78), showed two bands in the d-d transition the can be assigned to the  ${}^6\text{A}_{1g} \rightarrow {}^4\text{T}_{1g}(20366\text{cm}^{-1})$  and  ${}^6\text{A}_{1g} \rightarrow {}^4\text{T}_{2g}(12195\text{cm}^{-1})$  and one obscured by the intense charge-transfer band ( $34013\text{cm}^{-1}$ ). 294nm observed at nm.these assignments are comparable to the other earlier report made for ferric ion Fe(III) complexes <sup>(94,98)</sup>. The value of the measured magnetic moment .Table (3-35), is (5.14 B.M.) in accordance with the presumption of high-spin  $d^5$  Fe(III) in octahedral geometry <sup>(87,95,100)</sup>. Figure (3-79).

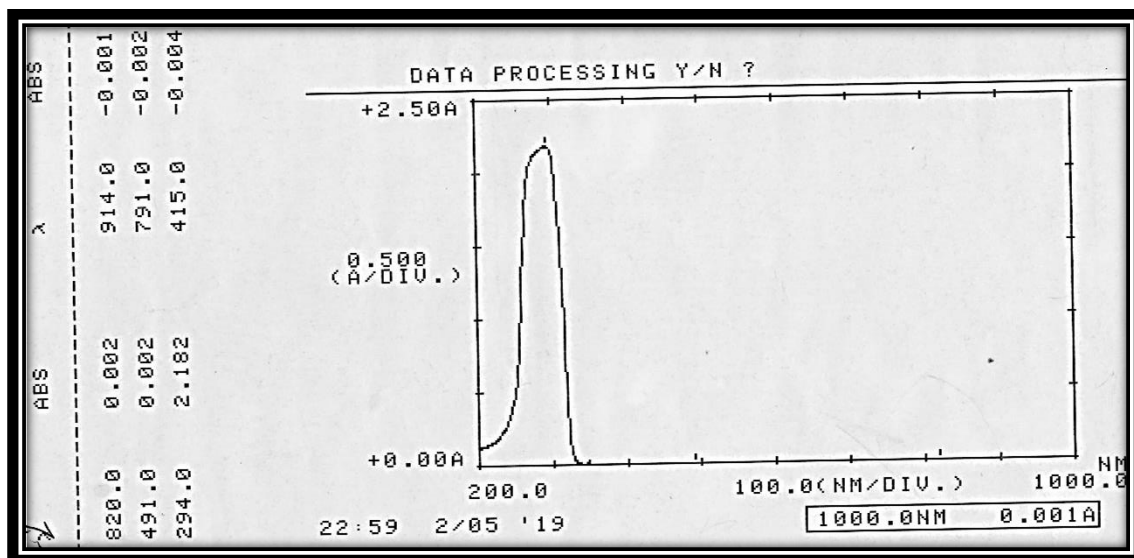


Figure (3-78) Electronic Spectrum of  $[\text{Fe}(\text{SMZ})_3]\text{Cl}_3$

### 3.7 The proposed molecular structure for $\text{M}'(\text{III})-\text{SMZ}$ complexes

Studying complexes on bases of the above analysis, spectral observations suggest the octahedral geometry for the  $[\text{Al}(\text{III})$ ,  $\text{Cr}(\text{III})$ , and  $\text{Fe}(\text{III})$ ] complexes, exhibit the coordination number six and may be formulated as  $[\text{Al}(\text{SMZ})_3]\text{Cl}_3$ ,  $[\text{Cr}(\text{SMZ})_3]\text{Cl}_3$  and  $[\text{Fe}(\text{SMZ})_3]\text{Cl}_3$ . It was found that (SMZ) interacts with all of three metal ions coordinates as a bidentate ligand, The general structure of the complexes is 3D as shown in Figure (3-79).

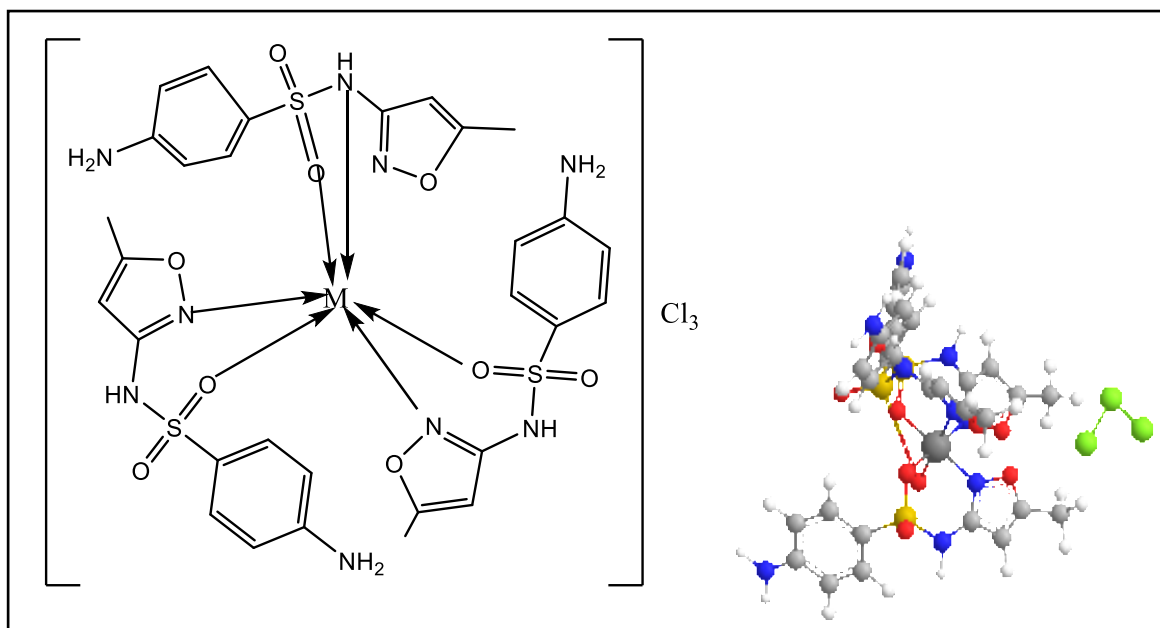


Figure (3-79) : 3D Molecular Modeling Proposed  $[M'(SMX)_3]Cl_3$

$[M'$  Al(III), Cr(III), and Fe(III)]

Chapter  
Four

**Biological  
activity**

## 4 Biological activity

### 4.1. Introduction

Biological [pharmacological] activity spectrum of a compound represents the biochemical vs, physiological such as antibacterial, anti-inflammatory, antifungal and anti-HIV, Inspired by the groundbreaking work of Domagk (sulfa drugs ) and Fleming, (Penicillin), [111]. The mechanisms of action of antimicrobial drugs, Figure (4-1) , can be discussed under inhibition of DNA synthesis , cell membrane function, cell wall synthesis , and protein synthesis. The broad-spectrum drug affects a wide range of disease-causing bacteria, Gram-positive and Gram-negative bacteria [112].

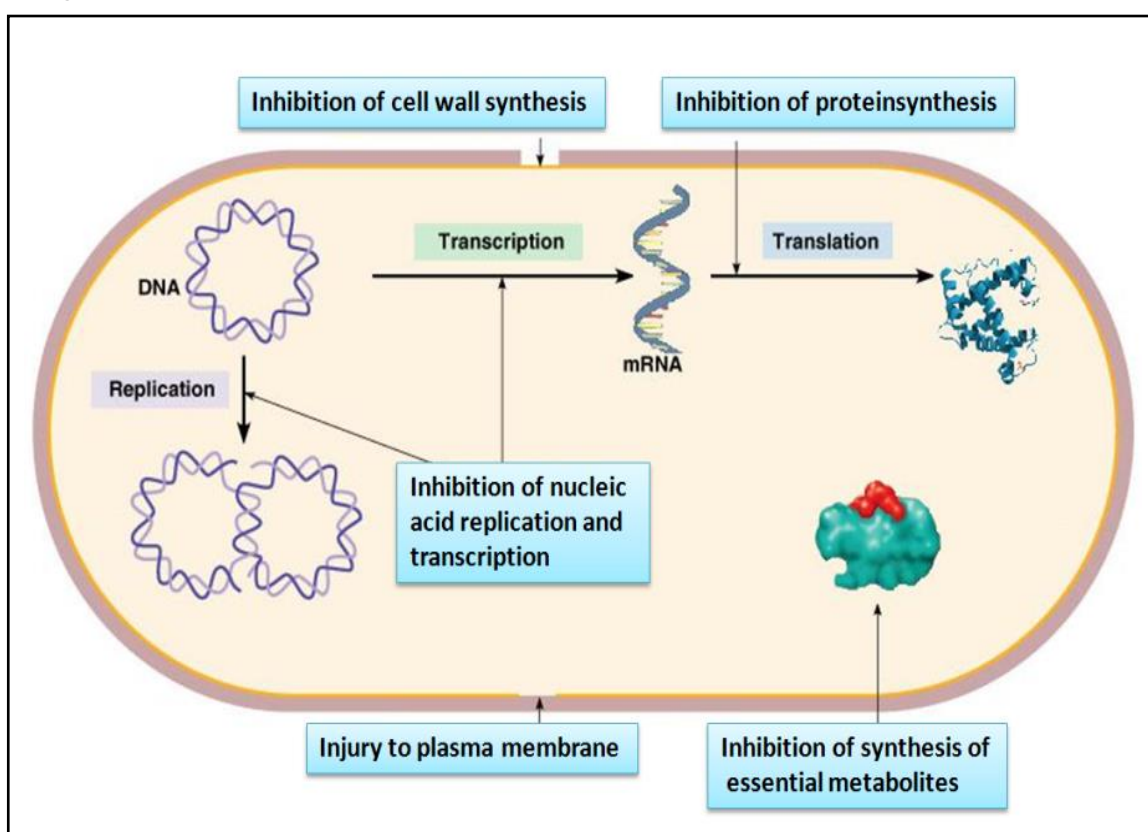


Figure (4-1) :The mechanisms of action of antimicrobial drugs

For a better understanding, in Figure (4-2) The classification of different types of antimicrobial drugs and their applications

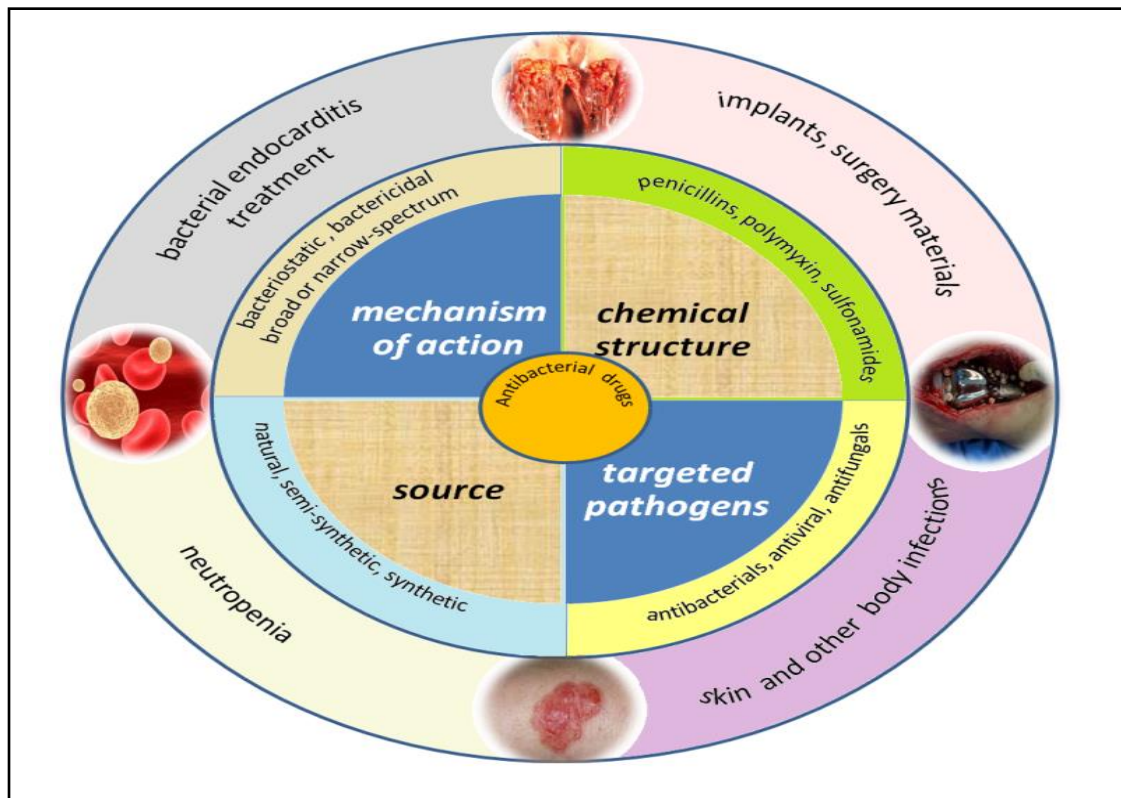


Figure (4-2) : applications of antimicrobial drugs

sulfonamides and Aminoglycosides are only effective against aerobic organisms, while nitroimidazoles are only effective for anaerobes [113].

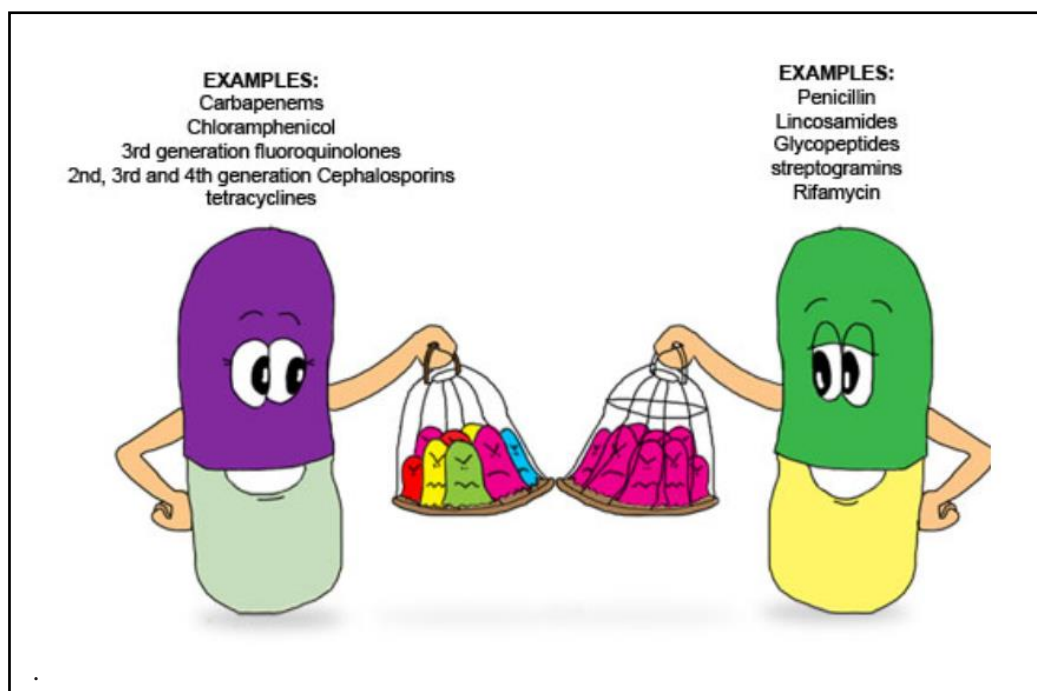


Figure (4-3) : Aerobic And anaerobes organisms

The interest in antimicrobial amino acids opens new perspectives in antimicrobial drug design. Such as Hunter-killer peptides as a novel class of targeted peptides efficacy including therapeutics for cancer <sup>[51]</sup>

## 4.2 Material & equipment's

Nutrient agar medium, Macferr land tube ,Cork borer Dish,. Autoclave Refrigerator petri Distilled water and DMSO as (solvent & control)

## 4.3 Principle of antimicrobial susceptibility test

The test solution ( $3 \times 10^{-3}$  Molar ) was prepared by dissolving the compounds in DMSO and filled with the test solution using micropipette. The size of the zone of inhibition (ZI) is compared with control to determine the sensitivity of the organism to the compounds , The diameter of (ZI) is determined intermediately susceptible or resistant. any samples since the (ZI) interpretation chart is as listed in Table (4-1)

Table (4-1):-Observation and Report of Diameter of the (IZ) around the Hole (mm) by scale.

Observation	Report
Inhibition zone > 15mm	Highly active
Inhibition zone >10mm	moderately active
Inhibition zone > 5mm	Slightly active
Inhibition zone ≤5-0 mm	Inactive

The results of the tested samples in this study was compared with the control (DMSO).



#### 4.4 Types of Pathogenic Bacteria and fungus in this Study

Table (4-2):- Types of bacteria , fungus and their report.

Bacteria	Report	Ref.
<i>Staphylococcus S.P</i> ( Gram-positive )	effects skin and causes skin wound and skin necrosis and later on pus discharge. This may progress to cause bacteria in blood and lymph system	[ 113-114]
<i>Acinetobacter baumannii</i> (Gram-negative "Iraqi bacter")	spread to civilian hospitals in part due to the transport of infected soldiers through multiple medical facilities. <sup>[123]</sup>  due to its seemingly sudden emergence in military treatment facilities during the Iraq War.	[ 113 -114]
Fungi	Report	
<i>Candida albicans</i> yeast-type Figure (4-5)	appear as white patches on the skin or mucus membrane, mainly in people with impaired immune system (i.e., cancer, transplant, or HIV patients).	[113]

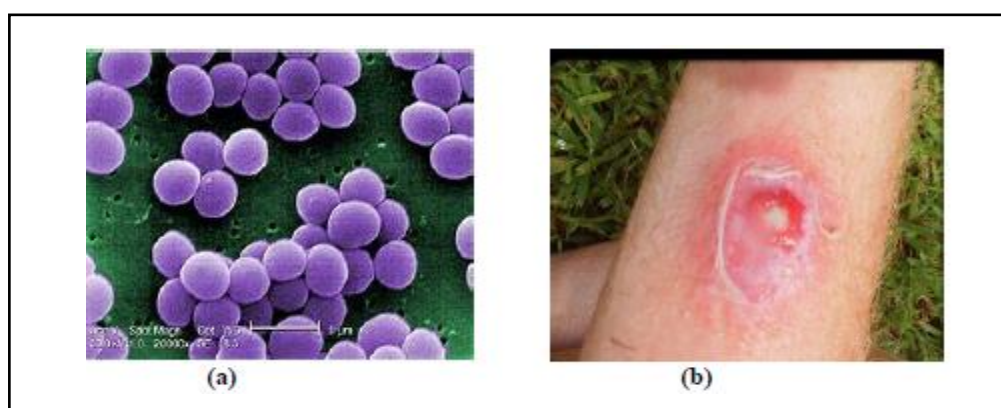


Figure (4-4) :(a) *S. aureus* cells and (b) skin infection by *S. aureus*.

Compounds were tested against the *Candida albicans* Figure (4-3) using agar plate technique .The linear growth of the fungus was obtained by

measuring the diameter of colony in a petri plate after 96 h and the Percentage of Inhibition  $(I) = 100(C-T)/C$ , where .

C = diameters of the fungus colony in the control plate

T = diameters of the fungus colony in the test plates.



Figure (4-5) : *Candida albicans*

## 4.5 Results and Discussion

All the compounds including DMSO (as solvent and control), ligands and their complexes and were screened against two bacterial strains *Staphylococcus aureus*, and *Acinetobacter*. and *Candida albicans* fungal strains to assess their potential as antimicrobial agent by Disc Diffusion method. The Zones of inhibition (IZ) based upon zone size around the discs were measured. and listed in Tables (4-3) and (4-4).As mentioned in Chapter (1), sulfamethoxazole, , amino acids and mixed ligand Complexes are known for a wide variety of biological activities. Higher bacteriacidal activity exhibited by the complexes than ligand reveals positive impact of coordination of metals with the ligand in enhancing the activity. The increase activity of the metal complexes can be explained on the Tweedy's chelation theory.<sup>[114]</sup> and overtones concept. On chelation, the polarity of the metal ion will subside to a greater extent due to the overlap of the (ligand orbital) and partial sharing of the positive charge of the metal ion

with donor groups. complex have shown highest bactericidal activity against both bacterial strains and fungicidal activity. Furthermore, The rate of inhibition diameter was varied according to the variation in the ligands type , bacteria type ,covenant of metals and types of structure Th or octahedral as in Sn(II) complexes , Comparative study of the control DMSO, free ligands and its metal complexes indicates that most of the metal complexes exhibit higher biological activity <sup>[52]</sup>.

Table (4-3) : The (IZ mm) data of ligands

Ligands	<i>Acineto</i>	<i>staphylococcus</i>	<b>Candida albicans</b>
(SMZ)	11	23	-
L-_Valin	12	20	-
L-_prolin	10	25	-

Table (4-4) : The (IZ mm) data of [M (SMZ)(L-Pro)<sub>2</sub>] and [M' (SMZ)(L-Pro)<sub>2</sub>]

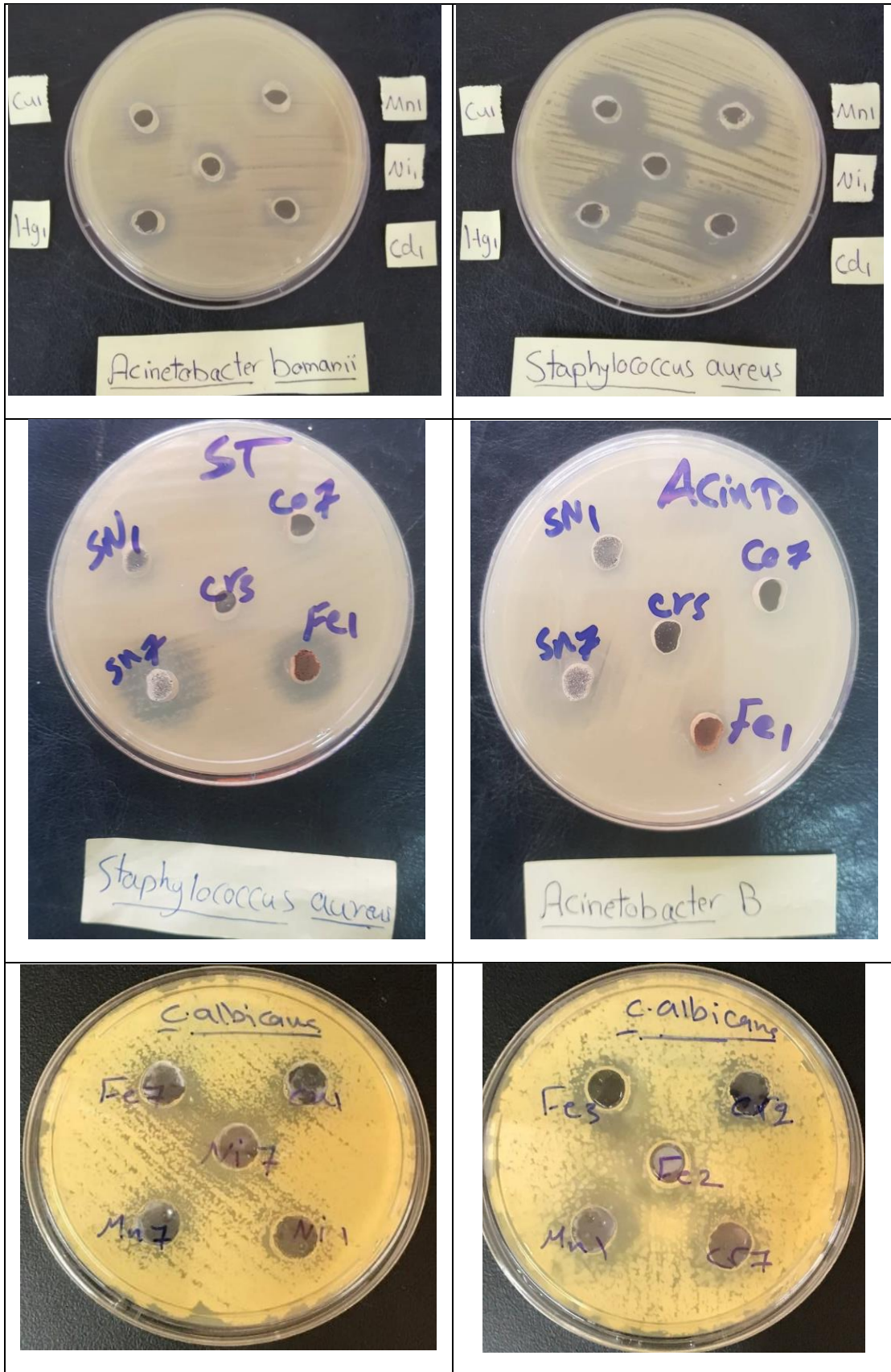
Complexes	<i>Acineto</i>	<i>staphylococcus</i>	<b>Candida albicans</b>	Symbol
[Mn(SMZ)(L-Pro) <sub>2</sub> ]	10	19	12	Mn1
[Sn(SMZ)(L-Pro) <sub>2</sub> ]	-	-	-	Sn1
[Cd(SMZ)(L-Pro) <sub>2</sub> ]	11	20	-	Cd1
[Cu(SMZ)(L-Pro) <sub>2</sub> ]	11	22	-	Cu1
[Ni(SMZ)(L-Pro) <sub>2</sub> ]	12	19	-	Ni1
[Hg(SMZ)(L-Pro) <sub>2</sub> ]	12	17	14	Hg1
[Sn (SMZ)(L-Pro) <sub>2</sub> ]Cl			-	Sn5
[Al(SMZ)(L-Pro) <sub>2</sub> ]Cl	10	19	14	Al3
[Cr(SMZ)(L-Pro) <sub>2</sub> ]Cl	-	-	15	Cr3
[Fe(SMZ)(L-Pro) <sub>2</sub> ]Cl	-	20	14	Fe3

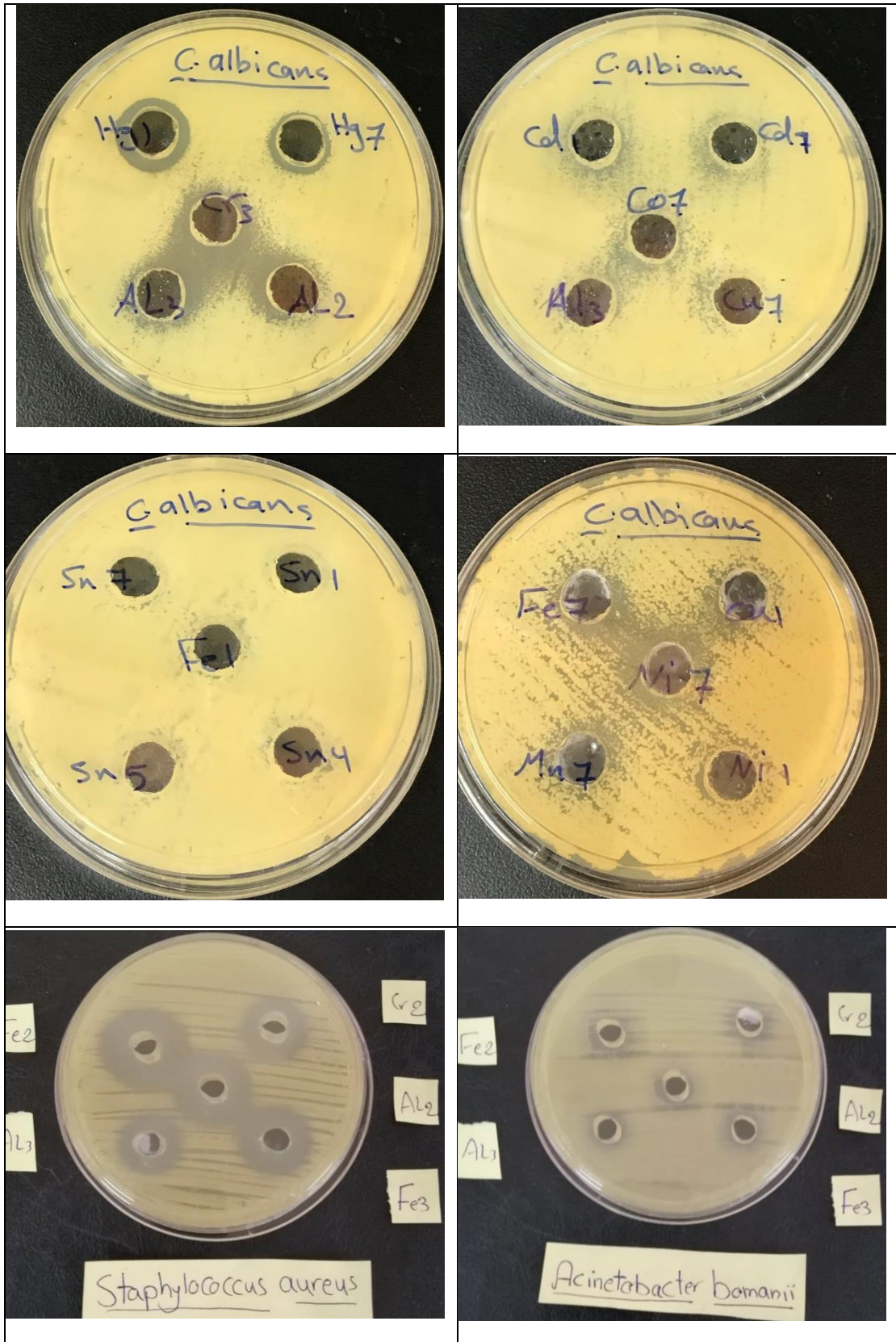
Table (4-5) The (IZ mm) data of  $[M(\text{SMZ})(\text{L-Val})_2]$  and  $[M'(\text{SMZ})(\text{L-Val})_2]\text{Cl}$ 

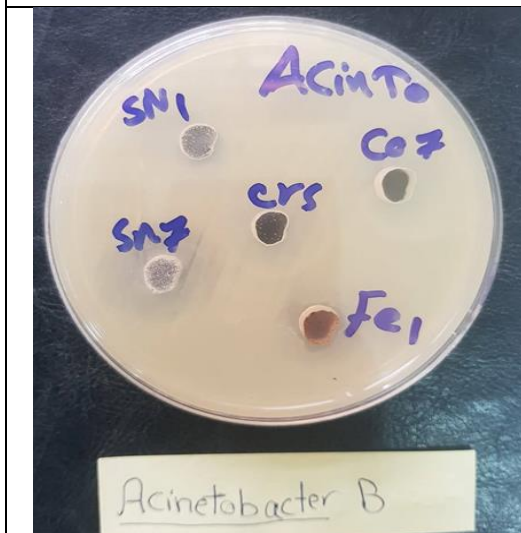
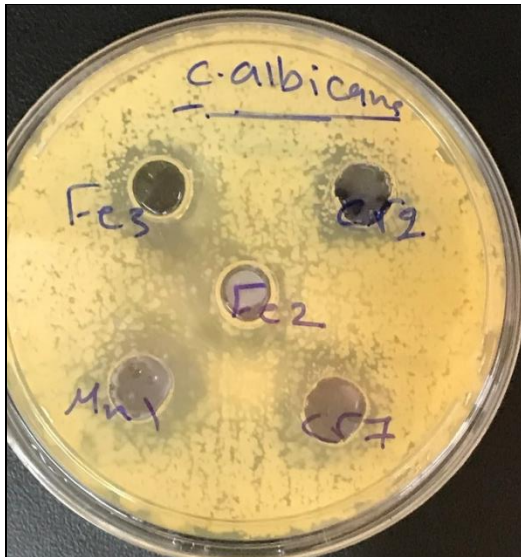
Complexes	<i>Acinetobacter bomanii</i>	<i>Staphylococcus aureus</i>	<i>Candida albicans</i>	Symbol
$[\text{Mn}(\text{SMZ})(\text{L-Val})_2]$	11	20	-	Mn7
$[\text{Sn}(\text{SMZ})(\text{L-Val})_2]$	16	21	-	Sn7
$[\text{Cd}(\text{SMZ})(\text{L-Val})_2]$	11	27	-	Cd7
$[\text{Cu}(\text{SMZ})(\text{L-Val})_2]$	13	29	--	Cu7
$[\text{Ni}(\text{SMZ})(\text{L-Val})_2]$	-	10	15	Ni7
$[\text{Co}(\text{SMZ})(\text{L-Val})_2]$	-	-	-	Co7
$[\text{Hg}(\text{SMZ})(\text{L-Val})_2]$	10	21	11	Hg7
$[\text{Fe}(\text{SMZ})(\text{L-Val})_2]\text{Cl}$	11	25	12	Fe7
$[\text{Cr}(\text{SMZ})(\text{L-Val})_2]\text{Cl}$	11	27	-	Cr7
$[\text{Al}(\text{SMZ})(\text{L-Val})_2]\text{Cl}$	11	25	14	Al7

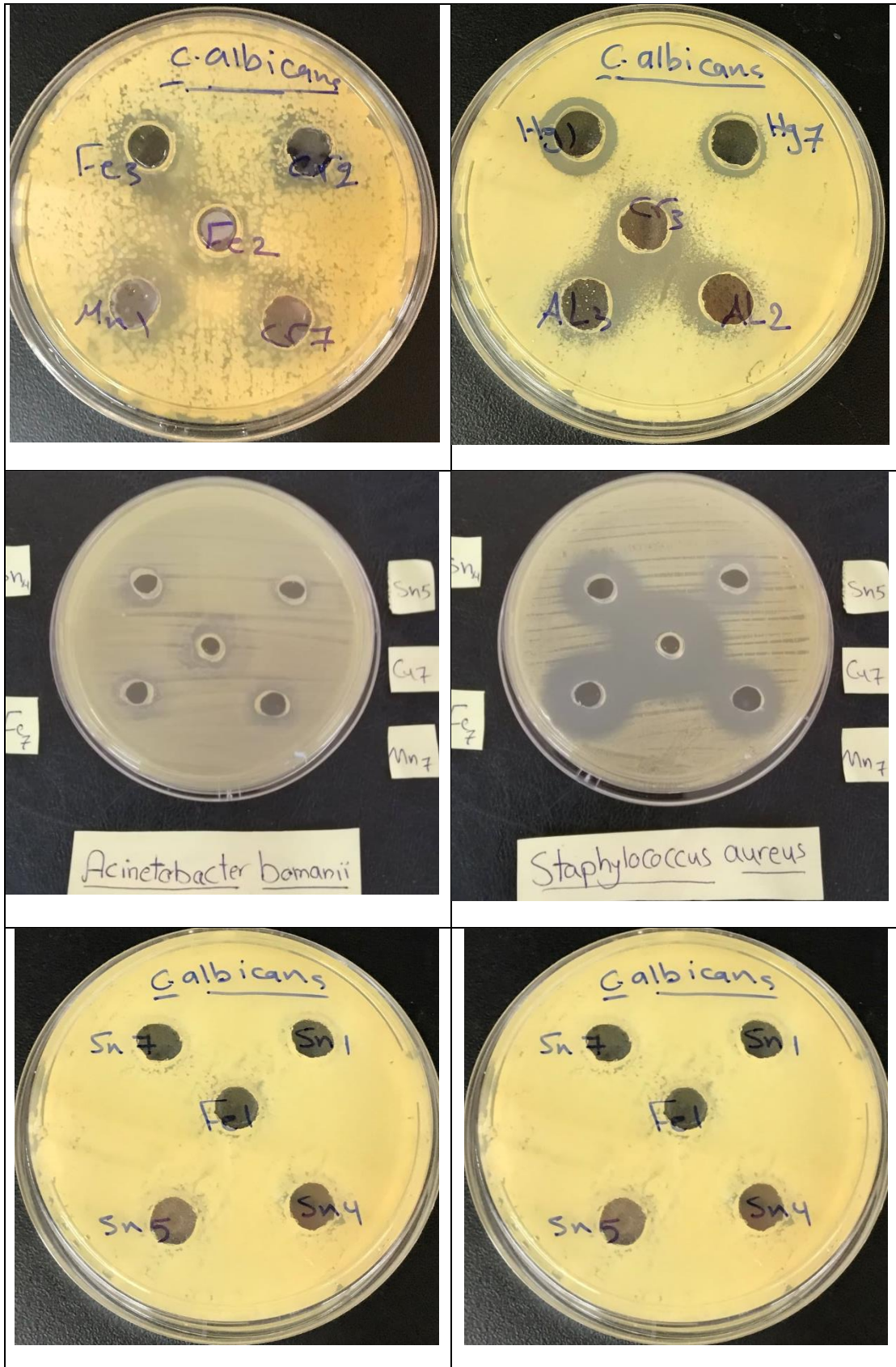
Table (4-6): The (IZ mm) data of  $M'$  (III) and Sn(II) mono ligand complexes

Complexes	<i>Acineto</i>	<i>staphylococcus</i>	<i>Candida albicans</i>	Symb ol
$[\text{Al}(\text{SMZ})_3]\text{Cl}_3$	11	23	-	Al2
$[\text{Cr}(\text{SMZ})_3]\text{Cl}_3$	12	20	-	Cr2
$[\text{Fe}(\text{SMZ})_3]\text{Cl}_3$	10	25	-	Fe2
$[\text{Sn}(\text{SMZ})_2]\text{Cl}_2$	11	20	-	Sn4

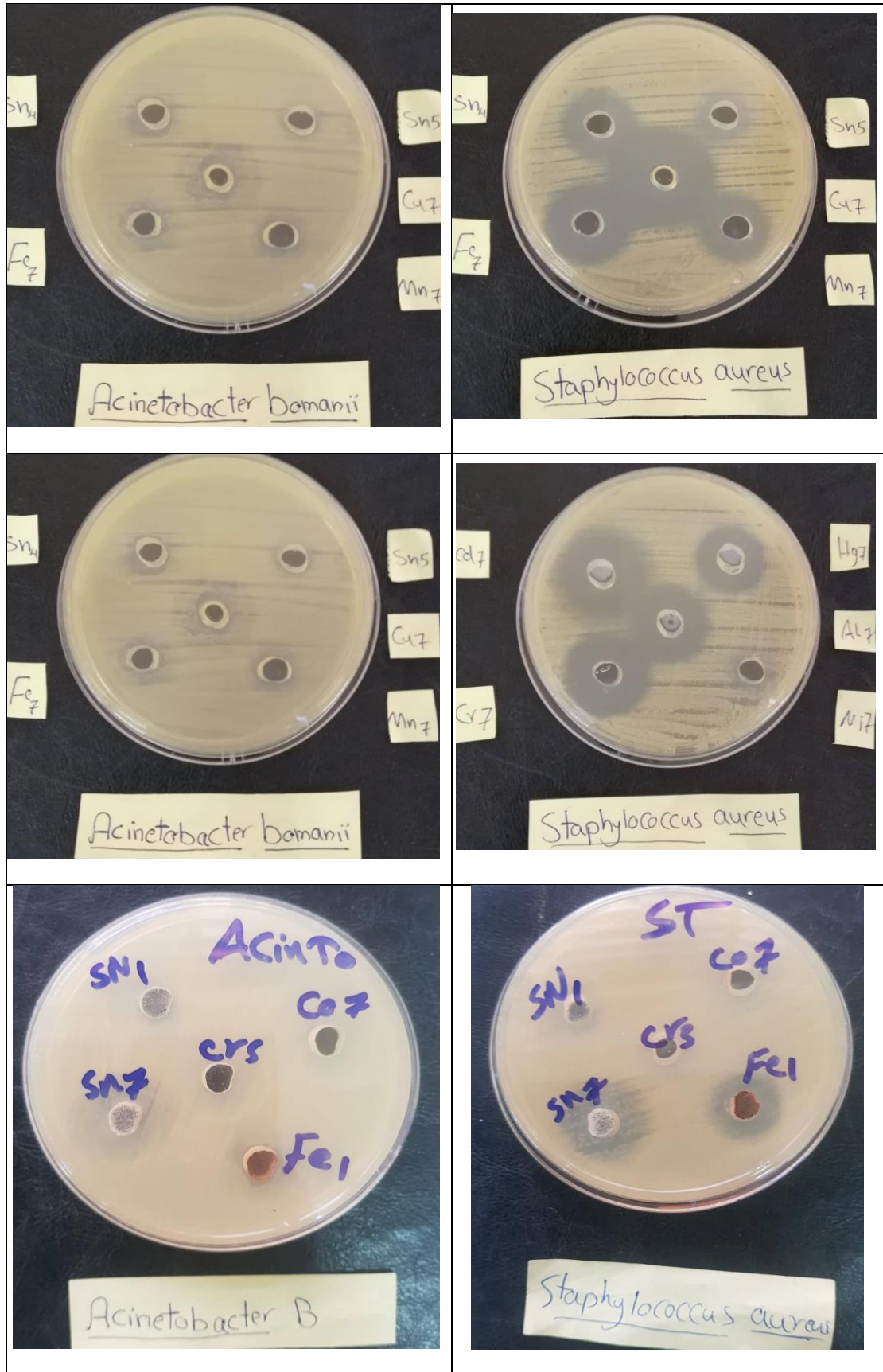


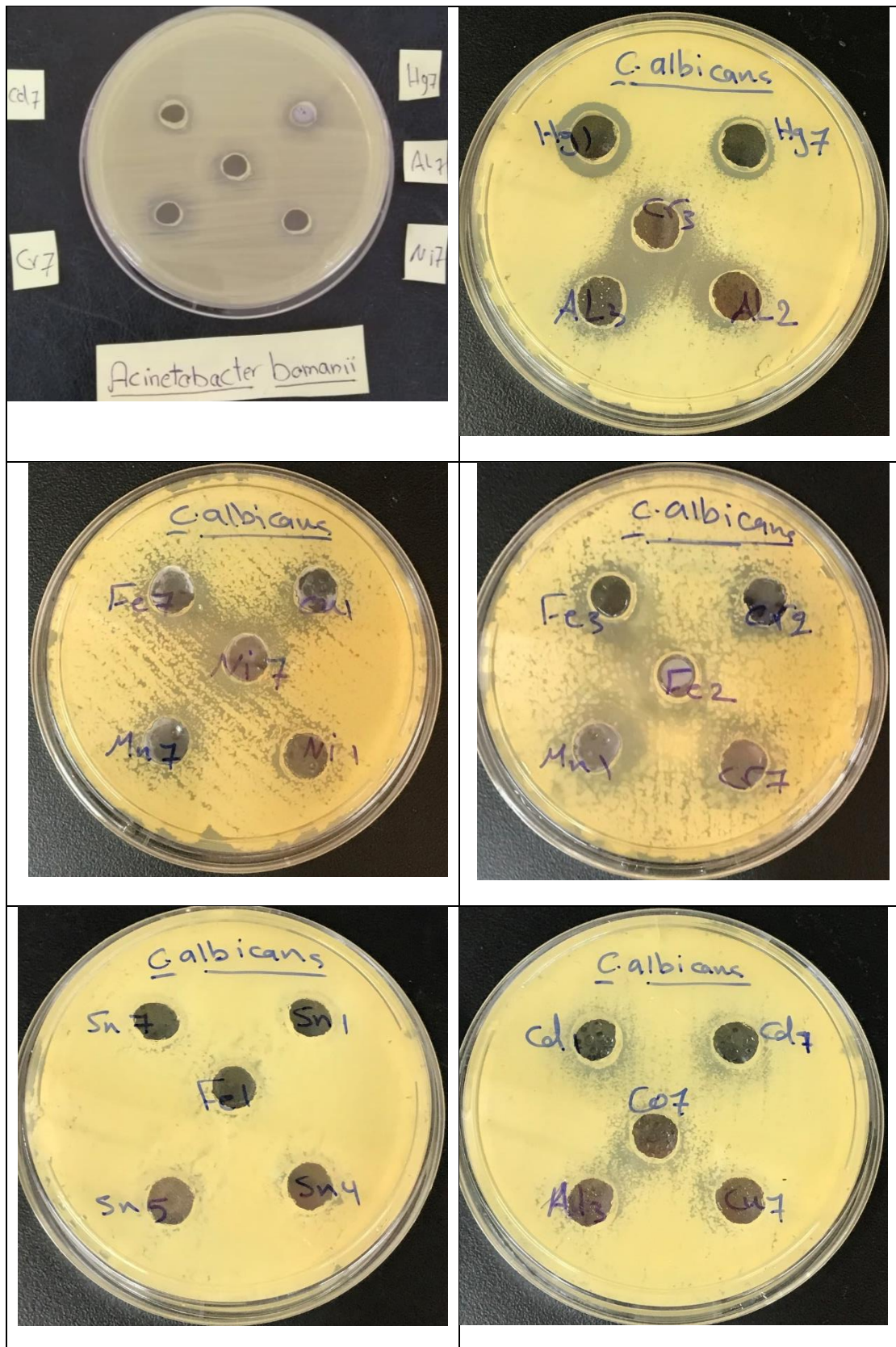












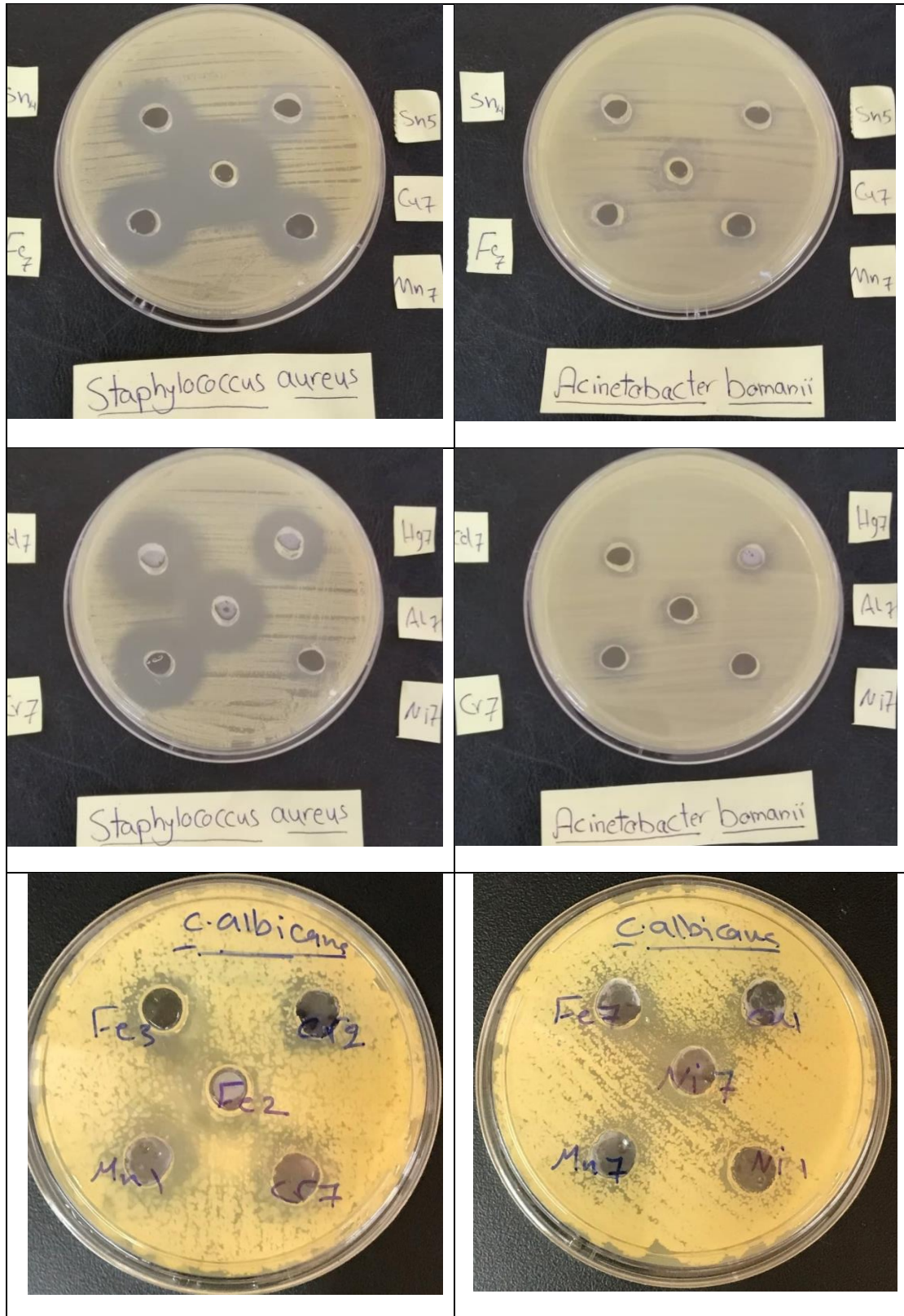




Figure (4-6): Photograph of Antimicrobial Activity of complexes

## Conclusion

1. The different ligands have been used in this study showed different physical properties.
2. All the prepared complexes were soluble in DMSO.
3. All mixed ligand complexes showed octahedral(Oh) geometry
4. In some the ligand field calculations showed different strength (according to the  $10Dq$  value and electron-repulsion parameter ( $\beta$ ), which refers to different ionic character between the metal and (O and N) donor atoms of the ligands. These complexes showed (Oh) geometry.
5. All mono M (II) ligand complexes showed tetrahedral (Th) geometry while M' (III) showed (Oh) geometry.
6. Comparing the spectral data (Ft-IR and (U.V- Vis) L- L-Valin and L-Proline ligands with corresponding M(II) and M' (III)- complexes may provide the idea about such peaks which either have newly formed or disappeared or even changed their position after complexation.
7. In all complexes the sulfamethoxazole ligand behaves as a bidentate ligand and coordinate to the metal ions through sulfonamide  $-NH$  [26,95].
8. Some the values data for C, H, N, and M % obtained are in the range of accepted theoretical values except for Sn complex which shows large difference range between the actual than theoretical values for the differences exists probably because of the presence of impurities or solvent in the analyzed compound [104].



# References

## References

1. Orving C. and M. Abrams (1999) *Chem. Rev.*, 99, 2201-2203.
2. Finney LA, O'halloran TV (2003) "Transition metal speciation in the cell: insights from the chemistry of metal ion receptors" *Science* 300(5621): 931-936.
3. Yang P, Kong X, Cheng C, Li C, Yang X . (2011) Synthesis and biological evaluation of 8-substituted and deglucuronidated scutellarin and baicalin analogues as antioxidant responsive element activators. *Science China Chemistry* 54(10): 1565.
4. Jolly W. L. (1984) "Modern Inorganic Chemistry, Principles of Inorganic chemistry", Ed. Mc.Graw hill, New York,
5. Ranjan K. Mohapatra, Pradeep K. Das, Manoj K. Pradhan, Marei M. El-Ajaily, Debadutta Das, Halima F. Salem, Umakanta Mahanta, Gouranga Badhei, Pankaj K. Parhi, Abdussalam A. Maihub & Md. Kudrat -E-Zahanm (2019), *Comments on Inorganic Chemistry*, on *Inorganic Chemistry*, 39:3, 127-187 .
6. Thompson K. H., Orvig C. *J Inorganic Biochem.* (2006) ,100, 12, 1925-1935.
7. Clarke M. J., Sadler P. J., Springer Verlag, Berlin, (1999) ; 1, 1-43.
8. Leo Di, Berrettin D., and Renzo F, C. *J. Chem. Soc. Dalton Trans.*, (1998). 1, 1993-2000.
9. Chartone SE, Loyola TL, Bucclarelli RW, Menezes MA, Rey NA and Pereira ME. *J Inorg Biochem.*, (2005); 99, 1001-08.
10. Jessica Lemke, Antonio Pinto, Philip Niehoff, Vera Vasylyeva and Nils Metzler-Nolte. (2009) , *Dalton Transactions*. 35, 6873 to 7316
11. Essien, E.E., Coker, H.A.B. *J. Pharm.* (1987) ; 18(4)21-22.
12. Abram U., Rhenium (2004), *Compr. Coord. Chem. II* ,5, 271 – 402.

## References

13. Osella, D.; Ferrali, M.; Zanello, P.; Laschi, F.; Fontani, M., Nervi, C., Cavigiolo, G. *Inorg. Chim. Acta.* (2000) ; 306, 42
14. Rudzinski, W.E., Aminabhavi, T.M., Biradar, N.S., and Patil, C.S. *Inorg. Chim. Acta.*, (1982) ; 67, 177-182.
15. Rehman W., Baloch M. K., Muhammad B., Badshah A. and Khan, K. M. ,*Chinese Science Bulletin*, (2004) 49, 2, 119-122.
16. Wei Lu, Yongxin Li, Rei Kinjo. *J. Am. Chem. Soc.* 2019,
17. Büşra Kaya, Zehra Kübra Yılmaz, Onur Şahin, Belma Aslim, Ümmügülsüm Tükenmez Bahri Ülküseven, *Journal of Biological Inorganic Chemistry* (1975). 24,3, 365-376
18. Yeon-Joo Cheong, Seunghyeon Lee, Sang Joon Hwang, Woojin Yoon, Hoseop Yun, Hye-Young Jang . (2019), *European Journal of Organic Chemistry*.
19. Panhwar, Q.K., and Shahabuddin Memon. (2014), *The Scientific World Journal* Vol. 2014.
20. Ma, M.; Cheng, Y.; Xu, Z.; Xu, P.; Qu, H.; Fang, Y.; Xu, T.; Wen, L. (2007), *European journal of medicinal chemistry*; 42 (1), 93–98.
21. Garg, S.K.; Ghosh, S.S.; Mathur, V.S. (1986), *International journal of clinical pharmacology, therapy, and toxicology* ;24 (1), 23–25.
22. Larson, A. M., Polson, J. and Fontana, R. J. (2005), *Hepatology*, 42 (6) 1364–1372
23. Ma, M., Cheng, Y., Xu, Z., Xu, P., Qu, H., Fang, Y., Xu, T. and Wen, L. (2007) , *European journal of medicinal chemistry*, 42 (1) 93–8
24. Monti, L., Ana Pontoriero N. M., Giulidori, C., Hure, E. and Patricia, A. M. W., Rodríguez, M. V., Feresin, G., Campagnoli, D. and Rizzotto, M. (2010), *Biometals*, 23 1015-1028
25. Bellú, S.; Hure, E.; Trapé, M.; Rizzotto, M.; Sutich, E.; Sigrist, M.; Moreno, V. *Quim. Nova.* (2003), 26(2), 188



## References

26. Bankole, F.O. *Journal of Pharm. and Med. Sci.* (1979), 4(5), 249-250.
27. Malgorzata Baranska, Joel Bowman, Sylvio Canuto, Judy Kim, Werner Mäntele, Siva Umapathy (2001), *JOURNAL OF Spectrochim Acta A Mol Biomol Spectrosc.* Apr;57A(5):1031-6.
28. Yasmin M.S. Jamil, Maher Ali Al-Maqtari and Mohammed K. Al-Qadasi (2017), *journal of European Pharmaceutical And Medical Research*, 4(07), 95-105.
29. Fatima A.I. Al-Khodir (2015), *Oriental Journal of Chemistry* 31(3):1277-1285 .
30. Bamigboye, Mercy Oluwaseyi, Obaleye, Joshua Ayoola And Abdulmolib (2012), *Journal of International. Chem.* ; 22 (2), 105-108
31. G. Karthikeyan , K. Mohanraj , K. P. Elango and K. Girishkumar J. (2006), *Russian Journal of Coordination Chemistry* ; 32(5), 380–385
32. Ameen, S.M.; Drancourt, M. (2013), *Antimicrob. Journal of Agents Chemotherapy* .57, 6370–6371.
33. Ameen, S.M.; Drancourt, M. (2013), *Antimicrob. Journal of Agents chemotherapy* 42, 281–288
34. Bharti Jaina, Suman Malikb, Neha Sharmaa and Shrikant Sharma (2013), *Journal of Der Chemica Sinica*, 4(5):40-45
35. Shrikant Sharmaa, Neha Sharmab, Bharti Jainb and Suman Malik (2014), *Journal of Der Chemica Sinica*, 5(5):61-66
36. Julia HelenaBormio NunesRaphael Enoque Ferrazde PaivaAlexandreCuinWilton RogérioLustriPedro PauloCorbi (2015), *Journal of Polyhedron* . 85 (8), 437-444
37. Naggara A.H., Mauofb H.A., Ekshibab A.A., Farghaly O.A. (2016), *The Pharmaceutical and Chemical Journal*, 3(1),125-137

## References

38. Varghese, B., Suliman, F. E. O., Al-Hajri, A., Al Bishri, N. S. S., & Al-Rwashda, N. (2018), *Journal of Spectrochimica Acta - Part A: Molecular and Biomolecular Spectroscopy*, 190, 392-401.
39. Hany M. Z. El-Alfy, Ali M Hassan<sup>2</sup>, Essam Shawky A. E. H Khattab, Bassem H. Heakal Egypt. *J. Chem. Vol. 61*, No.4 pp. 569 - 580
40. Rostamizadeh S, Daneshfar Z, Moghimi H. (2019) , *journal of European Med Chem.* 171, 474 .
41. Farkas E., Sóvágó I., (2007), *Metal Complexes of Amino Acids and Peptides, Amino Acids, Peptides and Proteins.* 36, 287 – 345.
42. Cerdá M. F., Méndez E., Malacrida L., Zinola C. F., Melián C., Martins M. E., Luna A. M. C., Kremer C. (2002), *Journal of Colloid and Interface Sci.* 249(2), 366 – 371.
43. K. J. Waldron, N. J. Robinson (2009), *Nature Reviews Microbiology* .7, 25 – 35
44. Mertz, E.T., (1972) , *The protein and amino acid needs.* In *Fish nutrition*, edited by J.E. Halver. New York, Academic Press, pp. 106-43
45. Sakiyan L., Logoglu E., Arslan S., Sari N. and Sakiyan N. (2004), *Biometals*, Vol. 17, No. 2, pp. 115-120.
46. Wujec M., Kosikowska U., Paneth P. and Malm A. (2007), *Journal of Heterocycles.*Vol. 71, No. 12.
47. Sutha Shobanal, Perumal Subramaniaml, Jeyaprakash Dharmaraja and Sundram Arvindnarayan (2015) ,*Journal of Pharmaceutics and Nanotechnology* . 8 (13), 5226-5241.
48. Hadjer F., Tahar B., Djallal A.. Eddine, Sofiane D. *Journal of Mater. Environ. Sci.* 9 (17), 2153-2157.
49. Rajendrakumar, C.S. (1994), *Proline-protein interactions: protection of structural and functional integrity of M4 lactate*

## References

- dehydrogenase. *Biochem. Biophys. Res. Commun.* 201, 957–963
50. Aijaz Ahmad Tak, Farukh Arjmand and Sartaj Tabassum (2014) , "Proline". *pubchem.ncbi.nlm.nih.gov*.
51. Aijaz Ahmad Tak, Farukh Arjmand and Sartaj Tabassum , "New Five Coordinated Copper(II) and Nickel(II) Complexes of L-Valine and Kinetic Study of Copper(II) with Calf Thymus DNA" t'ol. 9, Nos, I-2, (2002), *Metal-Based Drugs*".
52. Nursen S. Gazi (2003) , *University Journal of Science* , 16(2), 283-288 .
53. Ammar R. A., Al-Mutiri E. M., Abdalla M. A. (2011), *Fluid Phase Equilibria*, 301,51.
54. Noor K Fayad, Taghreed Hashim Al-Noor, Atheer A Mahmood, Ibtihaj Kadhim Malih (2013), *Chemistry and Materials Research* [www.iiste.org](http://www.iiste.org) ISSN 2224- 3224 (Print) ISSN 2225- 0956 (Online) Vol.3 No.5.
55. Peketi Bhushanavathi & Gollapalli Nageswara Rao (2013), "Speciation studies of Co(II), Ni(II) and Cu(II) complexes of L-valine in acetonitrile–water mixtures" , *Chemical Speciation & Bioavailability*, 25(4), 258-264.
56. Shilpi Mandal, Gunajyoti Das and Hassan Askari (2014), "Physicochemical investigations of the metal complexes of L-valine with doubly charged ions of nickel, copper and zinc a combined experimental and computational approach" *RSC Journal*.47 (4), 24796-24809 .
57. Takeshita, Y.; Takakura, K.; Akitsu, T. (2015), "Multifunctional Composites of Chiral Valine Derivative Schiff Base Cu(II) Complexes and TiO<sub>2</sub>". *Int. J. Mol. Sci.* 16, 3955-3969.
58. Nanami Yoshidal , Tomoka Shimadal , Haruka Hirokil , Masahiro Takasel , Takashiro Akitsu (2016), "L-Valine and salicylaldehyde

## References

- derivative Schiff base Zn(II) complexes as UVA sunscreen".  
*Jacobs Journal of Inorganic Chemistry* .
59. Saravanan P. C., Krishnan M. M., Arumugham M. N. (2017),  
"DNA Binding and Biological Activities of Ternary Copper(II)  
Complexes Containing L-Valine and Urea". *Indian J. Adv. Chem.  
Sci.* 5(4), 324–329.
60. Thakur G.A., Dhaigude U.N. and Bhise P.V. (2018), *Asian Journal  
of Chemistry*; Vol. 30, No. 11 .
61. Saravanan P. C., Murali Krishnan M. and Arumugham M. N.  
(2019), Vol. 10(1): 148-156
62. Teo S.G., Teoh C.H., Ng H.K. Fun and J.P. Declercq (1995),  
*Polyhedron*, 14,1447.
63. Yamaguchi T., Shibata A. and Ito T. (1996), *J. Chem. Soc., Dalton  
Trans.*4031.
64. Ramakrishna Rao a , Ashis K. Patra b , P.R. Chetana (2007),  
*Polyhedron*. 26, 5331–5338
65. Rao, P.S.; Thakur, G.A.; Lahiri, G.K. (2006), (IAEA) Proceedings  
of the fifteenth national symposium on thermal analysis  
"RADIATION CHEMISTRY, RADIOCHEMISTRY AND  
NUCLEAR CHEMISTRY" (S38).
66. Fintan Kelleher, Sinead Kellya and Vickie McKee (2007),  
*Spirobicyclic Diamines.: Synthesis and Metal Complexation of  
Proline-Derived [4,4]-Spirodiamines. Tetrahedron*, Vol. 63 (37)  
10th September, 9235-9242,
67. Boddu Veeraswami, Peketi Bhushanavathi, Uppuleti  
Viplavaprasad and Gollapalli Nageswara Rao (2014), *Chemical  
Speciation & Bioavailability*, 26(1),13-20.
68. Anna Rathgeb, Andreas Böhm, Maria S. Novak, Anotolie  
Gavrilita, Orsolya Dömötör, Jean Bernard Tommasino, Éva A.

## References

- Enyedy, Sergiu Shova, Samuel Meier, Michael A. Jakupec, Dominique Luneau, and Vladimir B (2014), "Arion · Ruthenium-Nitrosyl Complexes with Glycine, L-Alanine, L-Valine, L-Proline, D-Proline, L-Serine, L-Threonine, and L-Tyrosine: Synthesis, X-ray Diffraction Structures, Spectroscopic and Electrochemical Properties, and Antiproliferative Activity" *Inorg Chem.* Mar 3; 53(5): 2718–2729.
69. Junyi Du, Jisheng Zhang, Jianhua Zhu, Chungu Xia and Wei Sun (2018), *New J. Chem.*, 42, 8315- 8319
70. Mosarrat *Parveen*, Mohammad Mobin, *Saman Zehra & Ruby Asla* (2018), L-proline mixed with sodium benzoate as sustainable inhibitor for mild steel corrosion in 1M HCl: An experimental and theoretical approach . 8:7489
71. Mala Nath ,Partha Roy ,Rutusmita Mishra and Mridula Thakur (2019) , *applied organometallic chemistry* 33, 2 .
72. Geary W. J., *Coord J.* (1971). *Chem. Rev.* 7, 81-122.
73. Vogel AIA (1978), "Text Book of Quantitative Inorganic Analysis " 2<sup>nd</sup> Ed Longman, London. 694.
74. Dutta R. L. and Syamal A. (1996), "Elements of Magnatochemistry", 2<sup>nd</sup> Ed., East west press, New Delhi.
75. Z. Szafran, R.M. Pike, M.M. Sing (1991), *Microscale Inorganic Chemistry*, John Wiley, INC., New York.
76. Lorian and Boyd, 1984, *Antibiotic in Laboratory Medicine*, in: Einstein, A. (Ed.), *Collage of Medicine*, Bronx, New York; page 176, Boyd, R.F., *.General Microbiology Times Mirror*.
77. Fayad N.K., Taghreed H. Al-Noor and Ghanim F.H, (2012) , *J. Chemistry and Materials Research*, 2, (5), 18-29.

## References

78. Pabilane, Alma L. dela Cruz, Marie Giecel V. (2011), Group 6, Chem 27.1, SEJ1.
79. Daniales, F and Albert, R. (1975), "Physical Chemistry" 4th Ed
80. Halima F Salem<sup>1</sup>, Hind A Alzletni Marei M El-ajaily<sup>1,3</sup> and Hanan M Eghreibeel (2019), Antimicrobial Activity and Antioxidant Studies of (Z)-2-(2-Methoxybenzylideneamino)-3-Methylbutanoic Acid with Mixed Ligand Complexes, *Acta Scientific Microbiology* 2, 7.
81. Erdem, E., Sarı, E.Y., Kılıncarslan R., Kabay, N. (2009), "Synthesis and characterization of azo-linked Schiff bases and their nickel(II), copper(II), and zinc(II) complexes", *Trans. Met. Chem.*, 34(2):167-174.
82. A.B.P. Lever (1968), "Inorganic Electronic Spectroscopy", Elsevier, New York.
83. M.H. Soliman, Gehad G. Mohamed (2012), *Spectrochim. Acta (A)* 91, 11–17.
84. L.M. Vieira, M.V. de Almeida, M.S. Lourenço (2009), F.F.M. Bezerra, A.S. Fontes, *Euro. J. Med. Chem.* 44, 4107–4111.
85. A.S. Sadeek (2005), *J. Mol. Struct.* 753, 1–12.
86. K. Nakamoto (1996), "Infrared and Raman Spectra of Inorganic and Coordination Compounds", Wiley, New York.
87. C. Preti (1974), G. D. Tosi and Verani, *J. Inorg. Chem.*, 6, 3725.
88. S. F. Aikettle (1975), *Coord. Compounds London*, 168.
89. E. Farkas, I. Sóvágó, (2007), "Metal Complexes of Amino Acids and Peptides, Amino Acids, Peptides and Proteins 36, 287 – 345.
90. Wilkinson G. (1987), *Comprehensive Coordination Chemistry*, vol. 5, Pergamon, Oxford.

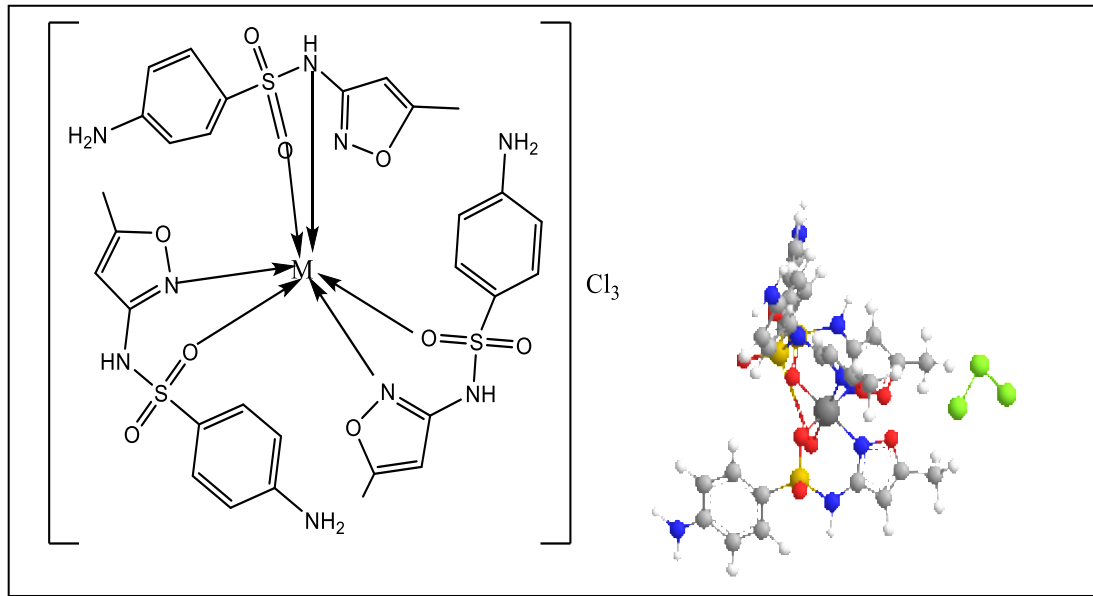
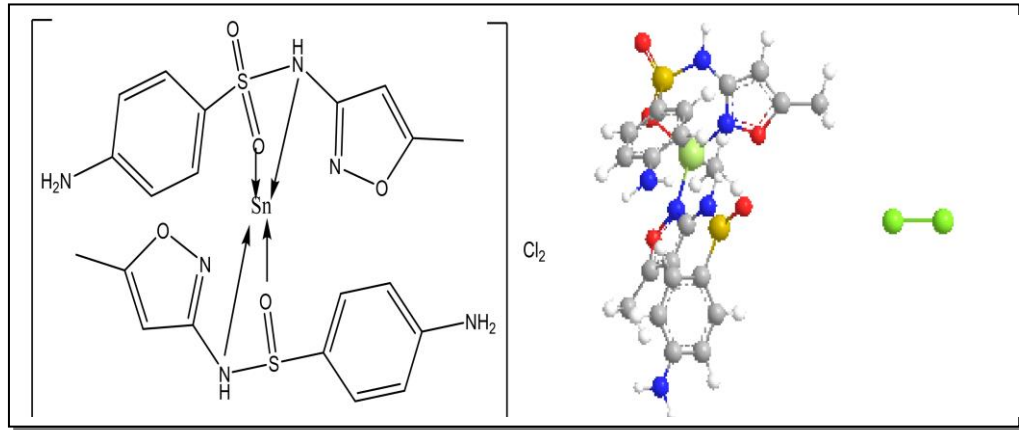
## References

91. B. Mahapatra, P.K. Bhoi, S.K. Kar and S.R. Prasad (1995), *J. Indian Chem. Soc.* 72, 399.
92. Curtis N.F. (1968), *J. Chem. Soc.* 4, 1579 .
93. Soliman M.H., Gehad G. Mohamed (2012), *Spectrochim. Acta (A)* 91 ,11–17.
94. A. Hori, M. Yonemura, M. Ohbe, H. Okawa (2001), *Bull. Chem. Soc. Jpn.* 74 ,495.
95. Sankhala D S, Mathur R C and Mishra S N (1980), *Indian J Chem*, ; 19A: 75-76.
96. L. Mishra and M. K. Said (1993), *Indian J. Chem.*, 32A, 417.
97. N. N. Greenwood and A. Earnshaw (1984), "Chemistry of Elements", Pergamon Press.
98. L. Mishra, A. Kumar, Pandey and R. P. Singh (1992), *Indian J. Chem.*, 31A, 195-198.
99. R. K. Agrawal, D. Sharma, L. Singh and H. Agarwal (1977), *Indian J. Chem. Soc.*, 119, 4599-4607.
100. Xiaofeng Tan and Paul J. Dagdigian , *J. Phys. Chem. A* 2001, 105, 11009-11017.
101. Masoud M.S., El-Husseiny A.F., Abd El-Ghany M.M., Hammud Bull H.H.(2006) , *ac.Sci. Alex. Univ.* 44 ,41–54.
102. E. W. Ainsceugh, A . M. Brodie, W. A. Denny, G.J. Finlay, J.D.Renford (1999), *J. Inorg. Biochem.*, 77, 125 .
103. E. W. A. Insko, A. M. Brodie, W. A. Denny, G. J. Finlay, J. D. Ranford (1998), *J. Indian Biochem.*, 70, 175-185.
104. . Aishah S. S (2009), "Synthesis and characterization of thiourea derivatives. with the reactivity towards the selected microbacteria," , University Malaysia Terengganu.

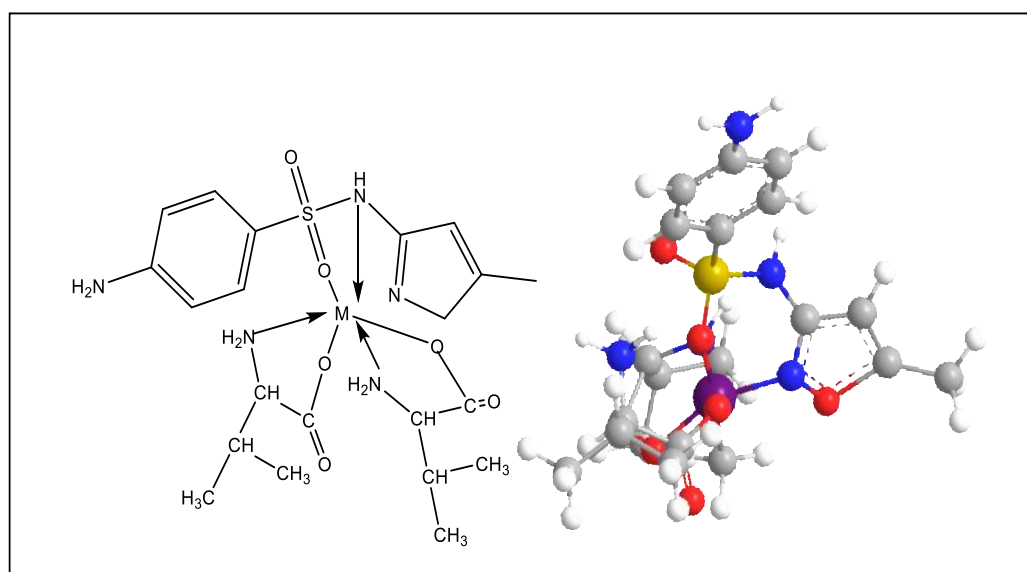
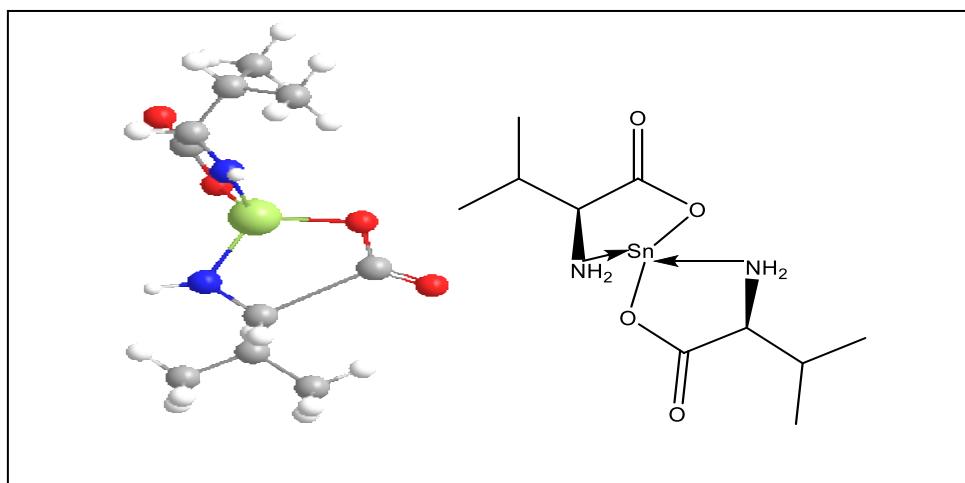
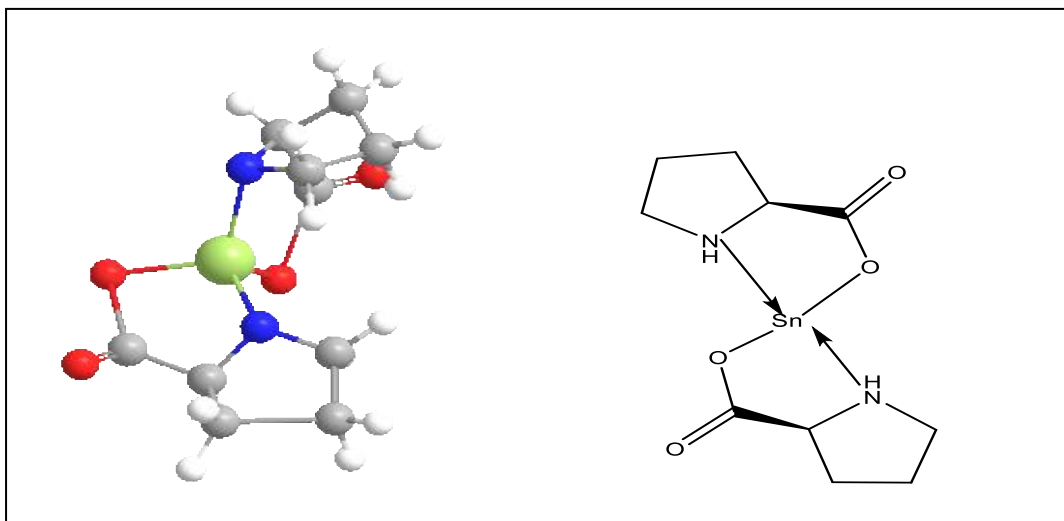
## References

105. Badriah. S. Al-Farhan<sup>1</sup>, Gamal. A. Gouda , Farghaly O. A. and EL Khalafawy A.K. (2019) ,Potentiometric Study of New Schiff Base Complexes Bearing Morpholine in Ethanol-water Medium with some Metal Ions , 14 ,3350 – 3362.
106. Naggara AH, Mauofb HA , Ekshibab AA, Farghalya OA (2016), "Potentiometric and conductometric studies of binary and ternary complexes of sulphamethoxazole and glycine with metal ions "The Pharmaceutical and Chemical Journal, 3(1):125-137.
107. Irving, H., Williams, R.J.P. (1953), "The stability of transition–metal complexes". J. Chem. Soc. 3192–3210 .
108. Amindzhanov A., Manonov K. A., Kabirov N. G. And. Abdelrahma G. A. H (2016), J. Russ. Inorg. Chem., 61 ,81–85.
109. MelinaM., Fernando P., Paula C. de Souza, Clarice Q. Leite , Javier E., Otaciro R. Nascimento, Gianella F., María H. Torre. J. (2013 ),Mol. Struct., 1036: 180–187.
110. Tolesa Egeta Dufera , Sofani Tafesse and Ramesh Duraisamy (2019) International Research Journal of Science and Technology 1, (1) 56 - 56 .
111. Estebanez A, Pascual R, Gil V (2009), "Fosfomycin in a single dose versus a 7-day course of amoxicillin–clavulanate for the treatment of asymptomatic bacteriuria during pregnancy". Eur J Clin Microbiol Infect Dis 28:1457-1464.
112. Wright PM, Seiple IB, Myers AG (2014). The evolving role of chemical synthesis in antibacterial drug discovery. Angew Chem Int Ed Engl. 53:8840-8869.
113. Rogers T, Birnbaum J. (1974), Biosynthesis of Fosfomycin by *Streptomyces fradiae*. Antimicrob Agents Chemother. 5:121-132.
114. Davidson I. and Henry J.B. (1974), Clinical Diagnosis by Laboratory Methods. p 848.





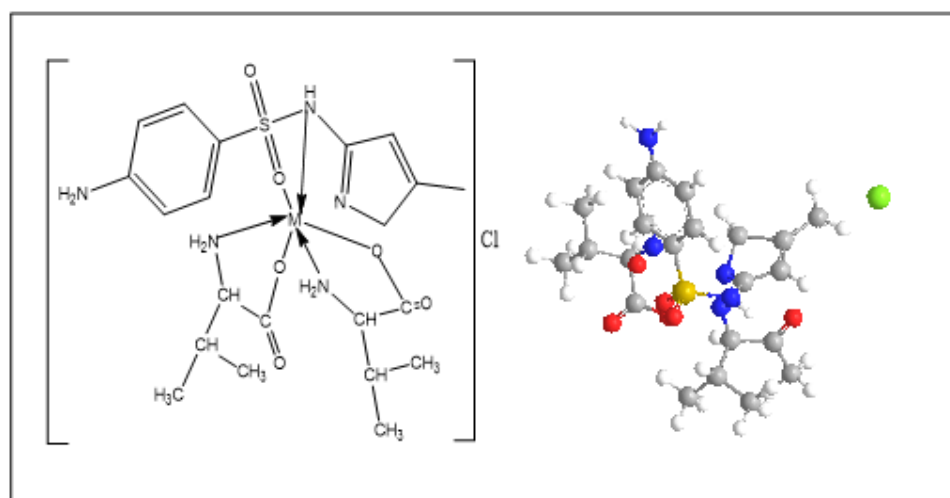
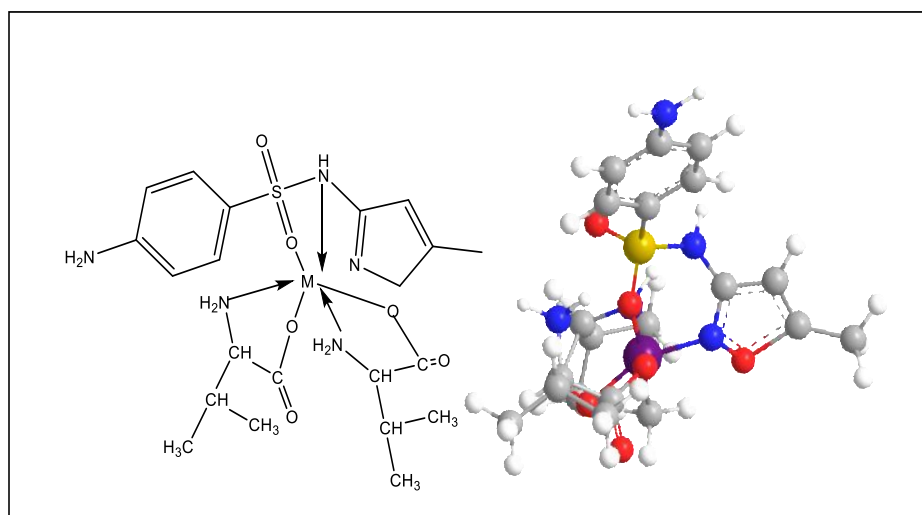
كما تم تقييم الفعالية البيولوجية (المضادة للبكتريا والفطريات) لليكاندات الحرة مع معقداتها المحضرة بقياس منطقة التنشيط (ZI).



Type	ligands	Compositions
Style 1	Sulfamethoxazole (SMZ)	$[\text{Sn}(\text{SMZ})_2]\text{Cl}_2$
Style 2	amino acid L-Proline ( L-ProH)	$[\text{Sn}(\text{L-Pro})_2]$
Style 3	amino acid L-Valine ( L-ValH)	$[\text{Sn}(\text{L-Val})_2]$
Style 4	Sulfamethoxazole (SMZ)	$[ \text{M}'(\text{SMZ})_3]\text{Cl}_3$ $\text{M}'=\text{Fe}(\text{III}),\text{Cr}(\text{III})$ and $\text{Al}(\text{III})$

المعقدات المحضرة (راسب بشكل باودر) درست من النواحي الآتية :-

التوصيلية المولارية ، الدراسات الطيفية (الأشعة تحت الحمراء، الأشعة فوق البنفسجية- المرئية و مطيافية الامتصاص الذري) ومن خلال النتائج التي تم الحصول عليها من التقنيات المختلفة، افترضت الأشكال الفراغية الآتية للمعقدات.



## الخلاصة

تضمن البحث تحضير مجموعة من المعقدات

أ- معقدات مختلطة الليكاند : تم استعمال (المضاد الحيوي) السلفاميثاكرول (SMZ) كليكاند اولي مع / أو ل-البرولين (L-ProH) و ل-الفالين (L-ValH) كليكاند ثانوي مع الايونات M(II) و M'(III) كما تم ادراجه في الجدول الاتي :

Type Mixed ligand complexes	Primary ligand	Secondary Ligand amino acid	Compositions
Style 1 SMZ- L ProH - M 1.1.2 1.1.1	Sulfamethoxazole (SMZ)	L-Proline ( L-ProH)	[M (SMZ)( L-Pro) <sub>2</sub> ] M= Mn(II), Fe (II),Ni(II), Cu(II),Cd(II), Hg(II)and Sn(II)
	Sulfamethoxazole (SMZ)	L-Proline ( L-ProH)	[ M' (SMZ)( L-Pro) <sub>2</sub> ]Cl M' = Al(III) ,Cr(III) and Fe(III)
	Sulfamethoxazole (SMZ)	L-Proline ( L-ProH)	[ Sn(SMZ)( L-Pro)]Cl
Style 2 SMZ. M. L-Val 1.1.2	Sulfamethoxazole (SMZ)	L-Valine ( L-ValH)	[M (SMZ)( L-Val) <sub>2</sub> ]Cl M= Mn (II), Fe (II), Co(II),Ni(II), Cu(II), ,Cd(II), Hg(II) and Sn(II)
	Sulfamethoxazole (SMZ)	L-Valine ( L-ValH)	[M' (SMZ)( L-Val ) <sub>2</sub> ]Cl M' = Fe(III) ,Cr(III) and Al(III)

ب- معقدات أحادية الليكاند : تم استعمال السلفاميثاكرول (SMZ) و ل-البرولين (L-ProH) و ل-الفالين (L-ValH) كليكاندات مع الايونات M(II) و M'(III) كما تم ادراجه في الجدول الاتي :



جمهورية العراق  
وزارة التعليم العالي والبحث العلمي  
جامعة بغداد  
كلية التربية للعلوم الصرفة / ابن الهيثم  
قسم الكيمياء

## تحضير , تشخيص وتقييم الفعالية البيولوجية لبعض الايونات الفلزية مع ادوية مختارة

رسالة مقدمة الى مجلس كلية التربية للعلوم الصرفة-ابن الهيثم- جامعة بغداد

وهي جزء من متطلبات نيل شهادة الماجستير في الكيمياء

من قبل

**سجى احمد عبد الله**

بكلوريوس / جامعة بغداد (2016)

بإشراف

**أ.د تغريد هاشم النور**